Euscorpius

Occasional Publications in Scorpiology

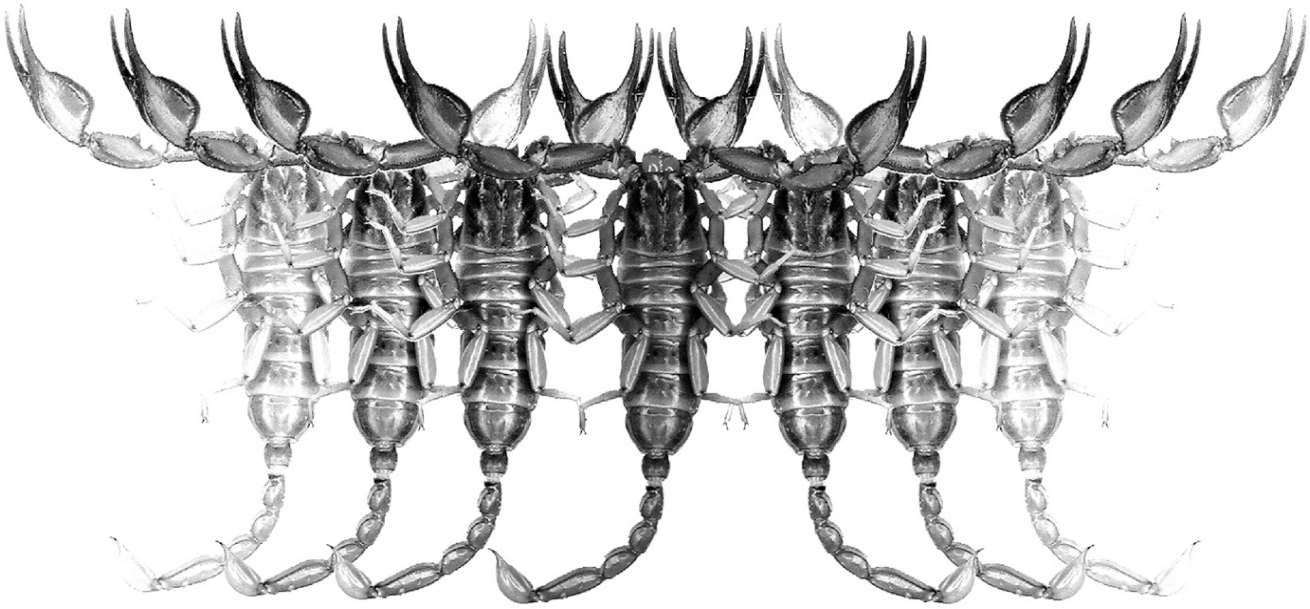

Review of *Grosphus* Simon, 1880, with description of *Teruelius* gen. n., a new buthid genus from Madagascar (Scorpiones: Buthidae)

Graeme Lowe & František Kovařík

May 2019 — No. 281

Euscorpius

Occasional Publications in Scorpiology

EDITOR: **Victor Fet**, Marshall University, **'fet@marshall.edu'**

ASSOCIATE EDITOR: **Michael E. Soleglad, 'msoleglad@gmail.com'**

Euscorpius is the first research publication completely devoted to scorpions (Arachnida: Scorpiones). ***Euscorpius*** takes advantage of the rapidly evolving medium of quick online publication, at the same time maintaining high research standards for the burgeoning field of scorpion science (scorpiology). ***Euscorpius*** is an expedient and viable medium for the publication of serious papers in scorpiology, including (but not limited to): systematics, evolution, ecology, biogeography, and general biology of scorpions. Review papers, descriptions of new taxa, faunistic surveys, lists of museum collections, and book reviews are welcome.

Derivatio Nominis

The name ***Euscorpius*** Thorell, 1876 refers to the most common genus of scorpions in the Mediterranean region and southern Europe (family Euscorpiidae).

Euscorpius is located at: https://mds.marshall.edu/euscorpius/
Archive of issues 1-270 see also at: http://www.science.marshall.edu/fet/Euscorpius

(Marshall University, Huntington, West Virginia 25755-2510, USA)

ICZN COMPLIANCE OF ELECTRONIC PUBLICATIONS:

Electronic ("e-only") publications are fully compliant with ICZN (*International Code of Zoological Nomenclature*) (i.e. for the purposes of new names and new nomenclatural acts) when properly archived and registered. All ***Euscorpius*** issues starting from No. 156 (2013) are archived in two electronic archives:

- **Biotaxa,** http://biotaxa.org/Euscorpius (ICZN-approved and ZooBank-enabled)
- **Marshall Digital Scholar**, http://mds.marshall.edu/euscorpius/. (This website also archives all *Euscorpius* issues previously published on CD-ROMs.)

Between 2000 and 2013, ICZN ***did not accept online texts*** as "published work" (Article 9.8). At this time, *Euscorpius* was produced in two ***identical*** versions: online (*ISSN 1536-9307*) and CD-ROM (*ISSN 1536-9293*) (laser disk) in archive-quality, read-only format. Both versions had the identical date of publication, as well as identical page and figure numbers. ***Only copies distributed on a CD-ROM*** from ***Euscorpius*** in 2001-2012 represent published work in compliance with the ICZN, i.e. for the purposes of new names and new nomenclatural acts.

In September 2012, ICZN Article 8. What constitutes published work**,** has been amended and allowed for electronic publications, disallowing publication on optical discs. From January 2013, ***Euscorpius*** discontinued CD-ROM production; only online electronic version (ISSN 1536-9307) is published. For further details on the new ICZN amendment, see http://www.pensoft.net/journals/zookeys/article/3944/.

Publication date: 22 May 2019

http://zoobank.org/urn:lsid:zoobank.org:pub:FEBA0106-02A3-4465-8D39-9FF32634EEF

Euscorpius — Occasional Publications in Scorpiology. 2019, No. 281

Review of *Grosphus* Simon, 1880, with description of *Teruelius* gen. n., a new buthid genus from Madagascar (Scorpiones: Buthidae)

Graeme Lowe[1] & František Kovařík[2]

[1] Monell Chemical Senses Center, 3500 Market St., Philadelphia, PA 19104-3308, USA
[2] P. O. Box 27, CZ - 145 01 Praha 45, Czech Republic www. scorpio.cz

http://zoobank.org/urn:lsid:zoobank.org:pub:FEBA0106-02A3-4465-8D39-9FF32634EEF

Summary

We review the taxonomy of the Madagascar endemic buthid genus *Grosphus* Simon, 1880. We split the genus and describe *Teruelius* **gen**. **n**. on the basis of nine morphological characters, six of them new for *Grosphus*: positions of trichobothria d_2 on pedipalp femur and Eb_3 on chela manus, number of pectine teeth, shape of female basal pectinal tooth, form of hemispermatophore capsule posterior lobe, spiracle shape, metasoma I ventromedian carination, telotarsal setation and UV fluorescence. We discuss functional and taxonomic aspects of these characters, and propose that *Teruelius* **gen**. **n**. is monophyletic, while *Grosphus* (sensu stricto) is paraphyletic. Some characters of *Teruelius* **gen**. **n**. suggest adaptations to xeric environments, some of *Grosphus* to humid environments. *Neogrosphus* Lourenço, 1995 shares characters with both *Grosphus* and *Teruelius* **gen**. **n**. Scenarios for origins of these genera by vicariance or dispersal are discussed. New synonymies proposed are: *Grosphus simoni* Lourenço, Goodman & Ramilijaona, 2004 = *Grosphus madagascariensis* (Gervais, 1843), **syn**. **n**.; *Grosphus halleuxi* Lourenço, Wilmé, Soarimalala & Waeber, 2017 = *Grosphus madagascariensis* (Gervais, 1843), **syn**. **n**.; *Grosphus mandena* Lourenço, 2005 = *Grosphus madagascariensis* (Gervais, 1843), **syn**. **n**.; *Grosphus hirtus garciai* Lourenço, 2001 = *Grosphus hirtus* Kraepelin, 1900, **syn**. **n**.; *Grosphus makay* Lourenço & Wilmé, 2015 = *Teruelius feti* (Lourenço, 1996) **comb. n., syn**. **n**.; *Grosphus rossii* Lourenço, 2013 = *Teruelius mahafaliensis* (Lourenço, Goodman & Ramilijaona, 2004) **comb. n., syn**. **n**.

Introduction

The 'island continent' of Madagascar is legendary as a biodiversity jewel endowed with a treasure trove of endemic biota. A Gondwanan fragment isolated since its separation from Africa in the Upper Jurassic ca. 160 Mya, and from India in the Late Cretaceous ca. 88 Mya, it has a long and complex geoclimatic history, making it an enticing natural laboratory for studies on biogeography, evolution and speciation (Goodman et al., 2003; Vences et al., 2009; Wilmé et al., 2006). Like many other animal groups in Madagascar, scorpions display high diversity and are comprised largely or entirely of endemic taxa, currently numbering 94 endemic species in 10 genera (9 endemic, one Gondwanan) and 3 families (one endemic) (e.g., Lourenço, 1996a, 1996b, 2000a, 2000b, 2003a, 2004b; Lourenço et al., 2006a, 2016a, 2018a, 2018c). Buthids account for 74 (79%) of these species, with the largest number (31) in the endemic genus *Grosphus* Simon, 1880. This genus includes both putative microendemic species known only from restricted localities, and more widespread species that together populate all major biomes in the country (Lourenço & Wilmé, 2016). The taxonomic scope of *Grosphus* has expanded in recent years by steady incremental addition of new species. However, our understanding of the systematics of this large genus has not progressed beyond informal species groups like those formulated by earlier workers (Fage, 1929). Here, we offer a fresh perspective on the taxonomy of *Grosphus*, partitioning it into two distinct genera based on a combination of classical morphological characters. The two genera are compared to the genus *Neogrosphus* and other related buthids.

Taxonomic history

The first scorpion to be described from Madagascar was *Scorpio* (*Androctonus*) *madagascariensis* Gervais, 1843, based on a male type collected for the Paris museum (Muséum National d'Histoire Naturelle) by French explorer and avid insect collector Jules Prosper 'Bibikely' Goudot in the 1830s. Placement in the subgenus *Androctonus* associated it with other Old World buthids known at the time (i.e., species now in *Androctonus*, *Buthacus*, *Buthus*, *Leiurus*, *Hottentotta*, *Lychas*, *Mesobuthus* and *Parabuthus*) (Gervais, 1844). Later, Simon (1880) separated it from the others, placing it into its own genus *Grosphus*, differentiated by an enlarged, oval, basal pectine tooth (a female character), and a single denticle on the ventral margin of the chelicera movable finger (in contrast to two denticles in other buthids). The latter character was not valid as there are actually two such teeth in *Grosphus*,

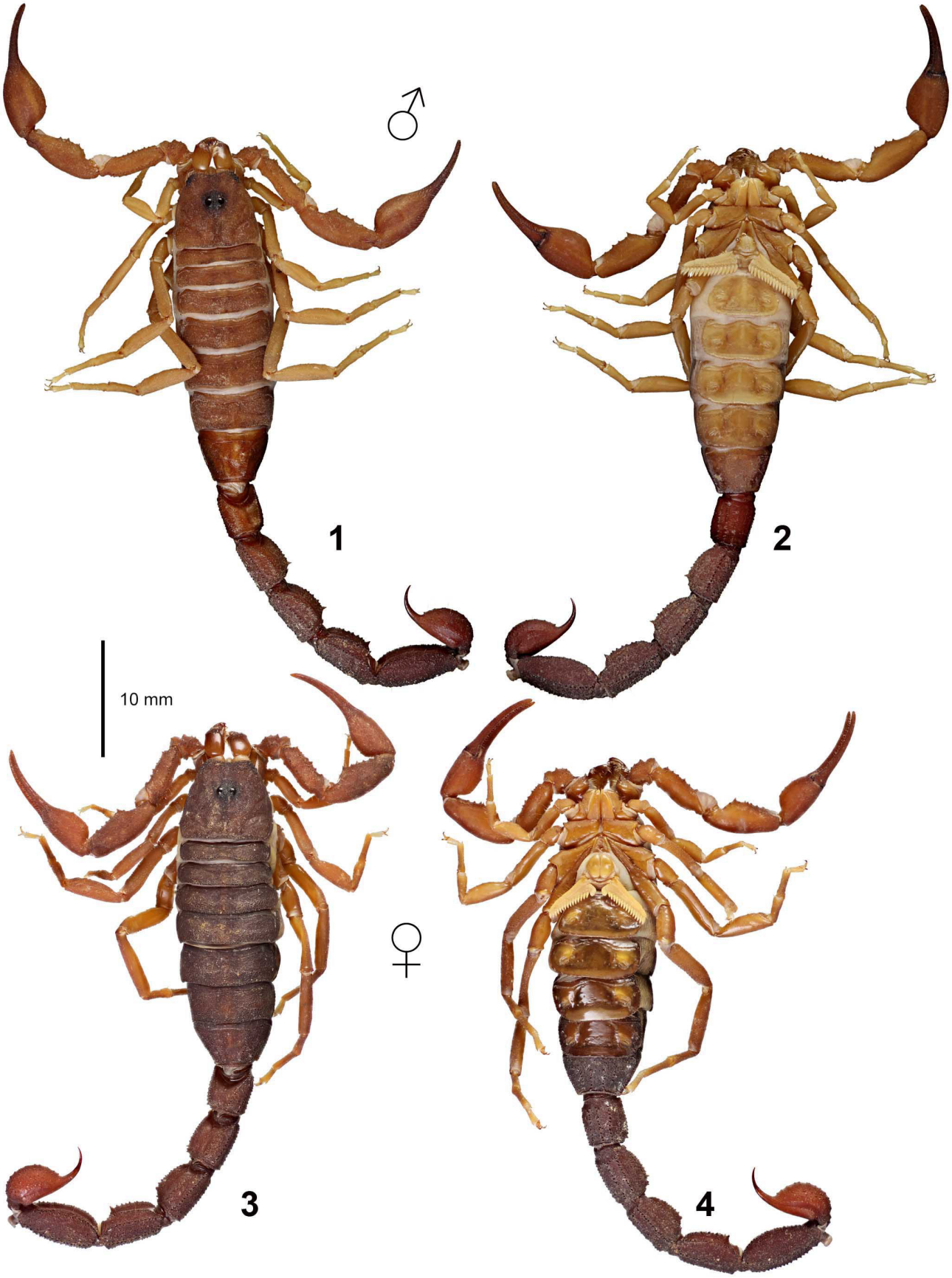

Figures 1–4. *Grosphus madagascariensis*. Type species of *Grosphus* Simon, 1880. Habitus. Male (1–2) and female (3–4), in dorsal (1, 3) and ventral (2, 4) views. Scale bar: 10 mm.

and Simon may have studied an abnormal specimen. This diagnosis of *Grosphus* was, however, accepted by Karsch (1886).

Nine years later, Pocock (1889a) described two additional buthids from Madagascar: *Buthus limbatus* and *B. piceus*. Both were also characterized by an enlarged basal pectine tooth in females, flask-shaped in the former, and oval (as in *G. madagascariensis*) in the latter. In spite of this shared character, Pocock retained the two new species under '*Buthus*' because they bore two denticles (not one) on the ventral margin of the cheliceral movable finger. Moreover, the metasoma of *B. limbatus* was more similar to those of *Buthus hottentotta*, *B. judaicus* (now in *Hottentotta*) and *B. liosoma* (now in *Parabuthus*). The species appeared intermediate between those taxa and *G. madagascariensis*, and Pocock claimed this to "weaken the basis upon which *Grosphus* was founded". Later that same year, Pocock (1889b) described a third new species from Madagascar, *Buthus lobidens*, similar to *B. piceus* but differentiated by a more slender metasoma, longer chela fingers, lack of subaculear tubercle on the telson, and narrower spiracles on the sternites. In contrast, the spiracles were conspicuously ovate in *B. piceus*, a character that Pocock considered possibly significant at the genus level. In his subsequent revision of buthid genera, Pocock (1890) suggested that the single cheliceral denticle was an abnormality and placed all four species under *Grosphus*, which he downgraded to a subgenus of *Buthus*.

Kraepelin (1891) accepted *Grosphus* as a valid genus in his revision of buthids. He dismissed Pocock's concerns about differences in cheliceral movable finger dentition and placed *B. piceus* in *Grosphus*, listing as a likely junior synonym *G. madagascariensis* (which should have had precedence). He also synonymized *B. lobidens* under *G. piceus*, citing variability in Pocock's diagnostic characters among six specimens of *B. piceus*. Variation was reported in chela and metasomal morphometrics, telson vesicle sculpture, and in spiracle shape such as narrower spiracles on posterior sternites. In his monograph (Kraepelin, 1899), the generic diagnosis was emended to 2 denticles on the ventral margin of the cheliceral movable finger, and *G. madagascariensis* was listed as senior synonym of *G. piceus*. Known diversity of *Grosphus* was increased when Kraepelin (1900) described four additional species from materials in the Paris museum: *G. hirtus*, *G. grandidieri*, *G. flavopiceus* and *G. bistriatus*. Strand (1908) concurred that *G. piceus* and *G. lobidens* were synonyms of *G. madagascariensis*, and described a subspecies *G. limbatus pallicauda*.

The next major work on the genus was a review of Madagascar scorpions by Fage (1929) who redescribed all four species of *Grosphus* and detailed their variation, geographic distribution and habitats. He added another subspecies, *G. limbatus annulata*, and synonymized *G. limbatus pallicauda* under *G. bistriatus*. In his species key, Fage organized the genus into three species groups: Group I: *G. madagascariensis* and *G. hirtus*, dark species with granular ventral metasomal carinae, lower pectinal tooth counts, oval or sub-quadrangular basal pectine tooth in females, occurring mostly in humid eastern region and Sambirano rainforest in the northwest; Group II: *G. flavopiceus*, *G. limbatus* and *G. bistriatus*, light- and dark-striped or patterned species with smooth ventral metasomal carinae, higher pectinal tooth counts, conical or saber-like basal pectine tooth in females, occurring mostly in central plateau, western and southern regions; and Group III: *G. grandidieri*, a large black species with smooth ventral metasomal carinae, high pectinal tooth count and a very long basal pectine tooth in females, restricted to the southern sub-arid region. Characters for separation at the species level included body size, coloration patterns, pectinal tooth count, number of denticle rows on the chela fingers, and the form of the enlarged basal pectine tooth in females.

Vachon (1969) described a seventh species, *G. griveaudi*, from the southwestern coast north of Tulear (= Toliara), but listed several differences compared to other species of the genus. On the basis of these differences, it was later transferred to its own genus, *Neogrosphus*, by Lourenço (1995). Another comprehensive review of Madagascar scorpions was provided by Lourenço (1996b) that included a summary of *Grosphus* species, the description of *G. feti* from Cap Sainte Marie, and promotion to species status of *G. annulatus* Fage, 1929. Characters used to diagnose and key out species were similar to those used in earlier works (Fage, 1929; Kraepelin, 1900; Vachon, 1969).

Since then, Lourenço and collaborators continued surveying Madagascar scorpions, describing many additional *Grosphus* species. The count progressively increased by over four-fold, to its current total of 31 species. Lourenço (1999) described *G. intertidalis*, one of the few scorpions known from a littoral habitat, near Tulear (= Toliara) on the southwestern coast. *G. garciai* Lourenço, 2001, was described from what is now Ankarafantsika National Park in the northwest. Lourenço (2003c) provided redescriptions of the two older species, *G. limbatus* and *G. bistriatus*. Their identities were clarified by freshly collected materials with better color preservation. The former species was confined to central highlands, and the latter to the southwest coast. Another related species, *Grosphus ankarafantsika* Lourenço, 2003, was described from Ankarafantsika National Park from specimens previously misidentified as *G. bistriatus*, distinguished by its different shaped female basal pectine tooth. The largest known member of the genus (> 11 cm), *G. ankarana* Lourenço & Goodman, 2003, was discovered in the Ankarana Massif in the northern end of the country. A much smaller species, *G. olgae* Lourenço, 2004, was found in Mikea Forest along the southwest coast. Lourenço, Goodman & Ramilijaona (2004) added three more species: *G. mahafaliensis* from the limestone karst Mahafaly Plateau in the southwest, *G. darainensis* from Daraina Forest in the northeast, and *G. simoni* from humid Makira Forest in the northeast and northwestern dry forest (Ankarafantsika National Park). Lourenço (2005) described *G. mandena*, from material collected in remnant southeastern rainforest that he previously determined as *G. hirtus* (Lourenço, 2000b). To better clarify the status of similar species, Lourenço &

Goodman (2006) redescribed *G. madagascariensis* and *G. hirtus*, and added a closely related species, *G. goudoti* from the northeast Daraina Forest. Another close relative of *G. hirtus* was *G. polskyi* from the subarid southwest coast (Lourenço et al., 2007a). The systematics and ecology of the southwestern *Grosphus* spp. was reviewed by Lourenço et al., 2007c, and an emended diagnosis of *G. mahafaliensis* given to include the form of the female basal pectine tooth.

A synopsis of *Grosphus* species distributed in the northern and humid eastern regions of Madagascar was given by Lourenço et al. (2009b). The species *G. tavaratra* was described from limestone karst of Montagne des Français, near Antsiranana in the extreme north, and *G. garciai* was downgraded to a subspecies, *G. hirtus garciai*. In the same year Lourenço & Goodman (2009) reported the interesting discovery of a new species, *G. mayottensis*, from the island of Mayotte in the Comoros Archipelago in the Mozambique Channel. This remains to date the only record of *Grosphus* outside Madagascar. Lourenço (2012c) described *G. bicolor* from a single juvenile male specimen from the southwest region, that appears to be related to *G. grandidieri*, which occurs across the same region (Lourenço et al., 2009a). It was differentiated by having two yellow stripes on the tergites. Lourenço (2013b) added another species, *G. rossii*, based on an isolated male type from higher elevations of central Madagascar and related it to *G. limbatus*, which occurs widely in the same region. Lourenço (2014) gave an updated review of systematics and ecology of southwestern *Grosphus*, adding another species, *G. magalieae* from Cap Sainte Marie, associating it with *G. limbatus*/ *G. rossii*. Also associated with these was *G. makay* Lourenço & Wilmé, 2015, from Makay mountains in the southwest. Recent additions to this species complex also included: *G. eliseanneae* and *G. waeberi* from the northeast, and *G. sabineae* from southern cape (Lourenço & Wilmé, 2016), *G. ganzhorni* from Ankarana Massif in the north (Lourenço et al., 2016c), and *G. bemaraha* from Tsingy Bemaraha in central western region, which was related to *G. mahafaliensis* (Lourenço et al., 2018b). Additions to the '*G. madagascariensis*/ *hirtus* group'(= Fage's Group I) were also made: *G. voahangyae*, a small, dark, mottled species from dense humid Torotorofotsy forest in the central eastern mountains (Lourenço & Wilmé, 2015); *G. halleuxi* also from Torotorofotsy forest, *G. rakotoariveloi* from Ankarafantsika National Park (Lourenço et al., 2017), a population previously classified as *G. simoni*; and *G. ambre* from Montagne d'Ambre at the north end of the island (Lourenço et al., 2018b).

In summary, Simon's initial recognition of *Grosphus* as a unique Madagascar genus was followed by an early stage of sporadic description of species. After the review by Fage (1929), there was a long period of inactivity until a renewed focus on Madagascar scorpiofauna by Lourenço (1995a, 1996a–d). Over the last 22 years, collective efforts by Lourenço and collaborators accelerated the discovery process and the species richness of *Grosphus* now rivals that of some other Madagascar endemic faunas. When genera reach a critical mass or become heterogeneous, analysis is warranted to identify putative lineages for splitting into smaller taxonomic units that better encode phylogeny and ecological or evolutionary developments. Our recent work has addressed this for some buthid genera: *Babycurus* Karsch, 1886 (Kovařík et al., 2018b), *Butheolus* (Lowe, 2018) and *Buthacus* Birula, 1908 (Kovařík et al., 2013; Lowe et al., 2019). We diagnosed new genera by identifying consistent differences in previously overlooked external characters and by comparing hemispermatophore capsule structures. Here we extend our approach to *Grosphus* (sensu lato).

Methods, Material & Abbreviations

Anatomical nomenclature and measurements. Morphological terminology generally follows Vachon (1963), Stahnke (1971), Sissom (1990), Kovařík (2009), and Kovařík & Ojanguren Affilastro (2013), except for trichobothria (Vachon 1974, 1975), tarsal segments (Haradon, 1984) and hemispermatophores (Kovařík et al., 2018a). The enlarged sclerite on the posterior marginal base of the female pectine, in line with other comb teeth, is herein termed an enlarged pectine tooth (Fage, 1929; Kraepelin, 1891, 1899, 1900; Prendini, 2001, 2004a; Simon, 1880; Pocock, 1889a, 1889b, 1890; Vachon, 1969), as opposed to an enlarged 'basal middle lamella' (cf. Lourenço, 1996b, and subsequent). The latter term is both inaccurate and ambiguous: (i) the position of the structure is posterior marginal, not middle; (ii) a distinct, separate sclerite occupying the basal middle position of the comb exists, and is better described as 'basal middle lamella'. Our choice of terminology is empirical, purely for the purpose of resolving ambiguity and does not endorse any hypothesis about origins of this sclerite. In specifying pectinal tooth counts (PTC), we only include normal teeth and omit the enlarged basal tooth of females, which differs ultrastructurally in lacking peg sensillae. This convention facilitates comparison with PTC data cited in most published descriptions by Lourenço and collaborators, who presumably did not enumerate the enlarged basal tooth.

General laboratory methods follow Sissom et al., 1990. White light and UV imaging methods were applied as described in Lowe et al. (2014) and Lowe (2018). Biometric analyses utilized the software Image J 1.44p (http://rsbweb.nih.gov/ij), Origin 7.0 (https://www.originlab.com) and Microsoft Excel 2010. Summary statistics are reported as mean ± SE (standard error of the mean), and coefficient of variation CV = standard deviation (SD)/ mean. In some graphs, we plot ranges (minimum, maximum, and mid-range values) as these limits have potential diagnostic application.

Study material. Specimens were loaned from several museums, donated by colleagues, or legally imported into the Czech Republic. Although we did not directly analyze materials representing all described species of *Grosphus*, we assembled a sufficiently representative and consistent dataset to support our conclusions. Some character states of taxa not examined were extracted from published descriptions or figures.

Fluorometry. For ultraviolet (UV) fluorescence measurements, scorpions were mounted ventral side up in 70% isopropyl alcohol under a Tiffen 58 mm glass filter on a custom-built stage, and viewed by an Olympus BX50 WI microscope with UPlanApo 10×/ NA 0.4 objective (2.2 mm diameter field of view). Excitation light was provided by a 395 nm LED with current driven by a linear DC power supply (0.35 A), directed through a BX-URA2 epifluorescence unit, and reflected onto the medial area of sternite VI of the specimen by a dichroic mirror (460 nm cutoff). Fluorescence wavelengths were isolated with a 515–570 nm band-pass emission filter (Chroma Technology), and detected by a Photomax 200 avalanche photodiode (Dagan Corporation) at 130 V bias voltage, cooled to –44 °C. The photocurrent signal was conditioned by a 4-pole Bessel filter (20 Hz) and digitized by Instrutech ITC-18 interface controlled by WinEDR V.3.8.6 software (Strathclyde).

Abbreviations. Specimen depositories: BMNH (The Natural History Museum, London, United Kingdom), CUPC (Charles University in Prague, Faculty of Science, Czech Republic), FKCP (František Kovařík, private collection, Prague, Czech Republic), FMNH (Field Museum of Natural History, Chicago, USA), GLPC (Graeme Lowe, private collection, Philadelphia, USA), MHNG (Muséum d'Histoire Naturelle de la Ville de Genève, Geneva, Switzerland); ZMUH (Centrum für Naturkunde (CeNak), Center of Natural History Universität Hamburg, Zoological Museum, Hamburg, Germany). Other abbreviations: nr, near; Mya, million years ago; PTC, pectinal tooth count. In citing figures, capitalized 'Fig(s).' cite illustrations in this paper, lower case 'fig(s).' cite illustrations in other papers.

Results

Systematics

Family Buthidae C. L. Koch, 1837

Diagnosis of the '*Grosphus*' group

The three buthid genera *Grosphus* Simon, 1880, *Neogrosphus* Lourenço, 1995, and *Teruelius* **gen**. **n**. comprise a distinct assemblage of Madagascar buthids (= '*Grosphus*' group) sharing the following set of characters:

Carapace subrectangular, weakly trapezoidal or nearly parallel-sided, surface densely granular, carinae indistinct except for superciliary carinae; frontal region of carapace flat, not sloped towards anterior margin; median eyes large, median ocular tubercle prominent, located forward of the carapace centroid (Figs. 165–180); 5 pairs of lateral eyes (3 large, 2 small) (Figs. 227–230); chelicerae with typical buthid dentition on fixed and movable fingers (Vachon, 1963), two enlarged denticles on ventral surface of fixed finger (Figs. 231–238); sternum type 1, subtriangular; tergites granular, tergites I–VI with single, weak median carina, tergite VII with weak median carina and 2 pairs of strong lateral carinae; metasoma moderately elongate, segments I–III with 8–10 carinae, IV with 8 carinae, V with 3–5 carinae; telson vesicle bulbous, ovoid or elongate, with or without subaculear tubercle (Figs. 181–195); pectines with fulcra, 13–41 teeth, female with basal pectinal tooth dilated or elongated, lacking peg sensillae (Figs. 40–51, 196–210); hemispermatophore flagellum thicker at base, narrowed proximally, thickened distally (Figs. 52, 58, 60, 67, 71, 75, 78, 84); pedipalp chela elongate, smooth, carinae obsolete, surface typically with numerous short macrosetae (Figs. 21–24); finger dentition composed of 8–15 discrete linear rows of granules or denticles, each slightly oblique with proximal ends directed externally; rows either non-overlapping or slightly imbricated, proximal 3 granules in each row enlarged, 2 of these slightly displaced outwards as 'external accessory' granules; series of large, dentate internal accessory granules present, offset from main rows; both chela fingers with enlarged apical teeth, 3–4 external subdistal granules; pedipalps sexually dimorphic, dentate margins of fingers weakly or strongly scalloped proximally in males, straight in females, manus of males broader than that of females; trichobothrial pattern orthobothriotaxic, type A (Vachon, 1974), with femur d_1-d_3-d_4 in α-configuration (Vachon, 1975), patella d_3 external to dorsomedian carina (Fet et al., 2005); patella *em* much closer to *est* and *et*, than to esb_1 and esb_2, with *em-est-et* usually forming a compact triad (Figs. 345, 481a); chela manus with Eb_1-Eb_2 angled distally, Eb_1-Eb_2-Eb_3 acute angle opening in proximal direction (γ-configuration) (Figs. 342, 478a); chela with *db* in proximal half to middle of fixed finger; legs III–IV with tibial spurs (Figs. 211–226, 261–262, 318–319, 364–365, 414–417, 487–488, 514–515, 540–541, 578–579, 618–619), tarsi without bristle-combs.

Remarks. In describing the first '*Grosphus*' group species, *Scorpio* (*Androctonus*) *madagascariensis*, Gervais (1844: pl. XI, fig. 3) illustrated the carapace showing forward placement of the median eyes, and also accurately depicted five pairs of lateral eyes, now recognized to be the prevalent buthid configuration (Loria & Prendini, 2014; Yang et al., 2013). In spite of this, Fage (1929) incorrectly declared that *Grosphus* (sensu lato) only bore 3 pairs of lateral eyes, and Lourenço (1996b) cited only 3–4 pairs. Moreover, only 3 pairs were described for: *Grosphus ambre*, *G. darainensis*, *G. garciai*, *G. goudoti*, *G. halleuxi*, *G. hirtus*, *G. madagascariensis*, *G. makay*, *G. mandena*, *G. mayottensis*, *G. polskyi*, *G. rossii*, *G. simoni*, *G. rakotoariveloi*, *G. tavaratra*, *G. voahangyae*, *Teruelius ankarana*, *T. ankarafantsika*, *T. bemaraha*, *T. bicolor*, *T. bistriatus*, *T. eliseanneae*, *T. feti*, *T. ganzhorni*, *T. intertidalis*, *T. limbatus*, *T. magalieae*, *T. mahafaliensis*, *T. olgae*, *T. sabineae*, *T. waeberi* (Lourenço, 1996b, 1999, 2001b, 2003c, 2005, 2012c, 2013b, 2014; Lourenço & Goodman, 2006, 2009; Lourenço & Wilmé, 2015a, 2015b, 2016; Lourenço et al., 2004, 2007a, 2009b, 2016c, 2017, 2018b). We confirm here that 5 pairs are indeed present in all species that we have examined: *G. garciai* (= *G. hirtus*), *G. goudoti*, *G.* '*halleuxi*', *G. hirtus*, *G.* sp. nr *hirtus*, *G. madagascariensis*, *G.* '*mandena*', *G. voahangyae*, *Neogrosphus griveaudi*, *Teruelius ankarafantsika*, *T. ankarana, T. annulatus*, *T. bistriatus*, *T. feti*, *T. flavopiceus*, *T. grandidieri*, *T. intertidalis*, *T. limbatus*,

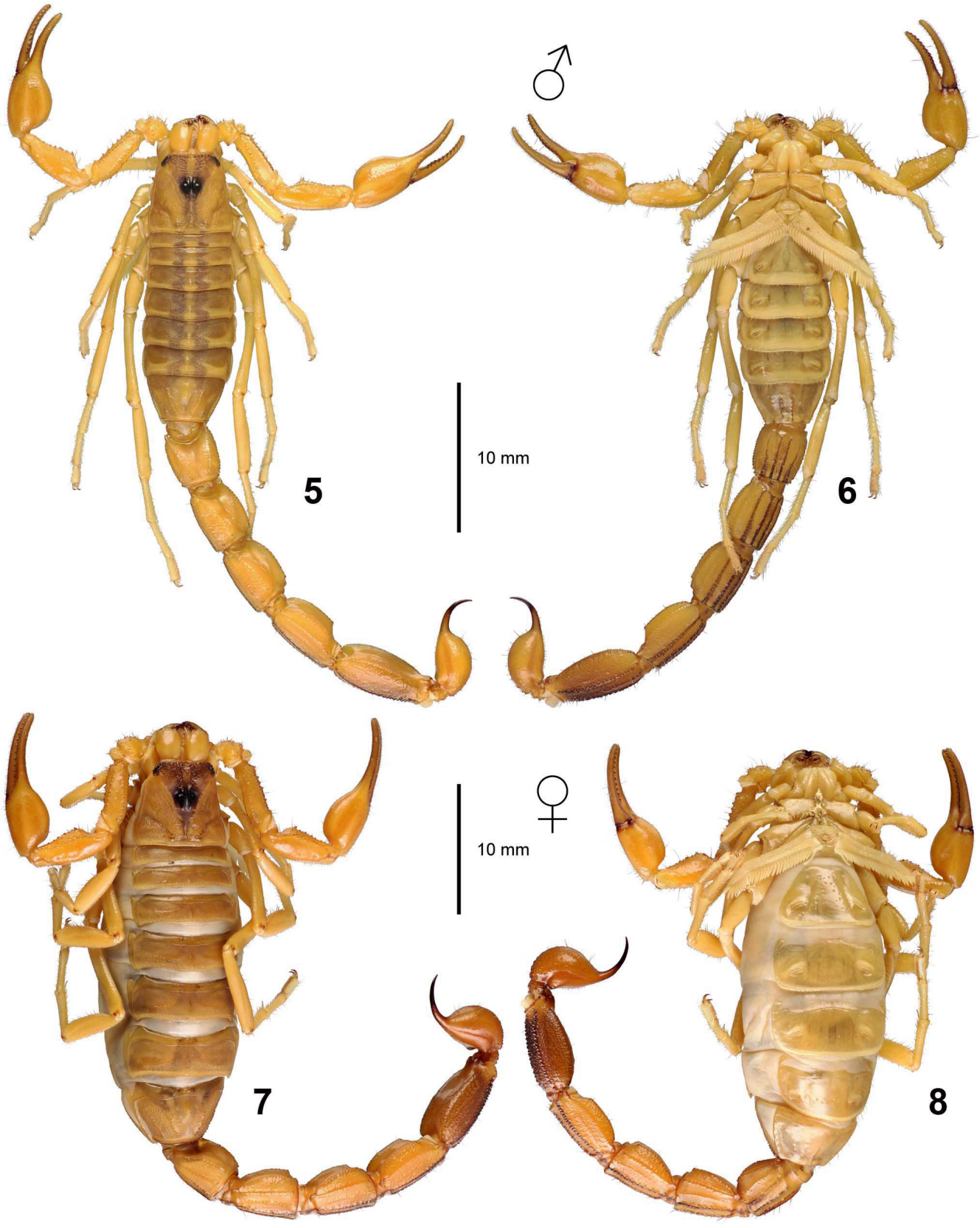

Figures 5–**8**. *Teruelius limbatus*. Type species of *Teruelius* **gen**. **n**. Habitus. Male (5–6) and female (7–8), dorsal (5, 7) and ventral (6, 8) views. Scale bars: 10 mm.

T. mahafaliensis and *T. olgae* (e.g., Figs. 227–230). We found only a few individual deviations from the standard pattern, such as 2 large and 2 small ocelli, that we regarded as developmental anomalies. We predict that other '*Grosphus*' group species will also comply with the 5-eye pattern. Although undercounting of lateral eyes is perhaps attributable to overlooking of the smaller posterior and upper ocelli, 10 of the published 3-eye counts post-date introduction of the 5-eye model by Yang et al. (2013, coauthor Lourenço) and Loria & Prendini (2014). Paradoxically, Lourenço et al. (2007a) claimed 3 lateral eyes in boilerplate descriptions of *G. hirtus* and *G. polskyi*, yet their figures clearly depict all 5 lateral eyes as being present in both species. Vachon (1969) correctly reported 5 "nettement visibles" lateral eyes, 3 large and 2 small, in both sexes of *Neogrosphus griveaudi*. Although 3 pairs were described for *N. blanci* and *N. andrafiabe* (Lourenço, 1996b; Lourenço et al., 2015), we are skeptical that these counts are accurate.

Genus ***Grosphus*** Simon, 1880

(Figs. 1–4, 9–12, 21–22, 25–43, 52–68, 86, 94–98, 106–125, 133–136, 145–149, 158–160, 165–169, 181–185, 196–200, 211–215, 227–228, 231–234, 239–386, 580–583, Tabs. 1–4)

Grosphus Simon, 1880: 377–378; Karsch, 1886: 77; Pocock, 1889a: 348–349; Kraepelin, 1891: 70 (in part); Pocock, 1893: 312 (in part); Kraepelin, 1895: 84 (in part); Kraepelin, 1899: 32 (in part); Kraepelin, 1900: 11–12 (in part); Birula, 1917a: 164 (in part); Birula, 1917b: 55 (in part); Fage, 1929: 640–642 (in part); Werner, 1934: 270 (in part); Vachon, 1969: 483 (in part); Legendre, 1972: 428 (in part); Stahnke, 1972: 130 (in part); Vachon, 1974: 906 (in part); Vachon, 1975: 1598 (in part); Lamoral & Reynders, 1975: 507 (in part); Francke, 1985: 8, 15 (in part); Sissom, 1990: 101 (in part); Lourenço, 1995a: 101 (in part); Lourenço, 1996a: 44; Lourenço, 1996b: 5, 8 (in part); Kovařík, 1998: 109 (in part); Fet & Lowe, 2000: 130 (in part); Lourenço, 2001b: 640 (in part); Prendini, 2001: 16–17, 32, 33–35; Fet et al., 2003: 2, 5–6; Lourenço, 2003a: 577 (in part); Lourenço, 2003c: 153–154 (in part); Lourenço & Goodman, 2003a: 26–27; Soleglad & Fet, 2003a: 26; Soleglad & Fet, 2003b: 19, 66–68, 78–79, 88, 90, 154 (in part); Lourenço, 2004a: 31–33 (in part); Lourenço et al., 2004: 232 (in part); Prendini, 2004a: 39, 41–42; Prendini, 2004b: 115; Fet et al., 2005: 3, 7–8, 10, 23, 26, 29; Prendini & Wheeler, 2005: 481 (in part); Dupré, 2007: 5, 13, 17 (in part); Lourenço et al., 2007a: 176 (in part); Lourenço et al., 2007b: 369 (in part); Kamenz & Prendini, 2008: 6, 8 (in part); Volschenk et al., 2008: 63 (in part); Kovařík, 2009: 22, 31 (in part); Lourenço et al., 2009b: 145 (in part); Lourenço & Wilmé, 2015: 209, 211; Lourenço et al., 2017: 62; Lourenço et al., 2018b: 74 (in part).

Buthus (*Grosphus*): Pocock, 1890: 123 (in part).

Type species. *Scorpio* (*Androctonus*) *madagascariensis* Gervais, 1843.

Diagnosis. A member of the '*Grosphus*' group differentiated as follows: medium-sized scorpions, adults ca. 25–75 mm in length; pedipalp finger granule rows 11–14 (Figs. 252, 286, 302, 330, 376), movable finger typically with 4 external subdistal granules; femur trichobothrium d_2 located on internal surface, or straddling dorsointernal carina (Figs. 9–12); chela manus with petite trichobothrium Eb_3 usually well separated from Eb_2, by more than half the distance between Eb_1 and Eb_2 (Figs. 21–22); manus trichobothrium V_2 roughly collinear with V_1 along chela axis or slightly displaced internally; lower pectinal tooth counts: ♂ 15–23, ♀ 12–19 (Figs. 28–31); basal pectinal tooth of females wide, oval to subrectangular, not distinctly longer than other teeth (Figs. 40–43, 196–200, 289); hemispermatophore capsule long or short, posterior lobe with long, lanceolate extension (Figs. 52–68); sternites with broad ovoid, elliptical or hemi-elliptical spiracles (Figs. 94–98); metasoma I with ventromedian carinae moderately to strongly crenulate or granulate (Figs. 122–125); telson with oval or bulbous vesicle, with or without subaculear tubercle in adults (Figs. 181–185); legs with ventral surface of telotarsus sparsely setose, with two rows of < 20 short, setiform macrosetae (Figs. 133–137, 211–215, 259–262, 316–319, 362–365); telotarsus with dorsal terminal process of normal size; cuticle with weak UV fluorescence (Figs. 145–149).

Subordinate taxa.

Grosphus ambre Lourenço, Wilmé & Waeber, 2018
Grosphus darainensis Lourenço, Goodman & Ramilijaona, 2004
Grosphus goudoti Lourenço & Goodman, 2006
Grosphus hirtus Kraepelin, 1900
Grosphus madagascariensis (Gervais, 1843)
Grosphus mayottensis Lourenço & Goodman, 2009
Grosphus polskyi Lourenço, Qi & Goodman, 2007
Grosphus rakotoariveloi Lourenço, Wilmé, Soarimalala & Waeber, 2017
Grosphus tavaratra Lourenço, Soarimalala & Goodman, 2009
Grosphus voahangyae Lourenço & Wilmé, 2015

See Tables 1–3 for diagnostic characters used to place the above taxa under *Grosphus*.

Remarks. We consider *Grosphus* paraphyletic and define two species groups distinguished by major differences in hemispermatophore capsule form: (i)'*madagascariensis*' group: capsule elongate, monocarinate, with basal lobe located far proximal to base of flagellum (*G. madagascariensis*); (ii) '*hirtus*' group: capsule short, carination variable, with basal lobe located distally near base of flagellum (*G. goudoti*, *G. hirtus* and *G. voahangyae*). Phylogenetic polarity of capsule form is unclear. Possible group affiliations of other species are suggested by some similarities in external characters, e.g.: (i) '*madagascariensis*' group: elliptic spiracles, more elongate metasomal segments, maculation patterns weak or absent, subaculear tubercle small or absent; may include *G. ambre*, *G. mayottensis* and *G. rakotoariveloi*; (ii) '*hirtus*' group:

SPECIES	femur d_2	R_{123}	PTC ♂	PTC ♀	basal pectine tooth ♀
Grosphus goudoti	carinal	0.82	19–22	17–19	short, wide
Grosphus hirtus	internal/carinal	0.32–0.83	17–20	14–18	short, wide
Grosphus madagascariensis	internal/carinal	0.45–1.04	15–20	13–18	short, wide
Grosphus voahangyae	carinal	0.44–0.64	15–19	14–16	short, wide
Neogrosphus griveaudi	internal/ dorsal?	0.55	29–31	27–29	short, wide
Teruelius ankarafantsika	dorsal	< 0.50	27–31	24–27	long, narrow
Teruelius ankarana	dorsal/carinal	< 0.50	36–41	31–35	long, narrow
Teruelius annulatus	dorsal	< 0.50	32–34	24–29	long, narrow
Teruelius bistriatus	dorsal	< 0.50	27–30	24–25	long, narrow
Teruelius feti	dorsal	< 0.50	30	25–28	long, narrow
Teruelius flavopiceus	dorsal	< 0.50	27–32	24–30	long, narrow
Teruelius grandidieri	dorsal	< 0.50	34–40	30–34	long, narrow
Teruelius intertidalis	dorsal	< 0.50	32–34	28–30	long, narrow
Teruelius limbatus	dorsal/carinal	< 0.50	25–32	23–29	long, narrow
Teruelius mahafaliensis	dorsal	< 0.50	28–40	27–31	long, narrow
Teruelius olgae	dorsal	< 0.50	29–33	26–29	long, narrow

Table 1. **Character states for species examined**. States of 5 characters for *Grosphus* (4 spp., blue panels), *Neogrosphus* (1 sp., magenta panels) and *Teruelius* **gen**. **n**. (11 spp., yellow panels) examined in this study: position of trichobothrium d_2 on pedipalp femur; ratio R_{123} = d(Eb_2, Eb_3)/ d(Eb_1, Eb_2) of distances between pedipalp manus trichobothria Eb_1, Eb_2 and Eb_3; ranges of pectinal tooth counts (PTC) of males (♂) and females (♀); and size and shape of female basal pectinal tooth.

ovoid spiracles, more stout metasomal segments, stronger maculation patterns, subaculear tubercle more developed; may include *G. polskyi*, *G. tavaratra*. However, external characters can be misleading and definitive group assignment requires study of hemispermatophore capsules. For example, *G. goudoti* resembles species of the '*madagascariensis*' group in external characters (metasoma slender, weak maculation, elliptic spiracles, lack of subaculear tubercle) but possesses a '*hirtus*' group type of capsule.

New synonymies.

Grosphus halleuxi Lourenço, Wilmé, Soarimalala & Waeber, 2017 = *Grosphus madagascariensis* (Gervais, 1843), **syn**. **n**.

Grosphus mandena Lourenço, 2005 = *Grosphus madagascariensis* (Gervais, 1843), **syn**. **n**.

Grosphus simoni Lourenço, Goodman & Ramilijaona, 2004 = *Grosphus madagascariensis* (Gervais, 1843), **syn**. **n**.

The single holotype male of *G. madagascariensis* used for description by Gervais (1843, 1844) is in poor condition after 176 years. It is disarticulated into several fragments: metasoma III–V + telson, metasoma I–II, hollowed carapace and tergites with most of coxosternal area and sternites III–VI missing, and 4 partial leg fragments (cf. https://science.mnhn.fr/taxon/species/grosphus/madagascariensis). The type locality is given only as 'Madagascar'. Gervais (1844: pl. XI, figs. 1–3) published a color painting of the dorsal habitus, and drawings of two consecutive metasomal segments in lateral view (segments not specified, but possibly III–IV), showing enlarged spiniform granules on posterior dorsal carinae, and the carapace with median and lateral eyes. With only limited information available about the holotype, which has lost many body parts bearing key taxonomic characters, it is difficult to precisely pin down the identity of *G. madagascariensis* in relation to a group of several other currently-named similar taxa (i.e., *G. darainensis*, *G. halleuxi*, *G. mandena*, *G. rakotoariveloi* and *G. simoni*). Previous diagnoses of Kraepelin (1900), Fage (1929) and Lourenço (1996b) listed some characters that differentiate *G. madagascariensis* from *G. hirtus* or *Teruelius* **gen**. **n**. Meristic characters were: PTC ♂18–20, ♀16–18, and pedipalp movable finger granule rows 12. Lourenço & Goodman (2006) suggested that Goudot, collector of the holotype, travelled in the north eastern region. They selected a male and female from Forêt de Plateau de Makira, in humid northeastern forest near Antongil Bay, as reference material for a redescription. The redescription is generic for the group, with few diagnostic characters: PTC ♂20, ♀15–16, pedipalp movable finger granule rows 13. Lateral eyes were incorrectly cited only as only 3 pairs, contradicting Gervais (1844).

SPECIES	hemisperm. basal lobe	hemisperm. posterior lobe	spiracles	met. I ventro-med. carinae	telotarsus setation	UV fluorescence
Grosphus goudoti	distal	long	elliptic	granulate	sparse	weak
Grosphus hirtus	distal	long	ovoid	granulate	sparse	weak
Grosphus madagascariensis	proximal	long	elliptic	granulate	sparse	weak
Grosphus voahangyae	distal	long	ovoid	granulate	sparse	weak
Neogrosphus griveaudi	distal	short	narrow elliptic	granulate	dense	strong
Teruelius ankarafantsika	distal	short	narrow	smooth	dense	strong
Teruelius ankarana	distal	short	narrow	smooth	dense	strong
Teruelius annulatus	distal	short	narrow	smooth	dense	strong
Teruelius bistriatus	–	–	narrow	smooth	dense	strong
Teruelius feti	–	–	narrow	smooth	dense	strong
Teruelius flavopiceus	distal	short	narrow	crenulate/ smooth	dense	strong
Teruelius grandidieri	distal	short	narrow	crenulate/ smooth	dense	strong
Teruelius intertidalis	distal	short	narrow	smooth	dense	strong
Teruelius limbatus	distal	short	narrow	crenulate/ smooth	dense	strong
Teruelius mahafaliensis	distal	short	narrow	crenulate/ smooth	dense	strong
Teruelius olgae	short	short	narrow	weakly crenuate	dense	strong

Table 2. **Character states for species examined**. States of 6 characters for *Grosphus* (4 spp., blue panels), *Neogrosphus* (1 sp., magenta panels) and *Teruelius* **gen**. **n**. (11 spp., yellow panels) examined in this study: position of hemispermatophore basal lobe relative to base of flagellum; size of hemispermatophore posterior lobe; shape of spiracles; condition of metasoma I ventromedian carinae; telotarsal setation; and intensity of UV fluorescence.

Grosphus simoni was described by Lourenço, et al. (2004) from two specimens: the holotype male from Forêt de Plateau de Makira, Forêt de Sahantaha, which is humid tropical forest in the northeast; and a paratype male from Station Forestière d'Ampijoroa, Ankarafantsika National Park, which is dry deciduous forest in the northwest. The differential diagnosis was brief: paler coloration, metasoma with strong granules and carinae, including several larger posterior spiniform granules on dorsal carinae on segments II–IV. Recently, Lourenço, et al. (2017) moved the paratype to a different species, *G. rakotoariveloi*, invalidating the original diagnosis of *G. simoni* based on both specimens. They revised the diagnosis of *G. simoni* as: moderately darker coloration, several larger posterior spiniform granules on dorsal carinae of metasoma II–IV, PTC ♂15–17, ♀14–15, pedipalp finger granule rows ♂11–12, ♀12–13, male chela with weak to moderate scalloping. Photographs were included for *G. simoni* specimens of both sexes from Forêt de Sahantaha (figs. 2–5), although the male was misidentified as a female, and the female misidentified as a male. The holotype male of *G. simoni* is well documented in high resolution images published on the FMNH website: https://collections-zoology.fieldmuseum.org/catalogue/963985. We studied FMNH materials (5♂, 1♀) from Andasibe determined as *G. simoni*. We further compared other materials, including a male determined by M. Vachon as *G. madagascariensis* (MHNG). We found no convincing diagnostic characters to support a distinction between *G. simoni* and *G. madagascariensis*. Diagnostic characters for *G. simoni* involve relatively minor differences in darker vs. lighter shades of color, differences in size of spiniform granules on dorsal metasomal segments, meristic differences of one or two pectine teeth with contiguous or overlapping ranges of PTC, and/ or pedipalp finger granule row counts. These characters are subject to inter-population and geographic variation in many scorpion taxa. Allowing for typical genetic variation, the metasoma and telson of holotypes of *G. simoni* and *G. madagascariensis* do not differ significantly in carination, spination or morphometrics. In the absence of quantitative analysis showing discontinuous variation either in characters

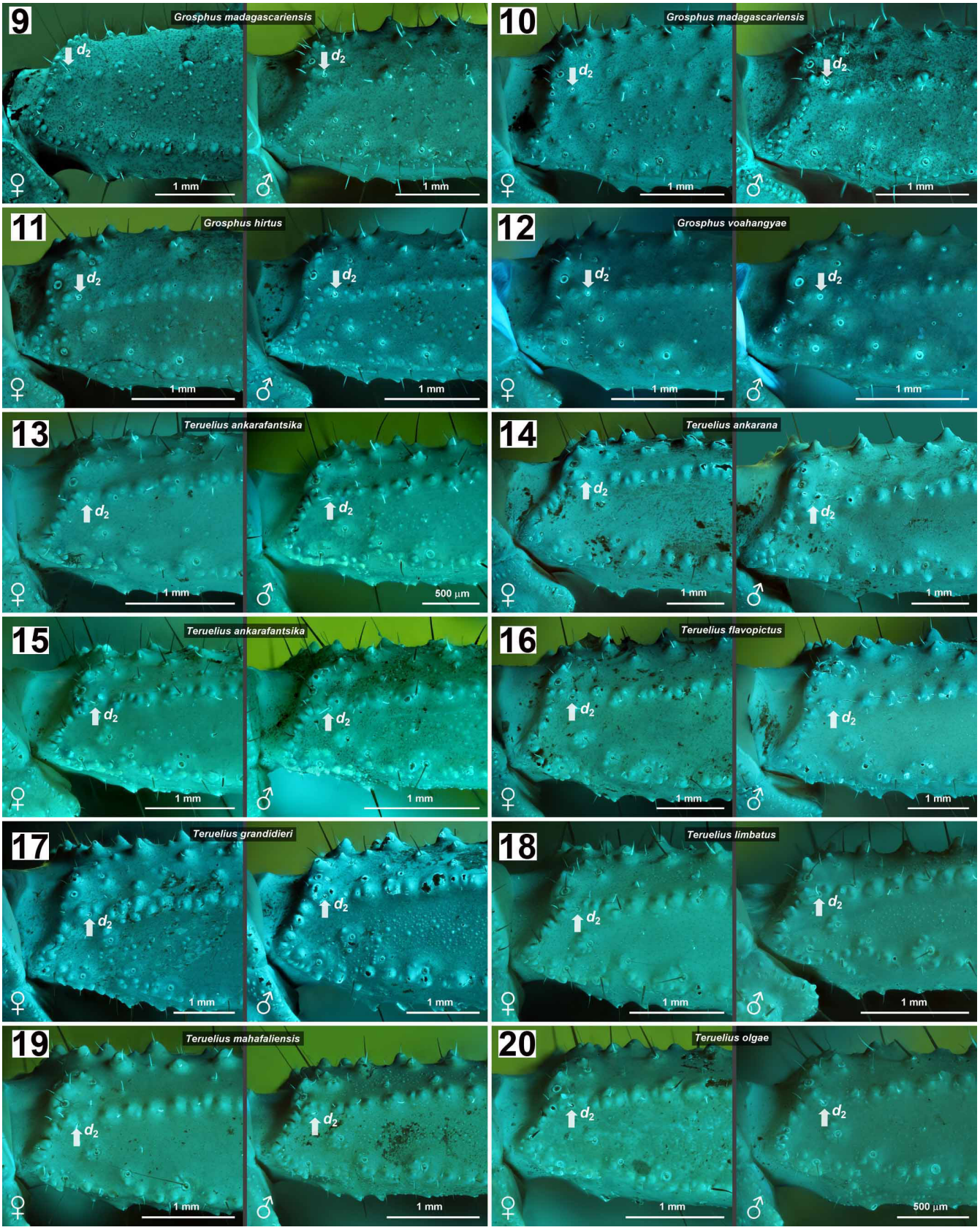

Figures 9–20. Position of femur trichobothrium d_2 in *Grosphus* and *Teruelius* **gen**. **n**. Dorsal surfaces of proximal pedipalp femur of adult females (♀, left panels) and adult males (♂, right panels), under UV fluorescence to highlight granulation, carinae and trichobothrial areolae. White arrows indicate positions of trichobothrium d_2 in each image. *G. madagascariensis* (9, 10; 2 samples from Anjiro (9) and Andasibe (10) show consistency of d_2 position), *G. hirtus* (11), *G. voahangyae* (12), *T. ankarafantsika* (13, 15; 2 samples from Ampijoroa show consistency of d_2 position), *T. ankarana* (14), *T. flavopiceus* (16), *T. grandidieri* (17), *T. limbatus* (18), *T. mahafaliensis* (19), and *T. olgae* (20). Scale bars: 1 mm (9–20♀) or 500 µm (20 ♂).

or morphometrics to support splitting into discrete species, we regard them as synonyms. Localities of *G. simoni* overlap or are sympatric with the distribution for *G. madagascariensis* in northeastern humid forests.

The species *G. rakotoariveloi* has meristics (PTC ♂18–19, pedipalp granule rows ♂13–14) that also overlap or are contiguous with those of *G. madagascariensis*. However, the type (and only known) locality is in a different bioclimatic region with dry deciduous forest, disjunct from eastern humid forests. It has much lighter coloration and relatively wide pedipalp chelae. We provisionally list this species, until additional data are available.

Grosphus halleuxi was described by Lourenço, et al. (2017) from a series of males from Torotorofotsy Forest, ca. 20 km NW of Moramanga, in a central humid forest area that is locally less humid than other eastern forests. The diagnostic characters for differentiating it from *G. simoni* were: darker coloration, smaller size of 55 mm, PTC ♂16–19, pedipalp granule rows ♂11–12, and weaker scalloping of pedipalp fingers. The meristic counts do not yield a differential diagnosis as they overlap those of *G. simoni* (= *G. madagascariensis*). We analyzed a series of near topotypic specimens (5♂, 6♀) from Moramanga and ca. 30 km E of Moramanga, whose males closely match photos of the *G. halleuxi* male holotype (Figs. 1–2, cf. Lourenço, et al., 2017: figs. 16–17). We obtained meristics: PTC ♂15–18, ♀13–15, pedipalp finger granule rows ♂♀12, which are not distinguishable from meristic ranges of *G. madagascariensis*. Other characters of darker or lighter shades, and degree of pedipalp finger scalloping can also be variable between populations. For example, in Figs. 1 & 3, a female from Moramanga area is darker than a male from the same area, showing that intensity of coloration varies within the same population, weakening this diagnostic character. *G. halleuxi* was diagnosed as "much darker", but '*G. simoni*' appears as dark, if not darker (Lourenço, et al., 2017: figs. 2–5 vs. 16–17). It was argued that *G. halleuxi* is a narrow-ranged species adapted to a less humid local microclimate. The existence of local microendemic taxa should be supported by strong diagnostic characters. Until such characters are defined, we regard this species as a local population of *G. madagascariensis*.

Grosphus mandena was described by Lourenço (2005) from near Fort Dauphin, in the Mandena region of southeastern coastal rainforest. Differential diagnostic characters were: lighter coloration, weaker metasomal carination, one larger spiniform granule on metasoma II–IV, and a more granulated telson. Meristics were: PTC ♂19–20, ♀15–17, pedipalp granule rows ♂12–13. As discussed above, these characters fall within ranges of variation for *G. madagascariensis*, including local populations given other species names. We loaned and studied the male holotype and a female paratype from MHNG and found them to be indistinguishable from *G. madagascariensis*. We note that the female paratype is considerably darker than the male holotype. This shows that intensity of coloration varies even within the type population, and is not a reliable diagnostic character (Figs. 348–351, 580–583). Lourenço & Wilmé (2016: fig. 36) showed a non-overlapping discontinuous transition, at latitude ca. 22°S between the northern range of *G. madagascariensis* and the southern range of *G. mandena*. The transition latitude does not correspond to any boundary between centers of endemism as defined by the watershed model of Wilmé et al. (2006). Lourenço et al., (2009b) suggested that the disjunction is recent, due to extirpation of south littoral rainforest by humans. More robust diagnostic characters and analysis of clinal vs. discontinuous variation is necessary to delimit the southern populations as a distinctive species. Until such characters are defined, we regard this species as a southern population of *G. madagascariensis*. The synonymies of *G. halleuxi* and *G. mandena* with *G. madagascariensis* are further supported by their identical hemispermatophores, all of which have a unique, elongated capsule architecture with a proximal basal lobe (cf. Figs. 52–53, 56–57 vs. Figs. 54–55).

Grosphus hirtus garciai Lourenço, 2001 = *Grosphus hirtus* Kraepelin, 1900, **syn**. **n**.

Grosphus garciai was described by Lourenço (2001b) from Station Forestière d'Ampijoroa, Ankarafantsika National Park, based on an adult male holotype and a juvenile, collected by García Herrero. In the diagnosis, it was differentiated from *G. madagascariensis*, a quite different species, by: smaller size, maculated light and dark pigmentation, pedipalp granule rows ♂13, weaker spiniform granules on pedipalp and metasoma, and weaker scalloping of pedipalp fingers. Curiously, it was not compared to *G. hirtus*, which bears a much greater similarity. Subsequently, Lourenço & Goodman (2006) redescribed *G. hirtus* based on material also from Station Forestière d'Ampijoroa, Ankarafantsika National Park, also collected by García Herrero. *G. hirtus* was separated from *G. garciai* by yellowish rather than reddish brown color, and larger size (40–50 mm vs. 32 mm). Subsequently, Lourenço & Wilmé, (2015a) downgraded *G. garciai* to the status of subspecies, *G. hirtus garciai*, supposedly a microendemic taxon in a "local isolated population". It is morphologically identical to, and differentiated from the nominotypical *G. hirtus* only by smaller size. The subspecies is known only from the type locality and the nominotypical *G. hirtus* also occurs in the same area (Lourenço & Goodman, 2006). The species *G. hirtus* is distributed more widely over northwest Madagascar (Lourenço & Wilmé, 2016: fig. 36). We loaned and studied the holotype of *G. garciai*, as well as male and female topotypes from FMNH. We confirmed that it is morphologically indistinguishable from *G. hirtus* (Figs. 263–305). We question whether an animal population of somewhat smaller average body size compared to closely neighboring conspecifics, but otherwise identical to them, merits subspecies status. Local size variations of species may be caused by varying environmental conditions that limit growth rates and development. The size differential is exaggerated by the reported body lengths, a measurement that can vary with mesosomal expansion: *G. hirtus* 40–50 mm (Lourenço & Goodman, 2006); *G. h. garciai* 28–32 mm (Lourenço & Wilmé, 2015a). These numbers imply that *G. hirtus* is at least 25% longer. A more reliable size comparison for morphometrically similar scorpions would use carapace

length. For example, we measured carapaces of *G. hirtus*: ♂5.5 mm, ♀5.0 mm, vs. *G. h. garciai*: ♂5.2 mm, ♀4.4 mm, i.e., only 6–12% longer. Lourenço et al. (2007a) redescribed *G. hirtus* with body lengths of ♂34.3 mm, ♀31.8 mm, and carapace lengths ♂4.1 mm, ♀4.3 mm. These are small enough to overlap measurements for *G. h. garciai*. Considering this overlap, we regard *G. h. garciai* as a synonym of *G. hirtus*.

Grosphus polskyi is another species that is quite similar to *G. hirtus*. It was diagnosed by having paler color, with weaker, more diffuse maculate patterns restricted to carapace and tergites, slightly more elongate metasoma segment I, weak spination on dorsal metasomal carinae, and a slightly larger subaculear tubercle. The only known record is the single male holotype from Mikea Forest near Toliara, on the southwestern coast. Although this is quite far south of the southern-most record of *G. hirtus* (Lourenço & Wilmé, 2016), records of the latter are sparse, so it is unclear if it represents a disjunction. We provisionally list this species, until it can be critically evaluated by more material and analysis of variation.

Genus ***Neogrosphus*** Lourenço, 1995

(Figs. 25–39, 69–70, 87, 106–121, 606–619, Tabs. 1–4)

Neogrosphus Lourenço, 1995a: 100–101; Lourenço, 1996a: 444, 447; Lourenço, 1996b: 16; Kovařík, 1998: 115; Fet & Lowe, 2000: 187; Lourenço, 2003a: 577; Soleglad & Fet, 2003b: 88; Fet et al., 2005: 3, 22, 26; Prendini & Wheeler, 2005: 481; Lourenço et al., 2006b: 266; Dupré, 2007: 7, 13, 17; Kovařík, 2009: 22; Loria & Prendini, 2014: 25; Lourenço et al., 2015: 769, fig. 2, 6; Loria & Prendini, 2018: 184.

Diagnosis. A member of the '*Grosphus*' group differentiated as follows: small-sized scorpions, adults ca. 24–30 mm in length; pedipalp finger granule rows 8–9 (Fig. 612–613, 616), movable finger with no more than 3 external subdistal granules; femur trichobothrium d_2 located on dorsal, carinal or internal surface; chela manus with petite trichobothrium Eb_3 usually well separated from Eb_2, by more than half the distance between Eb_1 and Eb_2 (Figs. 25–27); manus trichobothrium V_2 strongly displaced internally relative to V_1; higher pectinal tooth counts: ♂ 27– 31, ♀ 27–29 (Figs. 28–31); basal pectinal tooth of females wide, oval, only slightly longer than other teeth (Fig. 614); hemispermatophore capsule short, posterior lobe rounded, without lanceolate extension (Fig. 70); sternites with moderately narrow spiracles (Figs. 610, 614); metasoma I with ventromedian carinae moderate, finely granulate; telson with elongate vesicle, without subaculear tubercle; legs with ventral surface of telotarsus densely setose, with > 20 long, filiform setae (Figs. 618–619); telotarsus with dorsal terminal process very small; cuticle with strong UV fluorescence.

Subordinate taxa.
Neogrosphus andrafiabe Lourenço, Wilmé & Waeber, 2015
Neogrosphus blanci Lourenço, 1996
Neogrosphus griveaudi (Vachon, 1969)

Remarks. *Neogrosphus* shares some primitive characters with *Grosphus*, and some derived characters with *Teruelius* **gen. n.** (summarized in Table 4). One interpretation of this is that *Neogrosphus* is descended from an intermediate stage in the evolution of *Teruelius* **gen. n.** from a *Grosphus*-like ancestor. Other characters, such as small size, internal displacement of V_2, reduced dorsal terminal process of telotarsus and elongated telson appear to be autapomorphies for the genus.

Genus ***Teruelius*** **gen. n.**

(Figs. 5–8, 13–20, 23–39, 44–51, 71–85, 90–93, 99–105, 106–121, 137–144, 150–160, 170–180, 186–195, 201–210, 216–226, 229–230, 235–238, 387–579, 584–605, Tabs. 1–4)

http://zoobank.org/urn:lsid:zoobank.org:act:54CB8128-BCFD-4B1F-A947-153C7CDD5B83

Grosphus Vachon, 1940: 254, 256; Lourenço et al., 2007b: 375; Prendini & Esposito, 2010: 675–676; Loria & Prendini, 2014: 25; Loria & Prendini, 2018: 184.

Type species. *Buthus limbatus* Pocock, 1889.

Etymology. The generic epithet *Teruelius* (masculine) is a patronym honoring Rolando Teruel from Cuba in recognition of his many important contributions to the knowledge of scorpions.

Diagnosis. A member of the '*Grosphus*' group differentiated as follows: medium-sized to large-sized scorpions, adults ca. 35–120 mm in length; pedipalp finger granule rows 10–15 (Figs. 402, 431, 452, 485–486, 508, 521, 529, 560), movable finger typically with 4 external subdistal granules; femur trichobothrium d_2 straddling dorsointernal carina, or located on dorsal surface (Figs. 13–20); chela manus with petite trichobothrium Eb_3 near Eb_2, closer than half the distance between Eb_1 and Eb_2 (Figs. 23–24); manus trichobothrium V_2 roughly collinear with V_1 along chela axis or slightly displaced internally; higher pectinal tooth counts: ♂ 25– 41, ♀ 24–35 (Figs. 28–31); basal pectinal tooth of females wide, with elongate, tapering distal extension, distinctly longer than other teeth (Figs. 44–51, 201–210, 411, 510, 526); hemispermatophore capsule short, carinate, posterior lobe rounded, without lanceolate extension (Figs. 71–85); sternites with narrow, slit-like spiracles (Figs. 99–105); metasoma I with ventromedian carinae moderately to weakly crenulate or smooth to obsolete (Figs. 126–132); telson with oval or bulbous vesicle, without subaculear tubercle in adults (Figs. 186–195); legs with ventral surface of telotarsus densely setose or scopulate, with broad, brush-like strips of > 20 long filiform macrosetae (Figs. 138–144, 216–226, 409–417, 487–490, 512–515, 538–541, 576–579); telotarsus with dorsal terminal process of normal size; cuticle with strong UV fluorescence (Figs. 150–157).

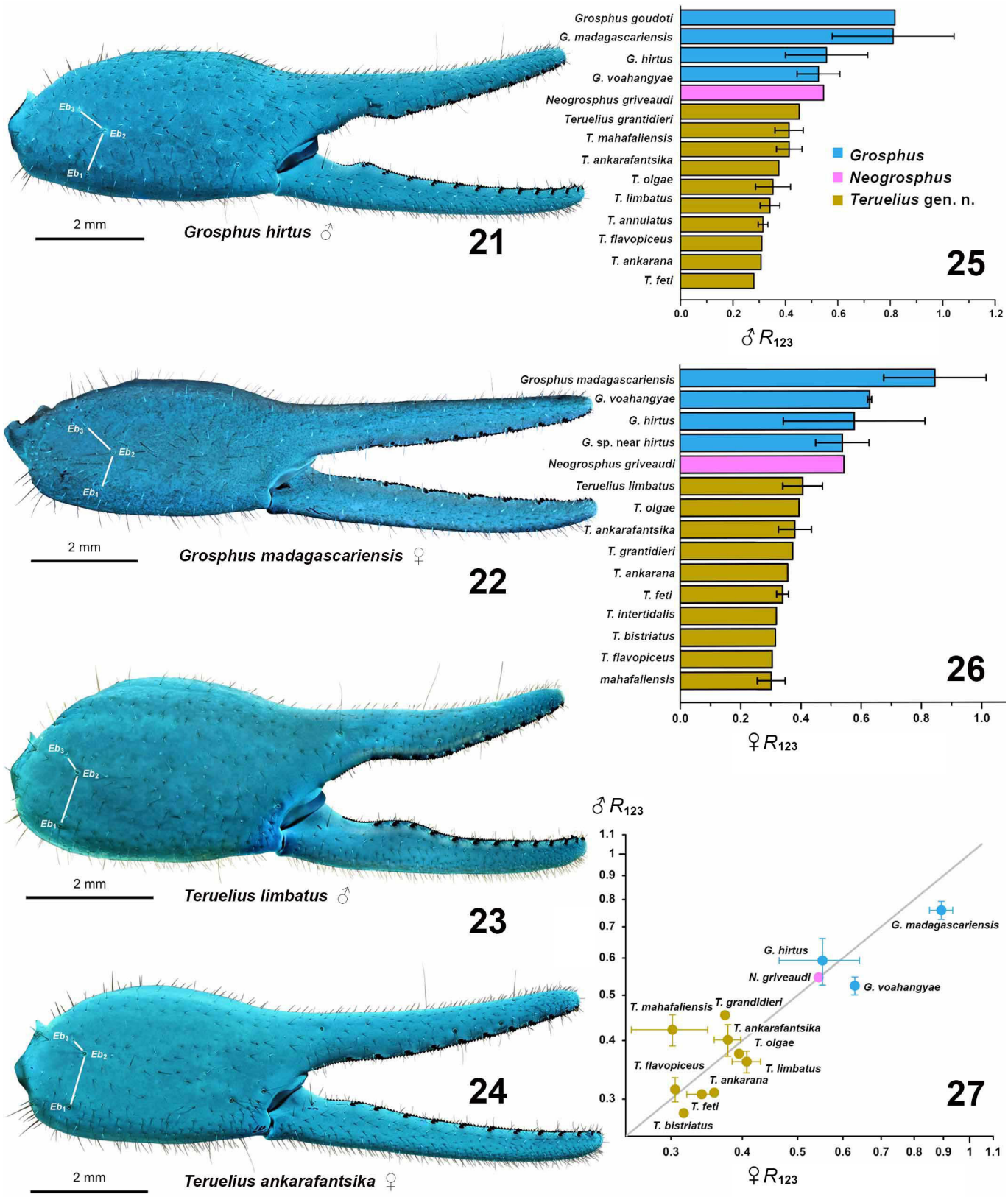

Figures 21–27. Positions of trichobothria Eb_1, Eb_2 and petite Eb_3 on manus of pedipalp chela in *Grosphus*, *Neogrosphus* and *Teruelius* **gen. n. Figures 21–24**. External views of pedipalp chela, shown under UV fluorescence to highlight trichobothrial areolae. *G. hirtus* ♂ (21), *G. madagascariensis* ♀ (22), *T. limbatus* ♂ (23), *T. ankarafantsika* ♀ (24). Positions of Eb_1, Eb_2 and Eb_3 and lines joining them shown as white overlays. Scale bars: 2 mm. **Figures 25–26**. Horizontal histograms comparing ratios, R_{123} = d(Eb_2, Eb_3)/ d(Eb_1, Eb_2), of Eb_2-Eb_3 distance, to Eb_1-Eb_2 distance, in males (25), and females (26) of *Grosphus*, *Neogrosphus* and *Teruelius* **gen. n**. Error bars indicate ranges (minimum, maximum), histogram bars mid-range values. **Figure 27**. Scatter plot of male vs. female ratios R_{123}. Ratio is larger in males if points fall above the diagonal (gray) line, larger in females if they fall below it.

Subordinate taxa.
Teruelius ankarafantsika (Lourenço, 2003) **comb**. **n**.
Teruelius ankarana (Lourenço & Goodman, 2003) **comb**. **n**.
Teruelius annulatus (Fage, 1929) **comb**. **n**.
Teruelius bemaraha (Lourenço, Wilmé & Waeber, 2018) **comb**. **n**.
Teruelius bicolor (Lourenço, 2012) **comb**. **n**.
Teruelius bistriatus (Kraepelin, 1900) **comb**. **n**.
Teruelius eliseanneae (Lourenço & Wilmé, 2016) **comb**. **n**.
Teruelius feti (Lourenço, 1996) **comb**. **n**.
Teruelius flavopiceus (Kraepelin, 1900) **comb**. **n**.
Teruelius ganzhorni (Lourenço, Wilmé & Waeber, 2016) **comb**. **n**.
Teruelius grandidieri (Kraepelin, 1900) **comb**. **n**.
Teruelius intertidalis (Lourenço, 1999) **comb**. **n**.
Teruelius limbatus (Pocock, 1889) **comb**. **n**.
Teruelius magalieae (Lourenço, 2014) **comb**. **n**.
(= *T. mahafaliensis* ?)
Teruelius mahafaliensis (Lourenço, Goodman & Ramilijaona, 2004) **comb**. **n**.
Teruelius olgae (Lourenço, 2004) **comb**. **n**.
Teruelius sabineae (Lourenço & Wilmé, 2016) **comb**. **n**.
Teruelius waeberi (Lourenço & Wilmé, 2016) **comb**. **n**.

See Tables 1–3 for diagnostic characters used to place the above species under *Teruelius* **gen**. **n**.

Remarks. Recognition of *Teruelius* **gen**. **n**. as a separate genus, distinct from *Grosphus*, necessitates revision of some previous concepts about taxonomy and biogeography of *Grosphus*. Lourenço et al. (2017) associated *G.* '*simoni*'(= *G. madagascariensis*) with *G. rakotoariveloi* and *G.* '*halleuxi*', and subsequently Lourenço et al. (2018b) elaborated on a '*Grosphus simoni*' group, treating it as a monophyletic unit of closely related "sister" species including the aforementioned three, plus *G. ambre*, *G. bemaraha* and *G. mahafaliensis*. A group diagnosis was not provided but, for *G. bemaraha*, mention was made of "a number of features such as spiniform granules on the dorsal carinae of metasomal segments II-IV and on internal carinae of pedipalp femur and patella". We place *G. bemaraha* under *Teruelius* **gen n**., on the basis of narrow spiracles, dense tarsal setation and high pectinal tooth count (Table 3), and consider spiniform granules shared with *G. simoni* to be a homoplasy. *G. bemaraha* was claimed to be closer to *G. rakotoariveloi*, but these species belong to different genera. Lourenço et al. (2018b: 74, fig.1) included *G. mahafaliensis* in the '*simoni*'group, perhaps due to similarities to *G. bemaraha*, noting in particular a high number of pectine teeth (but it lacks spiniform granules on metasomal carinae). In contrast, we find that *T. mahafaliensis* **comb**. **n**. is very far removed from *G.* '*simoni*' (= *G. madagascariensis*), differing in all nine genus-level diagnostic characters, and in the fundamental architecture of the hemispermatophore capsule (cf. Fig. 84 vs. Figs. 52–57).

Lourenço et al. (2018b) discussed biogeographic hypotheses attempting to explain the distribution of the incongruous, polyphyletic '*Grosphus simoni*' group. The very wide distribution of the group meant that it was "adapted to humid, dry and subarid environments", and the two most disjunct species, *G. bemaraha* and *G. mahafaliensis* from western and southern localities, were speculated to "belong to relict populations, which may have survived in humid refugia encountered in the sedimentary basins during the dry episodes of the paleoclimate oscillations". However, these two species are not closely related to the other four group members, but belong to *Teruelius* **gen**. **n**., whose ancestors may have already been adapted to dry environments. Although Pleistocene climatic fluctuations could be relevant for recent speciation events in *Grosphus* and *Teruelius* **gen**. **n**., the many correlated characters separating these two genera suggest a far earlier split, as in other taxa. For example, dated molecular phylogenies of Madagascar archaeid spiders (Wood et al., 2015), *Brookesia* and other chameleons (Tolley et al., 2013; Townsend et al., 2009) and *Zonosaurus* plated lizards (Blair et al., 2015) have revealed that the majority of divergences in these other endemic taxa are quite deep, occurring long before the advent of Pleistocene climate cycles.

Species of *Teruelius* **gen**. **n**. can be loosely subdivided by size and coloration: large species, *T. flavopiceus*, *T. ankarana*, *T. grandidieri* and *T. bicolor*; species with patterns of dark stripes on tergites ('*bistriatus*' group of Lourenço & Wilmé, 2016): *T. ankarafantsika*, *T. bistriatus*, *T. eliseanneae*, *T. feti*, *T. limbatus*, *T. sabineae* and *T. waeberi*; species with almost uniform yellow, orange or brown tergites, and maybe darker metasoma IV or V: *T. annulatus*, *T. bemaraha*, *T. ganzhorni*, *T. intertidalis*, *T. magalieae*, *T. mahafaliensis* and *T. olgae*. These groupings have been used to construct species keys, in conjunction with some other characters including shapes of female basal pectine teeth (Fage, 1929; Lourenço, 2003c, 2004a, 2014; Lourenço et al., 2007b; Vachon, 1969). Monophyly of these groupings remains to be tested.

New synonymies.
Grosphus makay Lourenço & Wilmé, 2015 = *Teruelius feti* (Lourenço, 1996) **comb**. **n**., **syn**. **n**.

Grosphus feti was described by Lourenço (1996b) from a juvenile male holotype, ostensibly collected from "Prov. Tulear, Tanjon' I Vohimena [= Cap Sainte Marie] Réserve spéciale, X.1995" and deposited in FMNH. We loaned and studied the holotype and a second juvenile male labeled as "♂ paratype" (which we concur is conspecific with the holotype). Until now, this species was only known from these two types. Associated with the type, we found locality labels (Fig. 459) that differ from the published type locality: "MADAGASCAR: Province de Toliara, Fôret de Vohimena, 35 km SE Sakaraha, 17-24.i.1996, MyrCE-7541, 22°41.0'S 44°49.8'E, 780 m, S. M. Goodman 0000 011 031 FMNH-INS *Grosphus feti* Lourenço HOLOTYPE: det. 1996 ". This locality is ca. 325 km roughly north of the published type locality at Cap Sainte Marie and the collection date of January 1996 is several months later. Either a labeling error occurred after description, or the published type locality is incorrect.

SPECIES	femur d_2	R_{123}	PTC ♂	PTC ♀	basal pectine tooth ♀	spiracles	telotarsus setation
Grosphus ambre	internal	> 0.5	17	–	–	elliptic	sparse
Grosphus darainensis	?	?	17–18	–	–	–	–
Grosphus mayottensis	internal	~ 0.5	–	17–18	short, wide	–	–
Grosphus polskyi	internal	< 0.5	18–19	–	–	–	–
Grosphus rakotoariveloi	internal	> 0.5	18–19	–	–	–	sparse
Grosphus tavaratra	internal	> 0.5	22–23	–	–	elliptic	sparse
Neogrosphus andrafiabe	dorsal/ carinal	–	27–28	–	–	–	–
Neogrosphus blanci	dorsal	–	27	–	–	–	–
Teruelius bemaraha	carinal	?	29–30	–	–	narrow	dense
Teruelius bicolor	–	?	36	–	–	–	–
Teruelius eliseanneae	internal	< 0.5	–	24	long, narrow	–	–
Teruelius ganzhorni	dorsal	> 0.5?	–	25–28	long, narrow	narrow	dense
Teruelius magalieae	dorsal	< 0.5	36	–	–	narrow	dense
Teruelius sabineae	dorsal	< 0.5	–	25	long, narrow	narrow	dense
Teruelius waeberi	dorsal	~ 0.5	26–30	–	–	narrow	dense

Table 3. **Character states for species not examined**. States of 6 characters for *Grosphus* (6 spp., blue panels), *Neogrosphus* (2 spp., magenta panels) and *Teruelius* **gen**. **n**. (7 spp., yellow panels) not examined in this study: position of trichobothrium d_2 on pedipalp femur; ratio R_{123} = d(Eb_2, Eb_3)/ d(Eb_1, Eb_2) of distances between pedipalp manus trichobothria Eb_1, Eb_2 and Eb_3; ranges of pectinal tooth counts (PTC) of males (♂) and females (♀);size and shape of female basal pectinal tooth; shape of spiracles; and telotarsal setation. Character states inferred from published descriptions and figures. PTC and basal pectinal tooth characters not indicated in cases where either males or females are not known or described. Other characters not indicated in cases where published descriptions did not yield clear information.

Cap Sainte Marie is a biological study area and frequent source of scorpion materials (e.g., Lourenço & Wilmé, 2016) so data labels of specimens could have been confused.

The FMNH label site is ca. 145 km south and slightly west of the type locality of *Grosphus makay* (Lourenço & Wilmé, 2015b): "Region Atsimo-Andrefana, ex Province of Toliara, Makay Mts., General Collection, dry-Forest on sandy soil, 12/III/2010 (B. L. Fisher et al.). BLF25549. Female holotype (CAS)". These two localities have sandstone substrates, similar elevation and are located in the same general bioclimatic region. Comparison of the published habitus of the holotype adult female of *T. makay* and the holotype juvenile male of *T. feti* revealed very similar morphology and morphometrics even though sex and age differ. Most notably, their color patterns are identical in all details including: pattern of fuscosity on interocular triangle of carapace with pale cut-out behind lateral eyes; thin median line, precise fuscous banding patterns and transverse lateral striping on all tergites; darkly marked ventrolateral and ventromedian carinae on metasoma I–IV; fuscous patterns on metasoma V and telson; short fuscous strip on interno-proximal margin of pedipalp patella; leg femora with distal short, pale cut-outs on distal dark areas of prolateral surfaces and pale narrow lines on dorsal margins; and leg patellae with fuscous ventral margins on prolateral surfaces (compare Fig. 459 to fig. 13 of Lourenço & Wilmé, 2015b). These very particular details of pigmentation pattern are not found in *T. limbatus* which was regarded as a closely related species (Figs. 5–8, 516–521). We also examined two adult females, near topotypes of *G. makay* from the Makay Mountains, that exhibited the same coloration patterns and morphometrics as *T. feti* (Fig. 459a). We allowed for the fact that juveniles of pigmented scorpions usually display darker, more intense markings, and that in adults these color patterns are somewhat faded. Details of

GENUS	*Pseudolychas*	*Grosphus*	*Neogrosphus*	*Teruelius* gen. n.
femur d_2	dorsal	carinal/ internal	internal/carinal/ external	carinal/ dorsal
R_{123}	2/3 spp. ≥ 0.50	0.32–1.04	0.54	< 0.50
PTC ♂	11–17	15–23	27–31	25–41
PTC ♀	9–14	12–19	27–28	24–35
basal pectine tooth ♀	short, ovoid (2/3 spp.)	short, ovoid	short, ovoid	elongate, falcate
hemispermatophore basal lobe	distal	distal/ proximal	distal	distal
hemispermatophore posterior lobe	long	long	short	short
spiracles	elliptic, L/W < 5	elliptic, L/W < 5	elliptic, L/W < 5	narrow, L/W > 5
met. I ventral carinae	granulate	crenulate/ granulate	granulate	weakly granulate to smooth
telotarsus setation	sparse, 2 rows	sparse, 2 rows	dense, irregular	dense, irregular
UV fluorescence	weak	weak	strong	strong

Table 4. **Character states for '*Grosphus*' group genera and outgroup genus *Pseudolychas***. States of 11 characters for *Grosphus*, *Neogrosphus*, *Teruelius* **gen**. **n**. and *Pseudolychas*, summarizing data of Tables 1–3. *Pseudolychas* character states determined by study of materials, and from published descriptions. Primitive states indicated by green panels, derived states by red panels, with polarities determined by comparison to *Pseudolychas* which is assumed primitive. Unpolarized characters indicated by dark green panels.

coloration pattern have been given high priority as characters for species-level taxonomy of *Grosphus* (Lourenço et al., 2009b; Lourenço, 2014). We therefore consider *Grosphus makay* to be a junior synonym of *T. feti*, and the correct type locality of the latter to be that indicated on FMNH data labels. *T. feti* was never again collected from Cap Sainte Marie in over two decades of fieldwork since its description, although other scorpion species (e.g., *T. sabineae*) were discovered there. The adult male remains unknown. Our opinion could be verified by collection and analysis of topotypic adult and juvenile specimens from the FMNH locality. The description of *T. feti* (Lourenço, 1996b: 14) noted the juvenile status of the holotype which is ca. 30 mm, but Lourenço (2014: 636) diagnosed the species as "of small size with a total length of 30 to 40 mm". Small size cannot be a species diagnostic character if it is a property of the juvenile, and adult males are probably medium-sized, comparable to an adult female of *G. makay*, ca. 56 mm in body length. Our synonymy also implies that this is not a microendemic species of the upper Central Menabe, as suggested of Lourenço & Wilmé (2015b). The *T. feti* emended type locality lies a significant distance south of the Makay mountains, in the Mangoky watershed (Wilmé et al., 2006).

Grosphus rossii Lourenço, 2013 = *Teruelius mahafaliensis* (Lourenço, Goodman & Ramilijaona, 2004) **comb**. **n**., **syn**. **n**.

Grosphus rossii was described by Lourenço (2013b) from a single adult male holotype collected from "Central region, NE Manandona, S of Antsirabe, in secondary growth forest, under log, 8 August 2004, W. R Lourenço" and deposited in ZMUH. We loaned and studied the holotype and found that it was virtually identical in coloration, external morphological characters and morphometrics to *Teruelius mahafaliensis* (Lourenço, Goodman & Ramilijaona, 2004) **comb**. **n**. Our comparative materials of the latter included a male collected near the type locality of that species (Figs. 522–525), and determined material loaned from FMNH including two adult males. In his description, Lourenço (2013b: 59) compared and

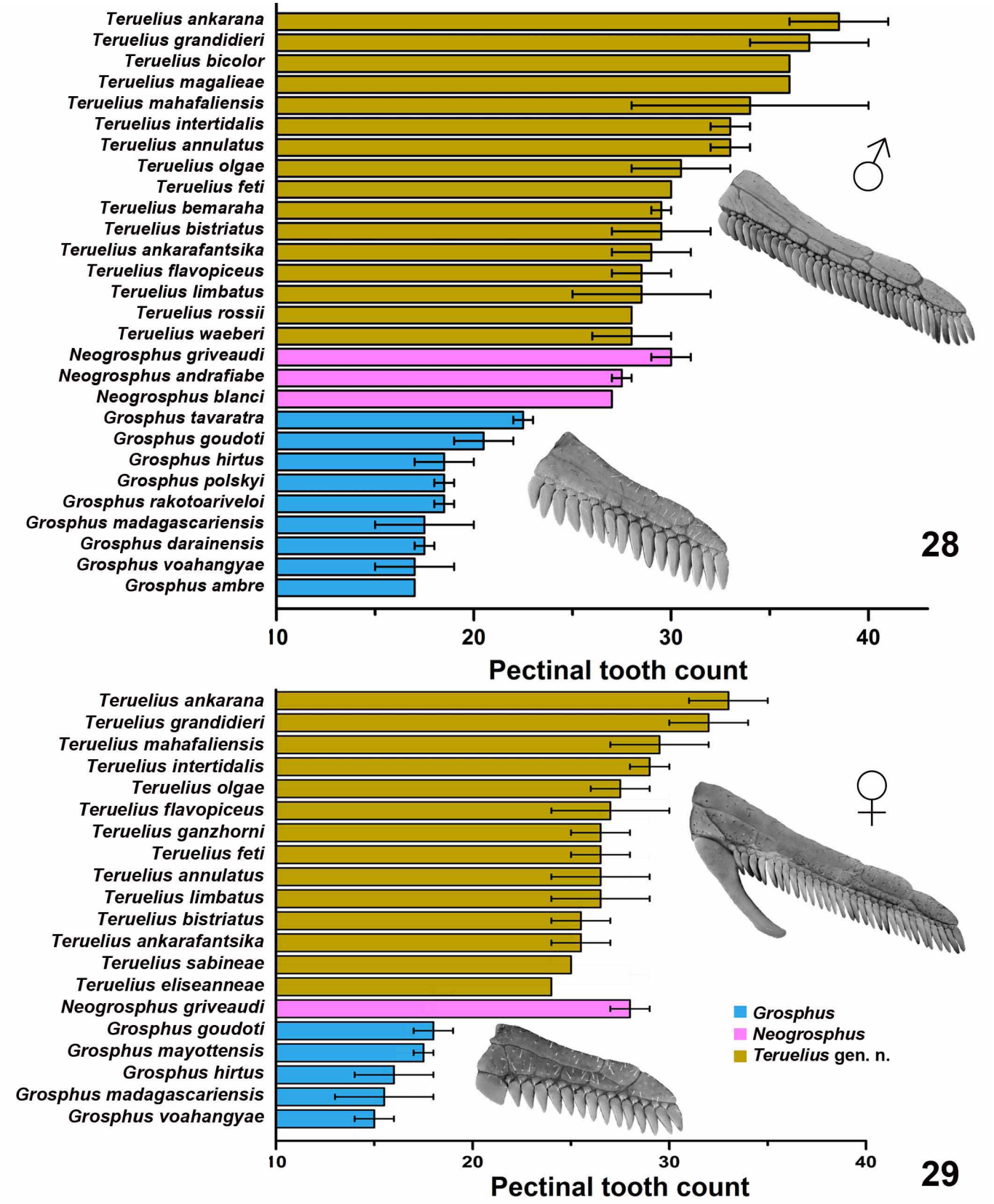

Figures 28–29. Variation in pectinal tooth count (PTC) in *Grosphus*, *Neogrosphus* and *Teruelius* **gen**. **n**. Horizontal histograms comparing PTC in males (28), and females (29) of *Grosphus*, *Neogrosphus* and *Teruelius* **gen**. **n**. Error bars indicate ranges (minimum, maximum), bars mid-range values.

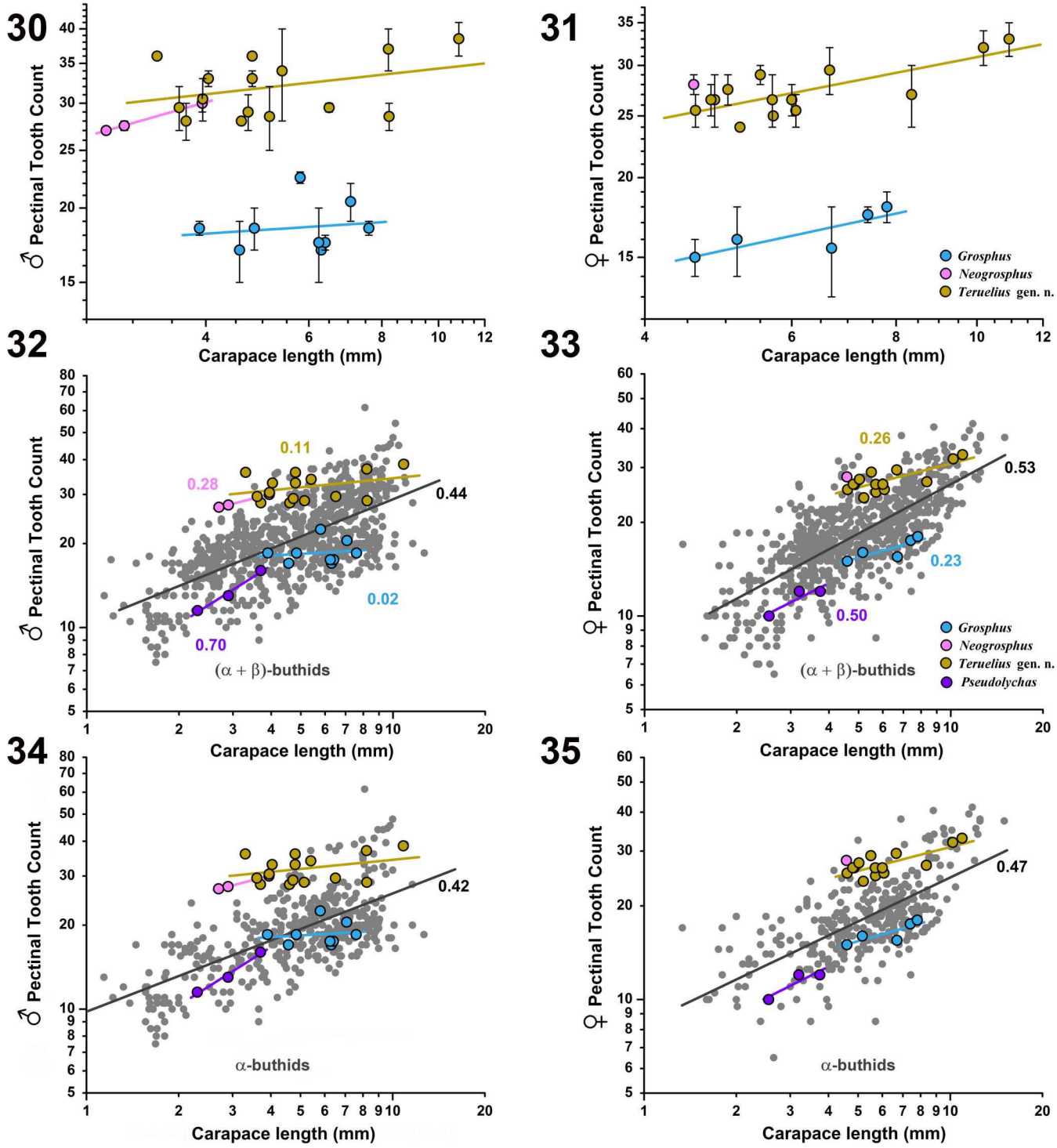

Figures 30–35. Variation in pectinal tooth count (PTC) in *Grosphus*, *Neogrosphus* and *Teruelius* **gen. n.** **Figures 30–31**. Logarithmic scatter plots showing scaling of PTC vs. carapace length in males (30), and females (31) of *Grosphus*, *Neogrosphus* and *Teruelius* **gen. n.** Color lines are least squares linear regression fits of scaling trends for the different genera. **Figures 32–33**. Logarithmic scatter plots showing scaling of PTC vs. carapace length in Figs. 30–31 superposed upon overall scaling trends for a larger sample of male (32) and female (33) buthids including both α and β trichobothrial configurations (gray symbols; 1055♂, 1046♀). Dark lines: least squares linear regression fits of scaling trends for larger sample of buthids. **Figures 34–35**. Logarithmic scatter plots showing scaling of PTC vs. carapace length in Figs. 30–31 superposed upon overall scaling trends for a larger sample of male (34) and female (35) α-buthids restricted to α trichobothrial configurations (gray symbols; 445♂, 371♀). Dark lines: least squares linear regression fits of scaling trends for α-buthids. Numbers: slopes of regression lines (= allometric exponents). Purple symbols and lines: outgroup *Pseudolychas*.

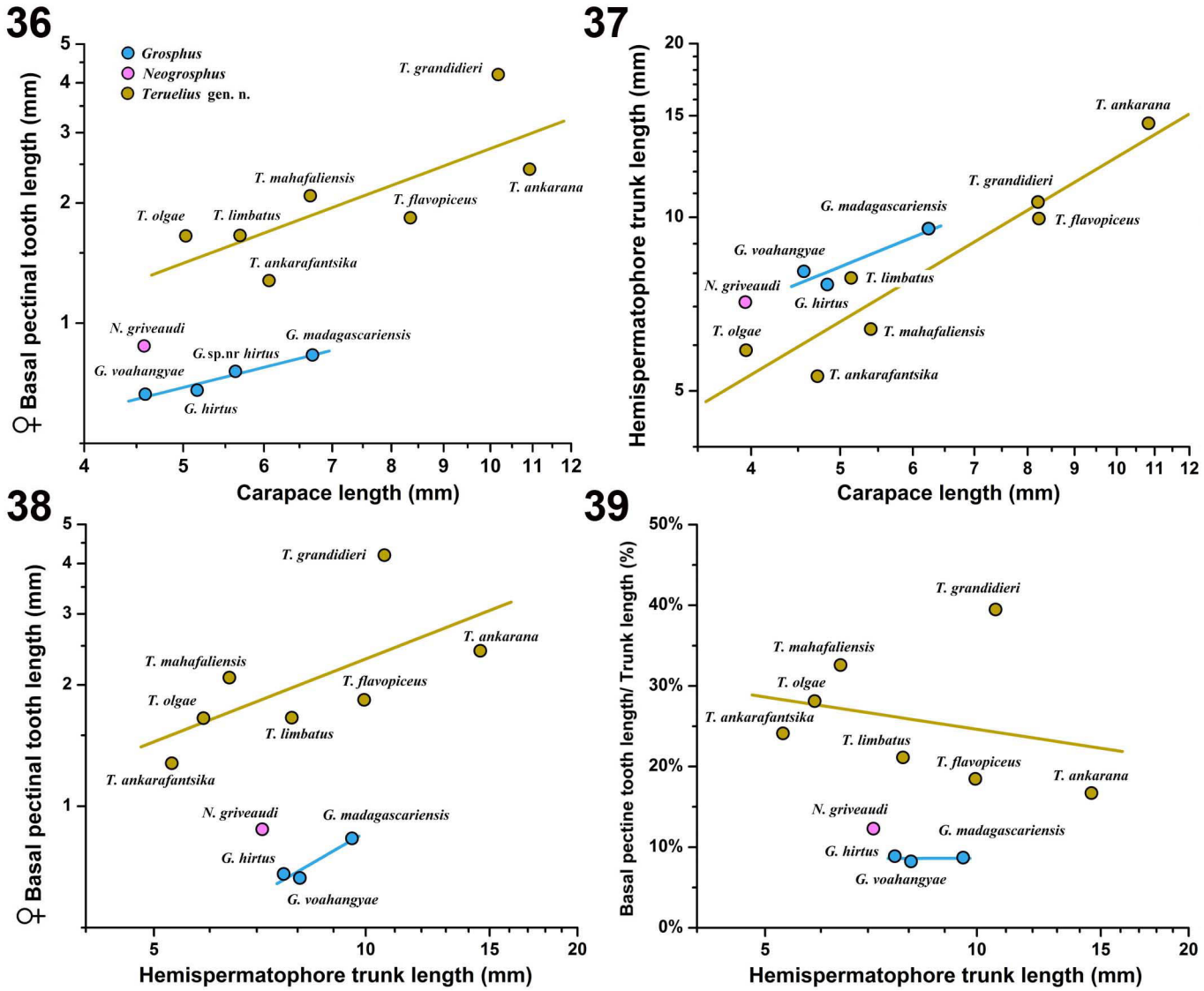

Figures 36–39. Comparative biometrics of female basal pectinal tooth and hemispermatophore trunk of *Grosphus*, *Neogrosphus* and *Teruelius* **gen. n. Figures 36–37**. Logarithmic scatter plots showing scaling of length of female basal pectinal tooth vs. carapace length (36), and hemispermatophore trunk length vs. carapace length (37). Color lines: least squares linear regression fits of scaling trends for the different genera. **Figures 38–39**. Logarithmic scatter plots of female basal pectinal tooth length vs. hemispermatophore trunk length (38), and the ratio of basal pectinal tooth length/ hemispermatophore trunk length (%) vs. hemispermatophore trunk length, showing fraction of trunk spanned by the female tooth (39). Female basal pectinal tooth length measured as chord length, from more proximal corner (along comb axis) at base of tooth, to more distal corner (along comb axis) at tip of tooth. Trunk length measured from proximal edge of basal lobe to pedicel (foot). Color lines: least squares linear regression fits of scaling trends for the different genera.

contrasted *G. rossii* to *T. limbatus*, but not to *T. mahafaliensis*. A potential diagnostic difference is the pectinal tooth count (= 28) in *G. rossii* being lower than the range (35–40) reported for male *T. mahafaliensis* by Lourenço et al., (2007b: 373, tab. III). However, we examined a male *T. mahafaliensis* collected near the species type locality with PTC of 29–33 (Figs. 524–525). The type locality of *G. rossii* on the central plateau at ca. 1400 m a. s. l., is in a cooler, more humid zone, quite far from the other records of *T. mahafaliensis* concentrated on the Mahafaly Plateau, a region of subarid thorn scrub along the southwest coast (ca. 120 m a.s.l.). It was suggested that *G. rossii* was evidence of microendemism. We take a more conservative position and interpret the very close morphologies of *G. rossii* and *T. mahafaliensis* as indicative of a eurytopic species with wider distribution. Broad elevation ranges of > 1400 m are known for some widely distributed scorpions that inhabit varied bioclimatic zones (e.g., *Anuroctonus pococki* Soleglad & Fet, 2004, 300–1850 m a.s.l., Soleglad & Fet, 2004; *Bothriurus burmeisteri* Kraepelin, 1894 and *Brachistosternus weijenberghi* (Thorell, 1876), 1000–3000 m a.s.l., Campón et al., 2014; *Compsobuthus maindroni* (Kraepelin, 1901), *Hottentotta jayakari* (Pocock, 1895), *Nebo omanensis* Francke, 1980 and *Orthochirus glabrifrons* (Kraepelin, 1903), 0–1850 m a.s.l., Lowe, 2010c). The status

of *G. rossii* should be reviewed when topotypic females are collected and their basal pectinal tooth compared to that of *T. mahafaliensis*, as this is a more reliable diagnostic character in *Teruelius* **gen. n.**

Another potential synonym of *T. mahafaliensis* is *T. magalieae* (Lourenço, 2014). According to its description, the morphometrics, coloration, and meristics of *T. magalieae* are very close to those of *T. mahafaliensis*. The type locality of Cap Saint Marie (holotype male as only known specimen) lies on the southwestern coast in the same bioclimatic region as the latter species. Lourenço (2014: 633) did not compare *T. magalieae* to *T. mahafaliensis*, but claimed that the most closely related species was *G. rossii*, which we here synonymize under *T. mahafaliensis*. The diagnostic differences between *T. magalieae* and *G. rossii* are not compelling: (i) pectines with 36 vs. 28 teeth (a range of variation allowed here for *T. mahafaliensis*); (ii) pedipalp fingers with 12–13 vs. 12–12 granule rows (overlapping counts); and (iii) overall paler coloration (differences in color shade are not uncommon for different populations of a species inhabiting areas with different substrates). We provisionally list this species, until it can be critically evaluated by study of more material and analysis of variation. The female of *T. magalieae* is unknown, and the species might be better diagnosed if the female basal pectinal tooth were determined to be unique.

Taxonomic characters

Trichobothria

The position of petite trichobothrium d_2 on the femur was recorded for 16 examined species (4 *Grosphus*, 1 *Neogrosphus*, 11 *Teruelius* **gen. n.**) and found to comply with our diagnoses: either internal or straddling the dorsointernal carina in *Grosphus* (Figs. 9–12, 346); dorsal or internal, or straddling the dorsointernal carina in *Neogrosphus*; and dorsal or straddling the dorsointernal carina in *Teruelius* **gen. n.** (Figs. 13–20, 483a) (summarized in Table 2). Locating d_2 can be challenging due to its small areolar diameter and very short shaft and may require scanning electron microscopy (Navidpour et al., 2008). We took advantage of UV fluorescence to positively identify d_2 by its areolar diameter and bright shaft fluorescence. The areole is smaller than in non-petite trichobothria, but larger than presumed chemotactic, fluorescent microsetae. UV fluorescence also accentuated the granules defining the dorsointernal carina. Near the base of the femur, in the vicinity of d_2, these granules may deviate from a linear series, dispersing as they course externally towards the dorsoexternal carina. Demarcation between dorsal vs. internal femoral surfaces may become imprecise, in which case we recorded a straddling position of d_2 as 'carinal' (i.e., it splits the granule series near the base of the femur). Positions of d_2 in other *Grosphus* (sensu lato) species that we inferred from published descriptions are largely consistent with our generic division (Table 3).

On the external surface of the patella in *Grosphus* and *Teruelius* **gen. n.**, the pair of trichobothria esb_1-esb_2 was consistently oriented with the more ventral esb_2 being distal to the more dorsal esb_1, usually by a substantial gap (Figs. 345, 481a). This agrees with preliminary observations of Fet et al. (2005) suggesting that a more distal position is a feature of '*Uroplectes*' and '*Tityus*' groups (the gap is even larger in the '*Tityus*' group). Conversely, in the '*Buthus*' group (β-configuration on femur, patella d_3 internal to dorsomedian carina) esb_2 is usually much closer to, level with, or even proximal to esb_1. Available data shows a similar arrangement in *Neogrosphus*, which could distinguish it from both *Grosphus* and *Teruelius* **gen. n.** (cf. Lourenço, 1996b, fig. 24, for *N. blanci*; Vachon, 1969, fig. 3, for *N. griveaudi*). The position of esb_2 in *N. andrafiabe* is unknown because the external patellar trichobothrial map was omitted from its description (Lourenço et al., 2015).

On the chela manus the relative positions of the triad of trichobothria, Eb_1-Eb_2-Eb_3, are also informative in buthid taxonomy. In a preliminary survey of 188 buthids, we observed that within the '*Buthus*' group, this triad usually forms an acute angle opening in the distal direction (herein termed *delta* (δ)-configuration), whereas in other buthids they usually are either collinear (= *lambda* (λ)-configuration) or open in the proximal direction (= *gamma* (γ)-configuration). There were some exceptions, and the rule may not be as exact as the α-β dichotomy on the femur. Nevertheless, it correlates with and supports the subdivision of buthids by patellar d_3 positioning (Fet et al., 2005). We confirmed that *Grosphus*, *Neogrosphus* and *Teruelius* **gen. n.** all comply with γ-configuration and included this in our diagnosis of the '*Grosphus*' group.

Comparisons of Eb_1-Eb_2-Eb_3 positioning among species within the '*Grosphus*' group revealed another trend. In *Teruelius* **gen. n.**, petite Eb_3 was usually close to Eb_2, separated from it by less than half the distance between Eb_1 and Eb_2 (e.g., Figs. 23–24). In *Grosphus*, Eb_3 was often (but not always) more remote from Eb_2 (e.g., Figs. 21–22), and in some cases the separation exceeded the distance between Eb_1 and Eb_2. Statistically, the difference between distance ratios (R_{123}) was highly significant (♂: *Grosphus*, 0.66 ± 0.03, N = 27, vs. *Teruelius* **gen. n.**, 0.37 ± 0.06, N = 23, P = 2.52×10^{-11}; ♀: *Grosphus*, 0.65 ± 0.04, N = 25, vs. *Teruelius* **gen. n.**, 0.37 ± 0.01, N = 20, P = 1.40×10^{-7}; one-tailed t-test). The ratio of the two distances showed much greater variability for *Grosphus* (CV: ♂ 0.235, ♀ 0.315), compared to *Teruelius* **gen. n.** (CV: ♂ 0.165, ♀ 0.144). The ratio for our sample of *Neogrosphus griveaudi* was intermediate (R_{123}: ♂ 0.546, ♀ 0.544), higher than all *Teruelius* **gen. n.** values, and within the lower range of *Grosphus* values (Figs. 25–27) but smaller than their mean.

On the ventral surface of the manus, Vachon (1969) noted that in *N. griveaudi*, trichobothrium V_2 was strongly displaced internally relative to V_1, whereas the V_1-V_2 axis was roughly parallel to the long axis of the chela (or only slightly oblique to it) in *Grosphus*. This was one of the characters used by Lourenço (1995) to diagnose *Neogrosphus* and separate it from *Grosphus.* The same character state is inherited from *Grosphus* (sensu lato) by *Teruelius* **gen. n.** We confirmed near parallel orientation in all examined species of *Grosphus* and *Teruelius* **gen. n.**

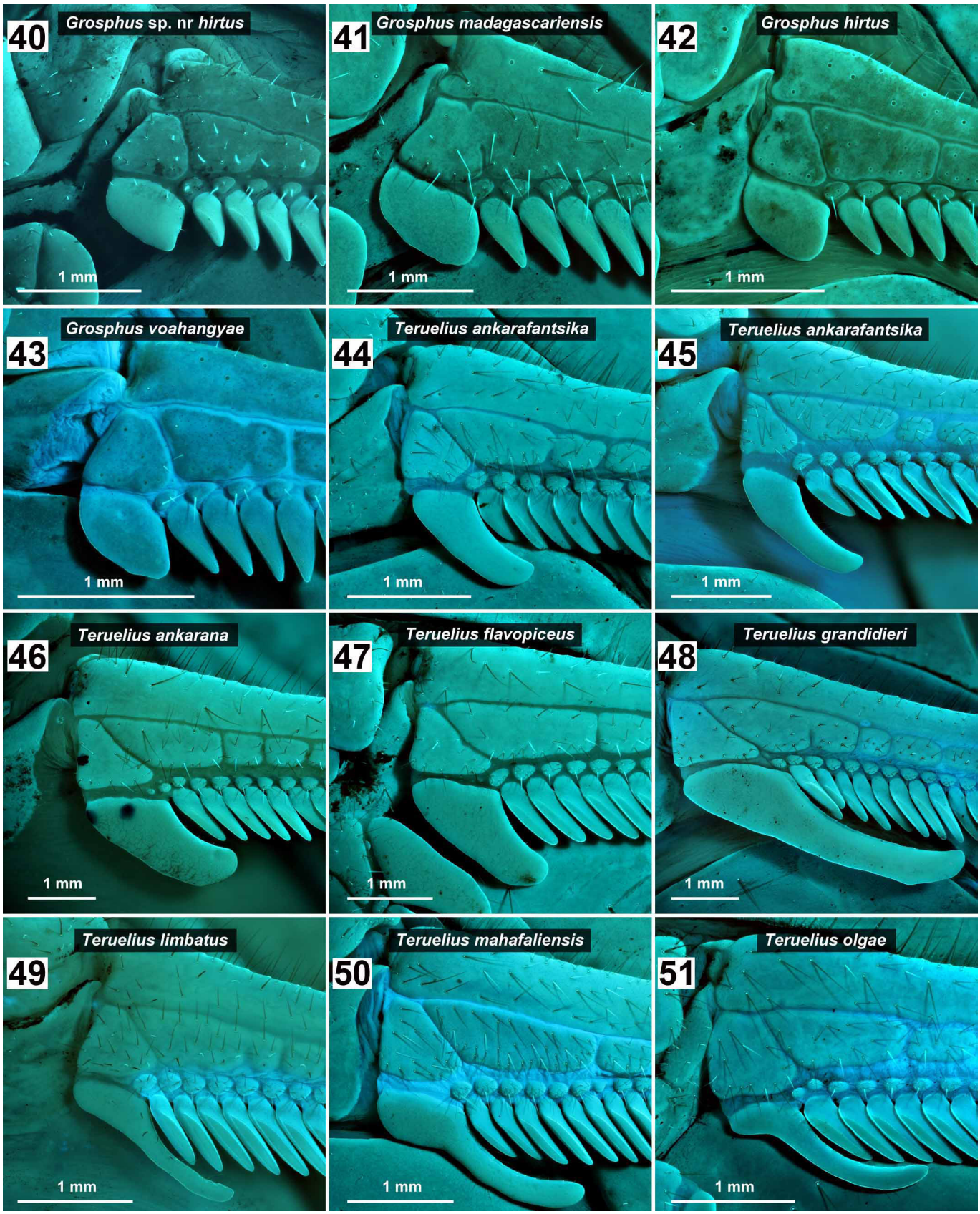

Figures 40–51. Female basal pectinal teeth in *Grosphus* and *Teruelius* **gen. n**. Ventral views of proximal left pectine of females shown under UV fluorescence to highlight cuticular surface texture, setation and absence of peg sensillae on basal tooth vs. their presence on other teeth. *G*. sp. nr *hirtus* (40), *G. madagascariensis* (41), *G. hirtus* (42), *G. voahangyae* (43), *T. ankarafantsika* (44–45; 2 samples from Ampijoroa show variation in tooth shape), *T. ankarana* (46), *T. flavopiceus* (47), *T. grandidieri* (48), *T. limbatus* (49), *T. mahafaliensis* (50), and *T. olgae* (51). Scale bars: 1 mm.

Pectine teeth

The number of pectine teeth has been used to discriminate between species of *Grosphus* (sensu lato) and to key out species groups (e.g., Fage, 1929; Kraepelin, 1900; Lourenço, 1996b, 2003c; Vachon, 1969). At the genus level, we found that *Grosphus* and *Teruelius* **gen**. **n**. are clearly separable by numbers of teeth per comb, with the former exhibiting a lower (♂ < 24, ♀ < 22), and the latter a higher (♂ > 24, ♀ > 22) range of counts (Figs. 28–29, Tabs. 1–3). The inter-generic separation was greater for females than for males, which showed more variability. Soleglad's Law, encapsulating the positive scaling of pectinal tooth count with body size (Kovařík et al., 2016d), was found to be significant for male *Neogrosphus* (R = 0.81, P = 0.0005, N = 3; Fig. 30), and female *Teruelius* **gen**. **n**. (R = 0.68, P = 0.001, N = 14; Fig. 31).

The form of the basal pectinal tooth in females is another character previously used in the taxonomy of '*Grosphus*' group scorpions. Our diagnosis of *Grosphus* (sensu stricto) includes only those species with an oval or sub-rectangular tooth that is widened along the comb axis, but not much elongated relative to other pectine teeth (Figs. 40–43). This corresponds to 'Group I' defined by Fage (1929), which is also characterized by a lower range of pectinal tooth counts. In *Teruelius* **gen**. **n**., the tooth is elongated to varying degrees, is always distinctly longer than the other pectine teeth (sometimes overlapping them), and is angled in a distal direction (Figs. 44–51). The shape of the basal tooth is diverse and species-specific and has been used to differentiate *Teruelius* **gen**. **n**. species. It differs from other teeth in lacking peg sensillae, as revealed by SEM (Lourenço, 2003c, 2004b; Lourenço & Goodman, 2003a) and UV microscopy (Figs. 40–51), and often in bearing either macrosetae or fluorescent microsetae (e. g., Figs. 40, 49). The most distal pectine tooth of the comb may also bear macrosetae or microsetae, but differs from the basal teeth by bearing peg sensillae. In *Neogrosphus*, the basal tooth of females is enlarged, with a form intermediate between that of *Grosphus* and *Teruelius* **gen**. **n**., being oval and slightly longer than other pectine teeth, but not as elongated as in *Teruelius* **gen**. **n**.

Regarding the enlarged female basal teeth of *Buthus limbatus*, Pocock (1889a: 394) remarked: "The usefulness of some such modification could scarcely be more clearly demonstrated; but of its function I believe nothing is certainly known." Alexander (1959) suggested that the enlarged female teeth of *Uroplectes triangulifer* (Thorell, 1876), or the enlarged basal middle lamellae of female *Parabuthus planicauda* (Pocock, 1889) and *Tityus trinitatis* Pocock, 1897, were used during mating to clasp the basal lobes of the spermatophore. She envisaged sperm being ejected as the male rocked the female back and forth while the enlarged basal pectine structures held the basal lobes, compressing the trunk. However, the basal lobes are too distal to permit such a function (Monod et al., 2017). Alternatively, the enlarged teeth or middle lamellae may serve either to directly embrace, or to impose constraints on lateral flexure of the spermatophore trunk, preventing it from bending too far sideways during rocking. This could facilitate transmission of axial compressive forces down the trunk as the genital opercula push on the basal lobes during rocking, promoting sperm ejection. Similar enlargements of basal pectinal structures in females have evolved independently in a number of other buthids, perhaps to serve similar functions, e.g., *Somalicharmus*, *Isometrus*, *Tityopsis*, and the *Tityus* '*asthenes*' complex (Kovařík et al., 2016e). It may be no coincidence that buthids with modified basal pectinal structures in females possess spermatophores with slender, narrow trunks more prone to lateral deflection. The trunk must be elastic to permit compression, but elasticity also allows lateral bending, a motion that may be less effective for driving sperm expulsion. The problem might be solved by use of the basal pectine teeth to stabilize the trunk against lateral deflection. Enlargement or modification of basal pectine teeth or basal middle lamellae is uncommon in non-buthids. Lamelliform spermatophores of non-buthids have a shorter, thicker trunk that may not require lateral support during sperm release mechanics. An exception is the vaejovid tribe Stahnkeini, in which female basal pectine teeth are modified, slightly enlarged or reduced, and smooth with peg sensillae either much diminished or completely absent (Ayrey, 2011; Graham & Soleglad, 2007; Sissom & Stockwell, 1991; Soleglad, 1974; Soleglad & Fet, 2006, 2008; Stahnke, 1974). These modified teeth may serve a different function than the enlarged basal teeth of buthid pectines.

Another possibility is that the basal pectinal teeth are utilized by the female during courtship before the capsule lodges between her opercula. They could make initial, tactile contact with the spermatophore and enable her to feel and guide herself towards it until the distal hooks latch onto her opercula. Accounts of scorpion mating describe the male as the active partner, bending the spermatophore backwards via the flagella and pulling the female over it by jerking motions (Alexander, 1959; Polis & Sissom, 1990). It is not clear how the male would determine precisely where to position the female, and some sensory feedback from the female would make it a collaborative effort. Aside from mating purposes, another suggestion is that modified female basal teeth could play a role in parturition (Soleglad & Fet, 2006).

In *Teruelius* **gen**. **n**., there are varying degrees of elongation of the female basal tooth, ranging from modest length (e.g., *T. ankarafantsika*, *T. ankarana, T. flavopiceus*) to conspicuous extension that overlaps many peg-bearing teeth (e.g., *T. grandidieri*, *T. limbatus*, *T. mahafaliensis*, *T. olgae*). Fig. 36 compares body size scaling of tooth length for *Grosphus* and *Teruelius* **gen**. **n**. species. Tooth length increases with body length, and the logarithmic regression lines have similar slopes, but the line for *Teruelius* **gen**. **n**. is located higher than for *Grosphus*, reflecting the greater tooth enlargement in that genus. In *Grosphus*, the tooth has a rather uniform shape, and the points lie close to the fitted line. In *Teruelius* **gen**. **n**., there is more diversity in basal tooth size and shape, and hence more scatter about the average trend. For instance, *T. ankarana* and *T. flavopiceus* have shorter teeth than predicted from their larger body sizes, whereas *T. grandidieri* is an outlier with

Figures 52–**70**. Hemispermatophores and capsule regions of *Grosphus* and *Neogrosphus*. Multi-panel figures show: whole hemispermatophore; whole hemispermatophore and capsule with flagellum; capsule region in convex (and/ or convex compressed), anterior and posterior views (panels in left to right sequence). Right hemispermatophores unless indicated as mirrored left images. **Figure 52**. *G. madagascariensis*, whole hemispermatophore (scale bar: 2 mm), capsule and flagellum (scale bar: 1 mm). **Figure 53**. *G. madagascariensis*, capsule, Sc1197, Andasibe, GLPC, FKCP. Scale bar: 500 µm. **Figure 54**. *G. madagascariensis*, capsule, Anjiro, *G. halleuxi* nr topotype, GLPC. Scale bar: 500 µm. **Figure 55**. *G. madagascariensis*, capsule, Mandena- Fort Dauphin, *G. mandena* paratype, MHNG. Scale bar: 500 µm. **Figure 56**. *G. madagascariensis*, capsule, Madagascar, det. Vachon, MHNG. Scale bar: 500 µm. **Figure 57**. *G. madagascariensis*, capsule, Andasibe, GLPC, FKCP. Scale bar: 500 µm. **Figure 58**. *G. goudoti*, whole hemispermatophore. Scale bar: 2 mm. **Figure 59**. *G. goudoti*, capsule, Forêt de Bobankota, holotype, MHNG. Scale bar: 500 µm. **Figure 60**. *G. hirtus*, whole hemispermatophore (scale bar: 2 mm), capsule and flagellum (scale bar: 1 mm), Antsiranana, Ramena vill., mirrored left, GLPC, FKCP. **Figure 61**. *G. hirtus*, capsule, Mahajamba River, GLPC, FKCP. Scale bar: 500 µm. **Figures 62**–**65**. *G. hirtus*, capsules in convex view. Antsiranana, Ramena vill., mirrored left, GLPC, FKCP (62), Jardin Botanique, MHNG (63), Ranohira-Llakaka, ZMUH, mirrored left (64), Forêt de Vohitaly, MHNG (65). Scale bars: 500 µm. **Figure 66**. *G. hirtus*, capsule, Forest Station Ampijoroa, *G. garciai* holotype, MHNG. Scale bar: 500 µm. **Figure 67**. *G. voahangyae*, whole hemispermatophore. Scale bar: 2 mm. **Figure 68**. *G. voahangyae*, capsule, Analamy Forest, FMNH. Scale bar: 500 µm. **Figure 69**. *N. griveaudi*, whole hemispermatophore (flagellum truncated). Scale bar: 2 mm. **Figure 70**. *N. griveaudi*, capsule, mirrored left, Tsimanampetsotsa National Park, GLPC, FKCP.

much a longer tooth than predicted, even for a large scorpion. In these plots, *Neogrosphus* groups with *Grosphus* in having a smaller basal tooth.

In contrast to female basal tooth length, the length of the hemispermatophore trunk showed similar length scaling relations in *Grosphus* and *Teruelius* **gen**. **n**. (Fig. 37). This geometric scaling is expected for a substrate-borne insemination device. A longer hemispermatophore is needed to reach the genital opening of a larger female standing taller on the substrate. In the context of our 'trunk-clasper' hypothesis, we asked whether there was a simple match of trunk length with length of female basal pectine tooth. Fig. 38 shows that there are size scaling relations for tooth length vs. trunk length, as would be expected from body size scaling of both parameters. Tooth length was not directly matched to trunk length, but was consistently smaller. However, partial trunk clasping by a pair of basal teeth could be effective to restrain lateral bending. The percentage of possible trunk overlap by the basal tooth is plotted in Fig. 39, as a function of trunk length. The teeth cover at most 40% of the trunk, and usually much less. The overlap is constant and small (< 10%) in *Grosphus*, slightly higher in *Neogrosphus* (12.3%), and moderate to high in *Teruelius* **gen**. **n**. (16–40%). There was a slight negative trend in *Teruelius* **gen**. **n**., with a lower fractional trunk coverage in larger species, but *T. grandidieri* was again an outlier with its very elongated basal tooth. The very long basal teeth seen in some *Teruelius* **gen**. **n**. occur in only a few other scorpions, e.g., *Uroplectes planimanus* and *U. tumidimanus*. They may well be a reproductive adaptation important for the ecological success of this genus.

Hemispermatophore

Comparative morphology of buthid hemispermatophores was pioneered by Vachon (1940, 1952), and although less studied than hemispermatophores of some other scorpion families, can provide informative taxonomic characters at the genus level (e.g., Botero-Trujillo & Flórez, 2011; Esposito et al., 2017; Francke & Stockwell, 1987; Kovařík et al., 2016c, 2018b; Levy & Amitai, 1980; Lowe, 2018; Lowe et al., 2019). The hemispermatophores of '*Grosphus*' group scorpions have not been characterized in detail. Vachon (1940: 254, figs. 30, 34) illustrated the hemispermatophore of *Grosphus* (= *Teruelius*) *limbatus*. He depicted a sperm hemiduct with a '2+1' lobe configuration: i.e., two short, broad lobes (*li*, lobe interne = posterior lobe; *le*, lobe externe = anterior lobe), both simple in structure without folds or carinae, and a large, robust, hook-like basal lobe (*lb*, lobe basal). This was contrasted with '3+1' lobes of *Buthus occitanus* (Amoreux, 1789), a typical '*Buthus*' group configuration (Kovařík et al., 2016c; Lowe et al., 2018), and '2+0' lobes of *Babycurus buettneri* Karsch, 1886 (basal lobe vestigial, reduced to a short carina, cf. Kovařík et al., 2018b: 5, fig. 39). Vachon (1969: 482, fig. 10) illustrated the hemispermatophore of *Neogrosphus griveaudi*, showing a large basal lobe and short capsule, but details of the capsule were not shown. Lourenço (2001b: 458, fig. 7) illustrated the distal profile of the hemispermatophore of *Grosphus garciai* (= *G. hirtus*), showing a strong basal lobe near the base of a short flagellum and an unusually elongated lobe of the sperm hemiduct. The same specimen is shown here again in more detail (Fig. 66). The elongated lobe differs markedly from the lobes that Vachon (1940) showed for *Grosphus* (= *Teruelius*) *limbatus*. We use this as a key character to separate *Teruelius* **gen**. **n**. from *Grosphus*.

Figs. 52–93 show hemispermatophores and capsules of *Grosphus*, *Neogrosphus* and *Teruelius* **gen**. **n**. species. In all cases, the trunk was very long and slender with a short capsule. The flagellum was well separated from the posterior lobe. When intact, it was relatively short compared to the trunk, and divided into pars recta and pars reflecta (the latter slightly thickened). A large, thick, hook-like basal lobe was always present. In *Grosphus*, a long, lanceolate projection of the posterior lobe extended distally, tapering to a blunt tip (Figs. 52–68, 86, 88–89; Fig. 66 consistent with Lourenço, 2001b: fig. 7). In contrast, *Neogrosphus* and *Teruelius* **gen**. **n**. had short, blunt posterior lobes lacking blade-like projections (Figs. 69–85, 90–93, consistent with Vachon, 1940, 1969). This difference in lobe shape was diagnostic. In many species, one or more sclerotized carinae ran axially along the capsule at the base of the posterior lobe (stereoscopically visualized in Figs. 86–93). The anterior lobe was short, sometimes indistinct, and connected to the posterior lobe by the sperm hemiduct membrane.

A remarkable observation was the profound difference in capsule shape and basal lobe position between *G. madagascariensis* and other *Grosphus* species. The capsule of *G. madagascariensis* was elongated and narrow, with a single sclerotized carina running along its length, and a basal lobe placed far proximal to the base of the flagellum (Figs. 52–57, 86). This differed strikingly from capsules of other species ('*hirtus*' group: *G. goudoti*, *G. hirtus* and *G. voahangyae*), which were short with the basal lobe positioned near the base of the flagellum, and in some cases with one or more sclerotized folds or carinae on the posterior lobe (Figs. 58–68, 88–89). The distal lanceolate projection was longer and broader in the '*hirtus*' group, and shorter and narrower in *G. madagascariensis*. Structurally, the '*hirtus*' group capsule appears more similar to the capsule of *Teruelius* **gen**. **n**., than *G. madagascariensis*. This was surprising because *G. madagascariensis* and '*hirtus*' group species are otherwise quite similar in external morphology, and were often misidentified or confused with each other in the past. In other animals, rapid divergence of male genital apparatus between externally similar taxa is well known and attributed to sexual selection or other mechanisms (Eberhard, 1985; Hosken & Stockley, 2004). In bothriurid scorpions, the rate of evolution of hemispermatophore structures varies, and parts deemed essential for sperm transfer may be more conserved by stabilizing selection and relay more phylogenetic signal (Mattoni et al., 2012). In buthids, we have found that as a rule, capsule and lobe structure tends to be well conserved in species belonging to the same genus (e.g., Kovařík et al., 2018a; Lowe, 2010b, 2018; Lowe et al., 2014, 2019).

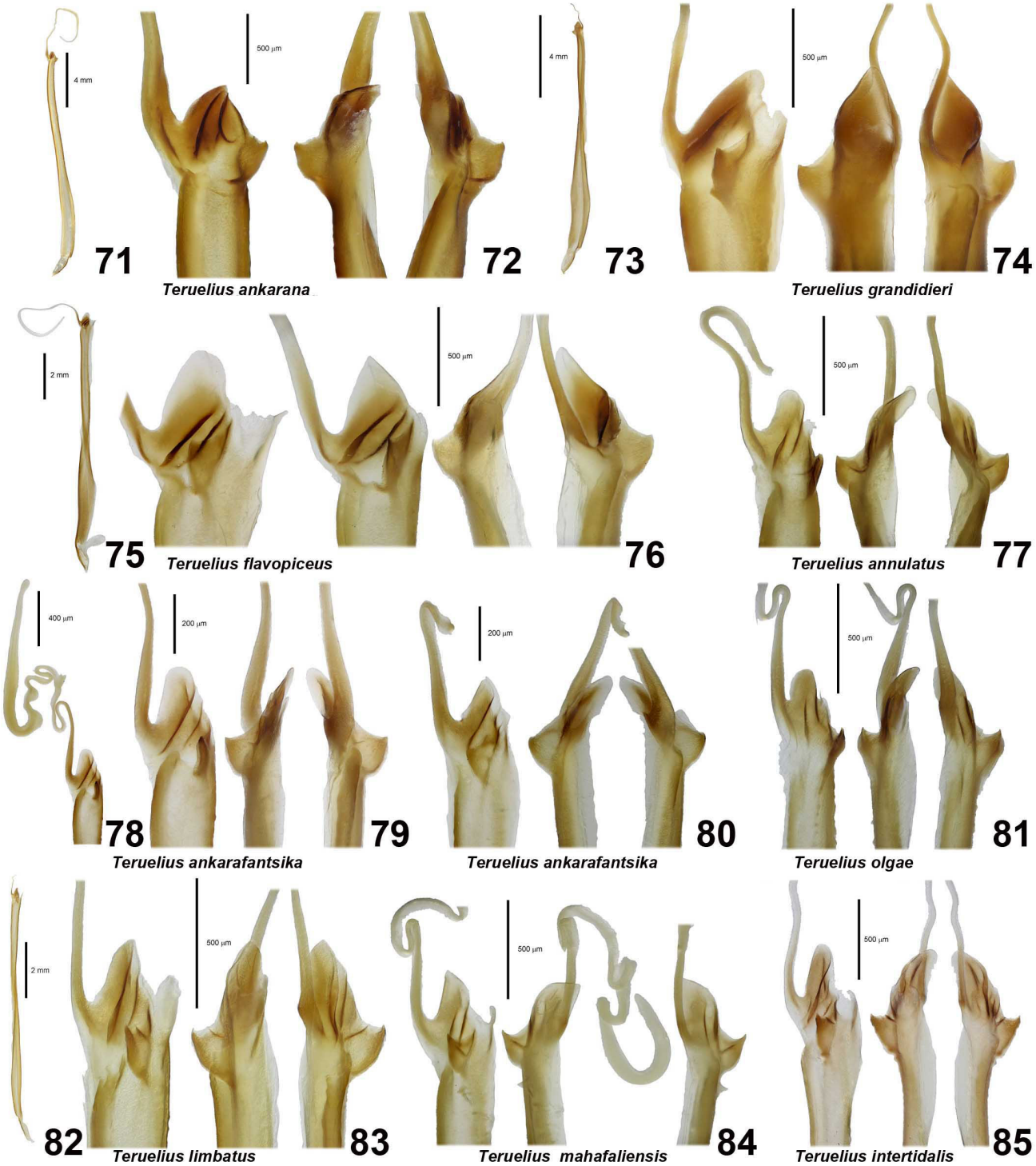

Figures 71–85. Hemispermatophores and capsule regions of *Teruelius* **gen n**. Multi-panel figures show: whole hemispermatophore; whole hemispermatophore and/or capsule with flagellum; capsule region in convex (or convex compressed), anterior and posterior views (panels in left to right sequence). Right hemispermatophores. **Figure 71**. *T. ankarana*, whole hemispermatophore. Scale bar: 4 mm. **Figure 72**. *T. ankarana*, capsule, left mirrored, Forêt d'Ankavanana, FMNH. Scale bar: 500 µm. **Figure 73**. *T. grandidieri*, whole hemispermatophore (flagellum truncated). Scale bar: 4 mm. **Figure 74**. *T. grandidieri*, capsule, Antsakabe River, FMNH. Scale bar: 500 µm. **Figure 75**. *T. flavopiceus*, whole hemispermatophore. Scale bar: 2 mm. **Figure 76**. *T. flavopiceus*, capsule, Madagascar, GLPC, FKCP. Scale bar: 500 µm. **Figure 77**. *T. annulatus*, capsule, Tsimanampetsotsa National Park, GLPC, FKCP. Scale bar: 500 µm. **Figure 78**. *T. ankarafantsika*, capsule and flagellum. Scale bar: 400 µm. **Figure 79**. *T. ankarafantsika*, capsule, Forêt d'Ankavanana, FMNH. Scale bar: 200 µm. **Figure 80**. *T. ankarafantsika,* capsule, Réserve Forestière de l'Ankarafantsika, FMNH. Scale bar: 200 µm. **Figure 81**. *T. olgae*, capsule, Itampolo village, FMNH. Scale bar: 500 µm. **Figure 82**. *T. limbatus*, whole hemispermatophore (flagellum truncated). Scale bar: 2 mm. **Figure 83**. *T. limbatus*, capsule, Forêt d'Ianasana, FMNH. Scale bar: 500 µm. **Figure 84**. *T. mahafaliensis*, capsule views, Zombitse-Vohibasia National Park, GLPC, FKCP. Scale bar: 500 µm. **Figure 85**. *T. intertidalis*, capsule, Madagascar, GLPC, FKCP. Scale bar: 500 µm.

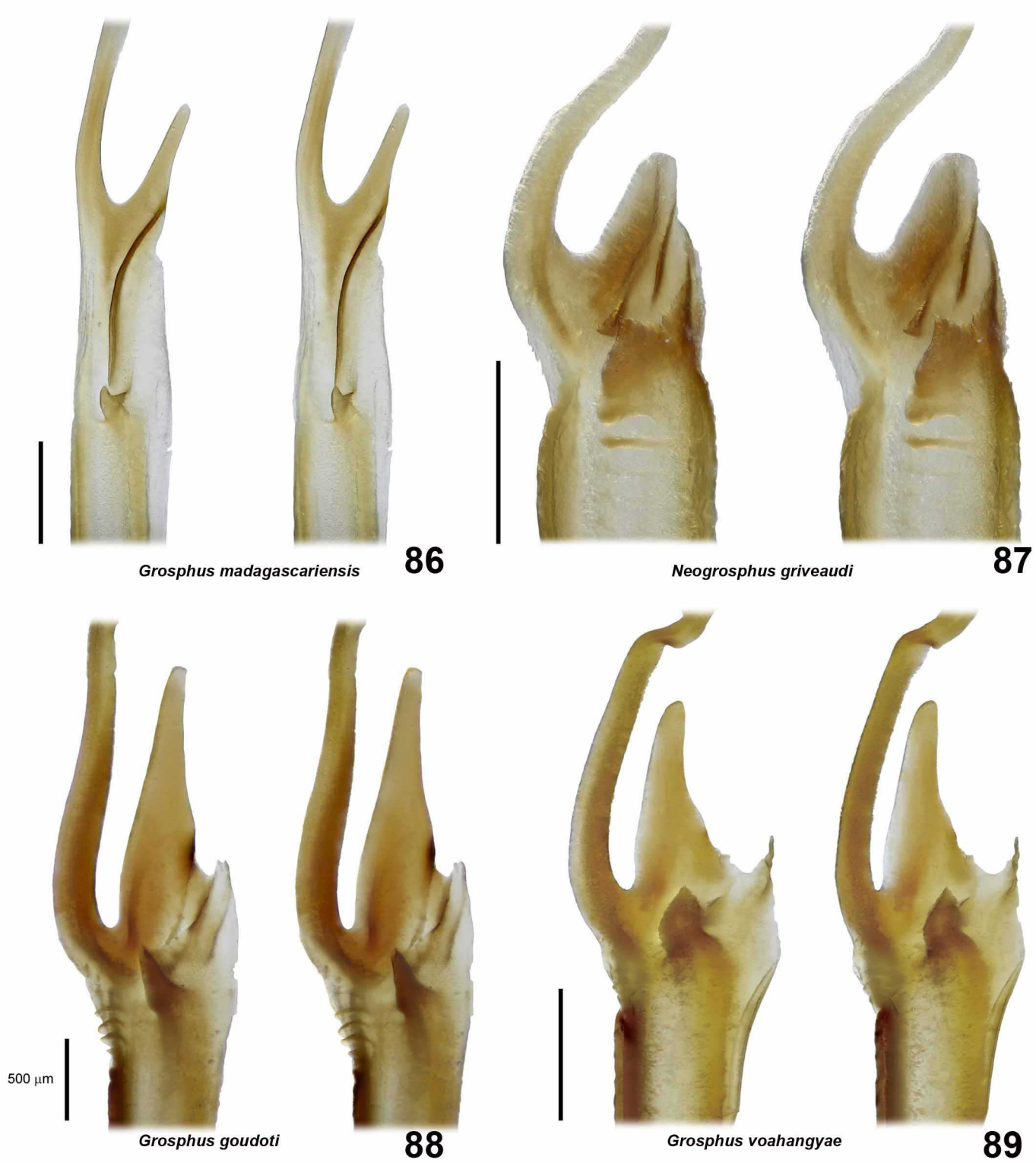

Figures 86–**89**. Hemispermatophores and capsule regions of *Grosphus* and *Neogrosphus*. Cross stereoscopic convex views. Scale bars: 500 µm. **Figure 86**. *G. madagascariensis*, Sc1197, Andasibe, GLPC, FKCP. **Figure 87**. *N. griveaudi*, mirrored left, Tsimanampetsotsa National Park, GLPC, FKCP. **Figure 88**. *G. goudoti*, Forêt de Bobankota, holotype, MHNG. **Figure 89**. *G. voahangyae*, Analamy Forest, FMNH.

Across a major clade, the '*Buthus*' group, we have not found differences in capsule shape as profound as those between *G. madagascariensis* and '*hirtus*' groups. This implies that either special selection mechanisms operated in *Grosphus* to drive a more rapid evolution of capsule size and shape, or there is a deeper divergence in the genus that is masked by highly conserved external morphology.

In a formed *Grosphus* spermatophore, the lanceolate posterior lobes would be fused into a single long blade that may function to pry apart the female genital opercula

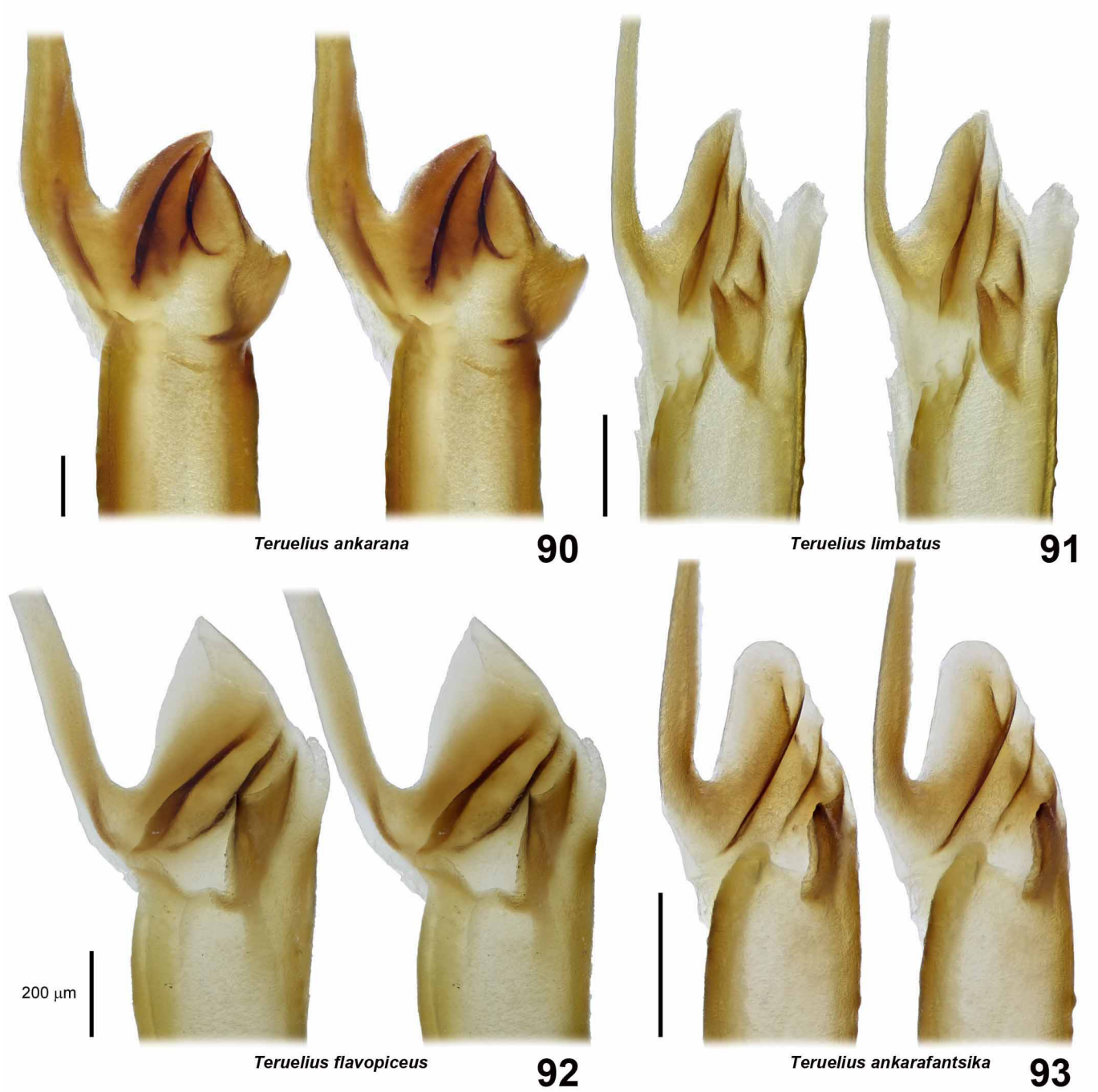

Figures 90–**93**. Hemispermatophores and capsule regions of *Teruelius* **gen**. **n**. Cross stereoscopic convex views. **Figure 90**. *T*. *ankarana*, left mirrored, Forêt d'Ankavanana, FMNH. **Figure 91**. *T*. *limbatus*, Forêt d'Ianasana, FMNH. **Figure 92**. *T*. *flavopiceus*, Madagascar, GLPC, FKCP. **Figure 93**. *T*. *ankarafantsika*, Forêt d'Ankavanana, FMNH. Scale bars: 200 µm.

along the midline. The longitudinal grooves and carinae of the lobes are oriented to engage medial rims of the opercula, allowing the sperm duct to glide smoothly into place until posterior margins of the opercula wedge against the basal lobes (Francke, 1979). In this position, the long '*madagascariensis*' capsule will be deeply inserted into the genital tract, securely lodged for 'safe sperm transfer' (Monod et al., 2017). The distal blade should contact the anterior margin of the genital opening, anchoring the capsule in position. Indeed, in *G*. *madagascariensis* we found that the length of the capsule (basal lobe to blade apex 1.46 ± 0.06 mm, N = 5) was approximately matched to the longitudinal span of the female genital opening (1.62 ± 0.03 mm, N = 7). In the '*hirtus*' group, the capsule is much shorter, but the longer projection of the posterior lobe may permit deeper penetration and carinae may help to lock it into an intromittent position. In *G*. *goudoti*, the posterior margin of the capsule below the flagellum bears regular costate sculpturing that could also engage opercular margins and stabilize the capsule.

In *Neogrosphus* and *Teruelius* **gen**. **n**., the capsule is short and lacks a prominent projecting lobe. The large, robust, hook-like basal lobe is located distally at the level of the flagellar base. If the hooks are wedged against the female opercular margins, then a short sperm duct precludes a deeper insertion that can better stabilize the intromittent position. However, in most species the sperm hemi-duct is furnished with two or more strong carinae, with intercarinal grooves that can fit over female opercular margins to prevent dislodging of the capsule. In some species (*N. griveaudi*, *T. mahafaliensis*, *T. intertidalis* and *T. olgae*), barbs or corrugations are developed below the basal lobe on the anterior convex surface (Figs. 70, 81, 84–85, 87). These could grip the female integument behind the genital opercula, holding the capsule more firmly in place.

Spiracles

The spiracles (= stigmata) on sternites IV–VII provide useful diagnostic characters for '*Grosphus*' group scorpions. Pocock (1889a) in his description of *Buthus piceus* (= *Grosphus madagascariensis*) first drew attention to the small ovoid spiracles (clearly illustrated on sternite IV in fig. 8a of his article) and wrote: "In the shape of the pulmonary stigmata this species stands by itself in the family Buthidae, and should in consequence perhaps constitute a new genus". He did not create a new genus, noting variability in spiracle shape, but emphasized the difference from *Buthus* (= *Teruelius*) *limbatus*, which has slit-shaped spiracles. Pocock (1889b) described *B. lobidens*, differentiating it from *B. piceus* by a longer, more slender metasoma and narrower spiracles: "These apertures in *B. piceus* are ovate; but in *B. lobidens* they are more slit-like and furnish to a certain extent a link between the ovate form of *B. piceus* and the slit-like form found in most other Scorpions". As noted in the **Introduction**, Kraepelin (1891) disregarded these differences and synonymized both species with *G. madagascariensis*. Spiracles of *Grosphus* were not referenced in his subsequent keys to the genus (Kraepelin, 1899, 1900). Here, we reaffirm Pocock's character by showing that *Teruelius* **gen**. **n**. is separable from *Grosphus* by spiracle shape.

As is apparent from Figs. 94–105, there is a clear difference between the wide, ovoid or hemi-elliptical spiracles of *Grosphus* species, and the narrow slit-like spiracles of *Teruelius* **gen**. **n**. species. Interestingly, the more elongate spiracles *G. madagascariensis* compared to those of *G. hirtus* recalls Pocock's observations about the difference between *B. lobidens* (elongate spiracles, longer metasoma) and *B. piceus* (ovoid spiracles, shorter metasoma). The types of *B. lobidens* and *B. piceus* should be restudied to reassess possible synonymy with *G. madagascariensis* vs. *G. hirtus*. We show spiracles of both sexes for comparison. Sexual dimorphism in spiracle biometrics is summarized in Figs. 114–116. On these plots, most species are near diagonal, with little difference between the sexes. Scatter was within expected variation for small sample sizes, and not significant.

In Figs. 106–107, plots of spiracle IV length/ width (L/W) vs. carapace length (a measure of body size) for males and females reveal the clear separation between *Grosphus* (L/W < 5) and *Teruelius* **gen**. **n**. (L/W > 5). In *Teruelius* **gen**. **n**., the L/W ratio is independent of size, all spiracles being narrow slits with L/W ~ 7.0–9.0. In *Grosphus*, there is a size scaling relation, with the openings being rounder in smaller species, and narrower in larger species. *Neogrosphus* has moderately narrow spiracles, at the upper end of the L/W range for *Grosphus*, but it deviates from the *Grosphus* scaling line, due to its small size. We also examined body size scaling for the ratio of spiracle width, W, to carapace length, i. e., spiracle relative width, normalized to body size (Figs. 108–109). There was an inverse scaling of relative width in *Grosphus* and again no scaling (constant relative width) for *Teruelius* **gen**. **n**., correlated with the L/W scaling relations. This indicates that shape scaling in *Grosphus* is mediated in part by changes in relative width. Relative width was also a good criterion for clearly separating *Grosphus* from *Teruelius* **gen**. **n**.

Plots in Figs. 110–111 show scaling of spiracle IV area, normalized to the square of carapace length, a ratio that measures fractional body surface area of book lung openings. There was no body size scaling of normalized area in both sexes of *Grosphus*, and a positive scaling trend for male *Teruelius* **gen**. **n**.. Spiracle area was generally higher for *Grosphus* than *Teruelius* **gen**. **n**., but there was some overlap so this ratio did not yield a numerical index for separating the two genera. The smallest species, *Neogrosphus griveaudi*, had the smallest relative spiracle area, in agreement with the positive scaling trend of *Teruelius* **gen**. **n**., but falling well below the regression line for that genus.

Relative area of spiracle openings is a physical parameter relevant to transpiration water loss from the book lungs. Thus, a possible interpretation of these data is in terms of gas exchange and respiratory water loss in humid vs. dry environments. Some *Grosphus* species are distributed in more humid regions of Madagascar, including rainforests along the eastern side of the mountains that divide the island (e.g., *G. madagascariensis*, *G. ambre*, *G. voahangyae*). Others occur in mesic or drier areas in the north and west (e.g., *G. goudoti*, *G. hirtus*, *G. polskyi*, *G. rakotoariveloi*). The ancestral state of the genus may be reflected by the first group, with adaptations to relatively cooler, more humid habitats where transpiration water loss is lower. The second group may have evolved later, radiating and adapting to more xeric habitats. In contrast, *Teruelius* **gen**. **n**. is most prevalent in southwestern and southern sectors with relatively warmer, subarid climates where transpiration water loss is greater due to higher temperatures and higher partial pressure differences of water vapor (Figs. 117–118). This correlates with their narrow slit-like spiracles with smaller areas, potentially allowing tighter control of water loss. Slit-like spiracles occur in many species of the '*Buthus*' group, the dominant scorpions of Palearctic deserts. Figs. 117–121 show climatic distributions of the '*Grosphus*' group genera. Compared to *Grosphus*, the distributions of *Teruelius* **gen**. **n**. and *Neogrosphus* have lower mean rainfall and higher mean temperature (Figs. 119–120). *Teruelius* **gen**. **n**. and *Neogrosphus* tolerate a broader precipitation range than *Grosphus*, overlapping the latter. With

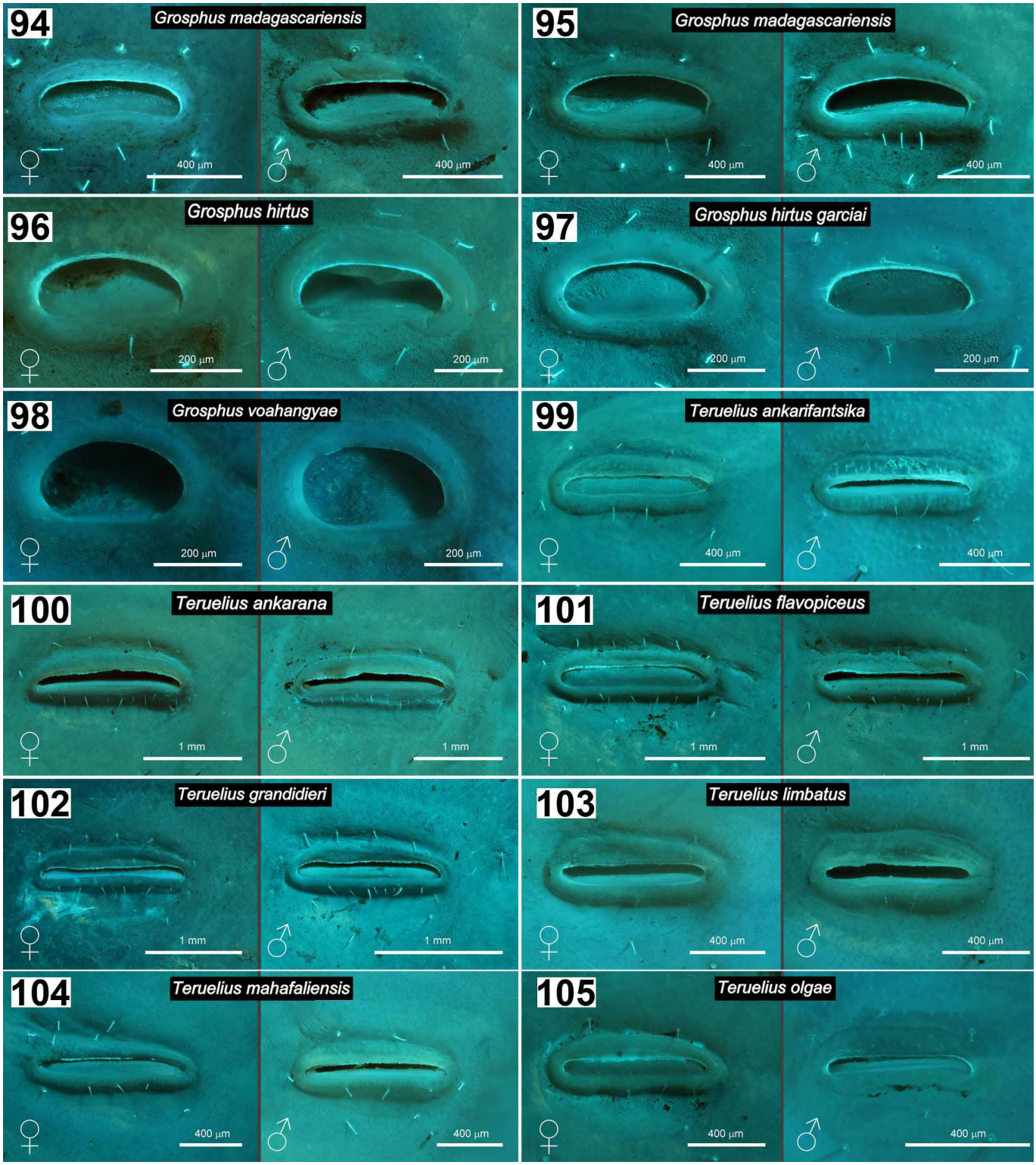

Figures 94–105. Spiracles on sternite IV in *Grosphus* and *Teruelius* **gen. n**. Spiracle on right side of sternite IV in adult females (♀, left panels) and adult males (♂, right panels), shown under UV fluorescence. *G. madagascariensis* (94 from Anjiro, 95 from Andasibe), *G. hirtus* (96), *G. hirtus* (= *G. h. garciai*) (97), *G. voahangyae* (98), *T. ankarafantsika* (99), *T. ankarana* (100), *T. flavopiceus* (101), *T. grandidieri* (102), *T. limbatus* (103), *T. mahafaliensis* (104), and *T. olgae* (105). Scale bars: 200 µm (96–98), 400 µm (94–95, 99, 103–105) or 1 mm (100–102).

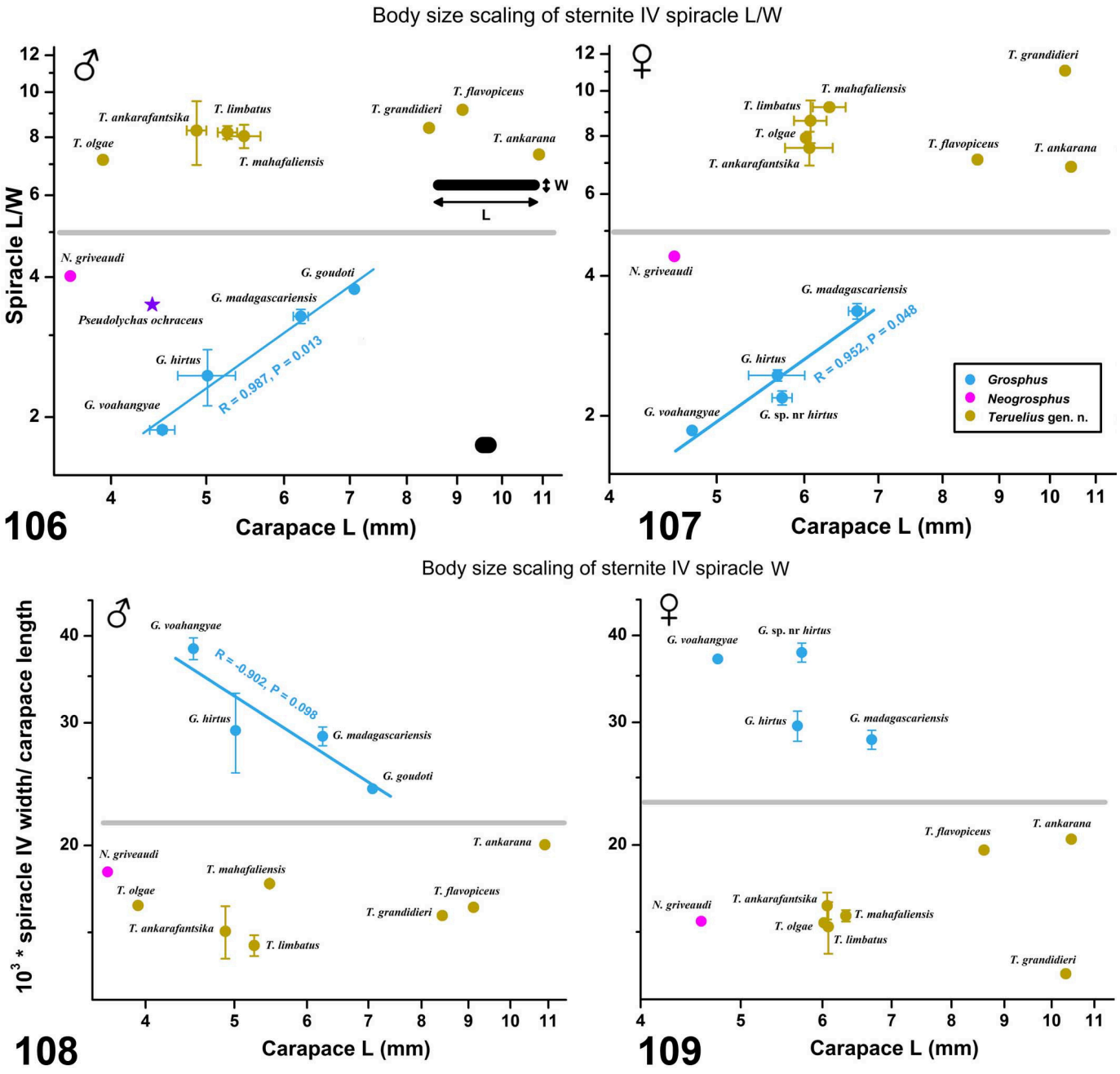

Figures 106–109. Biometric scaling of spiracles of sternite IV in *Grosphus*, *Neogrosphus* and *Teruelius* **gen**. **n**. **Figures 106–107**. Logarithmic scatter plots showing scaling of spiracle length/ width vs. carapace length in males (106), and females (107) of *Grosphus*, *Neogrosphus* and *Teruelius* **gen**. **n**. Male plot: purple star shows spiracle L/W of outgroup taxon *Pseudolychas ochraceus*. **Figures 108–109**. Logarithmic scatter plots showing scaling of spiracle width/ carapace length vs. carapace length in males (108), and females (109) of *Grosphus*, *Neogrosphus* and *Teruelius* **gen**. **n**. Blue lines are least squares linear regression fits of scaling trends for *Grosphus*. R = Pearson correlation coefficient, and P value as indicated. Horizontal gray lines are proposed diagnostic thresholds.

their narrower spiracles, they would be better adapted to low rainfall regions in the southwest, but they could also colonize more humid environments in the north. This is indicated by the bimodal distributions of *Teruelius* **gen**. **n**. over rainfall and temperature. However, *Teruelius* **gen**. **n**. and *Neogrosphus* do not extend into the humid rainforest belt along the east coast, where *Grosphus* is prevalent (Fig. 121).

Scorpions can directly control spiracle opening. An atrial chamber between the book lung lamellae and the spiracle acts as a valve in a normally closed state (Kamenz & Prendini, 2008). The valve opens under neural control by contraction of a poststigmaticus muscle attached to the posterior atrial membrane (Farley, 1990). This mechanism allows for discontinuous gas exchange (DGC), a gating mechanism used by insects for reducing respiratory water loss (Lighton, 1996). In the spiracle-closed state, reduction of O_2 and accumulation

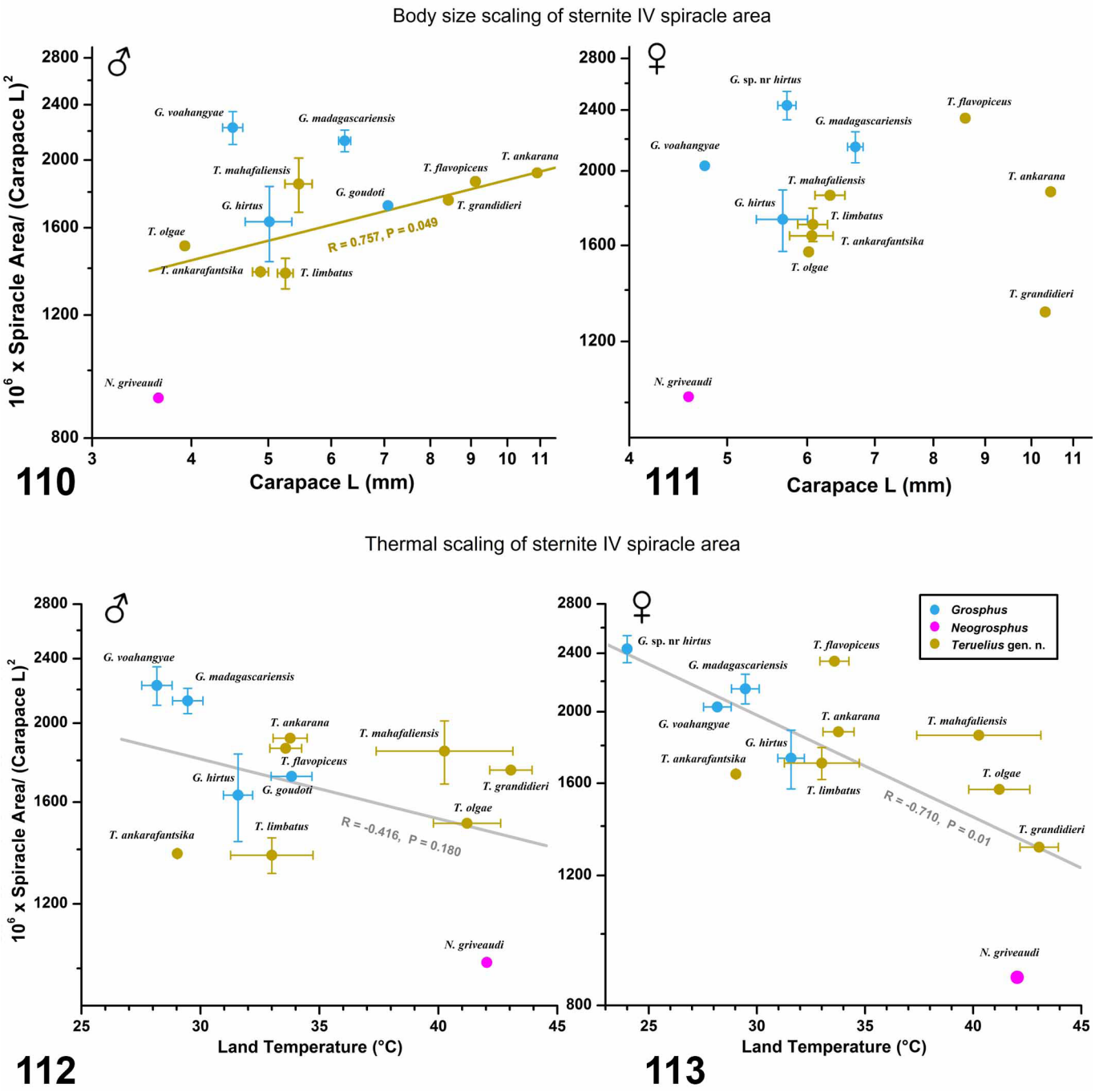

Figures 110–113. Biometric scaling of spiracles of sternite IV in *Grosphus*, *Neogrosphus* and *Teruelius* **gen. n.** **Figures 110–111**. Logarithmic scatter plots showing scaling of single spiracle area/ (carapace length)^2 vs. carapace length in males (110), and females (111) of *Grosphus*, *Neogrosphus* and *Teruelius* **gen. n.** Spiracle length was largest diameter (approximately along mediolateral axis), width was smallest diameter (approximately along rostrocaudal axis). Area was from closed boundary curve: anterior edge of opening sharply delineated, posterior edge sometimes less sharp and fitted with spline curve extrapolating lateral edge curvature and tracing shadow of raised posterior margin. Brown line is least squares linear regression fit of scaling trends for *Teruelius*. R = Pearson correlation coefficient, and P value as indicated. Plotted points are means, error bars SE. **Figures 112–113**. Logarithmic scatter plots showing thermal (terrestrial temperature) scaling of spiracle area/ (carapace length)^2 in males (112), and females (113) of *Grosphus*, *Neogrosphus* and *Teruelius* **gen. n.** Gray lines are least squares linear regression fits of scaling trends for all points. R = Pearson correlation coefficient, P value as indicated. Plotted points are means, error bars SE. Land surface temperatures at known collection sites were averaged over all sites for each species. Collection sites were extracted from published data and FMNH records. Temperatures were extracted from published model data of Chabot-Couture et al. (2014), who estimated annual mean daytime temperature by statistical processing and Kriging of remote sensing spectral radiance by AQUA satellite.

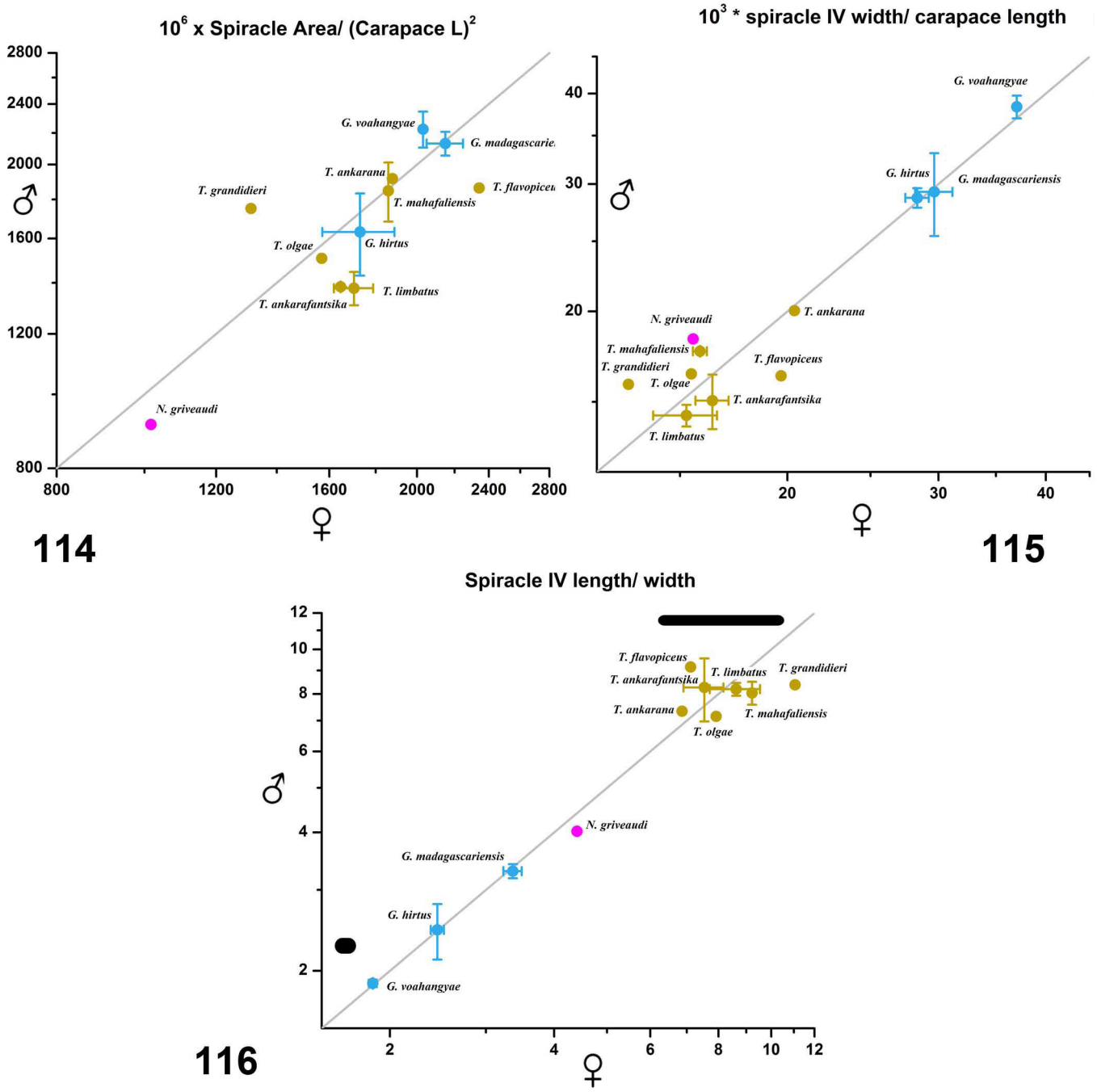

Figures 114–116. Biometrics of spiracles of sternite IV in *Grosphus*, *Neogrosphus* and *Teruelius* **gen**. **n**. Logarithmic scatter plots showing sexual dimorphism of spiracle area/ (carapace length)^2 (114), spiracle width/ carapace length (115), and spiracle length/ width (116) in *Grosphus*, *Neogrosphus* and *Teruelius* **gen**. **n**. Plotted points are means, error bars SE. Ratios are larger in males if points fall above the diagonal (gray) line, larger in females if they fall below it.

of buffered CO_2 in the hemolymph elevates partial pressure gradients of the gases, enhancing their fluxes during transient spiracle-open states when a normal H_2O gradient determines water loss. Desert scorpions have very low water loss rates compared to rainforest species (Hadley, 1974, 1990), and xerophilous buthids have lower respiratory water loss than mesic buthids or scorpionids (Gefen, 2011). This is probably achieved by a combination of low metabolic rate, secretion of a water-impermeant waxy layer on the cuticle (Hadley, 1990), and DGC (Fincke & Paul, 1989). The narrow slit-like geometry of the spiracles of *Teruelius* **gen**. **n**., and other buthids of more xeric habitats, may be better suited to atrial occlusion mechanics of DGC than the broad, ovoid or elliptical spiracles of *Grosphus*.

Fage (1929) appreciated the correlation of climatic factors with taxonomic divisions of the genus into his 'Group I' (= *Grosphus* sensu stricto) and Group II/III (= *Teruelius* **gen**. **n**.): "Tout se passe donc, en réalité, comme si les organes auxquels

nous empruntons les caractères spécifiques du genre *Grosphus* étaient dans une large mesure influencés par le climat." Speculating about respiratory function, Fage focused on pectines instead of spiracles, incorrectly thinking that pectines were used as oscillating fans to blow fresh air over spiracles (Ubisch, 1921). In fact, pectines do play a role in respiration, not as ventilators but as chemosensors for adaptively modulating spiracular responses to CO_2 (Farley, 1990).

Another potential benefit of the long, narrow spiracles of *Teruelius* **gen**. **n**. in drier environments is protection of booklungs from particulate contamination by sand and dust. Respiratory systems of some desert animals incorporate mechanisms to exclude fine particles (Stadler et al., 2016; Stebbins, 1943). Entry of sand and dust is probably not an important abiotic factor in humid rainforests where *Grosphus* is found. However, *Grosphus hirtus* has ovoid spiracles and occurs in dry deciduous forests, where there is often a sandy substrate (Lourenço & Wilmé, 2015a). It may have evolved ecological or behavioral adaptations to mitigate particulate contamination of the respiratory system.

The exceptionally low fractional spiracle area of *Neogrosphus griveaudi* may relate to its subarid habitat combined with its small size (Lourenço et al., 2006b). Mass-specific rate of diffusional water loss is greater in smaller arthropods due to a higher surface-to-volume ratio, which predicts inverse scaling of water loss vs. carapace length. This means larger species can afford higher spiracular areas without increasing water loss per unit body mass, and this may account for the positive scaling seen in Fig. 110. The allometric exponent for male *Teruelius* **gen**. **n**. was + 0.29, well below than the theoretical maximum of +1 for maintaining constant water loss based on a surface-to-volume model.

Respiratory water loss may explain other observations. The spiracles on the more posterior sternites have a narrower shape in *Grosphus*, a property noticed by Kraepelin (1891: 72). The posterolateral locations of the hindmost spiracles on sternite VI expose them more directly to ambient air flow and thus increased water loss. The foremost spiracles on sternite III are located near the mid-ventral part of the body, which is a more sheltered location closer to the substrate, with a more humid microenvironment.

If spiracle area is related to respiratory water loss, then it should be correlated with relevant environmental parameters. To test this, we plotted fractional spiracle area against mean land temperature of recorded collection sites for each species (Figs. 112–113). Spiracle area was inversely related to temperature, in accord with experimental findings of increased respiratory water loss at higher temperatures in scorpions (Gefen et al., 2009). Again, *Neogrosphus griveaudi* was a conspicuous outlier with much smaller spiracle area than predicted by thermal scaling lines of other genera, possibly a consequence of its small body size.

Metasoma I ventromedian carinae

Previously, Fage (1929) noted in his key that metasomal segments of species in his 'Group I' ('*Grosphus*' sensu stricto: *G. madagascariensis, G. hirtus*) have granulated ventromedian carinae, whereas those in his 'Group II/ III' (*Teruelius* **gen**. **n**.: *T. flavopiceus*, *T. annulatus*, *T. limbatus*, *T. bistriatus*, *T. grandidieri*) have smooth ventromedian carinae. The latter characterization is an over-simplification because carinae of posterior metasomal segments of *Teruelius* **gen**. **n**. spp. are granulate. We restricted this criterion to the ventromedian carinae of metasoma I, which show more consistent differences. These carinae are moderately to strongly granulate/ crenulate, usually with sharp granules, in *Grosphus* (Figs. 122–125), and moderately to weakly granulate/ crenulate, usually with blunt granules, or smooth, in most *Teruelius* **gen**. **n**. (Figs. 126–132). In *Neogrosphus*, these carinae are well defined and finely granulate.

Tarsal setation

Setation of tarsal segments has been applied to diagnose many scorpion taxa (Soleglad & Fet, 2003b), but was seldom applied to *Grosphus*. Fage (1929: 641) characterized *Grosphus* (sensu lato) as having a paired series of setae on the ventral surface of the telotarsus. However, inspection of the ventral surfaces of telotarsi reveals a conspicuous difference between setation of *Grosphus* and *Teruelius* **gen**. **n**. (Figs. 133–144). The telotarsi in *Grosphus* bear small numbers (< 20) of short socketed, tapered macrosetae arranged simply along its axis in two discrete rows (Figs. 133–137), whereas those in *Teruelius* **gen**. **n**. bear large numbers (> 20) of long, filiform socketed macrosetae not arranged in linear rows, but spread over the ventral surface to form a dense brush or scopula (Figs. 138–144; cf. also Soleglad & Fet, 2003b, fig. 16). A similar difference in the density of setation is seen on the ventral aspect of the distal basitarsus. Setation on the telotarsus of *Neogrosphus* resembles the condition in *Teruelius* **gen**. **n**., consisting of a dense cover of long, fine setae (Figs. 618–619; Vachon, 1969: figs. 8–9).

We suggest that the tarsal 'scopula' in *Teruelius* **gen**. **n**. is an adaptation to life on loose sandy or silty soils in more arid regions of Madagascar, where the genus is prevalent. It could offer biomechanical advantages for traction during locomotion over loose substrates, like the basitarsal bristle-combs of psammophilous scorpions (Fet et al., 1998).

UV fluorescence

Fluorescence of the hyaline exocuticle of scorpions under UV light is a well known phenomenon (Hjelle, 1990). It was not used as a taxonomic character until Lourenço (2012b) proposed a lack of fluorescence as a potential diagnostic character for chaerilids. He tested 9 species of *Chaerilus*, all of which exhibited greatly reduced or undetectable fluorescence compared to several other control scorpions (5 pseudochactids, 6 buthids). While applying UV imaging methods in our study, we noticed a consistent difference in fluorescence emission between *Grosphus*, and *Neogrosphus*/ *Teruelius* **gen**. **n**. The emission was quite weak in *Grosphus*, and strong in *Neogrosphus* and *Teruelius* **gen**. **n**. Figs. 145–

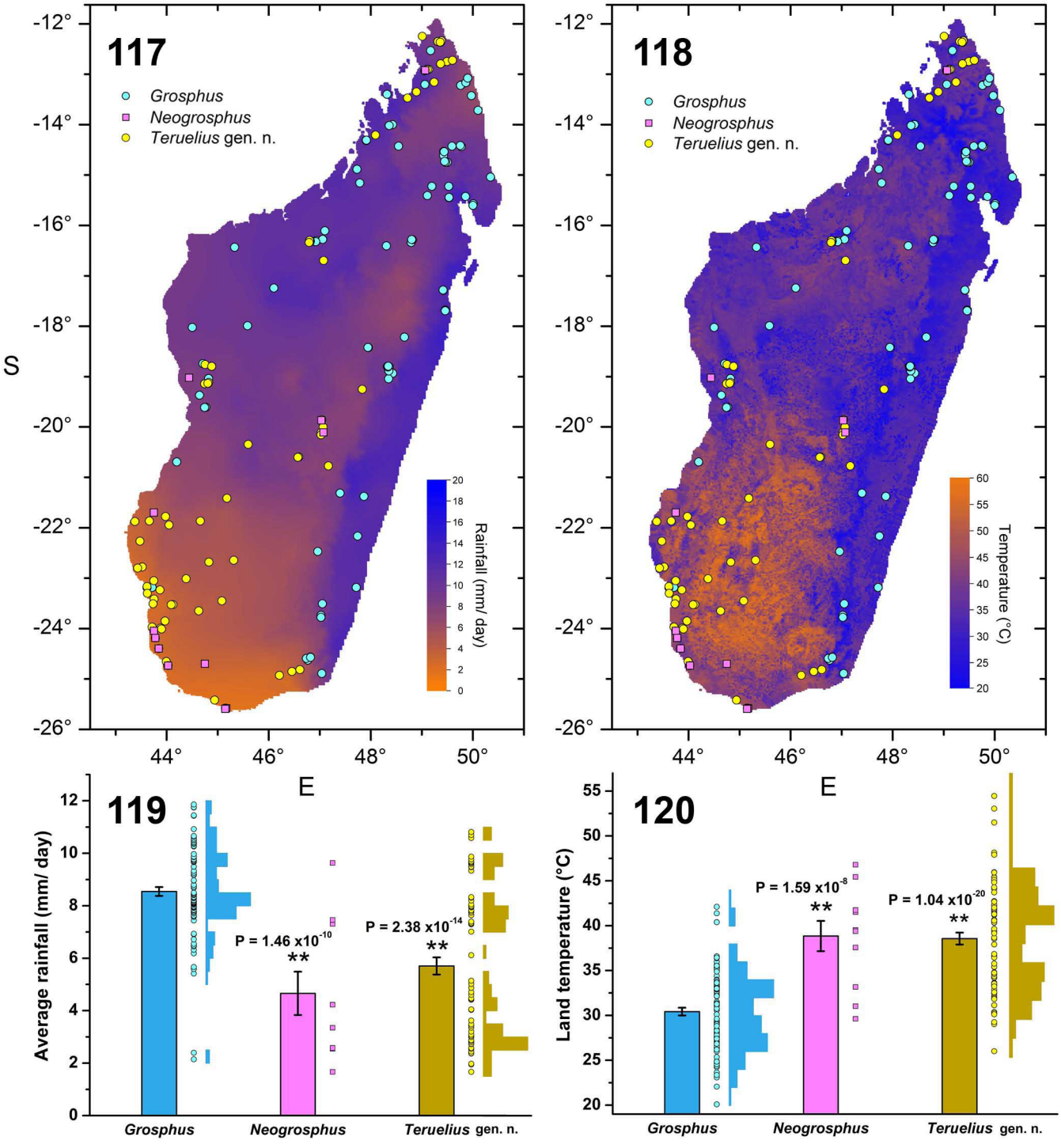

Figures 117–120. Distributions of *Grosphus*, *Neogrosphus* and *Teruelius* **gen. n.** superposed on climate maps. **Figure 117**. Collection sites superposed on average rainfall map. **Figure 118**. Collection sites superposed on land temperature map. **Figure 119**. Distribution of each genus according to average rainfall. **Figure 120**. Distribution of each genus according to land temperature. Vertical histogram bars in Figs 119–120 are means, error bars SE. P-values and asterisks indicate significant differences of *Neogrosphus* and *Teruelius* **gen. n.** means from *Grosphus* means. Symbols in bar charts are collection sites collapsed along rainfall axis (119), or temperature axis (120). Inset horizontal histograms show relative (normalized) densities of points vs. rainfall or temperature (vertical axes). Collection sites were extracted from published data and FMNH records. Rainfall and temperatures were extracted from published model data of Chabot-Couture et al. (2014), who estimated January and July rainfalls by interpolation of RFE 2.0 data, and annual mean daytime temperature by statistical processing and Kriging of remote sensing spectral radiance by AQUA satellite. We averaged January and July rainfalls to generate a single map.

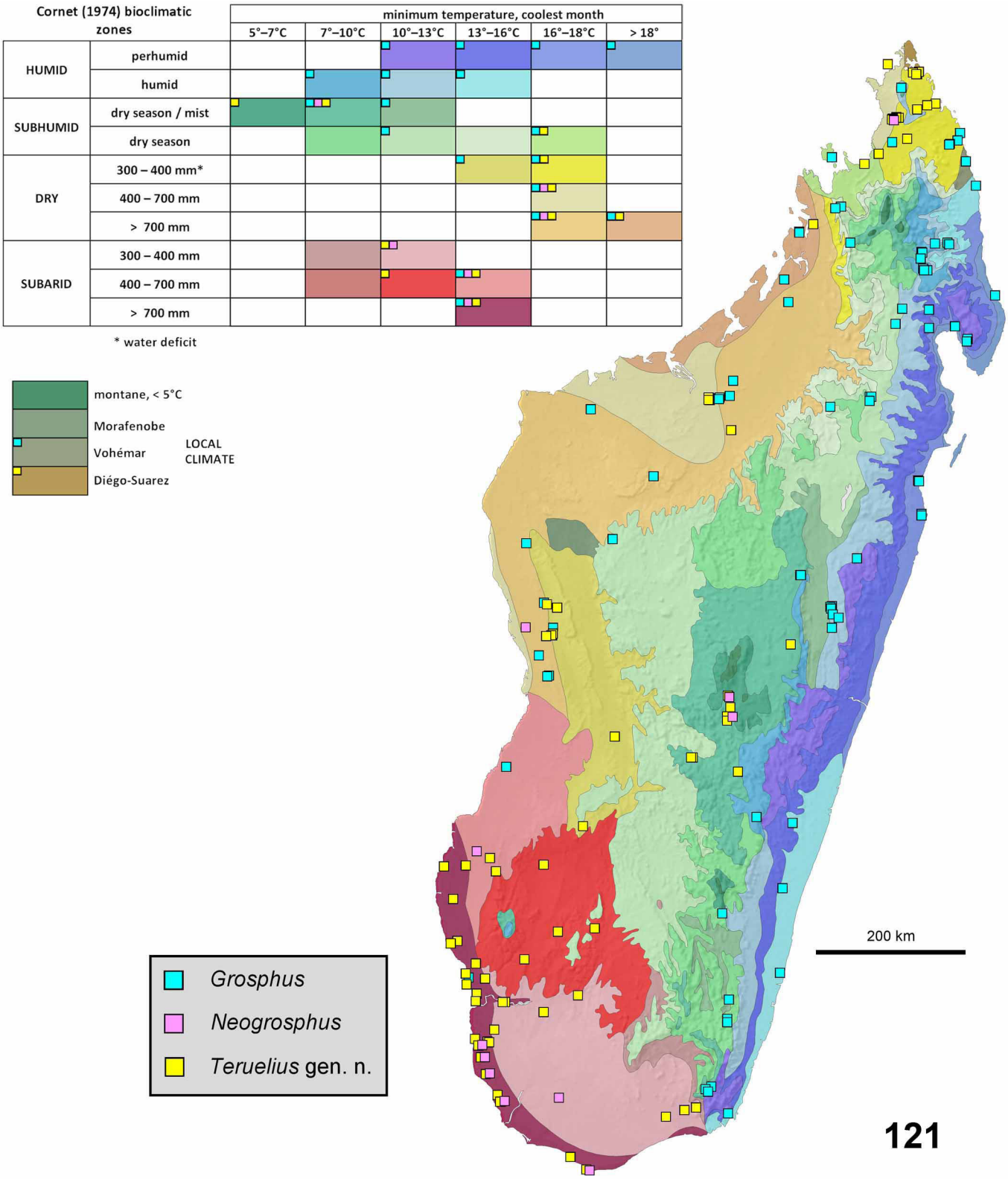

Figure 121. Bioclimatic zone distributions of *Grosphus*, *Neogrosphus* and *Teruelius* **gen. n.** in Madagascar. Collection sites were extracted from published data and FMNH records, and their bioclimatic classification visualized by superposition on zone boundaries defined by Cornet (1974). Colored regions show zones as delineated by Cornet, and symbols for genera are placed on the map and on zone keys of Cornet (upper left inset) to show ranges of humidity and temperature tolerance of each genus.

157 illustrate this difference between emission intensities of *Grosphus* and *Teruelius* **gen**. **n**. when excited by the same power UV source.

To quantify the differences, we measured fluorescence intensity from a standard reference spot on the medial area of sternite VI by fluorescence microscopy, using an avalanche photodiode to detect light emitted over 515–570 nm, a wavelength range capturing most of the longer half-peak of the emission spectrum (Hjelle, 1990; Kloock, 2009; Lowe et al., 2003). The measurement spot was chosen for easy access and uniform, smooth cuticle free of dense setation, strong granulation or carination that can introduce local inhomogeneity in fluorescence intensity. The horizontal histogram in Fig. 158 shows that the means of measured photodiode currents (proportional to intensity) from *Grosphus* all fell below the means from *Teruelius* **gen**. **n**. The error bars show variability across individuals of the same species. There was also variability across species in the same genus, but we do not consider this to be significant because our sample sizes were small. The fluorescence of an individual specimen is highly dependent on history of exposure to light, and observed variation could be caused by variations in photobleaching that occurred in the past (Kloock, 2009; Lourenço & Cloudsley-Thompson, 1996). Could the weaker fluorescence in *Grosphus* compared to *Teruelius* **gen**. **n**. also be due to random prior bleaching? This is statistically unlikely given the sample sizes and ranges of variation in fluorescence (means: *Grosphus* 5.45 ± 0.61, N = 4; *Teruelius* **gen**. **n**.: 12.43 ± 1.19, N = 7; means different at significance level P = 0.0012, t = -4.17, 9 degrees of freedom, one tailed t-test). Photobleaching of fluorophore(s) in scorpion cuticle is not as rapid as rates of some other fluorescent compounds, but there can be severe cumulative fading over years in museum specimens not stored in the dark. For example, we examined a sample of 12 *T. limbatus* that were packed together into a small bottle, and found specimens with fluorescence very unevenly distributed over their bodies. Some areas were strongly fluorescent while others were almost dark, indicating strong differential photobleaching. The bottle may have been stored on a shelf exposed to sunlight which bleached some body parts while other parts were shielded by other specimens in the bottle. Photobleaching of scorpion fluorescence by UV light was documented by Kloock (2009), and used as an experimental tool by Kloock et al. (2010). We predict that intrageneric variation of fluorescence in *Grosphus* and *Teruelius* **gen**. **n**. will prove to be less than what we found here if experiments are conducted on freshly collected materials, and we predict a clear gap between fresh emission intensities of *Grosphus* vs. *Teruelius* **gen**. **n**.

Figs. 159–160 show the kinetics of UV photobleaching in two representative species of *Grosphus* and *Teruelius* **gen**. **n**. There was a steady decrement in photodiode current during 10 min recording sessions. The normalized curves reveal that the speed and extent of photobleaching was different for each specimen, ranging from ca. 3% to 17% in *G. madagascariensis*, and ca. 5% in *T. limbatus*. Decays were mono-exponential, but with different time constants (654.4 s vs. 347.5 s, respectively in *G. madagascariensis*; 640.2 s in *T. limbatus*). To avoid confounds from photobleaching, data in the histogram Fig. 158 were obtained by averaging signal over the first 5 s after switching on the UV light, a sufficiently brief period for bleaching to be negligible. Bleaching kinetics was not specific to genus, as the decay curve for *T. limbatus* fell between the two curves for *G. madagascariensis*. The differences in photobleaching, expressed as a percentage of baseline fluorescence, may be due to differences in past histories of cumulative photobleaching in individual specimens. Specimen #2 of *G. madagascariensis* had a lower baseline fluorescence than specimen #1, and it also had greater percentage bleaching. The decay time constant of ca. 650 s for *T. limbatus* and the less bleached *G. madagascariensis* #1 may be a more accurate estimate of normal bleaching kinetics.

Discussion

Phylogeny.

Previously, cladistic analyses placed *Grosphus* in a monophyletic group together with *Parabuthus* and *Uroplectes*. *Grosphus* (represented by type species *G. madagascariensis*) was resolved as the sister taxon to *Uroplectes*, and *Uroplectes* (represented by *U. triangulifer*) as sister to *Parabuthus* (Prendini, 2001, 2003, 2004b). *Parabuthus* and *Uroplectes* are prevalent buthids in adjacent eastern and southeastern Africa, and have been considered to be related to *Grosphus* (e.g., Fage, 1929; Lourenço, 2003a; Pocock, 1890). Another cladistic analysis placed the southeast African genus *Pseudolychas* as sister to the clade (*Grosphus*, (*Uroplectes*, *Parabuthus*)) (Prendini, 2004a). We relied upon nine characters to diagnose *Teruelius* **gen**. **n**. and differentiate it from *Grosphus* (sensu stricto). Below, we discuss the polarity of each of these characters, making outgroup comparisons to the presumed basal sister genus *Pseudolychas* (Figs. 162–164, 620–641). We also compare these characters for *Parabuthus*, *Uroplectes*, other buthids with α-configuration of femoral trichobothria, and chaerilids and pseudochactids which are hypothesized to be primitive sister groups of all buthids (Prendini et al., 2006; Soleglad & Fet, 2003b; Sharma et al., 2018; Stockwell, 1989). Relationships of '*Grosphus*' group genera are inferred.

(i) position of femur trichobothrium d_2: dorsal or carinal in *Teruelius* **gen**. **n**.; dorsal, carinal or internal in *Neogrosphus*; carinal or internal in *Grosphus*.

Vachon (1975) established two mutually exclusive femoral trichobothrial configurations in buthids: *alpha* (α) with d_1-d_3-d_4 acute angle opening externally, petite d_2 on internal surface; and *beta* (β) with d_1-d_3-d_4 acute angle opening internally, petite d_2 on dorsal surface. This dichotomy was utilized by Sissom (1990) in his key to buthids, but without taking into account variations in location of d_2. Soleglad & Fet (2003b), presented a preliminary cladistic analysis of α and β patterns allowing d_2 location on either the dorsal or the internal surface. Comparing to basal outgroup

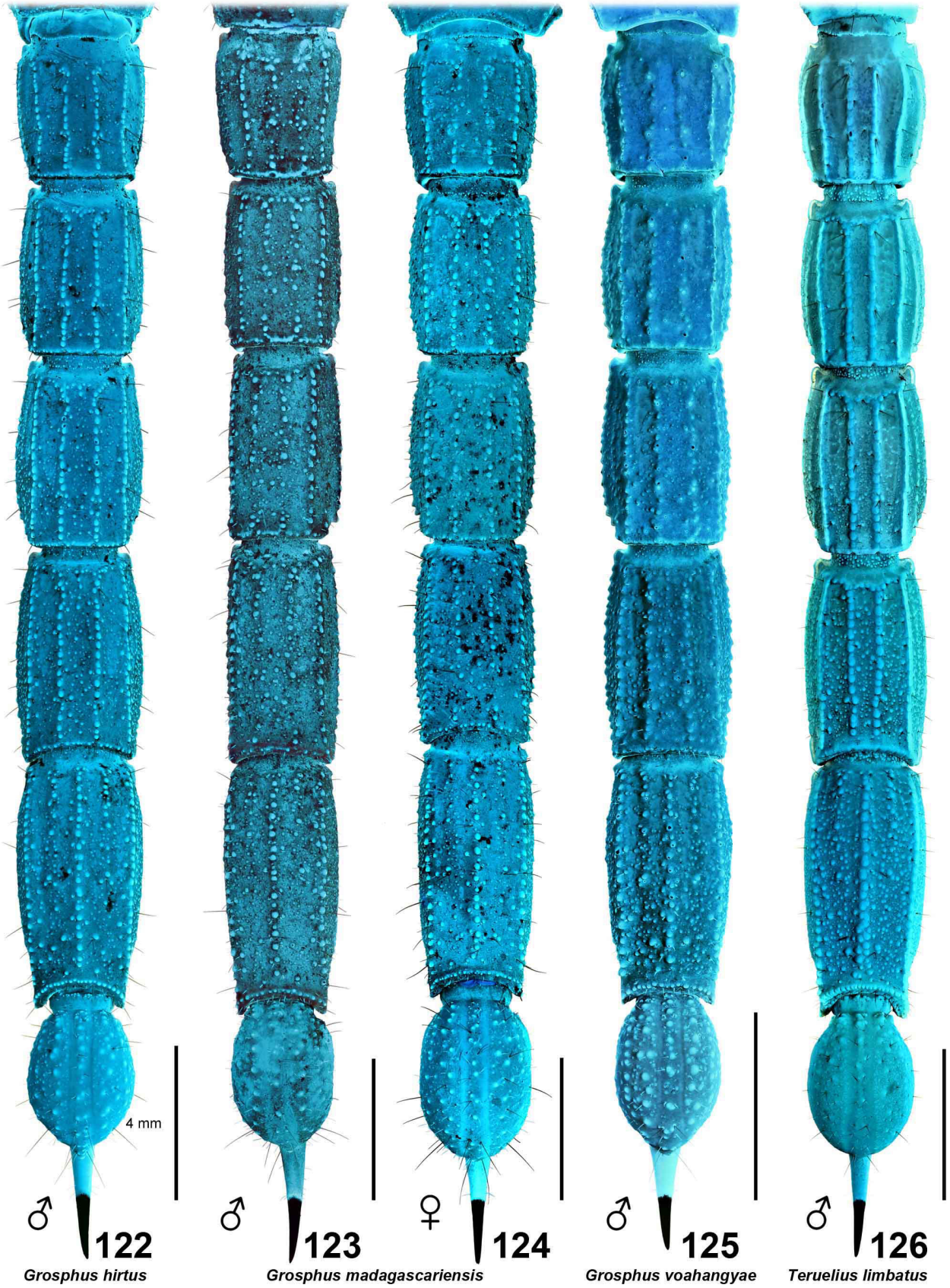

Figures 122–126. Ventral aspect of metasoma and telson of adult males (♂) or females (♀) of representative *Grosphus* spp. and *Teruelius limbatus* under UV fluorescence to reveal carination and granulation. *G. hirtus* (122), *G. madagascariensis* (123 from Anjiro, 124 from Andasibe), *G. voahangyae* (125), and *T. limbatus* (126). Scale bars: 4 mm.

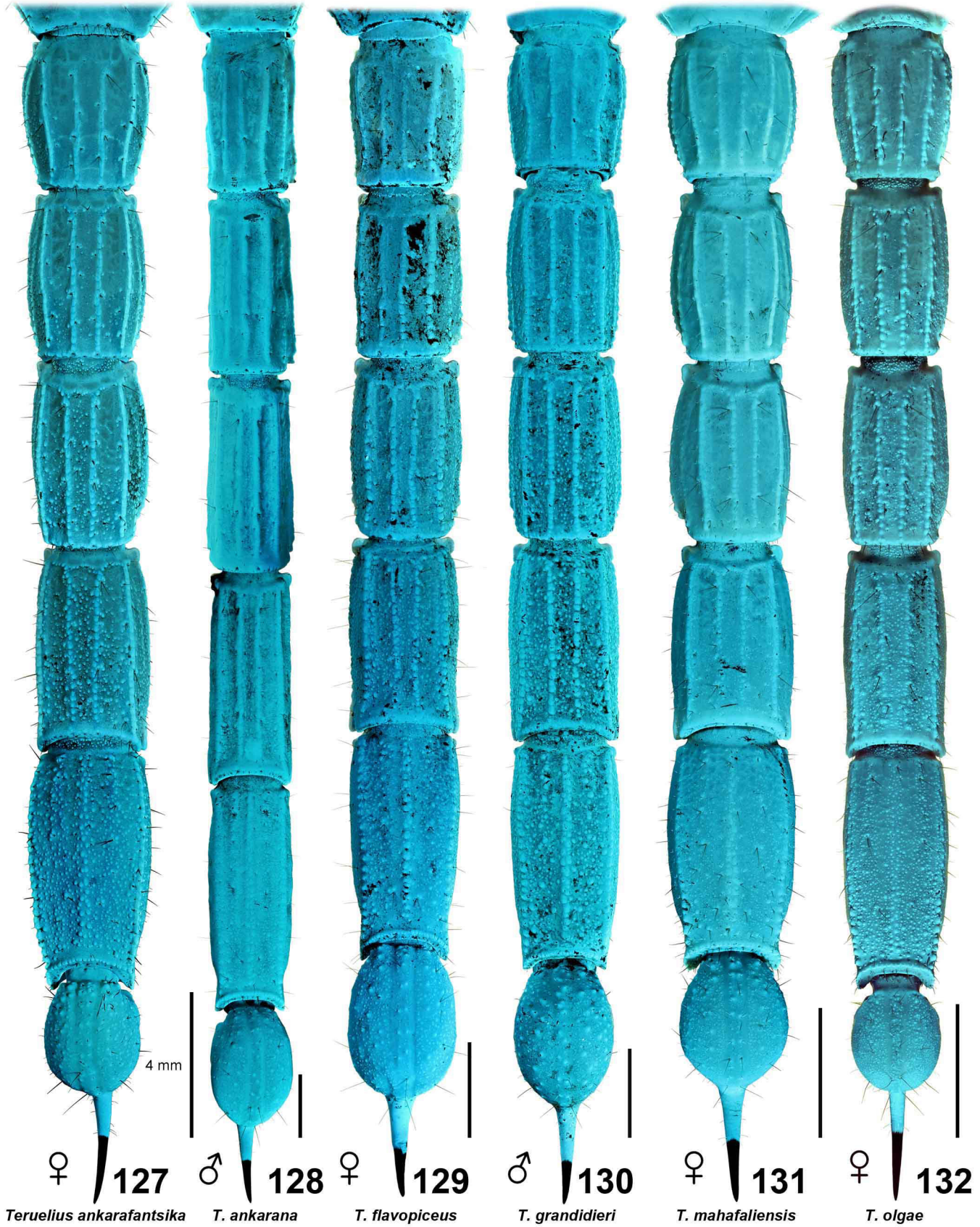

Figures 127–132. Ventral aspect of metasoma and telson of adult males (♂) or females (♀) of representative *Teruelius* **gen**. **n** under UV fluorescence to reveal carination and granulation. *T. ankarafantsika* (127), *T. ankarana* (128), *T. flavopiceus* (129), *T. grandidieri* (130), *T. mahafaliensis* (131), and *T. olgae* (132). Scale bars: 4 mm.

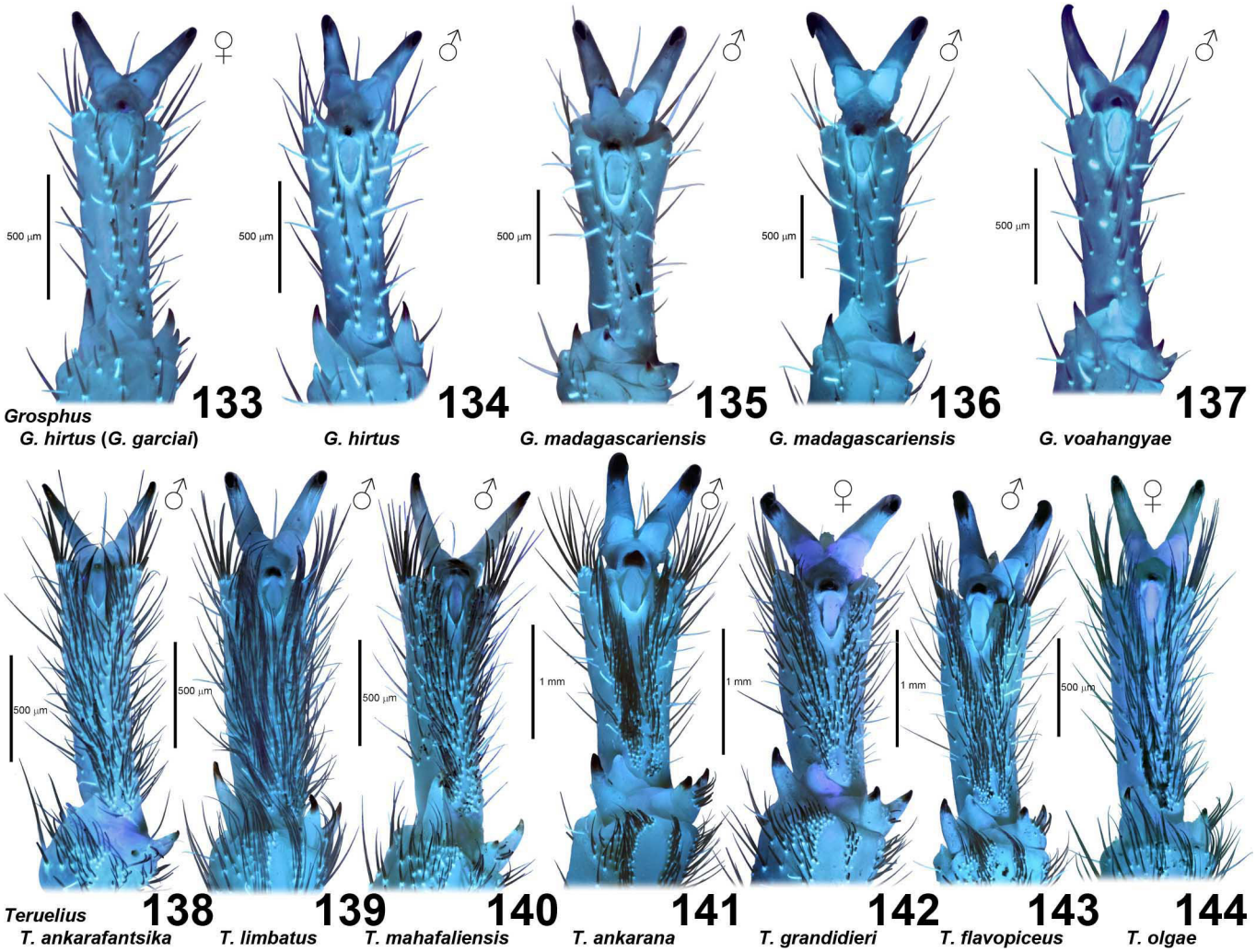

Figures 133–144. Ventral setation of telotarsus III in *Grosphus* and *Teruelius* **gen**. **n**. Ventral surfaces of right telotarsus III of adult males (♂) or females (♀), shown under UV fluorescence to highlight setation. Macrosetae appear dark with strongly fluorescent cuticular sockets at their base. Putative chemosensory microsetae appear bright. *G. hirtus* (= *G. h. garciai*) (133), *G. hirtus* (134), *G. madagascariensis* (135, from Anjiro, 136 from Andasibe), *G. voahangyae* (137), *T. ankarafantsika* (138), *T. limbatus* (139), *T. mahafaliensis* (140), *T. ankarana* (141), *T. grandidieri* (142), *T. flavopiceus* (143), and *T. olgae* (144). Scale bars: 500 µm (133–140, 144) and 1 mm (141–143).

taxa (*Pseudochactas* and *Archaeobuthus*), they inferred that dorsal d_2 was plesiomorphic. Fet et al. (2005) extended the analysis to incorporate position of patella d_3 relative to the dorsomedian carina, and divided buthids into 6 major clades. *Grosphus* and *Neogrosphus* were assigned to the '*Uroplectes*' group on the basis of retention of tibial spurs, α-configuration, and internal d_2 (with *G. madagascariensis* and *N. griveaudi* as representatives).

The dorsal placement of d_2 in *Teruelius* **gen**. **n**. conflicts with the formal definition of the '*Uroplectes*' group, and relegates it to the '*Charmus*' group. However, a comprehensive survey of d_2 was not presented by Fet et al. (2005). The position of d_2 is actually heterogeneous in the '*Uroplectes*' group (see **Appendix 1**). Prendini & Esposito (2010) showed that d_2 placement correlates with two major clades in *Parabuthus* that are well supported by other morphological characters (Prendini, 2001, 2003, 2004b). As in Soleglad & Fet (2003b), they took dorsal d_2 as primitive, but oddly chose *G. flavopiceus* (= *Teruelius* **gen**. **n**., d_2 dorsal) as outgroup species, instead of the type species *G. madagascariensis* (d_2 internal) that was used by Prendini in prior cladistic analyses which did not code d_2 position. Thus, their cladogram shows the relationship of *Parabuthus* to *Teruelius* **gen**. **n**. In their more proximate outgroup taxon, *U. triangulifer*, d_2 was coded as dorsal, but a different choice of *Uroplectes* species could have coded d_2 as internal. Nevertheless, the next level outgroup taxon, *Pseudolychas*, has d_2 dorsal in all 3 species (Prendini, 2004a).

The fact that each of the 3 major genera, *Grosphus* (sensu lato), *Parabuthus* and *Uroplectes* are nearly evenly split in numbers of species having d_2 either dorsal or internal, and *Pseudolychas* also has d_2 dorsal, invalidates the formal definition of the '*Uroplectes*' group. If dorsal d_2 is primitive, then internal d_2 arose independently as a derived state in multiple lineages of α-buthids. In particular, it implies that internal d_2 in *Grosphus* is derived, and dorsal d_2 in *Teruelius* **gen**. **n**. primitive. Conversely, if all four genera had an earlier

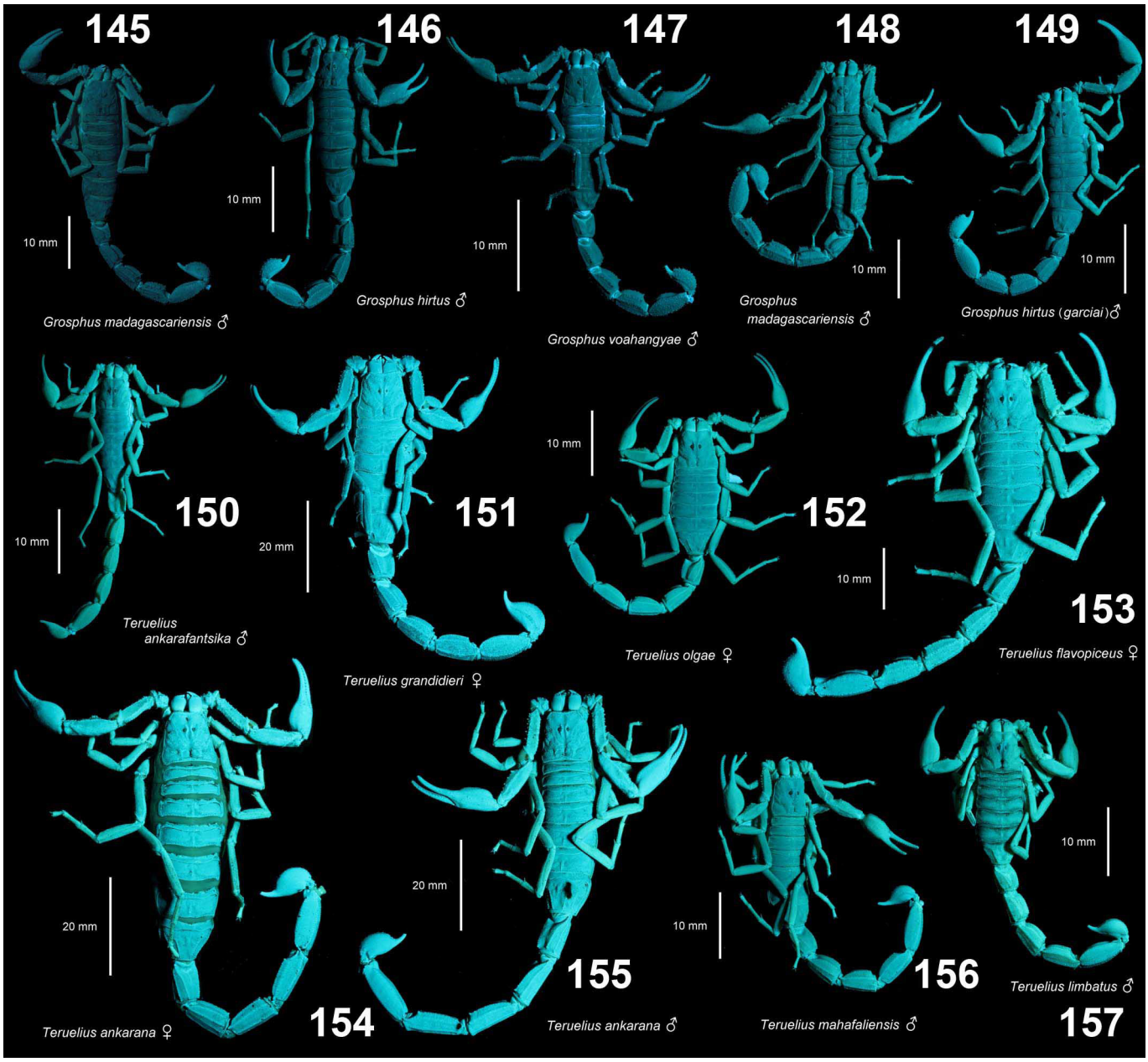

Figures 145–157. Comparative intensity of UV fluorescence in *Grosphus* and *Teruelius* **gen**. **n**. Photographic comparison of fluorescence emission intensities of representative species of each genus, including adult males (♂) or females (♀). *G. madagascariensis* (145 from Anjiro, 148 from Andasibe), *G. hirtus* (146), *G. voahangyae* (147), *G. hirtus* (= *G. h. garciai*) (149), *T. ankarafantsika* (150), *T. grandidieri* (151), *T. olgae* (152), *T. flavopiceus* (153), *T. ankarana* (154–155), *T. mahafaliensis* (156), and *T. limbatus* (157). Images acquired under identical intensities of UV excitation (395 nm LED source, 0.35 A current) and camera exposure (Canon EOS 7D Mark II, 100 mm f/13, 0.5 s, ISO 320), with 475 nm longpass filter to block excitation wavelengths. Scale bars: 10 mm (145–150, 152–153, 156–157), 20 mm (151, 154–155).

common ancestor with d_2 internal, like many other α-buthids (e.g., all of the '*Tityus*' group), then dorsal d_2 was derived repeatedly in these genera.

In *Neogrosphus* we found a dorsal d_2 in *N. griveaudi*, as opposed to the internal position reported by Vachon (1969: 478, fig. 2; 479). Illustrations in Lourenço (1996b: 62, fig. 25) for *N. blanci*, and Lourenço et al. (2015: 772, fig. 4b) for *N. andrafiabe*, appear to indicate d_2 with dorsal or carinal positions. In our diagnosis of *Neogrosphus* we admit all three possibilities until further study.

(ii) relative distance between chela manus trichobothria *Eb*$_3$ and *Eb*$_2$, expressed as a ratio R_{123} = d(*Eb*$_2$, *Eb*$_3$)/ d(*Eb*$_1$, *Eb*$_2$): far or close (0.32–1.02) in *Grosphus*; slightly far (> 0.5) in *Neogrosphus*; close (< 0.5) in *Teruelius* **gen**. **n**.

In *Pseudolychas*, $0.40 < R_{123} < -0.99$, a variable condition like that recorded in *Grosphus* (see **Appendix 1**). In *Parabuthus* and *Uroplectes*, R_{123} is variable, either < 0.5 or > 0.5. In other genera of the '*Uroplectes*' group $R_{123} \geq \sim 0.5$, and the same is true for the '*Tityus*' group (see **Appendix 2**). In the '*Charmus*' group (Fet et al., 2005): *Charmus*, R_{123}

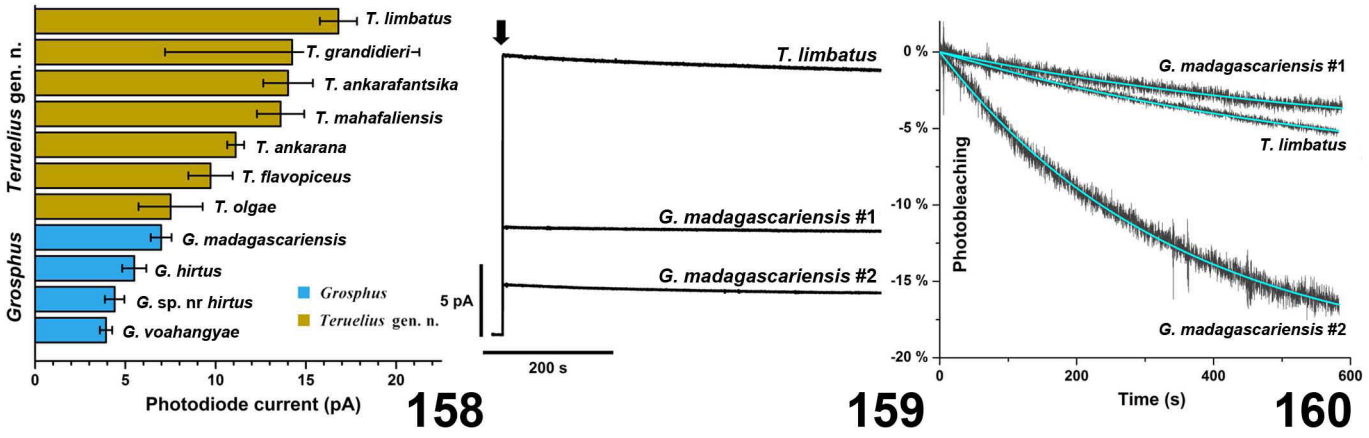

Figures 158-160. Comparative intensity of UV fluorescence in *Grosphus* and *Teruelius* **gen**. **n**. **Figure 158**. Horizontal histograms comparing relative fluorescence emission intensities measured by photodiode current, for *Grosphus* and *Teruelius* species. Histogram bars are means, error bars are SE, species averages over all samples, male and female (sexes not significantly different, P > 0.05). Sample sizes: *G. hirtus*, 1♂, 1♀; *G.* sp. nr *hirtus*, 6♀; *G. madagascariensis*, 9♂, 1♀; *G. voahangyae*, 4♂, 1♀; *T. ankarafantsika*, 2♂, 2♀; *T. ankarana*, 1♂, 1♀; *T. flavopiceus*, 1♂, 1♀; *T. grandidieri*, 1♂, 1♀; *T. limbatus*, 6♂, 5♀; *T. mahafaliensis*, 2♂, 2♀; *T. olgae*, 1♂, 1♀. Sample means may not reflect single specimen intensities recorded in Figs. 145–157. **Figure 159**. Time course of photodiode current in UV fluorescence emission measurement for *T. limbatus* (upper curve), and two specimens of *G. madagascariensis* (middle and lower curves) over 620 s. Arrow indicates time of shutter opening to initiate UV excitation.**160**. Photobleaching time course for UV fluorescence emission of *T. limbatus* (middle curve) and *G. madagascariensis* (upper and lower curves) over 600 s following shutter opening (see Fig. 159). Ordinate is percentage bleaching relative to initial fluorescence after shutter opening. Blue curves are mono-exponential fits with decay time constants: *T. limbatus*, 640.2 s; *G. madagascariensis*, #1 654.4 s and #2 347.5 s.

< 0.5, or > ~ 0.5 (Kovařík et al., 2016c; Sreenivasa-Reddy, 1966); *Somalicharmus*, R_{123} ~1 (Kovařík et al., 2016e); *Thaicharmus*, R_{123} > ~ 0.5 (Kovařík et al., 2007). Thus, in the majority of α-buthids, $R_{123} \geq 0.5$, and we also note that R_{123} > ~ 1 in chaerilids and pseudochactids. We conclude that the condition $R_{123} < 0.5$ in *Teruelius* **gen**. **n**. is derived. This is supported by homogeneity of R_{123} values in *Teruelius* **gen**. **n**. (low CV), compared to their heterogeneity in *Grosphus* (high CV) (Figs. 25–26). A more homogeneous state is consistent with a derived character state inherited from a common ancestor, whereas the higher variability seen in *Grosphus* is suggestive of a paraphyletic group. In *Neogrosphus*, R_{123} was slightly above 0.5, and separated from the range of *Teruelius* **gen**. **n**., so we group the character state with that of *Grosphus*, i.e., primitive relative to *Teruelius* **gen**. **n**.

(iii) pectinal tooth count (PTC): lower in *Grosphus*; higher in *Neogrosphus* and *Teruelius* **gen**. **n**.

Outgroup comparisons of pectinal tooth count are complicated by variations in numbers of teeth across individuals within species, and across species within genera. Interspecific variation shows a positive scaling relation with respect to body size, described by Soleglad's Law (Kovařík et al., 2016d). In Figs. 32–33 we compare body size scaling of PTC in *Grosphus* and *Teruelius* **gen**. **n**. to scaling in the majority of other buthids. The slopes of logarithmic regression lines are shallower for *Grosphus* and *Teruelius* **gen**. **n**., than for buthids overall, indicating weak or no size dependence of PTC. Over their respective size ranges, *Grosphus* counts fell below the average buthid trend, while *Teruelius* **gen**. **n**. counts stayed above it. In this sense, *Grosphus* PTC is indeed 'low', and *Teruelius* **gen**. **n**. PTC is 'high' even accounting for body size scaling. A similar result holds if the comparison is restricted to a subset consisting only of α-buthids, where *Grosphus* and *Teruelius* **gen**. **n**. are taxonomically grouped (Figs. 34–35).

The PTC ranges of *Pseudolychas* (♂ 11–17, ♀ 9–14) are lower than in *Grosphus*, but body size is smaller, so a comparison requires compensation for Soleglad's Law. Figs. 32–35 show that PTCs of outgroup *Pseudolychas* are displaced below the main buthid regression lines, similar to *Grosphus* PTCs. Low PTCs are also characteristic of chaerilids and pseudochactids, which fall far below the main buthid regression lines and well below *Pseudolychas* and *Grosphus* (data not shown). We conclude that the lower PTC range in *Grosphus* is primitive, and the higher range in *Teruelius* **gen**. **n**. is derived. *Neogrosphus* has higher PTCs which group with *Teruelius* **gen**. **n**. in scaling plots.

(iv) shape of female basal pectinal tooth: enlarged, oval or subrectangular, not longer than other pectine teeth in *Grosphus*; enlarged, oval, slightly longer than other pectine teeth in *Neogrosphus*; enlarged, elongated and curved or falcate (sickle-shaped) in *Teruelius* **gen**. **n**.

In *Pseudolychas*, the female basal pectinal tooth is modified in all three species (Lawrence, 1961; Prendini, 2004a). In *P. ochraceus* and *P. pegleri* it is enlarged with a simple, oval shape that most closely approximates the shape in *Grosphus* (Fig. 625). In *P. transvaalicus*, it is reduced in size compared to other pectine teeth, and has a different subtriangular shape (Fig. 632). The presence or absence of peg sensillae has not been reported. In female *Uroplectes*,

the basal tooth is often modified or enlarged, and although variable in size, is typically smaller and lobate or oval like that of *Grosphus* (Kovařík et al., 2016a; Lourenço, 2000c; Prendini, 2015a, 2015b ; Vachon, 1950b). Exceptions include *U. planimanus* (Karsch, 1879) and *U. tumidimanus* Lamoral, 1979, whose females bear a longer, falcate basal tooth, similar those found in *Teruelius* **gen. n.** (Lamoral, 1979; Pocock, 1896). Based on the prevalence of the simple, smaller oval tooth in other related genera, we propose that this a primitive condition in *Grosphus*, and that the more elaborate, elongated, falcate tooth, almost exclusively found in *Teruelius* **gen. n.**, is derived. In *Neogrosphus*, the female basal tooth most closely resembles the enlarged teeth of *Pseudolychas* or *Grosphus*, and we consider it primitive.

The origin of the modified basal tooth has been a subject of some speculation. In *Parabuthus*, the female basal tooth is unmodified, but the basal middle lamella is dilated and can intrude into the line of pectine teeth along the posterior margin of the comb. Pocock (1889a), in comparing *P. villosus* to *T. limbatus*, wrote: "clearly the same result has been attained in these two species by the modification of different structures, and therefore presumably independently in the two." In other words, the structure in *Parabuthus* represents an enlargement and posterior extension of the basal middle lamella, whereas the structure in *Teruelius* **gen. n.** represents an enlargement and modification of the basal pectine tooth. But in the following year he surmised that the structure in *Parabuthus* was derived from fusion of an enlarged basal pectine tooth with the basal middle lamella (Pocock, 1890). This would relegate *Grosphus* to a more basal position with respect to *Parabuthus*, as supported by cladistic analysis (Prendini, 2004a). The occurrence of an enlarged basal pectine tooth or middle lamella in closely related genera with adjacent or overlapping distributions makes it more plausible that these features are connected or homologous. On the other hand, if, as we propose, these organs are important female adaptations serving a reproductive function, for example sperm transfer, then they would enhance fitness and could arise independently. As mentioned above, similar basal pectinal structures are found in a number of other buthids that are not closely related to genera discussed here.

Lourenço (1996d) described the sub-fossil *Tityobuthus copalensis* from copal amber of northern Madagascar, and then renamed it *Palaeogrosphus copalensis*, suggesting that it was related to *Grosphus* because it has a dilated basal middle lamella. This implicitly assumes that the enlarged basal pectine tooth of *Grosphus* represents either a displaced basal middle lamella, or a piece derived from it by fission, i.e., the reverse of Pocock's fusion hypothesis. Fission would imply that the condition in *Parabuthus* is primitive, and precursor to the dilated basal pectine teeth in *Grosphus*, *Teruelius* **gen. n.**, *Uroplectes*, and *Pseudolychas*.

(v) posterior lobe of hemispermatophore capsule: long and blade-like in *Grosphus*; short and rounded in *Neogrosphus* and *Teruelius* **gen. n.**

The hemispermatophore capsule in *Pseudolychas* (Figs. 162–164) is short with a robust, hook-like basal lobe adjacent to the flagellum, and a moderately long, tapered, blade-like posterior lobe terminating in a rounded apex. It is most similar to the capsule and posterior lobe of the '*hirtus*' group of *Grosphus*, and differs from capsules of *Neogrosphus* and *Teruelius* **gen. n.** that lack a blade-like extension. This supports the long posterior lobe of *Grosphus* as being primitive, and the short lobe in *Teruelius* **gen. n.** as being derived. The *Pseudolychas* capsule differs from both in lacking well developed carinae, having an anterior lobe well separated from the posterior lobe by a deep incision of the sperm hemiduct membrane ('2+1' lobe configuration), and a coiled flagellum without a linear pars reflecta. *Parabuthus* has a different capsule layout, with a short posterior lobe and a flagellum that is not separated from it, but attached to its postero-distal margin (Fitzpatrick, 1994; Kovařík et al., 2016d; Lamoral, 1979; Vachon, 1940). *Uroplectes* is more like *Neogrosphus* and *Teruelius* **gen. n.** in having a short, compact posterior lobe separated from the flagellum, but the anterior lobe differs in being disconnected from the posterior lobe and having a finely incised or feathered margin (Alexander, 1959; Kovařík et al., 2016a; Lamoral, 1979; Vachon, 1950b). The capsules of *Parabuthus* and *Uroplectes* appear to be derived with their own specializations.

A perplexing puzzle is the status of *G. madagascariensis*, with its long, monocarinate capsule and a basal lobe far proximal to the flagellum. This condition contrasts with the short capsule of *Pseudolychas*. In the '*Uroplectes*' group, capsules with similar topology are found in *Butheoloides* (Vachon, 1952), *Buthoscorpio* (Kovařík et al., 2016c) and *Tityobuthus* (unpublished data). Among other α-buthids, it is found in '*Charmus*' and '*Tityus*' groups. In β-buthids, it occurs in *Australobuthus*, *Hemilychas*, *Isometroides*, *Isometrus*, *Lychas* and *Reddyanus* (Locket, 1990; Koch, 1977; Kovařík et al., 2016c). The fusiform hemispermatophore of chaerilids has a somewhat elongated monocarinate 'capsule' or sperm duct that lacks lobes, and a distal lamina instead of a flagellum (Bastawade, 1994; Kovařík et al., 2015b, 2016c; Monod et al., 2017; Stockwell, 1989). It is unclear whether the '*madagascariensis*' capsule represents a primitive or derived state, and we leave it here as an unpolarized character.

(vi) spiracle shape: broad, hemielliptic or ovoid in *Grosphus* and *Neogrosphus*, L/W < 5; narrow or slit-like in *Teruelius* **gen. n.**, L/W > 5.

In *Pseudolychas*, spiracles are small, elongate-ovoid or hemielliptic, similar to those of *Grosphus*. This argues for the spiracle shape in *Grosphus* and *Neogrosphus* being primitive, and that in *Teruelius* **gen. n.** being derived. Hemielliptic, ovoid or rounded spiracles are associated with scorpion taxa that have been considered primitive: chaerilids (e.g., Kovařík & Ojanguren Affilastro, 2013; Kraepelin, 1899; Kovařík et al., 2015b, 2018c; Tikader & Bastawade, 1983); pseudochactids (Lourenço, 2007; Lourenço & Pham, 2010; Prendini et al., 2006); and most known fossil buthoids (see **Appendix 1**). In

extant α-buthids, ovoid spiracles are present in several genera in the '*Uroplectes*' group, in all three genera of the '*Charmus*' group, and in many of the '*Tityus*' group. Consistent with our ecophysiological hypothesis, many of these are tropical taxa inhabiting mesic or humid microenvironments where there is likely to be less stress from respiratory water loss.

(vii) metasoma I ventromedian carinae: moderately to strongly crenulate or granulate in *Grosphus*, moderately to weakly crenulate, smooth or obsolete in *Teruelius* **gen**. **n**.

In *Pseudolychas*, metasoma I carinae, including ventromedials, are distinct and finely granulate (Fig. 634; Prendini, 2004a). This supports the weakly granulate or smooth condition in *Teruelius* **gen**. **n**. as derived. In *Neogrosphus*, the carinae are distinct and moderately or finely crenulate/ granulate (Lourenço et al., 2015; Vachon, 1969), similar to the primitive condition in *Pseudolychas*.

(viii) tarsal setation: sparse regular, with two discrete rows of < 20 short setiform setae in *Grosphus*; dense, irregular, with > 20 long, filiform setae in *Neogrosphus* and *Teruelius* **gen**. **n**.

In *Pseudolychas*, telotarsi have simple setation with paired rows of < 20 short macrosetae (Fig. 628; Prendini, 2004a). This supports the setation in *Grosphus* being primitive, and that in *Neogrosphus* and *Teruelius* **gen**. **n**. being derived. Other '*Uroplectes*' group genera bear two discrete rows of short to medium length setae, i.e., *Butheoloides* (Kovařík, 2015, 2016; Lourenço, 1996e, 2013a; Vachon, 1952), and *Buthoscorpio* (Javed et al., 2010; Tikader & Bastawade, 1983; Vachon, 1961). In pseudochactids, telotarsi bear two linear rows of non-socketed spinules, and in chaerilids they bear two linear rows of short, socketed macrosetae (Soleglad & Fet, 2003b).

In *Parabuthus*, there are numerous long macrosetae that may be roughly arrayed in two series, but tend to be scattered and not organized into discrete rows or paired (Fitzpatrick, 1994; Kovařík et al., 2016d; Prendini, 2000, 2004b; Prendini & Esposito, 2010). In *Uroplectes*, there is typically a dense brush of usually > 20 long, fine, filiform setae, scattered or arranged in two broad strips, not well aligned in rows (Kovařík et al., 2016a; Vachon, 1950b). We regard these as derived conditions. An exception is *U. planimanus* (Karsch, 1879) with two, linear rows of < 20 shorter, spiniform setae, which could represent a primitive condition within that genus.

(ix) UV fluorescence: weak in *Grosphus*; strong in *Neogrosphus* and *Teruelius* **gen**. **n**.

In the genus *Pseudolychas*, we observed relatively weak UV fluorescence, indicating the weak fluorescence of *Grosphus* to be the primitive state within this clade of buthids. In *Uroplectes* and *Parabuthus*, we observed strong UV fluorescence in most species. Two curious exceptions were very weak fluorescence in *U. flavoviridis* Peters, 1862 and *U. olivaceus* Pocock, 1896, whose dark green pigmentation is unusual for scorpions. Absence of fluorescence in chaerilids (Lourenço, 2012b), a potential buthid outgroup, suggests that buthid fluorescence is derived. However, another possible outgroup, the Pseudochactidae, exhibits stronger fluorescence (Lourenço, 2012b; Prendini et al., 2006). Lowe (2010a) reported weak UV fluorescence in *Microbuthus gardneri* Lowe, 2010. It appears that while strong fluorescence is widespread in scorpions, weakness or loss can occur in some lineages or taxa.

Fluorescence was hypothesized to be utilized by scorpions for their own nocturnal UV detection purposes (Gaffin & Barker, 2014; Kloock et al., 2010), or as UV shielding or sunblock (Frost et al., 2001; Lourenço & Cloudsley-Thompson, 1996). In this context, we point out that weaker fluorescence in *Grosphus* roughly correlates with its preference for forested habitats having more closed canopies and a lower UV index, while stronger fluorescence in *Neogrosphus*/ *Teruelius* **gen**. **n**. correlates with terrain having more open vegetation and a higher UV index. This could be relevant to either the UV detection hypothesis or the sunblock hypothesis. Although as nocturnal animals, sunblock may seem irrelevant for scorpions, circadian biology and UV microenvironments of *Grosphus*/ *Teruelius* **gen**. **n**. have not been documented. Diurnal activity is known in some scorpions: *Parabuthus villosus* (Peters, 1863) (Harington, 1982), *Euscorpius flavicaudis* (Cloudsley-Thompson, 1978; Wanless, 1977), *Scorpio maurus* Linné, 1758 (Krapf, 1986), and *Serradigitus littoralis* (Williams, 1980) (Due & Polis, 1985).

Rubin et al. (2017) argued that cuticular fluorescence is primitive for the order because it is found in the Xiphosura, a primitive sister group of scorpions. Like scorpions, xiphosurans possess a hyaline exocuticle, and it was suggested that the fluorescence originates from this cuticular layer. They argued that eurypterids, another basal outgroup of scorpions, were fluorescent because SEMs of fossils revealed a similar hyaline layer. However, possession of a hyaline layer may not be a sufficient condition for fluorescence, since non-fluorescent chaerilids presumably have this layer as well. According to the authors, the supposed fluorescence in aquatic ancestors implies that "it did not develop as a protection against UV light during terrestrialization (Lourenço & Cloudsley-Thompson, 1996)." But Lourenço & Cloudsley-Thompson (1996) did not discuss colonization of land by scorpions, only the possibility of sunblock. It is not inconceivable that UV blocking agents could have been an asset for aquatic scorpion-ancestors in brightly sunlit, shallow coastal waters. UV radiation can efficiently penetrate water (e.g., Quickenden et al., 2000; Morel et al., 2007; Smith & Baker, 1981), even in the presence of organic solutes (Bricaud et al., 1981; D'Sa et al., 1999) and is deleterious to aquatic life (Häder et al., 2011). Various marine organisms evolved UV screening compounds to protect against the damaging wavelengths (Dionisio-Sese et al., 1997; Dunlap et al, 1986, 1989; Häder et al., 2011).

Table 4 summarizes inferred polarities of our taxonomic characters for *Grosphus*, *Neogrosphus* and *Teruelius* **gen**. **n**., determined by outgroup comparisons to *Pseudolychas*. The hemispermatophore capsule shape and position of basal lobe was not polarized, but included to indicate the internal

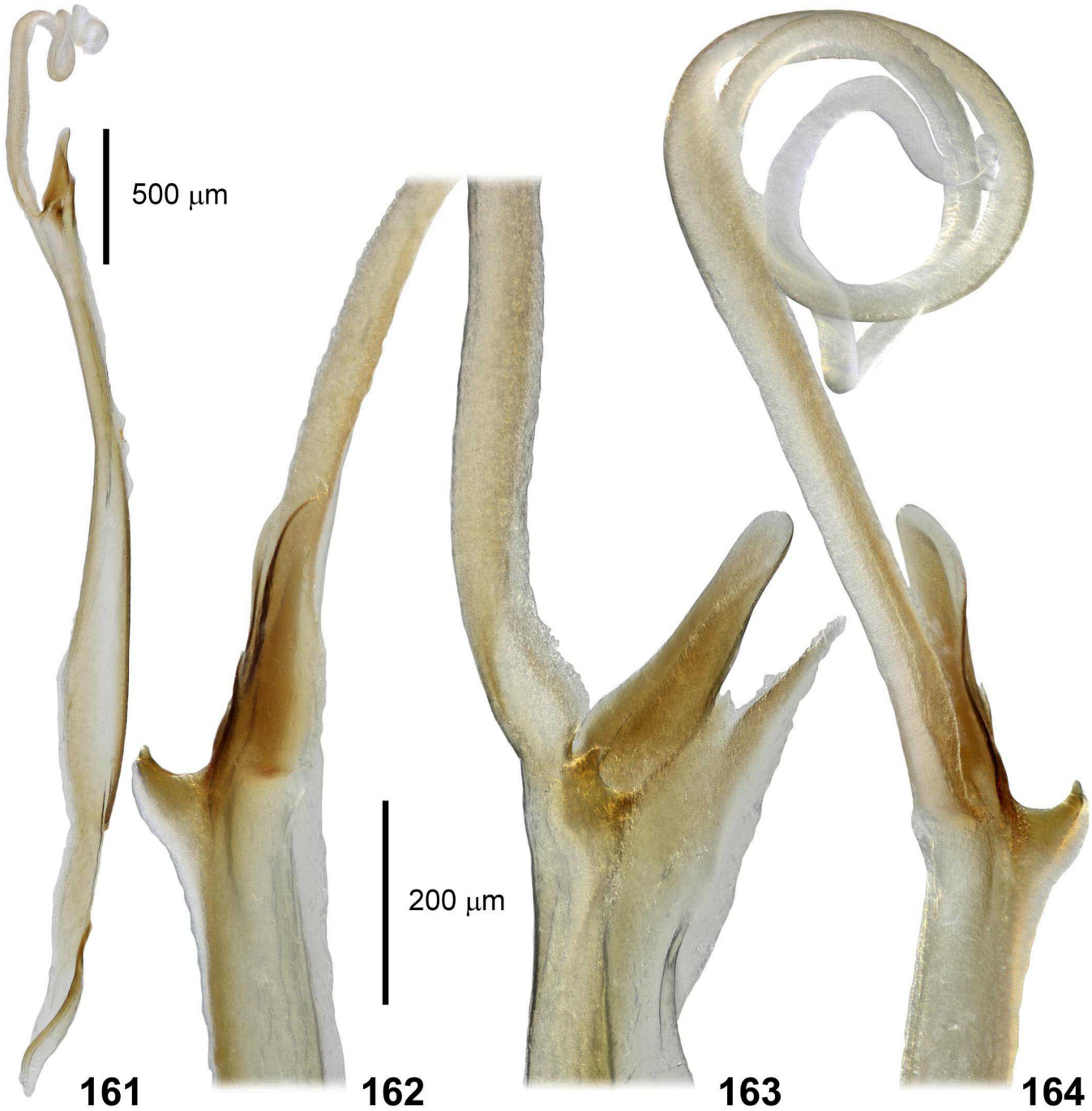

Figures 161–164. Hemispermatophore of *Pseudolychas pegleri* (Purcell, 1901). Whole hemispermatophore (161), and capsule region in anterior (162), convex compressed (163), and posterior (164) views. Scale bars: 500 μm (161), 200 μm (162–164). Right hemispermatophore (JA1418).

dichotomy between '*madagascariensis*' and '*hirtus*' groups of *Grosphus*. Species of *Teruelius* **gen**. **n**. have a majority of shared derived characters, whereas *Grosphus* species have mostly primitive characters. This supports the conclusion that *Teruelius* **gen**. **n**. is monophyletic, and *Grosphus* is paraphyletic. Monophyly of *Neogrosphus* is supported by 4 of 9 characters derived, vs. 4 primitive (femur d_2 position ambiguous). We suggest that *Neogrosphus* represents an intermediate form, descended from a common ancestor shared with *Teruelius* **gen**. **n**.

Biogeography.

What are the origins of *Grosphus*, *Neogrosphus* and *Teruelius* **gen**. **n**.? All three are Madagascar endemics, implying that either they evolved from ancestors present on the island after it was isolated from other landmasses by continental drift (vicariance model), or they are descendants of individuals that colonized it after isolation by marine barriers (dispersal model). In a vicariance model, during the breakup of Pangaea in the mid- to late-Jurassic, the rifting of Indo-Madagascar from Africa ca. 160–130 Mya (de Wit, 2003) separated ancient precursors of the

'*Grosphus*' group from ancestors of east African genera with nearest affinities, i.e., *Pseudolychas*, *Uroplectes* and *Parabuthus*. Subsequently, *Grosphus*, *Neogrosphus* and *Teruelius* **gen**. **n**. lineages evolved over a long period. Early *Grosphus* ancestors were adapted to more mesic or humid environments existing in the Late Cretaceous (Ohba et al., 2016), and persisted through the K-T mass extinction 66 Mya. In the early half of the Paleogene (66–30 Mya), it is theorized that Madagascar's climate was largely arid, due to its location in the 30°S subtropical belt of high atmospheric pressure (Wells, 2003). Physiological stress of aridity was further exacerbated during the Paleocene-Eocene thermal maximum 55 Mya (Gingerich, 2006). Conditions at this time spurred evolution of arid-adapted genera, *Neogrosphus* and *Teruelius* **gen**. **n**. A similar history was suggested for the hormurid genus *Opisthacanthus* which has a Gondwanan distribution (South America, Africa and Madagascar). It is also postulated to have persisted across the K-T boundary, after which species isolated on Madagascar became adapted to arid Paleogene conditions (Lourenço et al., 2018a).

During the arid Palaeogene, ancestral *Grosphus* could have survived in montane refugia. *Grosphus* eventually became more widespread again in the late Paleocene/ early Eocene when Madagascar drifted out of the arid belt into more northern latitudes where it received moisture laden southeasterly trade winds (Wells, 2003). Fed by orographic precipitation, rainforests flourished along the east and provided humid habitats where many contemporary *Grosphus* now reside. Wood et al. (2015) proposed similar refugia models for archaeid spiders, an ancient Gondwanan family that in Madagascar is found mostly in the rainforests. Their ancestral area estimation traces Madagascar archaeids back to rainforest habitat in the Upper Jurassic, 150 Mya. Extant diversity of the two groups is comparable: 21 known archaeid species in Madagascar, vs. 31 species of '*Grosphus*' group scorpions. In the *Paroedura* geckos of Madagascar, DNA data indicate that two eastern and northern rainforest species are basal, eight northwestern/ Comoros species are polyphyletic, and six southwestern arid zone species form a monophyletic clade (Jackman et al., 2008). This topology roughly parallels our biogeographic model of *Grosphus* as the more basal paraphyletic group mainly found in humid/ dry eastern and northern regions, and *Teruelius* **gen**. **n**. as the derived monophyletic genus mainly found in the dry/ subarid southwest.

If *Grosphus* has Cretaceous origins, the elongate spermatophore capsule of the '*madagascariensis*' group could be a relic from this era. Apart from *Tityobuthus*, the geographically closest α-buthids with elongate capsules are *Butheoloides* of Africa, and the '*Charmus*' group of peninsular India. Possible Gondwanan links between Madagascar endemics and Oriental/ Indian scorpions have been suggested, for example between *Microcharmus* and the '*Charmus*' group; and between *Tityobuthus* and *Himalayotityobuthus* (Lourenço, 1996b, 1997, 2003b, 2011). On the other hand, the elongate '*madagascariensis*' capsule could be an autapomorphy if the short capsule of *Pseudolychas* models the primitive state for the '*Grosphus*' group as a whole.

The vicariance model assumes that the '*Grosphus*' group is derived from an ancient paleaoendemic lineage. However, a dated molecular analysis of the '*Tityus*' group in South America (Ojanguren-Affilastro et al., 2017a) estimated that *Teruelius flavopiceus* split from *Parabuthus* much more recently, ca. 30–15 Mya (Oligocene to early Miocene). To explain this, we can invoke a dispersal model in which an ancestor of *Teruelius* **gen**. **n**. spreads from Africa to Madagascar by marine rafting (Simpson, 1940). The estimated time window of splitting overlaps the Eocene-Oligocene epochs, when such transport was still compatible with prevailing oceanic currents flowing eastward across the Mozambique Channel (Ali & Huber, 2010). Much of the endemic terrestrial vertebrate fauna of Madagascar is thought to have originated during the Cenozoic via colonization by rafting from Africa (Crottini et al., 2012; Yoder & Novak, 2006). The present day fauna is a mix of basal Mesozoic survivors and Cenozoic arrivals, with the latter comprising the majority (Samonds et al., 2013). Endemic scorpions could have similarly heterogeneous origins. Rafting would favor hardier species able to make landfall and colonize more arid biomes of western Madagascar (Crottini et al., 2012). A *Teruelius* **gen**. **n**. ancestor from east Africa that was pre-adapted to arid environments could have made the journey. Alternatively, an earlier taxon related to *Pseudolychas* may have rafted to Madagascar and given rise to both xerophilous *Teruelius* **gen**. **n**. and humicolous *Grosphus*. Multiple colonizations could have yielded multiple neoendemic lineages. *Neogrosphus* may represent a separate founder allied to *Parabuthus* (an affinity suggested by the oblique V_1-V_2 trichobothrial axis on the pedipalp chela shared by the two genera). The genus *Palaeogrosphus*, known from two subfossils of Pleistocene vintage in Malagasy copal (Lourenço, 1996d, 2000b; Lourenço & Henderickx, 2012), also shares a character with *Parabuthus* (enlarged basal middle lamella on female pectines), but its relationship to the '*Grosphus*' group is unclear. More recent local rafting events have been suggested as possible mechanisms to explain the presence of *Grosphus mayottensis* in the Comoros Archipelago (Lourenço & Goodman, 2009), and the widely separated distributions of *Teruelius bistriatus* and *T. waeberi* along the west coast (Lourenço & Wilmé, 2016).

Oceanic dispersal was also invoked by Ojanguren-Affilastro et al. (2017a) to address inconsistency between Cenozoic molecular dating of the origin of New World buthids and Gondwanan vicariance models (Fet et al., 2005). In doing so, they revived an old trans-Atlantic rafting hypothesis previously articulated by Newlands (1973) to explain disjunct New World and Old World distributions of *Opisthacanthus*. Lourenço (1991) rejected this hypothesis because *Opisthacanthus* of Madagascar are more similar to New World forms than to African forms of the genus. Similarly, the split of *Lychas* from *Ananteris* ca. 40–30 Mya in the cladogram of Ojanguren-Affilastro et al. (2017a) is not easily accommodated by a simple dispersal model. It was suggested that these and other members of the '*Ananteris*' buthid group share Gondwanan roots, along with the Madagascar genus *Tityobuthus* (Fet et al., 2005; Lourenço, 2003a, 2011; Lourenço et al., 2016a), which seems incompatible with a post-Cretaceous dating of major buthid lineages.

Acknowledgements

We sincerely thank the curators who generously arranged for loans of materials to support our work: Petra Sierwald and Crystal Maier (loan Z-51381, FMNH); Peter Schwendinger and Lionel Monod (MHNG); Nadine Dupérré and Danilo Harms (ZMUH). Special thanks to Victor Fet for continued support and facilitation of loans, and to Greg Shaffer, Monell Chemical Senses Center for assistance with computer hardware. We are grateful to all scientists, collectors and professionals who generously donated specimens for our studies, mainly: Victor Fet, Charles Haddad, David Hoferek, Charles Kristensen, František Šťáhlavský, Mark Stockmann. Special thanks Mada Flora Seeds company from Madagascar and Czech importers Jiří Krchov (Animalfarm CZ) and Miloslav Mareček. Some study materials were imported under their authorization. Comparative study materials from RSA were covered under permit no. MPB5582. We thank two anonymous reviewers for their comments.

References

ABALOS, J. W. 1953. El género *Zabius* Thorell, 1894 (Buthidae, Scorpiones). *Anales del Instituto de Medicina Regional Univercidad Nacional de Tucuman*, 3 (3): 349–356.

ACOSTA, L. E., D. M. CANDIDO, E. H. BUCKUP & A. D. BRESCOVIT. 2008. Description of *Zabius gaucho* (Scorpiones, Buthidae); a new species from southern Brazil, with an update of the generic diagnosis. *Journal of Arachnology*, 36 (3): 491–501.

ALEXANDER, A. J. 1959. Courtship and mating in the buthid scorpions. *Proceedings of the Zoological Society of London*, 133 (1): 145–169.

ALI, J. R. & M. HUBER. 2010. Mammalian biodiversity on Madagascar controlled by ocean currents. *Nature*, 463: 653–657.

ARMAS, L. F. DE. 1973. Escorpiones del Archipiélago Cubano. I. Nuevo género y nuevas especies de Buthidae (Arachnida: Scorpionidae). *Poeyana*, 114: 1–28.

ARMAS, L. F. DE. 1977. Tricobotriotaxia de *Alayotityus nanus* Armas y *Centruroides guanensis cubensis* Moreno (Scorpionida, Buthidae). *Poeyana*, 162: 1–9.

ARMAS, L. F. DE. 1981. Redescripción de *Rhopalurus princeps* (Karsch, 1879) (Scorpionida: Buthidae). *Poeyana*, 227: 1–7.

ARMAS, L. F. DE. 1999. Quince nuevos alacranes de La Española y Navassa, Antillas Mayores (Arachnida, Scorpiones). *Avicennia*, 10/11: 101–136.

ARMAS, L. F. DE, & E. MARTIN-FRIAS. 1998. Presencia del género *Tityopsis* en México y descripción de una especie nueva (Scorpiones: Buthidae). *Anales de l'Escuela Nacional de Ciencias Biologicas*, 43: 45–49.

ARMAS, L. F. DE & F. J. M. ROJAS-RUNJAIC. 2006. On the poorly known genus *Mesotityus* González-Sponga, 1981 (Scorpiones: Buthidae). *Euscorpius*, 47: 1–11.

ASWATHI, K., P. M. SURESHAN & W. R. LOURENÇO. 2015. A new scorpion of the genus *Buthoscorpio* Werner, 1936 (Scorpiones: Buthidae) from Kerala, India. *Taprobanica*, 7 (4): 213–218.

AYREY, R. F. 2011. *Serradigitus miscionei* (Scorpiones: Vaejovidae), a new species from southern Arizona. *Euscorpius*, 111: 1–15.

BAPTISTA, C., J. A. SANTIAGO-BLAY, M. E. SOLEGLAD & V. FET. 2006. The Cretaceous scorpion genus, *Archaeobuthus*, revisited (Scorpiones: Archaeobuthidae). *Euscorpius*, 35: 1–42.

BASTAWADE, D. B. 1994. A study of hemispermatophore in Indian scorpions of the families Chaerilidae, Vaejovidae and Ischnuridae. *Records of the Zoological Survey of India*, 94 (2-4): 435–437.

BIRULA, A. A. 1917a. *Arachnoidea Arthrogastra Caucasica. Pars I. Scorpiones*. Zapiski Kavkazskogo Muzeya (Mémoires du Musée du Caucase), Tiflis, Imprimerie de la Chancellerie du Comité pour la Transcaucasie. ser A, 5, 253 pp. (in Russian; published August 1917). English translation: Byalynitskii-Birulya, A. A. 1964. Arthrogastric Arachnids of Caucasia. 1. Scorpions. Israel Program for Scientific Translations, Jerusalem, 170 pp.

BIRULA, A. A. 1917b. *Faune de la Russie et des pays Limitrophes Fondee Principalement sur les Collections du Musée Zoologique de l'Académie des Sciences de Russie*. Arachnides (Arachnoidea), 1 (1): xx+227 pp. English translation: Byalynitskii-Birulya, A. A. 1965. Fauna of Russia and Adjacent Countries. Arachnoidea. Vol. I. Scorpions. Israel Program for Scientific Translations, Jerusalem, xix, 154 pp.

BLAIR, C., B. P. NOONAN, J. L. BROWN, A. P. RASELIMANANA, M. VENCES & A. D. YODER. 2015. Multilocus phylogenetic and geospatial analyses illuminate diversification patterns and the biogeographic history of Malagasy endemic plated lizards (Gerrhosauridae: Zonosaurinae). *Journal of Evolutionary Biology*, 28: 481–492.

BOTERO-TRUJILLO, R. & E. FLÓREZ D. 2011. A revisionary approach of Colombian *Ananteris* (Scorpiones, Buthidae): two new species, a new synonymy, and notes

on the value of trichobothria and hemispermatophore for the taxonomy of the group. *Zootaxa*, 2904: 1–44.

BRICAUD, A., A. MOREL & L. PRIEUR. 1981. Absorption by dissolved organic matter of the sea (yellow substance) in the UV and visible domains. *Limnology and Oceanography*, 26 (1): 43–53.

CAMPÓN, F. FERNÁNDEZ, S. LAGOS SILNIK & L. A. FEDELI. 2014. Scorpion diversity of the Central Andes in Argentina. *Journal of Arachnology*, 42: 163–169.

CHABOT-COUTURE, G., K. NIGMATULINA & P. ECKHOFF. 2014. An environmental data set for vector-borne disease modeling and epidemiology. *PLoS ONE*, 9 (4): e94741. doi:10.1371/journal.pone.0094741.

CORNET, A. 1974. *Essai de cartographie bioclimatique à Madagascar*. Paris, ORSTOM.

CROTTINI, A., O. MADSEN, C. POUX, A. STRAUSS, D. R. VIEITES & M. VENCES. 2012. Vertebrate time-tree elucidates the biogeographic pattern of a major biotic change around the K-T boundary in Madagascar. *Proceedings of the National Academy of Sciences*, 109 (14): 5358–5363.

DIONISIO-SESE, M. L. M. ISHIKURA, T. MARUYAMA & S. MIYACHI. 1997. UV-absorbing substances in the tunic of a colonial ascidian protect its symbiont, *Prochloron* sp., from damage by UV-B radiation. *Marine Biology*, 128: 455–461.

D'SA, E. J., R. G. STEWARD, A. VODACEK, N. V. BLOUGH & D. PHINNEY. 1999. Determining optical absorption of colored dissolved organic matter in seawater with a liquid capillary waveguide. *Limnology and Oceanography*, 44 (4): 1142–1148.

DUNLAP, W. C., B. E. CHALKER & J. K. OLIVER. 1986. Bathymetric adaptations of reef-building corals at Davies Reef, Great Barrier Reef, Australia. III. UV-B absorbing compounds. *Journal of Experimental Marine Biology and Ecology*, 104: 239–248.

DUNLAP, W. C., D. McB. WILLIAMS, B. E. CHALKER & A. T. BANASZAK. 1989. Biochemical photoadaptation in vision: U.V.-absorbing pigments in fish eye tissues. *Comparative Biochemistry and Physiology*, 93B (3): 601–607.

DUPRÉ, G. 2007. Conspectus genericus scorpionorum 1758–2006 (Arachnida: Scorpiones). *Euscorpius*, 50: 1–31.

EASTWOOD, E. B. 1977. Notes on the scorpion fauna of the Cape. Part 2. The *Parabuthus capensis* (Ehrenberg) species-group; remarks on taxonomy and bionomics (Arachnida, Scorpionida, Buthidae). *Annals of the South African Museum*, 73 (8): 199–214.

EBERHARD, W. G. 1985. *Sexual selection and animal genitalia*. Harvard University Press.

ESPOSITO, L. A., H. Y. YAMAGUTI, C. A. SOUZA, R. PINTO DA ROCHA & L. PRENDINI. 2017. Systematic revision of the neotropical club-tailed scorpions, *Physoctonus*, *Rhopalurus*, and *Troglorhopalurus*, revalidation of *Heteroctenus*, and descriptions of two new genera and three new species (Buthidae: Rhopalurusinae). *Bulletin of the American Museum of Natural History*, 415: 1–134.

FAGE, L. 1929. *Les scorpions de Madagascar, leur affinités, leur distribution géographique*. Pp. 637-693 in: Faune des Colonies Françaises. Société d'Editions Géographiques Maritimes et Coloniales, Paris.

FARLEY, R. D. 1990. Regulation of air and blood flow through the booklungs of the desert scorpion, *Paruroctonus mesaensis*. *Tissue and Cell*, 22 (4): 547–569.

FET, V., B. GANTENBEIN, A. V. GROMOV, G. LOWE & W. R. LOURENÇO. 2003. The first molecular phylogeny of Buthidae (Scorpiones). *Euscorpius*, 4: 1–10.

FET, V. & G. LOWE. 2000. Family Buthidae C. L. Koch, 1837. Pp. 54–286 in Fet, V., W. D. Sissom, G. Lowe & M. E. Braunwalder. *Catalog of the Scorpions of the World (1758–1998)*. New York: The New York Entomological Society, 689 pp.

FET, V., G. POLIS, & W. D. SISSOM. 1998. Life in sandy deserts: the scorpion model. *Journal of Arid Environments*, 39: 609–622.

FET, V., M. E. SOLEGLAD & G. LOWE. 2005. A new trichobothrial character for the high-level systematics of Buthoidea (Scorpiones: Buthida). *Euscorpius*, 23: 1–40.

FINCKE, T. & R. PAUL. 1989. Book lung function in arachnids. III. The function and control of the spiracles. *Journal of Comparative Physiology B*, 159 (4) : 433–441.

FITZPATRICK, M. J. 1994. A checklist of the *Parabuthus* Pocock species of Zimbabwe with a re-description of *P. mossambicensis* (Peters, 1861) (Arachnida: Scorpionida). *Transactions of the Zimbabwe Scientific Association*, 68: 7–14.

FRANCKE, O. F. 1978. Redescription of *Centruroides koesteri* Kraepelin (Scorpionida: Buthidae). *Journal of Arachnology*, 6: 65–71.

FRANCKE, O. F. 1979. Spermatophores of some north American scorpions (Arachnida, Scorpiones). *Journal of Arachnology*, 7 (1): 19–32.

FRANCKE, O. F. 1985. Conspectus genericus scorpionorum 1758-1982 (Arachnida: Scorpiones). *Occasional Papers of the Museum, Texas Tech University*, 98: 1–32.

FRANCKE, O. F. & STOCKWELL S. A. 1987. Scorpions (Arachnida) from Costa Rica. *Special Publications of the Museum, Texas Tech University*, 25: 1–64.

FRANCKE, O. F., R. TERUEL & C. E. SANTIBÁÑEZ-LÓPEZ. 2014. A new genus and a new species of scorpion (Scorpiones: Buthidae) from southeastern Mexico. *Journal of Arachnology*, 42: 220–232.

FROST, L. M., D. R. BUTLER, B. O'DELL & V. FET. 2001. A coumarin as a fluorescent compound in scorpion cuticle. Pp. 171–177 in FET, V & P. A. SELDEN (eds.) *Scorpions 2001. In Memoriam Gary A. Polis*. British Arachnological Society, Burnham Beeches, Bucks. xi + 404 pp.

GAFFIN, D. & T. N. BARKER. 2014. Comparison of scorpion behavioral responses to UV under sunset and nighttime irradiances. *Journal of Arachnology*, 42: 111–118.

GALLÃO, J. E. & M. E. BICHUETTE. 2016. On the enigmatic troglobitic scorpion *Troglorhopalurus translucidus*: distribution, description of adult females, life history and comments on *Rhopalurus lacrau* (Scorpiones: Buthidae). *Zoologia*, 33 (6): e20150193 | DOI: 10.1590/S1984-4689zool-20150193

GEFEN, E., C. UNG & A. G. GIBBS. 2009. Partitioning of transpiratory water loss of the desert scorpion, *Hadrurus arizonensis* (Iuridae). *Journal of Insect Physiology*, 55: 544–548.

GEFEN, E. 2011. The relative importance of respiratory water loss in scorpions is correlated with species habitat type and activity pattern. *Physiological and Biochemical Zoology*, 84 (1): 68–76.

GERVAIS, P. M. 1843. (Les principaux résultats d'un travail sur la famille des Scorpions). *Sociètè Philomatique de Paris. Extraits des Procès-Verbaux des Séances*, 5 (7): 129–131.

GERVAIS, P. M. 1844. *Scorpions*. Pp. 14-74 in: Walckenaer, C. A. (Ed.). Histoire Naturelle des Insectes. Aptères. Librarie Encyclopédique de Roret, Paris, 3 (8), 418 pp.

GINGERICH, P. D. 2006. Environment and evolution through the Paleocene–Eocene thermal maximum. *Trends in Ecology and Evolution*, 21 (5): 246–253.

GONZÁLEZ-SPONGA, M. A. 1981a. Seis nuevas especies del género *Tityus* en Venezuela (Scorpionida: Buthidae). *Monografias Cientificas* "*Augusto Pi Suner*" *del Instituto Pedagogico de Caracas*, 12: 1–87.

GONZALEZ-SPONGA, M. A. 1981b. Un nuevo género y dos nuevas especies de la familia Buthidae de Venezuela (Arachnida: Scorpiones). *Monografias Cientificas* "*Augusto Pi Suner*" *del Instituto Pedagogico de Caracas*, 13: 1–27.

GONZÁLEZ-SPONGA, M. A. 2001a. Aracnidos de Venezuela. Cuatro especies nuevas del género *Tityus* (Scorpionida: Buthidae). *Acta Biologica Venezuelica*, 21 (3): 69–83.

GONZÁLEZ-SPONGA, M. A. 2001b. Aracnidos de Venezuela. Seis nuevas especies del género *Microtityus* (Scorpionida: Buthidae) del sistema Montanoso de la Costa. *Boletin de la Academia de Ciencias Fisicas, Matematicas y Naturales* (*Venezuela*), 61 (1/2): 45–66.

GONZÁLEZ-SPONGA, M. A. 2002. Aracnidos de Venezuela. Cuatro nuevas especies del género *Tityus* (Scorpionida: Buthidae). *Boletin de la Academia de Ciencias Fisicas, Matematicas y Naturales* (*Venezuela*), 62 (2): 49–66.

GONZÁLEZ-SPONGA, M. A. 2007. Biodiversidad en Venezuela. Aracnidos. Descripcion de cuatro nuevas especie del género *Tityus* Koch, 1836 (Escorpiones: Buthidae) de la región centro occidental de Venezuela. *Boletin de la Academia de Ciencias Fisicas, Matematicas y Naturales* (Venezuela), 67 (1–2): 37–63.

GONZÁLEZ-SPONGA, M. A. 2008a. Biodiversidad de Venezuela. Descripcion de dos nuevas especie del género *Tityus* Koch, 1836 (Buthidae) y dos especies del género Chactas Gervais, 1844 (Chactidae). *Boletin de la Academia de Ciencias Fisicas, Matematicas y Naturales* (*Venezuela*), 68 (1): 39–65.

GONZÁLEZ-SPONGA, M. A. 2008b. Biodiversidad de Venezuela. Descripcion de cuatro nuevas especie del género *Tityus* Koch, 1836 (Scorpionida: Buthidae) de mos estados Monagas, Sucre y Bolivar. *Boletin de la Academia de Ciencias Fisicas, Matematicas y Naturales* (*Venezuela*), 68 (4): 9–30.

GONZÁLEZ-SPONGA, M. A. 2009. Biodiversidad en Venezuela. Aràcnidos. Descripcion de cuatro nuevas especies del género *Tityus* Koch, 1836 (Escorpiones: Buthidae) de los Estados Bolivar y Amazonas. *Revista de Investigacion*, 66: 227–255.

GOODMAN, S. M., J. P. BENSTEAD & H. SCHUTZ. 2003. *The Natural History of Madagascar*. University Of Chicago Press.

GRAHAM, M. R. & M. E. SOLEGLAD. 2007. A new scorpion genus representing a primitive taxon of tribe Stahnkeini, with a description of a new species from Sonora, Mexico (Scorpiones: Vaejovidae). *Euscorpius*, 5: 1–34.

HÄDER, D.-P, E. W. HELBLING, C. E. WILLIAMSON AND R. C. WORREST. 2011. Effects of UV radiation on aquatic ecosystems and interactions with climate change. *Photochemical & Photobiological Sciences*, 10: 242–260.

HADLEY, N. F. 1974. Adaptational biology of desert scorpions. *Journal of Arachnology*, 2: 11–23.

HADLEY, N. F. 1990. Environmental physiology. Pp. 321–340 in POLIS, G. A. (Ed.) *The Biology of Scorpions*. Stanford University Press, Stanford, California.

HARADON, R. M. 1984. New and redefined species belonging to the *Paruroctonus baergi* group (Scorpiones, Vaejovidae). *Journal of Arachnology*, 12: 205–221.

HARINGTON, A. 1982. Diurnalism in *Parabuthus villosus* (Peters) (Scorpiones, Buthidae). *Journal of Arachnology*, 10: 85–86.

HJELLE, J. T. 1990. Anatomy and morphology. Pp. 9–63 in POLIS, G. A. (Ed.) *The Biology of Scorpions*. Stanford University Press, Stanford, California.

HOSKEN, D. J. & P. STOCKLEY. 2004. Sexual selection and genital evolution. *Trends in Ecology and Evolution*, 19 (2): 87–93.

JACKMAN, T. R., A. M. BAUER, E. GREENBAUM, F. GLAW & M. VENCES. 2008. Molecular phylogenetic relationships among species of the Malagasy-Comoran gecko genus *Paroedura* (Squamata: Gekkonidae). *Molecular Phylogenetics and Evolution*, 46: 74–81.

JAVED, S. M. MAQSOOD, K. THULSI RAO, Z. A. MIRZA, R. V. SANAP & F. TAMPAL. 2010. A new species of scorpion of the genus *Buthoscorpio* Werner, 1936 (Scorpiones: Buthidae) from Andhra Pradesh, India. *Euscorpius*, 98: 1–11.

KAMENZ, C. & L. PRENDINI. 2008. An atlas of book lung fine structure in the order Scorpiones (Arachnida). *Bulletin of the American Museum of Natural History*, 316: 1–360.

KARSCH, F. 1886. Skorpionologische Beitrage (I. Ueber einen sizilianischen Skorpion. - II. Uebersicht der Gruppe Buthina (Androctonina). - III. Ueber einen neuen *Opisthacanthus* (Peters) Thor). *Berliner Entomologische Zeitschrift*, 30 (1): 75–79.

KLOOCK, C. T. 2009. Reducing scorpion fluorescence via prolonged exposure to ultraviolet light. *Journal of Arachnology*, 37: 368–370.

KLOOCK, C. T., K. ABRAHAM & R. REYNOLDS. 2010. Ultraviolet light detection: a function of scorpion fluorescence. *Journal of Arachnology*, 38: 441–445.

KOCH, L. E. 1977. The taxonomy, geographic distribution and evolutionary radiation of Australo-Papuan Scorpions. *Records of the Western Australian Museum*, 5 (2): 83–367.

KOVAŘÍK, F. 1998. *Štíři*. Madagaskar, Jihlava, 175 pp.

KOVAŘÍK, F. 2003. *Butheoloides cimrmani* sp. n. from Ghana (Scorpiones: Buthidae). *Serket*, 8 (3): 125–127.

KOVAŘÍK, F. 2009. *Illustrated catalog of scorpions. Part I. Introductory remarks; keys to families and genera; subfamily Scorpioninae with keys to* Heterometrus *and* Pandinus *species*. Prague: Clairon Production, 170 pp.

KOVAŘÍK, F. 2015. Scorpions of Ethiopia (Arachnida: Scorpiones). Part I. Genus *Butheoloides* Hirst, 1925 (Buthidae), with description of a new species. *Euscorpius*, 195: 1–10.

KOVAŘÍK, F. 2016. *Butheoloides grosseri* sp. n. (Scorpiones: Buthidae) from Uganda. *Euscorpius*, 230: 1–6.

KOVAŘÍK, F., G. LOWE, J. PLÍŠKOVÁ & F. ŠŤÁHLAVSKÝ 2013. A new scorpion genus, *Gint* gen. n., from the Horn of Africa (Scorpiones, Buthidae). *Euscorpius*, 173: 1–19.

KOVAŘÍK, F., G. LOWE, D. HOFEREK, M. FORMAN & J. KRÁL. 2015b. Two new *Chaerilus* from Vietnam (Scorpiones, Chaerilidae), with observations of growth and maturation of *Chaerilus granulatus* sp. n. and *C. hofereki* Kovařík et al., 2014. *Euscorpius*, 213: 1–23.

KOVAŘÍK, F., G. LOWE, P. JUST, A. I. AWALE, H. SH A. ELMI & F. ŠŤÁHLAVSKÝ. 2018a. Scorpions of the Horn of Africa (Arachnida: Scorpiones). Part XVI. Review of the genus *Gint* Kovařík et al., 2013, with description of three new species from Somaliland (Scorpiones, Buthidae). *Euscorpius*, 259: 1–41.

KOVAŘÍK, F., G. LOWE, D. HOFEREK, J. PLÍŠKOVÁ & F. ŠŤÁHLAVSKÝ. 2016a. Scorpions of Ethiopia. Part IV. Genus *Uroplectes* Peters, 1861 (Scorpiones: Buthidae). *Euscorpius*, 217: 1–16.

KOVAŘÍK, F., G. LOWE, K. B. RANAWANA, D. HOFEREK, V. A. SANJEEWA JAYARATHNE, J. PLÍŠKOVÁ & F. ŠŤÁHLAVSKÝ. 2016c. Scorpions of

Sri Lanka (Arachnida, Scorpiones: Buthidae, Chaerilidae, Scorpionidae) with description of four new species of the genera *Charmus* Karsch, 1879 and *Reddyanus* Vachon, 1972 stat. n. *Euscorpius*, 220: 1–133.

KOVAŘÍK, F., G. LOWE, J. PLÍŠKOVÁ & F. ŠŤÁHLAVSKY. 2016d. Scorpions of the Horn of Africa (Arachnida: Scorpiones). Part VII. *Parabuthus* Pocock, 1890 (Buthidae), with description of *P. hamar* sp. n. and *P. kajibu* sp. n. from Ethiopia. *Euscorpius*, 228: 1–58.

KOVAŘÍK, F., G. LOWE & F. STAHLAVSKY. 2016e. Scorpions of the Horn of Africa (Arachnida: Scorpiones). Part IX. *Lanzatus*, *Orthochirus*, and *Somalicharmus* (Buthidae), with Description of *Lanzatus somalilandus* sp. n. and *Orthochirus afar* sp. n. *Euscorpius*, 232: 1–40.

KOVAŘÍK, F., G. LOWE & F. ŠŤÁHLAVSKÝ. 2018b. Review of the genus *Babycurus* Karsch, 1886 (Arachnida, Scorpiones, Buthidae), with descriptions of *Barbaracurus* gen. n. and two new species from Oman and Yemen. *Euscorpius*, 267: 1–41.

KOVAŘÍK, F., G. LOWE & F. ŠŤÁHLAVSKÝ. 2018c. Three new *Chaerilus* from Malaysia (Tioman Island) and Thailand (Scorpiones: Chaerilidae), with a review of *C. cimrmani*, *C. sejnai*, and *C. tichyi*. *Euscorpius*, 268: 1–29.

KOVAŘÍK, F & A. A. OJANGUREN AFFILASTRO. 2013. *Illustrated catalog of scorpions Part II. Bothriuridae; Chaerilidae; Buthidae I., genera* Compsobuthus*,* Hottentotta*,* Isometrus*,* Lychas*, and* Sassanidotus. Prague: Clairon Production, 400 pp.

KOVAŘÍK, F., M. E. SOLEGLAD & V. FET. 2007. A new species of scorpion in the "*Charmus*" group from India (Scorpiones: Buthoidea). *Boletin de la Sociedad Entomologica Aragonesa*, 40: 201–209.

KOVAŘÍK, F. & R. TERUEL. 2014. Three new scorpion species from the Dominican Republic, Greater Antilles (Scorpiones: Buthidae, Scorpionidae). *Euscorpius*, 187: 1–29.

KOVAŘÍK, F., R. TERUEL & G. LOWE. 2016b. Two new scorpions of the genus *Chaneke* Francke, Teruel et Santibáñez-López, 2014 (Scorpiones: Buthidae) from southern Mexico. *Euscorpius*, 218: 1–22.

KOVAŘÍK, F., R. TERUEL, G. LOWE & S. FRIEDRICH. 2015a. Four new scorpion species (Scorpiones: Buthidae) from Amazonian Peru. *Euscorpius*, 210: 1–40.

KRAEPELIN, K. 1891. Revision der Skorpione. I. Die Familie der Androctonidae. *Jahrbuch der Hamburgischen Wissenschaftlichen Anstalten*, 8: 1–144.

KRAEPELIN, K. 1895. Nachtrag zu Theil I der Revision der Scorpione. *Beiheft zum Jahrbuch der Hamburgischen Wissenschaftlichen Anstalten*, 12: 73–96.

KRAEPELIN, K. 1899. Scorpiones und Pedipalpi. In: F. Dahl (Ed.). *Das Tierreich. Herausgegeben von der Deutschen Zoologischen Gesellschaft*. Berlin, R. Friedländer und Sohn Verlag, 8 (Arachnoidea): 1–265.

KRAEPELIN, K. 1900. Ueber einige neue Gliederspinnen. Abhandlungen aus dem Gebiete der Naturwissenschaften. *Herausgegeben vom Naturwissenschaftlichen Verein in Hamburg*, 16, 1 (4): 1–17.

KRAPF, D. 1986. Predator prey relations in diurnal *Scorpio maurus*. P. 133 in BARRIENTOS, J. A. (Ed.) *Actas X Congreso internacional de aracnologia, Jaca (España), septiembre 1986*. Bellaterra (Barcelona).

LAMORAL, B. H. & S. C. REYNDERS. 1975. A catalogue of the scorpions described from the Ethiopian faunal region up to December 1973. *Annals of the Natal Museum*, 22 (2): 489–576.

LAMORAL, B. H. 1977. *Parabuthus kalaharicus*, a new species of scorpion from the Kalahari Gemsbok national park in the Republic of South Africa (Buthidae, Scorpionida). *Koedoe*, 20: 101–107.

LAMORAL, B. H. 1979. The scorpions of Namibia (Arachnida: Scorpionida). *Annals of the Natal Museum*, 23 (3): 497–784.

LAMORAL, B. H. 1980. Two new psammophile species and new records of scorpions from the northern Cape province of South-Africa (Arachnida: Scorpionida). *Annals of the Natal Museum*, 24 (1): 201–210.

LAWRENCE, R. F. 1961. A new forest-living scorpion from the Transvaal. *Annals and Magazine of Natural History*, 38 (4): 123–126.

LENARDUCCI, A. R. I. P., R. PINTO-DA-ROCHA & S. M. LUCAS. 2005. Descriçao de uma nova espécie de *Rhopalurus* Thorell, 1876 (Scorpiones, Buthidae) do nordeste brasileiro. *Biota Neotropica*, 5 (1): 173–180.

LEVY, G. & P. AMITAI. 1980. *Scorpiones. Fauna Palaestina. Arachnida I*. The Israel Academy of Sciences and Humanities. Jerusalem 1980.

LEVY, G., P. AMITAI & A. SHULOV. 1973. New scorpions from Israel, Jordan and Arabia. Zoo-logical *Journal of the Linnaean Society*, 52: 113–140.

LEGENDRE, R. 1972. Les Arachnides de Madagascar. Pp. 427–457 in BATTISTINI, R. & G. RICHARD-VINDARD (Eds.) *Biogeography and Ecology in Madagascar*, *Monographiae Biologicae*, 21: 427–457.

LIGHTON, J. R. B. 1996. Discontinuous gas exchange in insects. *Annual Review of Entomology*, 41: 309–324.

LOCKET, N. A. 1990. A new genus and species of scorpion from South Australia (Buthidae: Buthinae). *Transactions of the Royal Society of South Australia*, 114 (1-2): 67–80.

LORIA, S. F. & L. PRENDINI. 2014. Homology of the lateral eyes of Scorpiones: a six-ocellus model. *PLoS ONE* 9 (12): e112913. doi:10.1371/journal.pone.0112913.

LORIA, S. F. & L. PRENDINI. 2018. Ultrastructural comparison of the eyespot and ocelli of scorpions, and implications for the systematics of Chaerilidae Pocock, 1893. *Zoologischer Anzeiger*, 273: 183–191.

LOURENÇO, W. R. 1980. Contribution à la connaissance systématique des Scorpions appartenant au complexe *Tityus trivittatus* Kraepelin, 1898 (Buthidae). *Bulletin du Muséum National d'Histoire Naturelle de Paris*, 4éme série, 2, A, 3: 793–843.

LOURENÇO, W. R. 1982. Révision du genre *Rhopalurus* Thorell, 1876 (Scorpiones, Buthidae). *Revue Arachnologique*, 4: 107–141.

LOURENÇO, W. R. 1984a. Analyse taxonomique des Scorpions du groupe *Tityus clathratus* Koch, 1845 (Scorpiones, Buthidae). *Bulletin du Muséum National d'Histoire naturelle de Paris*, 4éme série ie, 6, A, (2): 319–360.

LOURENÇO, W. R. 1984b. Considérations sur les espèces de *Tityus* (Scorpiones, Buthidae) décrites des Petites Antilles. *Revue Arachnologique*, 5 (3): 91–105.

LOURENÇO, W. R. 1991. *Opisthacanthus* genre gondwanien de´fini comme groupe naturel. Caractérisation des sous-genres et des groupes d'espèces (Arachnida, Scorpiones, Ischnuridae). *Iheringia, Série Zoologia*. 71: 5–42.

LOURENÇO, W. R. 1995a. Déscription de trois noveaux genres et quatre nouvelles espèces de scorpions Buthidae de Madagascar. *Bulletin du Musèum National d'Histoire naturelle, Paris (Zoologie, Biologie et Écologie Animale)*, (4), 17A (1-2): 95–106.

LOURENÇO, W. R. 1995b. Considérations sur la répartition géographique de genre *Butheloides* Hirst avec la description de *Butheloides wilsoni* nov. sp. (Scorpiones, Buthidae). *Bulletin du Muséum National d'Histoire Naturelle de Paris*, 4éme série, section A, 16 (2-4): 475–480.

LOURENÇO, W. R. 1996a. *Origins and affinities of the scorpion fauna of Madagascar*. Pp. 441–455 in: Lourenço, W. R. (Ed.). Biogéographie de Madagascar. ORSTOM, Paris.

LOURENÇO, W. R. 1996b. *Faune de Madagascar. 87. Scorpions (Chelicerata, Scorpiones)*. Muséum National d'Histoire Naturelle, Paris. 102 pp.

LOURENÇO, W. R. 1996c. A new species of *Tityobuthus* from Madagascar (Scorpiones, Buthidae). *Bollettino del Museo Regionale di Scienze Naturale, Torino*, 14 (1): 267–273.

LOURENÇO, W. R. 1996d. Premier cas connu d'un sub-fossile de scorpion dans le copal de Madagascar. *Comptes Rendus de l'Academie des Sciences*, *Paris*, Sér. IIa, 323: 889–891.

LOURENÇO, W. R. 1996e. A propos de deux espèces nouvelles appartenant au genre *Butheloides* Hirst (Scorpiones, Buthidae). *Revue Arachnologique*, 11 (9): 87–94.

LOURENÇO, W. R. 1997. Description of a new genus and new species of Buthidae scorpion from the Himalayas of India and Nepal, with some new biogeographic implications. *Entomologische Mitteilungen aus dem Zoologischen Museum Hamburg*, 13 (161): 133–138.

LOURENÇO, W. R. 1999. A new species of *Grosphus* Simon (Scorpiones, Buthidae), the first record of an intertidal scorpion from Madagascar. *Entomologische Mitteilungen aus dem Zoologischen Museum Hamburg*, 12 (156): 183–188.

LOURENÇO, W. R. 2000a. Un nouveau genre de Scorpion malgache, maillon possible entre les Microcharmidae et les Buthidae. *Comptes rendus de l'Académie des Sciences, Paris, Sciences de la vie*. 323: 877–881.

LOURENÇO, W. R. 2000b. More about the Buthoidea of Madagascar, with special references to the genus *Tityobuthus* Pocock (Scorpiones, Buthidae). *Revue Suisse de Zoologie*, 107: 721–736.

LOURENÇO, W. R. 2000c. Analyse taxonomique de quelques espèces du genre *Uroplectes* Peters, 1861 présentes en Angola et description d'une espèce nouvelle (Scorpiones, Buthidae). *Zoosystema*, 22 (3): 499–506.

LOURENÇO, W. R. 2001a. A remarkable scorpion fossil from the amber of Lebanon. Implications for the phylogeny of Buthoidea. *Comptes Rendus des Séances de l'Académie des Science, Paris*, 332: 641–646.

LOURENÇO, W. R. 2001b. Another new species of *Grosphus* Simon (Scorpiones, Buthidae) for Madagascar. *Revue Suisse de Zoologie*, 108 (3): 455–461.

LOURENÇO, W. R. 2002. Nouvelles considérations sur la systématique et la biogéographie du genre *Butheoloides* Hirst (Scorpiones, Buthidae) avec description d'un nouveau sous-genre et de deux nouvelles espèces. *Revue Suisse de Zoologie*, 109 (4): 725–733.

LOURENÇO, W. R. 2001c. A new genus and species of scorpion from Algeria, with taxonomic considerations on the genus *Lissothus* Vachon, 1948 (Scorpiones, Buthidae). *Zoosystema*, 23 (1): 51–57.

LOURENÇO, W. R. 2003a. Scorpiones, scorpions. Pp. 575–579 in GOODMAN, S., BENSTEAD, J. (Eds.). *The Natural History of Madagascar*. The University of Chicago Press, Chicago, Illinois.

LOURENÇO, W. R. 2003b. Description of a new species of scorpion belonging to the genus *Himalayotityobuthus* Lourenço (Scorpiones, Buthidae). *Revista Ibérica de Aracnologia*, 7: 225–229.

LOURENÇO, W. R. 2003c. New taxonomic considerations on some species of the genus *Grosphus* Simon, with description of a new species (Scorpiones, Buthidae). *Revue Suisse de Zoologie*, 110 (1): 141–154.

LOURENÇO, W. R. 2004a. *Scorpions du sud-ouest de Madagascar et en particulier de la forêt des Mikea*. Pp. 25-35, In: Raselimanana A. P. & Goodman S. M. (eds), Inventaire floristique et faunistique de la forêt de Mikea: Paysage écologique et diversité biologique d'une préoccupation majeure pour la conservation, Recherches pour le développement, Série Sciences Biologiques, 21: 105 pp.

LOURENÇO, W. R. 2004b. Humicolous microcharmid scorpions: a new genus and species from Madagascar. *Comptes Rendus Biologies*, 327: 77–83.

LOURENÇO, W. R. 2005. Scorpions from Mandena East Coastal rain forest in Madagascar, and description of a new species of *Grosphus* Simon (Scorpiones, Buthidae). *Boletin de la Sociedad Entomológica Aragonesa*, 37: 83–87.

LOURENÇO, W. R. 2007. First record of the family Pseudochactidae Gromov (Chelicerata, Scorpiones) from Laos and new biogeographic evidence of a Pangaean palaeodistribution. *Comptes Rendus Biologies*, 330 (10): 770–777.

LOURENÇO, W. R. 2009. A synopsis of the amber scorpions, with special reference to the Baltic fauna. *Denisia* 26, *zugleich Kataloge der oberösterreichischen Landesmuseen Neue Serie*, 86: 131–136.

LOURENÇO, W. R. 2010. A new species of *Butheoloides* Hirst, 1925 from Morocco (Scorpiones, Buthidae). *Entomologische Mitteilungen aus dem Zoologischen Museum Hamburg*, 15 (183): 183–187.

LOURENÇO, W. R. 2011. The "*Ananteris* group" (Scorpiones: Buthidae); suggested composition and possible links with other buthids. *Boletin de la Sociedad Entomologica Aragonesa*, 48: 105–113.

LOURENÇO, W. R. 2012a. Further taxonomic considerations on the genus *Buthoscorpio W*erner, 1936 (Scorpiones, Buthidae), with description of a new species from India. *Boletin de la Sociedad Entomologica Aragonesa*, 50: 187–192.

LOURENÇO, W. R. 2012b. Fluorescence in scorpions under UV light; can chaerilids be a possible exception? *Comptes Rendus Biologies*, 335: 731–734.

LOURENÇO, W. R. 2012c. A new species of *Grosphus* Simon, 1880 (Scorpiones, Buthidae) from the Southwest of Madagascar. *Entomologische Mitteilungen aus dem Zoologischen Museum Hamburg*, 16 (188): 33–40.

LOURENÇO, W. R. 2012d. Further considerations on scorpions found in Baltic amber, with a description of a new species (Scorpiones: Buthidae). *Euscorpius*, 146: 1–9.

LOURENÇO, W. R. 2013a. The remarkable peri-Saharan distribution of the genus *Butheoloides* Hirst (Scorpiones, Buthidae), with the description of a new species from Cameroon. *Comptes Rendus Biologies*, 336 (10): 515–520.

LOURENÇO, W. R. 2013b. A new species of *Grosphus* Simon, 1880 (Scorpiones, Buthidae) from Central Madagascar. *Entomologische Mitteilungen aus dem Zoologischen Museum Hamburg*, 16 (189): 57–62.

LOURENÇO, W. R. 2014. The genus *Grosphus* Simon, 1880 in South-Western Madagascar, with the description of a new species (Scorpiones, Buthidae). *Zoosystema*, 36 (3): 631–645.

LOURENÇO, W. R. 2016. A new genus and three new species of scorpions from Cretaceous Burmese amber (Scorpiones: Chaerilobuthidae: Palaeoeuscorpiidae). *Arthropoda Selecta*, 25 (1): 67–74.

LOURENÇO, W. R. 2017. A new species of *Physoctonus* Mello-Leitão, 1934 from the 'Campos formations' of southern Amazonia (Scorpiones, Buthidae). *ZooKeys*, 711: 67–80.

LOURENÇO, W. R. & A. BEIGEL. 2011. A new scorpion fossil from the Cretaceous amber of Myanmar (Burma). New phylogenetic implications. *Comptes Rendus Palevol*, 10: 635–639.

LOURENÇO, W. R. & A. BEIGEL. 2015. A new genus and species of Palaeoburmesebuthinae Lourenço, 2015 (Scorpiones: Archaeobuthidae) from Cretaceous amber of Myanmar. *Beiträge zur Araneologie*, 9: 476–480.

LOURENÇO, W. R. & J. L. CLOUDSLEY-THOMPSON. 1996. The evolutionary significance of colour, colour patterns and fluorescence in scorpions. *Revue Suisse de Zoologie*, H.S. 2: 449–458. Proceedings of the XIIIth International Congress of Arachnology, Geneva, 3-8. IX.1995.

LOURENÇO, W. R. & V. R. Von EICKSTEDT. 1983. Présence du genre *Microtityus* (Scorpiones, Buthidae) au Brésil. Description de *Microtityus vanzolinii* sp. n. *Revue Arachnologique*, 5 (2): 65–72.

LOURENÇO, W. R. & S. M. GOODMAN. 1994. Taxonomic and ecological observations on the scorpions collected in the Forest of Ankazomivady-Ambositra and on the ''RS d' Ivohibe'', Madagascar. *Revista Biologica Tropical*, 47 (3): 475–482.

LOURENÇO, W. R. & S. M. GOODMAN. 2003a. Description of a new species of *Grosphus* Simon (Scorpiones, Buthidae) from the Ankarana Massif, Madagascar. *Revista Ibérica de Aracnología*, 7: 19–28.

LOURENÇO, W. R. & S. M. GOODMAN. 2003b. New considerations on the genus *Tityobuthus* Pocock (Scorpiones, Buthidae), and description of a new species from the Ankarana in northern Madagascar *Revista Ibérica de Aracnología*, 8: 13–22.

LOURENÇO, W. R. & S. M. GOODMAN. 2006. Further considerations regarding the status of *Grosphus madagascariensis* (Gervais) and *Grosphus hirtus* Kraepelin, and description of a new species (Scorpiones, Buthidae). *Revue Suisse de Zoologie*, 113 (2): 247–261.

LOURENÇO, W. R. & S. M. GOODMAN. 2009. Scorpions from the Comoros Archipelago: description of a new species of *Grosphus* Simon (Scorpiones, Buthidae) from Mayotte (Maore). *Boletin de la Sociedad Entomológica Aragonesa*, 44: 35–38.

LOURENÇO, W. R., S. M. GOODMAN & B. L. FISHER. 2006a. A reappraisal of the geographical distribution of the endemic family Microcharmidae Lourenço (Scorpiones) in Madagascar and description of eight new species and subspecies. *Proceedings of the California Academy of Sciences*, ser. 4, 57 (26): 751–783.

LOURENÇO, W. R., S. M. GOODMAN & O. RAMILIJAONA. 2004. Three new species of *Grosphus* Simon from Madagascar (Scorpiones, Buthidae). *Revista Iberica de Aracnologia*, 9: 225–234.

LOURENÇO, W. R. & H. HENDERICKX. 2012. Another new sub-fossil species of scorpion of the genus *Palaeogrosphus* Lourenço, 2000 from Malagasy copal (Scorpiones: Buthidae). *Euscorpius*, 137: 1–4.

LOURENÇO W. R., E. A. LEGUIN & S. M. GOODMAN. 2009a. A reappraisal of the geographical distribution of *Grosphus grandidieri* Kraepelin, 1900 (Scorpiones: Buthidae). *Entomologische Mitteilungen aus dem Zoologischen Museum Hamburg*, 15 (180): 75–85.

LOURENÇO, W. R. & D. D. PHAM. 2010. A remarkable new cave scorpion of the family Pseudochactidae Gromov (Chelicerata, Scorpiones) from Vietnam. *ZooKeys*, 71: 1–13.

LOURENÇO, W. R., & R. PINTO-DA-ROCHA. 1997. A reappraisal of the geographic distribution of the genus *Rhopalurus* Thorell (Scorpiones, Buthidae) and description of two new species. *Biogeographica* (*Paris*), 73 (4): 181–191.

LOURENÇO, W. R., J.-X. QI & S. M. GOODMAN. 2007a. Scorpions of south-western Madagascar. A new species of *Grosphus* Simon, 1880 (Scorpiones, Buthidae). *Boletín de la Sociedad Entomológica Aragonesa*, 40: 171–177.

LOURENÇO, W. R., J.-X. QI & S. M. GOODMAN. 2008. The identity of *Tityobuthus baroni* (Pocock, 1890) (Scorpiones, Buthidae) and description of three new species from Madagascar. *Boletin de la Sociedad Entomologica Aragonesa*, 42: 89–102.

LOURENÇO, W. R., V. SOARIMALALA & S. M. GOODMAN. 2006b. Further considerations on the geographical distribution of the endemic Malagasy genus *Neogrosphus* Lourenço, 1995 (Scorpiones: Buthidae). *Boletin de la Sociedad Entomológica Aragonesa*, 39: 265–269.

LOURENÇO, W. R., V. SOARIMALALA & S. M. GOODMAN. 2007b. Scorpions of south-west Madagascar. II. The species of *Grosphus* Simon (Scorpiones, Buthidae). *Boletin de la Sociedad Entomológica Aragonesa*, 41: 369–375.

LOURENÇO, W. R., V. SOARIMALALA & S. M. GOODMAN. 2009b. The species of *Grosphus* Simon (Scorpiones, Buthidae) distributed in the northern and eastern regions of Madagascar with the description of a new species. *Malagasy Nature*, 2: 144–153.

LOURENÇO, W. R. & M. VACHON. 1996. Compléments à la phylogénie et à la biogéographie des genres *Alayotityus* Armas et *Tityopsis* Armas (Scorpiones, Buthidae). *Biogeographica*, 72 (1): 33–39.

LOURENÇO, W. R., P. O. WAEBER & L. WILMÉ. 2016a. The geographical pattern of distribution of the genus *Tityobuthus* Pocock, 1890, a typical Ananterinae element endemic to Madagascar (Scorpiones: Buthidae). *Comptes Rendus Biologies*, 339: 427–436.

LOURENÇO, W. R. & L. WILMÉ. 2015a. Species of *Grosphus* Simon, 1880, associated to the group *madagascariensis* / *hirtus* (Scorpiones: Buthidae); description of a peculiar new species from the humid eastern forests of Madagascar. *Entomologische Mitteilungen aus dem Zoologischen Museum Hamburg*, 17 (194): 207–223.

LOURENÇO, W. R. & L. WILMÉ. 2015b. Scorpions collected in the Makay mountain range, Madagascar (Scorpiones: Hormuridae, Buthidae) and with description of a new species. *Revista Iberica de Arachnologia*, 26: 55–61.

LOURENÇO, W. R. & L. WILMÉ. 2016. Three new species of *Grosphus* Simon 1880, (Scorpiones: Buthidae) from Madagascar; possible vicariant cases within the *Grosphus bistriatus* group of species. *Madagascar Conservation & Development*, 11 (2): 1–14.

LOURENÇO, W. R., L. WILMÉ & P. O. WAEBER. 2015. More about the geographical distribution of the Malagasy genus *Neogrosphus* Lourenço, 1995 (Scorpiones: Buthidae) and description of a vicariant new species. *Comptes Rendus Biologies*, 339: 37–43.

LOURENÇO, W. R., L. WILMÉ & P. O. WAEBER. 2016b. More about the geographical pattern of distribution of the genus *Pseudouroplectes* Lourenço, 1995 (Scorpiones: Buthidae) from Madagascar. *Comptes Rendus Biologies*, 339: 37–43.

LOURENCO, W. R., L. WILMÉ L, V. SOARIMALALA & P. O. WAEBER. 2017. Species of *Grosphus* Simon, 1880 associated to *Grosphus simoni* Lourenço, Goodman & Ramilijaona, 2004 with description of two new species (Scorpiones: Buthidae). *Revista Iberica de Arachnologia*, 30: 61–69.

LOURENCO, W. R., L. WILMÉ & P. O. WAEBER. 2016c. One more vicariant new species of *Grosphus* Simon, 1880 (Scorpiones: Buthidae) from Madagascar. *Revista Iberica de Arachnologia*, 29: 45–50.

LOURENÇO, W. R., L. WILME & P. O. WAEBER. 2018a. The genus *Opisthacanthus* Peters, 1861 (Scorpiones: Hormuridae), a remarkable Gondwanian group of scorpions. *Comptes Rendus Biologies*, 341: 131–143.

LOURENCO, W. R., L. WILMÉ & P. O. WAEBER. 2018b. Two more new species of *Grosphus* Simon, 1880, associated to the '*Grosphus simoni* group' (Scorpiones: Buthidae) from the regions of the Tsingy de Bemaraha and Montagne d'Ambre (Madagascar). *Revista Iberica de Arachnologia*, 32: 73–80.

LOURENCO, W. R., L. WILMÉ & P. O. WAEBER. 2018c. One more new species of *Tityobuthus* Pocock, 1890 (Scorpiones: Buthidae) from the SW of Madagascar with comments on the distributions of associated species. *Rivista Aracnologica Italiana*, 18: 15–25.

LOURENCO, W. R. & E. YTHIER. 2010. Another new species of *Pseudouroplectes* Lourenco, 1995 from Madagascar (Scorpiones, Buthidae). *ZooKeys*, 48: 1–9

LOWE, G. 2010a. New picobuthoid scorpions (Scorpiones: Buthidae) from Oman. *Euscorpius*, 93: 1–53.

LOWE, G. 2010b. The genus *Vachoniolus* (Scorpiones: Buthidae) in Oman. *Euscorpius*, 100: 1–37.

LOWE, G. 2010c. Two new species of *Hottentotta* Birula, 1908 (Scorpiones: Buthidae) from northern Oman. *Euscorpius*, 103: 1–23.

LOWE, G. 2018. The genera *Butheolus* Simon, 1882 and *Xenobuthus* gen. nov. (Scorpiones: Buthidae) in Oman. *Euscorpius*, 261: 1–73.

LOWE, G., F. KOVAŘÍK, M. STOCKMANN & F. ŠŤÁHLAVSKÝ. 2018. Review of *Microbuthus* with description of *M. satyrus* sp. n. (Scorpiones, Buthidae) from Oman and Yemen. *Euscorpius*, 263: 1–22.

LOWE, G., F. KOVAŘÍK, M. STOCKMANN & F. ŠŤÁHLAVSKÝ. 2019. *Trypanothacus* gen. n., a new genus of burrowing scorpion from the Arabian Peninsula (Scorpiones: Buthidae). *Euscorpius*, 277: 1–30.

LOWE, G., S. R. KUTCHER & D. EDWARDS. 2003. A powerful new light source for ultraviolet detection of scorpions in the field. *Euscorpius*, 8: 1–7.

LOWE, G., E. A. YAĞMUR & F. KOVAŘÍK. 2014. A review of the genus *Leiurus* Ehrenberg, 1828 (Scorpiones: Buthidae) with description of four new species from the Arabian Peninsula. *Euscorpius*, 191: 1–129.

MATTONI, C. I., J. A. OCHOA, A. A. OJANGUREN AFFILASTRO & L. PRENDINI L. 2012. *Orobothriurus* (Scorpiones: Bothriuridae) phylogeny, Andean biogeography, and the relative importance of genitalic and somatic characters. *Zoologica Scripta*, 41 (2): 160–176.

MAURY, E. A. & W. R. LOURENÇO. 1987. *Tityus roigi*, nouvelle espèce de scorpion de l'Equateur (Scorpiones, Buthidae). *Revue Arachnologique*, 7 (2): 79–84.

MONOD L., L. CAUWET, L., E. GONZÁLEZ-SANTILLÁN & S. HUBER. 2017. The male sexual apparatus in the order Scorpiones (Arachnida): a comparative study of functional morphology as a tool to define hypotheses of homology. *Frontiers in Zoology*, 14: 51: 1–48.

MOREL, A., B. GENTILI, H. CLAUSTRE, M. BABIN, A. BRICAUD, J. RAS & F. TIECHE. 2007. Optical properties of the "clearest" natural waters. *Limnology and Oceanography*, 52 (1): 217–229.

MORENO, A. 1940. Contribución al estudio de los escorpiónides cubanos. Part III. Familia Buthidae, Addendus. *Memorias de la Sociedad Cubana de Historia Natural*, 14 (2): 161–164.

NAVIDPOUR, S., F. KOVAŘÍK, M. E. SOLEGLAD & V. FET. 2008. Scorpions of Iran (Arachnida, Scorpiones). Part I. Khoozestan Province. *Euscorpius*, 65: 1–41.

NEWLANDS, G. 1973. Zoogeographical factors involved in the trans-Atlantic dispersal pattern of the genus *Opisthacanthus* Peters (Arachnida- Scorpionidae). Annals of the Transvaal Museum, 28 (7): 91–98, pl. 1.

OHBA, M., K. E SAMONDS, M. LAFLEUR, J. R. ALI & L. R. GODFREY. 2016. Madagascar's climate at the K/P boundary and its impact on the island's biotic suite. *Palaeogeography, Palaeoclimatology, Palaeoecology*, 441 (4): 688–695.

OJANGUREN-AFFILASTRO, A. A. 2005. Estudio monogràfico de los escorpiones de la Repùblica Argentina. *Revista Ibérica de Aracnologia*, 11: 75–241.

OJANGUREN-AFFILASTRO, A. A., R. S. ADILARDI, C. I. MATTONI, M. J. RAMIREZ & F. SARA CECCARELLI. 2017a. Dated phylogenetic studies of the southernmost American buthids (Scorpiones; Buthidae). *Molecular Phylogenetics and Evolution*, 110: 39–49.

OJANGUREN-AFFILASTRO, A. A., R. S. ADILARDI, R. CAJADE, M. J. RAMÍREZ, F. SARA CECCARELLI & L. M. MOLA. 2017b. Multiple approaches to understanding the taxonomic status of an enigmatic new scorpion species of the genus *Tityus* (Buthidae) from the biogeographic island of Paraje Tres Cerros (Argentina). *PLoS ONE* 12 (7): e0181337. https:// doi.org/10.1371/ journal.pone.0181337.

PINTO-DA-ROCHA, R. & W. R. LOURENÇO. 2000. Two new species of *Tityus* from Brazilian Amazonia (Scorpiones, Buthidae). *Revue Arachnologique*, 13 (13): 187–195.

POCOCK, R. I. 1889a. Notes on some Buthidae, new and old. *Annals and Magazine of Natural History*, 3: 334–351.

POCOCK, R. I. 1889b. Another new species of scorpion from Madagascar. *Annals and Magazine of Natural History*, 3: 461–463.

POCOCK, R. I. 1890. A revision of the genera of scorpions of the family Buthidae, with descriptions of some South-African species. *Proceedings of the Zoological Society*, 1890: 114–141.

POCOCK, R. I. 1893b. Notes on the classification of scorpions, followed by some observations on synonymy, with descriptions of new genera and species. *Annals and Magazine of Natural History*, (6), 12: 303–330.

POCOCK, R. I. 1896. A further revision of the species of Scorpions belonging to the South-African genera *Uroplectes*, *Lepreus* and *Tityolepreus*. *Annals and Magazine of Natural History*, 6 (16): 377–393.

POLIS, G. & SISSOM, W. D. 1990. Life history. Pp. 161–223 in POLIS, G. A. (Ed.) *The Biology of Scorpions*. Stanford University Press, Stanford, California.

PRENDINI, L. 2000. A new species of *Parabuthus* Pocock (Scorpiones, Buthidae), and new records of *Parabuthus capensis* (Ehrenberg), from Namibia and South Africa. *Cimbebasia*, 16: 201–214.

PRENDINI, L. 2001. Phylogeny of *Parabuthus* (Scorpiones, Buthidae). *Zoologica Scripta*, 30: 13–35.

PRENDINI, L. 2003. Discovery of the male of *Parabuthus muelleri*, and implications for the phylogeny of *Parabuthus* (Scorpiones: Buthidae). *American Museum Novitates*, 3408: 1–24.

PRENDINI, L. 2004a. Systematics of the Genus *Pseudolychas* Kraepelin (Scorpiones: Buthidae). *Annals of The Entomological Society of America*, 97 (1): 37–63.

PRENDINI, L. 2004b. The systematics of Southern African *Parabuthus* Pocock (Scorpiones, Buthidae): revisions to the taxonomy and key to the species. *Journal of Arachnology*, 32: 109–186.

PRENDINI, L. 2015a. Three new *Uroplectes* (Scorpiones: Buthidae) with punctate metasomal segments from tropical central Africa. *American Museum Novitates*, 3840: 1–32.

PRENDINI, L. 2015b. A remarkably small species of *Uroplectes* Peters, 1861 (Scorpiones: Buthidae), endemic to the Succulent Karoo of South Africa. *African Invertebrates*, 56 (2): 499–513.

PRENDINI, L. & L. ESPOSITO. 2010. A reanalysis of *Parabuthus* (Scorpiones: Buthidae) phylogeny with descriptions of two new *Parabuthus* species endemic to the Central Namib gravel plains, Namibia. *Zoological Journal of the Linnean Society*, 159: 673–710.

PRENDINI, L., L. A. ESPOSITO, J. C. HUFF & E. S. VOLSCHENK. 2009. Redescription of *Rhopalurus abudi* (Scorpiones, Buthidae), with first description of the male and first record from mainland Hispaniola. *Journal of Arachnology*, 37 (2): 206–224.

PRENDINI, L., E. S. VOLSCHENK, S. MAALIKI & A. V. GROMOV. 2006. A 'living fossil' from Central Asia: The morphology of *Pseudochactas ovchinnikovi* Gromov, 1998 (Scorpiones: Pseudochactidae), with comments on its phylogenetic position. *Zoologischer Anzeiger*, 245 (3-4): 211–248.

PRENDINI, L. & W. WHEELER. 2005. Scorpion higher phylogeny and classification, taxonomic anarchy, and standards for peer review in online publishing. *Cladistics*, 21: 446–494.

QUICKENDEN, T. I., C. G. FREEMAN & R. A. J. LITJENS. 2000. Some comments on the paper by Edward S. Fry on the visible and near-ultraviolet absorption spectrum of liquid water. *Applied Optics*, 39 (16): 2740–2742.

RUBIN, M., J. C. LAMSDELL, L. PRENDINI & M. J. HOPKINS. 2017. Exocuticular hyaline layer of sea scorpions and horseshoe crabs suggests cuticular fluorescence is plesiomorphic in chelicerates. *Journal of Zoology*, 303: 245–253.

SAMONDS, K. E., L. R. GODFREY, J. R. ALI, S. M. GOODMAN & M. VENCES, M. R. SUTHERLAND, M. T. IRWIN & D. W. KRAUSE. 2013. Imperfect Isolation: Factors and Filters Shaping Madagascar's Extant Vertebrate Fauna. *PLoS ONE*, 8 (4): e62086. doi:10.1371/journal.pone.0062086

SHARMA, P. P., C. M. BAKER, J. G. COSGROVE JG, J. E. JOHNSON, J. T. OBERSKI, R. J. RAVEN, M. S. HARVEY, S. L. BOYER & G. GIRIBET. 2018. A revised dated phylogeny of scorpions: Phylogenomic support for ancient divergence of the temperate Gondwanan family Bothriuridae. *Molecular Phylogenetics and Evolution*, 122: 37–45.

SIMON, E. 1880. Études arachnologiques 12e Mémorie (1). XVIII. Déscriptions de genres et espèces de l'ordre des Scorpiones. *Annales de la Sociètè Entomologique de France*, (5), 10: 377–398.

SISSOM, W. D. 1990. Systematics, biogeography and paleontology. Pp. 64–160 in POLIS, G. A. (Ed.) *The Biology of Scorpions*. Stanford University Press, Stanford, California.

SISSOM, W. D. 1995. Redescription of the scorpion *Centruroides thorelli* Kraepelin (Buthidae) and description of two new species. *Journal of Arachnology*, 23 (2): 91–99.

SISSOM, W. D. & O. F. FRANCKE. 1983. Redescription of *Centruroides testaceus* (DeGeer) and description of a new species from the Lesser Antilles (Scorpiones: Buthidae). *Occasional Papers. Tthe Museum, Texas Tech University*, 88: 1–13.

SISSOM, W. D. & W. R. LOURENÇO. 1987. The genus *Centruroides* in South America (Scorpiones, Buthidae). *Journal of Arachnology*, 15 (1): 11–28.

SISSOM, W. D. & S. A. STOCKWELL. 1991. The genus *Serradigitus* in Sonora, Mexico, with descriptions of four new species (Scorpiones, Vaejovidae). *Insecta Mundi*, 5 (3–4): 197–214.

SISSOM, W. D., G. A. POLIS & D. D. WATT. 1990. Field and laboratory methods. Pp. 445–461 in POLIS, G. A. (Ed.). *The Biology of Scorpions*. Stanford University Press, Stanford, CA.

SMITH, R. C. & K. S. BAKER. 1981. Optical properties of the clearest natural waters (200–800 nm). *Applied Optics*, 20 (2): 177–184.

SOLEGLAD, M. E. 1974. *Vejovis calidus*, a new species of scorpion from Coahuila, Mexico (Scorpionida: Vejovidae). *Entomological News*, 85: 109–115.

SOLEGLAD, M. E. & V. FET. 2003a. The scorpion sternum: structure and phylogeny (Scorpiones: Orthosterni). *Euscorpius*, 5: 1–34.

SOLEGLAD, M. E. & V. FET. 2003b. High-level systematics and phylogeny of the extant Scorpions (Scorpiones: Orthosterni). *Euscorpius*, 11: 1–175.

SOLEGLAD, M. E. & V. FET. 2004. The systematics of the scorpion subfamily Uroctoninae (Scorpiones: Chactidae). *Revista Ibérica de Aracnología*, 10: 81–128.

SOLEGLAD, M. E. & V. FET. 2006. Contributions to scorpion systematics. II. Stahnkeini, a new tribe in scorpion family Vaejovidae (Scorpiones: Chactoidea). *Euscorpius*, 40: 1–34.

SOLEGLAD, M. E. & V. FET. 2008. Contributions to scorpion systematics. III. Subfamilies Smeringurinae and Syntropinae. *Euscorpius*, 71: 1–117.

SREENIVASA-REDDY, R. P. 1966. Contribution à la connaissance des scorpions de l'Inde. I. *Charmus indicus* Hirst 1915 (fam. Buthidae). *Bulletin du Muséum d'Histoire Naturelle*, *Paris*, 38 (3): 247–256.

STADLER, A. T., V. BOŠTJAN VIHAR, M. GÜNTHER, M. HUEMER, M. RIEDL, S. SHAMIYEH, B. MAYRHOFER, W. BÖHME & W. BAUMGARTNER. 2016. Adaptation to life in aeolian sand: how the sandfish lizard, *Scincus scincus*, prevents sand particles from entering its lungs. *Journal of Experimental Biology*, 219, 3597–3604.

STAHNKE, H. L. 1971. Scorpion nomenclature and mensuration. *Entomological News*, 81: 297–316.

STAHNKE, H. L. 1972. A key to the genera of Buthidae (Scorpionida). *Entomological News*, 83 (5): 121–133.

STAHNKE, H. L. 1974. Revision and keys to the higher categories of Vejovidae (Scorpionida). *Journal of Arachnology*, 1 (2): 107–141.

STEBBINS, R. C. 1943. Adaptations of the nasal passages for sand burrowing in the saurian genus *Uma*. *American Naturalist*, 768: 38–52.

STOCKWELL, S. A. 1989. *Revision of the Phylogeny and Higher Classification of Scorpions* (*Chelicerata*). Ph.D. Dissertation, University of Berkeley, Berkeley, California. 319 pp. (unpublished). University Microfilms International, Ann Arbor, Michigan.

TIKADER, B. K. & D. B. BASTAWADE. 1983. *The fauna of India: Scorpions. Scorpionida, Arachnida*. Vol III. Zoological Survey of India, Calcutta, 668 pp.

TOLLEY, K. T., TOWNSEND & M. VENCES. 2013. Large-scale phylogeny of chameleons suggests African origins and Eocene diversification. *Proceedings of the Royal Society B*, 280: 20130184.

TOWNSEND, T. M., D. R. VIEITES, F. GLAW & M. VENCES. 2009. Testing species-level diversification hypotheses in Madagascar: the case of microendemic *Brookesia* leaf chameleons. *Systematic Biology*, 58 (6): 641–656.

UBISCH, M. von. 1921. Über eine neue *Jurus*-Art aus Kleinasien nebst einigen Bemerkungen über die Funktion der Kämme der Scorpione. *Zoologische Jahrbücher für Systematik*, 44: 503–516.

VACHON, M. 1940. Sur la systématique des Scorpions. *Mémoires du Muséum national d'Histoire Naturelle, Paris*, 13 (2): 241–260.

VACHON, M. 1950a. Quelques remarques sur le peuplement en scorpions du Sahara à propos d'une nouvelle espèce du Sénégal: *Butheoloides monodi*. *Bulletin de la Société Zoologique de France*, 75 (4): 170–176.

VACHON, M. 1950b. Remarques sur les scorpions de l' Angola (Première note). *Publicacoes Culturais da Companhia de Diamantes Angola*, 5–18.

VACHON, M. 1952. Études sur les scorpions. *Institut Pasteur d'Algérie*, *Alger*, 1–482. (published 1948–1951 in *Archives de l'Institut Pasteur d'Algérie*, 1948, 26: 25–90, 162–208, 288–316, 441–481. 1949, 27: 66–100, 134–169, 281–288, 334–396. 1950, 28: 152–216, 383–413. 1951, 29: 46–104).

VACHON, M. 1961. A propos d'un scorpion de l'Inde: *Buthiscorpio laevicauda* Werner (famille des Scorpionidae), synonyme de *Stenochirus politus* Pocock 1899 (famille des Buthidae). *Bulletin de la Société Zoologique de France*, 86 (6): 789–795.

VACHON, M. 1963. De l'utilité, en systématique, d'une nomenclature des dents de chélicères chez les scorpions. *Bulletin du Musèum national d'Histoire Naturelle, Paris*, (2), 35 (2): 161–166.

VACHON, M. 1969. *Grosphus griveaudi*, nouvelle espèce de Scorpion Buthidae malgache. *Bulletin du Musèum national d'Histoire naturelle, Paris*, (2), 41: 476–483.

VACHON, M. 1974. Étude des caractères utilisés pour classer les familles et les genres de Scorpions (Arachnides). 1. La trichobothriotaxie en Arachnologie, Sigles trichobothriaux et types de trichobothriotaxie chez les Scorpions. *Bulletin du Musèum National d'Histoire naturelle, Paris*, (3), 140 (Zool. 104), mai-juin 1973: 857–958.

VACHON, M. 1975. Sur l'utilisation de la trichobothriotaxie du bras des pédipalpes des Scorpions (Arachnides) dans le classement des genres de famille des Buthidae Simon. *Comptes Rendus Hebdomadaires des Séances de l'Académie des Sciences*, (D), 281 (21): 1597–1599.

VACHON, M. 1977a. Contribution à l'étude des scorpions Buthidae du nouveau monde. I. Complément à la connaissance de *Microtityus rickyi* Kj. W. 1956 de l'ile de

la Trinité. II. Description d'une nouvelle espèce et d'un nouveau genre mexicains: *Darchenia bernadettae*. III. Clé de détermination des genres de Buthidae du nouveau monde. *Acta Biologica Venezuelica*, 9 (3): 283–302.

VACHON, M. 1977b. Contribution à la connaissance de la trichobothriotaxie chez le scorpion cavernicole *Alayotityus delacruzi* Armas 1973 (famille des Buthidae), suivie de quelques 871 données biospéologiques. Pp. 93–97 in ORGHIDAN, T, A. NUNEZ JIMENEZ ET AL. (Eds.) *Résultats des expéditions biospéléologiques Cuba-no-Roumaines a Cuba*. Vol. 2. Bucharest: Institut de Spéologie "Emil Racovitza".

VENCES, M., K. C. WOLLENBERG, D. R. VIEITES & D. C. LEES. 2009. Madagascar as a model region of species diversification. *Trends in Ecology and Evolution*, 24 (8): 456–465.

VOLSCHENK, E. S., C. I. MATTONI & L. PRENDINI. 2008. Comparative anatomy of the mesosomal organs of scorpions (Chelicerata, Scorpiones), with implications for the phylogeny of the order. *Zoological Journal of the Linnean Society*, 154: 651–675.

WAGNER, F. W. 1977. Descriptions of *Centruroides* Marx from Yucatan Peninsula (Arachnida, Scorpionida, Buthidae). *Bulletin of the Association for Mexican Cave Studies*, 6: 39–47.

WANLESS, F. R. 1977. On the occurrence of the scorpion *Euscorpius flavicaudis* (DeGeer) at Sheerness Port, Isle of Sheppey, Kent. *Bulletin of the British Arachnological Society*, 4 (2): 74–76.

WELLS, N. 2003. Some hypotheses on the Mesozoic and Cenozoic paleoenvironmental history of Madagascar. Pp. 16–34 in GOODMAN, S., BENSTEAD, J. (Eds.). *The Natural History of Madagascar*. The University of Chicago Press, Chicago, Illinois.

WERNER, F. 1934. Scorpiones, Pedipalpi. In: H. G. Bronns *Klassen und Ordnungen des Tierreichs. Akademische Verlaggesellschaft*, Leipzig. 5, IV, 8, Lief. 1-2, Scorpiones, pp. 1–316.

WILMÉ, L., S. M. GOODMAN & J. U. GANZHORN. 2006. Biogeographic evolution of Madagascar's microendemic biota. *Science*, 312: 1063–1065.

WIT, M. J. DE. 2003. Madagascar: heads it's a continent, tails it's an island. *Annual Review of Earth and Planetary Sciences*, 31: 213–48.

WOOD, H. M., R. G. GILLESPIE, C. E. GRISWOLD & P. C. WAINWRIGHT. 2014. Why is Madagascar special? The extraordinarily slow evolution of pelican spiders (Araneae, Archaeidae). *Evolution*, 69 (2): 462–481.

YANG, X., Y. NORMA-RASHID, W. R. LOURENÇO & M. ZHU. 2013. True lateral eye numbers for extant buthids: a new discovery on an old character. *PLoS ONE*, 8 (1): e55125. doi:10.1371/journal.pone.0055125

YODER, A. D. & M. D. NOVAK. 2006. Has vicariance or dispersal been the predominant biogeographic force in Madagascar? Only time will tell. *Annual Review of Ecology, Evolution, and Systematics*, 37: 405–431.

Appendix 1. Characters of outgroup buthids compared to the '*Grosphus*' group.

I. Position of femur trichobothrium d_2 (petite) in '*Uroplectes*' group (Fet et al., 2005).

Uroplectes: d_2 dorsal in: *U. olivaceus* (GLPC), *U. planimanus* (Lamoral, 1979; GLPC), *U. teretipes* (Lamoral, 1979), *U. tumidimanus* (Lamoral, 1979), *U. zambezicus* (Prendini, 2015a); carinal in: *U. ansiedippenaarae* (Prendini, 2015b), *U. machadoi* (Lourenço, 2000c), *U. malawicus* (Prendini, 2015a), *U. vittatus* (GLPC); internal in: *U. carinatus* (Lamoral, 1979), *U. chubbi* (GLPC), *U. fischeri* (Kovařík et al., 2016a), *U. gracilior* (Lamoral, 1979), *U. longimanus* (Lamoral, 1979), *U. occidentalis* (Vachon, 1950b), *U. otjimbinguensis* (Lamoral, 1979), *U. pilosus* (Lamoral, 1979) and *U. schlecteri* (Lamoral, 1979).

Parabuthus: d_2 dorsal in: *P. capensis* (Eastwood, 1977), *P. brevimanus* (Lamoral, 1979), *P. distridor* (Lamoral, 1980), *P. glabrimanus* (Prendini & Esposito, 2010), *P. granulatus* (Lamoral, 1979; GLPC), *P. kalaharicus* (Lamoral, 1977), *P. laevifrons* (Lamoral, 1979), *P. liosoma* (GLPC), *P. namibensis* (Lamoral, 1979), *P. neglectus* (Eastwood, 1977), *P. stridulus* (Lamoral, 1979); internal in: *P. gracilis* (Lamoral, 1979), *P. granimanus*, *P. heterurus* (Prendini & Esposito, 2010), *P. kraepelini*, *P. kuanyamarum* (Lamoral, 1979), *P. mossambicensis* (Fitzpatrick, 1994) *P. muelleri* (Prendini, 2000, 2003), *P. nanus* (Lamoral, 1979), *P. pallidus* (GLPC), *P. planicauda* (Prendini & Esposito, 2010), *P. transvaalicus* (GLPC), *P. raudus*, *P. schlecteri* (Lamoral, 1979) and *P. villosus* (Lamoral, 1979).

II. Relative distance between chela manus *Eb* trichobothria: R_{123} = d(Eb_2, Eb_3)/ d(Eb_1, Eb_2).

Pseudolychas (estimated from UV photomicrographs in Prendini, 2004a): *P. ochraceus*, ♂ 0.48, ♀ 0.46; *P. pegleri*, ♂ 0.42, ♀ 0.40; *P. transvaalicus*, ♂ 0.99, ♀ 0.53.

'*Uroplectes*' group (Fet et al., 2005): *Butheoloides*, $R_{123} \geq \sim 0.5$ (Kovařík, 2003, 2015, 2016; Lourenço, 1995b, 1996e, 2002, 2010, 2013a; Vachon, 1950a); *Buthoscorpio*, $R_{123} \geq \sim 0.5$ (Aswathi et al., 2015; Maqsood Javed et al., 2010; Lourenço, 2012a; Tikader & Bastawade, 1983; Vachon, 1961); *Neoprotobuthus*, $R_{123} > 0.5$ (Lourenço, 2000a); *Pseudolissothus*, $R_{123} \sim 1$ (Lourenço, 2001c); *Pseudouroplectes*, $R_{123} > 0.5$, except *P. tsingy* (Lourenço & Ythier, 2010; Lourenço et al., 2016b); *Tityobuthus*, $R_{123} \geq \sim 0.5$ (Lourenço, 1996c; Lourenço & Goodman, 1994, 2003b; Lourenço et al., 2008, 2016a).

'*Tityus*' group (Fet et al., 2005): *Alayotityus*, $R_{123} > 0.5$ (e.g., Armas, 1977b; Lourenço & Vachon, 1996; Vachon, 1977b); *Centruroides*, $R_{123} > 0.5$ (e.g. Armas, 1977; Francke, 1978; Francke & Stockwell, 1987; Sissom, 1995; Sissom & Francke, 1983; Sissom & Lourenço, 1987; Wagner, 1977); *Heteroctenus*, $R_{123} > \sim 0.5$ (Armas, 1981; Lourenço, 1982; Prendini et al., 2009); *Ischnotelson*, $R_{123} < 0.5$ or > 0.5 (Esposito et al., 2017; Lenarducci et al., 2005); *Jaguajir*, $R_{123} > 0.5$ (Esposito et al., 2017; Lourenço, 1982; Lourenço & Pinto-da-Rocha, 1997); *Microtityus*, $R_{123} > 0.5$, typically $\geq \sim 1$ (González-Sponga, 2001b; Lourenço & Eickstedt, 1983; Vachon, 1977a); *Physoctonus*, $R_{123} > 0.5$ (Esposito et al., 2017; Lourenço, 2017); *Rhopalurus*, $R_{123} > 0.5$ (Esposito et al., 2017; Lourenço, 1982); *Tityopsis,* $R_{123} > 0.5$ (Lourenço & Vachon, 1996); *Tityus*, $R_{123} > 0.5$, typically $\geq \sim 1$ (e.g., Francke & Stockwell, 1987; González-Sponga, 1981a, 2001a, 2002, 2007, 2008a, 2008b, 2009; Lourenço, 1980, 1984a, 1984b; Maury & Lourenço, 1987; Ojanguren-Affilastro, 2005; Ojanguren-Affilastro et al., 2017b; Pinto-da-Rocha & Lourenço, 2000); *Troglorhopalurus*, $R_{123} > \sim 0.5$ (Gallão & Bichuette, 2016; Lourenço & Pinto-da-Rocha, 1997); *Zabius*, $R_{123} > 0.5$, typically $\geq \sim 1$ (Abalos, 1953; Acosta et al., 2008; Ojanguren-Affilastro, 2005).

III. Occurrence of round or ovoid spiracles.

'*Uroplectes*' group (Fet et al., 2005): *Ankaranocharmus* (Lourenço, 2004b), *Neoprotobuthus* (Lourenço, 2000a), and *Microcharmus* (Lourenço, 2000a; Lourenço & al., 2006a).

'*Charmus*' group (Fet et al., 2005): *Charmus* (Kovařík et al., 2016c), *Somalicharmus* (Kovařík et al., 2016e), and *Thaicharmus* (Kovařík et al., 2007).

'*Tityus*' group (Fet et al., 2005): *Alayotityus* (Armas, 1973; Lourenço & Vachon, 1996), *Chaneke* (Francke et al., 2014; Kovařík et al., 2016b), *Ischnotelson* (Esposito et al., 2017), *Mesotityus* (Armas & Rojas-Runjaic, 2006; González-Sponga, 1981b), *Microtityus* (Kovařík & Teruel, 2014), *Tityopsis* (Armas & Martin-Frias, 1998), Lourenço & Vachon, 1996; Moreno, 1940), at least some *Tityus* (*Archaeotityus*) (Armas & Rojas-Runjaic, 2006), at least some *Tityus* (*Caribetityus*) (Armas, 1999; Armas & Rojas-Runjaic, 2006; Kovařík & Teruel, 2014), *Troglorhopalurus* (Esposito et al., 2017) and *Zabius* (Abalos, 1953; Acosta et al., 2008; Ojanguren-Affilastro, 2005).

Fossil buthoids: from Cretaceous amber: *Archaeobuthus estephani* Lourenço, 2001; *Betaburmesebuthus kobberti* Lourenço & Beigel, 2015; *Chaerilobuthus complexus* Lourenço & Beigel, 2011; *Chaerilobuthus gigantosternum* Lourenço, 2016; and from Baltic (Middle Eocene) amber (cf. Lourenço, 2009, 2012): *Palaeoakentrobuthus knodeli* Lourenço & Weitschat, 2000; *Palaeoananteris ribnitiodamgartensis* Lourenço & Weitschat, 2001; *Palaeolychas weitschati* Lourenço, 2012; *Palaeoprotobuthus pusillus* Lourenço & Weitschat, 2000.

Appendix 2. Material examined.

Madagascar:

Grosphus goudoti Lourenco & Goodman, 2006

1♂ (holotype, Figs. 58–59, 88, 211, 239–262), Antsiranana Province, Forêt de Bobankota, Versant ouest, site No. 2, 11 km E of Daraina, 13°13.414'S 49°45.586'E, 350–550 m a. s. l., X.2002-III.2003, leg. M. Raheriarisena & H. A. Rakotondravony (MHNG).

Grosphus hirtus Kraepelin, 1901
1♂ (holotype of *Grosphus garciai* Lourenço, 2001, Figs. 66, 291–292, 294–305) 1juv. (paratype, Figs. 213, 293), Majunga Province, Ankarafantsika Reserve, Ampijoroa, 16°18'45.2"S 46°48'54.2"E, 73 m a. s. l., VI.2000, leg. García Herrero (MHNG); 1♀ (labeled *Grosphus madagascariensis*, Fig. 197), Majunga Province, Ankarafantsika Reserve, Forest Station Ampijoroa, Ampijoroa village, 16°18'45.2"S 46°48'54.2"E, 73 m a. s. l., VI.2000, leg. García Herrero (MHNG); 1♂ (labeled *Grosphus garciai*), Majunga Province, Ankarafantsika Reserve, Forest Station Ampijoroa, 16°18'S 46°48'E, sand area of Paquypodium (=*Pachypodium*), 27.II.2001-1.III.2001, leg. García Herrero (MHNG); 4♂4♀1juv. (Figs. 64, 196, 212, 263–290), southwestern region, inland zone between Ranohira and Llakaka, IX.2004, leg. W. R. Lourenço (ZMUH); 1♂ (Figs. 11, 21, 96, 122, 134, 181), Antsiranana Province, Reserve Special d'Analamerana, Fôret d'Ankavanana, 15.8 km SE Anivorano-Nord, 12°47.7'S 49°22.1'E, 200 m a. s. l., 23.I.2004, pitfall trap, in particularly disturbed mixed dry deciduous and humid forest, leg. S. M. Goodman, SMG#14135 (FMNH 86976); 1♀ (Figs. 11, 42, 96, 146, 167, 182), Mahajanga Province, Forêt de Beanka, 18°01'23"S 44°30'08"E, 220 m a. s. l., slightly disturbed dry deciduous forest, leg. Z. H. Harimpitia, Z.H H-032 (FMNH 3482761); 1♂ (Fig. 60, 62), N Antsiranana Province, Diego Suarez env., E of Ramena village, 12°15'9.95"S 49°21'31.05"E, ca. 50 m a. s. l., (FKCP, GLPC); 1♂ (Fig. 61), Mahajanga Province, Mahajamba riv., Ampatika env., 16°08'S 47°15'E, 2002 (FKCP, GLPC); 4♂3♀37juvs. (Fig. 63), Majunga Province, Ankarafantsika Reserve, Forest Station Ampijoroa, "Jardin Botanique A", 16°18'S 46°48'E, 24.-24.II.2001, leg. García Herrero (MHNG); 1♂1♀ (Figs. 65, 198), Toamasina Province, Forêt de Vohitaly, site F, 5 km SE village Anjiahely, 15°26'58"S 49°32'06"E, 540–680 m a. s. l., 28.XII.2002, leg. V. Andrianjakarivelo (MHNG); 1♂ (Fig. 64), southwestern region, inland zone between Ranohira and Llakaka, IX.2004, leg. W. R. Lourenço (ZMUH); 1♂1♀ (Figs. 21, 42, 97, 133, 149, 166), Mahajanga Province, SE d'Ampijoroa, 16°19.4'S 46°48.4'E, 160 m a. s. l., in dry deciduous forest on white sand, 20.IV.2003, leg. S. M. Goodman, SMG#13631,#13632 pitfall 2 (FMNH♂73434, ♀73436), det. as *G. garciai*.

Grosphus* sp. nr *hirtus
10♀ (Fig. 40), Moramanga env., Anjiro, 1995 (FKCP, GLPC).

Grosphus madagascariensis (Gervais, 1843)
3♂ (Fig. 56) 6♀2juvs., 'Madagascar', leg. Saussure, det. M. Vachon (MHNG); 11♂41♀ (Figs. 1–4, 9, 22, 41, 54, 94, 123, 135, 145, 159–160, 165, 183, 199, 214, 227, 231–234), Moramanga env., Toamasina, Anjiro, 18°52'S 47°59'E, 1995 (FKCP, GLPC); 1♂ (Figs. 52–53, 86), Andasibe, Marie Guest House, 18.94727°S 048.41782°E, No. 1197 (FKCP, GLPC); 1♂ (*G. mandena* holotype, Figs. 215, 348–349), 2♂1♀1juv. (*G. mandena* paratypes, Figs. 55, 200, 350–351), Toliara Province, Mandena - Fort Dauphin, littoral forest 10 km north of Fort Dauphin, 6-12/I/1999, leg. J.-B. Ramanamanjato (MHNG); 1♂2♀ (Figs. 341–347), Moramanga env., 1997, (FKCP); 1♂1♀, Andasibe-Mantadia, Anamalazaotra forest (FKCP); 1♀, Fianarantsoa district, Ranomafana env., 21°13'S 47°25'E, 1995 (FKCP); 5♂1♀ (Figs. 10, 95, 124, 136, 148, 168, 184, 306–340), Toamasina Province, Ambalafary Forest, 14.5 km SW Andasibe, 19°02'38"S 48°20'55"E, 995 m a. s. l., 11.III.2012, dense, humid lowland and montane forest, leg. V. Soarimalala VS-2142 (FMNH 3482757), det. as *G. simoni*; 2♂3♀1juv. (Fig. 57), Toamasina Province, Andasibe-Mantadia, near Andasibe, Camp Feon'ny Ala, 938 m a. s. l., 18°56.836'S 48°25.063'E, (FKCP, GLPC).

Grosphus voahangyae Lourenço & Wilmé, 2015
4♂1♀ (paratypes, Figs. 12, 43, 67–68, 89, 98, 125, 137, 147, 169, 185, 228, 352–386), Toamasina Province, region of Alaotra-Mangoro, Moramanga District, Analamy Forest, 10 km E Ambohimanarivo Village, 18°48'20.8"S 48°21'38.1"E, 1006 m a. s. l., 15–31.I.2009, dense humid forest, leg. V. Soarimalala VS-2142 (FMNH 2992958).

Neogrosphus griveaudi (Vachon, 1969)
1♂1♀2juvs. (Figs. 69–70, 87, 606–619), Toliara Province, Tsimanampetsotsa National Park, Andranovao camp, 15 m a. s. l., 24°01.505'S 43°44.306'E (FKCP, GLPC).

Teruelius ankarafantsika (Lourenço, 2003) **comb. n.**
1♀ (holotype, Figs. 219, 389–390, 394–403, 406–408, 410–415) 1♂ (paratype, Figs. 201, 220, 387–388, 391–393, 404–405, 409, 416–417), Majunga Province, Ankarafantsika Reserve, Forest Station Ampijoroa, 16°18'S 46°48'E, sand area of Paquypodium (=*Pachypodium*), 27.II.2001-1.III.2001, leg. García Herrero (MHNG); 1♀45 newborn (paratypes), Majunga Province, Ankarafantsika Reserve, Forest Station Ampijoroa, "Jardin Botanique A", 16°18'S 46°48'E, 24.-24.II.2001, leg. García Herrero (MHNG); 1♂ (Figs. 13, 78–79, 93, 99, 138, 150, 170), Mahajanga Province, SE d'Ampijoroa, 16°19.4'S 46°48.4'E, 160 m a. s. l., in dry deciduous forest on white sand, 17.IV.2003, leg. S. M. Goodman, SMG#13610 pitfall (FMNH 73423); 1♀ (Figs. 13, 44, 78–79, 99, 127), Mahajanga Province, SE d'Ampijoroa, 16°19.4'S 46°48.4'E, 100 m a. s. l., in dry deciduous forest on white sand, 22.IV.2003, leg. S. M. Goodman, SMG#13639 pitfall 3 bucket 74 (FMNH 73425); 1♂1♀ (Figs. 15, 24, 45, 80, 99, 171, 186–187), Mahajanga Province, Réserve Forestière de l'Ankarafantsika, 5 km SSE Ampijoroa, 16°20.3'S 46°47.6'E, 160 m a. s. l., 4–7.II.1997, slightly disturbed deciduous forest, pitfall, leg. S. M. Goodman (FMNH ♂73430, ♀73432), det. as *G. bistriatus*.

Teruelius ankarana (Lourenço & Goodman, 2003) **comb. n.**
1♂1♀ (Figs. 14, 46, 71–72, 90, 100, 128, 141, 154–155, 172, 188), Antsiranana Province, Reserve Special d'Analamerana, Forêt d'Ankavanana, 15.8 km SE Anivorano-Nord, 12°47.7'S 49°22.1E, 200 m a. s. l., 23.I.2004, pitfall trap, in particularly disturbed mixed dry deciduous and humid forest, leg. S. M. Goodman, SMG#14114 (FMNH 86978); 8♂10♀5juvs.♂3juvs.♀ (Figs. 100, 202, 216, 418–421), Antsiranana Province, Ankarana NP, Diego Suarez env., E of Ramena village, 12°57'43.4"S

49°07'13.48"E, 126 m a. s. l., (FKCP, GLPC); 2♂ (after 4th ecdysis) 2♂ (after 5th ecdysis) 2♀, 2011 (FKCP); 1♂, Mahajanga Province, Ankofia riv., Ambodimanga env. (Bora) (FKCP).

Teruelius annulatus (Fage, 1929) **comb. n.**
4♂1♀ (Figs. 77, 203, 218, 422–432) 1juv.(♂), Toliara Province, Tsimanampetsotsa National Park, Andranovao camp, 15 m a. s. l., 24°01.505'S 43°44.306'E, 2014 (FKCP, GLPC); 1♀, Isalo Mts, Ranohira near Tulear, 1998 (FKCP).

Teruelius bistriatus (Kraepelin, 1900) **comb. n.**
1♂1♀ (syntypes, Figs. 204, 221, 433–458), Tullear, Makabo, 5.VII.1900, ZMUH.

Teruelius feti (Lourenço, 1996) **comb. n.**
2 juv ♂ (holotype, Figs. 459–472, paratype), Toliara Province, Fôret de Vohilema, 35 km SE Sakaraha, 22°41.0'S 44°49.8'E, 780 m a. s. l., 17–24.I.1996, leg. S. M. Goodman (FMNH holotype 11031, paratype 11032); 2♀ (topotypes of *G. makay*, Figs. 210, 226, 459a), Toliara Province, Makay Mts., (FKCP).

Teruelius flavopiceus (Kraepelin, 1901) **comb. n.**
1♂ (Figs. 16, 101, 173, 189, 230), Toliara Province, Parc National de Bemaraha, Ankidrodroa, 2.5 km NE Bekopaka, 19°7.9'S 44°48.5'E, 100 m a. s. l., 25.XI.2001, secondary dry forest, leg. S. M. Goodman SMG12489 (FMNH 73453); 1♀ (Figs. 16, 47, 101, 129, 143, 153, 174), Majunga, Melaky, Antsalova, Antsalova, Tsiandro, Bemaraha Plateau, Ambakoa forest, near Befanazava River, 18°47.838'S 44°52.904'E, 1400 ft a. s. l., 17.I.2006, valley marsh, pitfall 3, bucket 7, leg. H. A. Rakotondravony, HER 02557 (FMNH 73428); 1♂ (Fig. 75–76, 92), No. 1196 (FKCP, GLPC); 1♂6♀2♂juvs.1♀juv., Montagne d`Ambre 30km south of Antseranana (FKCP); 1♂3♀, no exact locality data, 2011 (FKCP); 1juv. (Figs. 597–599, with duplicated metasoma, dead during 2nd ecdysis) (FKCP); 3♂6♀1♀juv. (Figs. 205, 217, 473–490), N Antsiranana Province, Tamatave, Plateau von Antsirana, Diego Suarez env., E of Ramena village, 12º15'9.95"S 49º21'31.05"E, ca 50 m a. s. l. (FKCP).

Teruelius grandidieri (Kraepelin, 1901) **comb. n.**
1♂ (Figs. 17, 71, 73–74, 102, 130, 175, 190, 491–494), Tuléar, Atsimo-Andrefana, Morombe, Nosy Ambositra, Antevankira, Antevankira forest, near the Antsakabe River, 21°56.753'S 44°02.781'E, 130–160 ft, 3.II.2007, riparian valley along the Antsakabe River, in a rotten tree trunk, leg. H. A. Rakotondravony HER 03685 (FMNH 73446); 1♀ (Figs. 17, 48, 102, 142, 151), Toliara Province, Maheleotse 124c River Onilahy, 23°31.600'S 44°05.366'E, 68 m, leg. Achile Rasehmionna (FMNH); 3♂1♀3juvs (Figs. 206, 223), Toliara Province, Ankotofotsy, No. 17, 2011 (FKCP); 1♂, Toliara Province, Tsimanampetsotsa, Mitoho camp, 10 m a. s. l., 24°02.838'S 43°45.138'E (FKCP).

Teruelius intertidalis (Lourenço, 1999) **comb. n.**
1♀ (holotype, Figs. 207, 222, 495–515), Toliara Province, 3.5 km north of Tulear, IV. 1998, leg. N. Lutzmann (ZMUH); 1♂1♀ (Fig. 85), No. 1485 (FKCP, GLPC).

Teruelius limbatus (Pocock, 1889) **comb. n.**
8♂6♀ (Figs. 5–8, 18, 23, 49, 82, 83, 91, 103, 126, 139, 157, 159–160, 176, 192, 229, 235–238), Fianarantsoa Province, Forêt d'Ianasana, 7 km W Itremo, at source of Atsirakamhaity River, 20°36.1'S 46°34.3'E, 1630 m a. s. l., 6.II.1999, under rocks in Tapia forest, leg. S. M. Goodman (FMNH 73449); 2♂7♀ (Fig. 208, 225, 516–521), Central region, south of Antsirabe, 2006 (FKCP); 1♂3♀, Central region, south of Antsirabe, 2010 (FKCP).

Teruelius mahafaliensis (Lourenço et al., 2004) **comb. n.**
1♂ (holotype of *Grosphus rossii*, Figs. 522–523, 536–541), Central Region, NE Manandona, S of Antsirabe, 8.IX.2004, leg. W. R. Lourenço in secondary growth forest, under log (ZMUH); 2♂2♀ (Figs. 19, 50, 84, 104, 131, 140, 156, 177–178, 193), Toliara Province, 10.5 km SE Itampolo (village), 24°44.2'S 44°01.39'E, 120 m a. s. l., 20.II.2005, pitfall trap in disturbed spiny bush on Mahafaly Plateau, leg. V. Soarimalala & S. M. Goodman (FMNH 73598); 2♂1♀ (Figs. 84, 209, 224, 524–535), Toliara Province, Zombitse-Vohibasia, Isoky forrest margin, 692 m a. s. l., 22°41.012'S 44°51.835'E, (FKCP, GLPC); 4♂1♀, Fianarantsoa Province, Isalo, Ananalava forest margin, Tanambao (Mandabe) vill. env., 724 m a. s. l., 22°35.028'S 45°7.672'E (FKCP).

Teruelius olgae (Lourenço, 2004) **comb. n.**
1♂ (paratype, Figs. 542–546, 552–563, 576–579), Toliara Province, Fôret des Mikeas, 9.5 km W Ankiloaka, 22°46.7'S 43°31.4'E, 16.III.2003, leg. S. Goodman & V. Soarmalala (MHNG); 1♂ (Figs. 20, 81, 105, 179, 194), Toliara Province, 10.5 km SE Itampolo (village), 24°44.2'S 44°01.39'E, 120 m a. s. l., 19.II.2005, pitfall trap in disturbed spiny bush on Mahafaly Plateau, leg. V. Soarimalala & S. M. Goodman SMG# 14539 (FMNH 86968); 1♀ (Figs. 20, 51, 105, 132, 144, 152, 180, 195, 547–551, 564–575), Toliara Province, Forêt des Milua, 19 km SW Tamotamo, 21°52.0'S 43°39.6'E, 70 m a. s. l., 23.III.2003, found in pitfall trap 16, leg. V. Soarimalala #VS376 (FMNH 73624); 1♂ (paratype), south region, Toliara Province, Fôret de Mikea, 7.5 km NE Tsifotsa, 22°48.0'S 43°26.'E, 60 m a. s. l., 21-25.II.2003, leg. S. M. Goodman, V. Soarimalala, hemispermatophore examined (MHNG).

RSA:
Pseudolychas ochraceus (Hirst, 1911)
1♀ (holotype, Figs. 622–623), Orange River Colony, Bethulie (BMNH No. 1905.3.30.45-54); 1♂1♀ (Figs. 106, 620–621, 624–628, 635–638, 641), no exact locality (CUPC).

Pseudolychas pegleri (Purcell, 1902)
1♂ (Figs. 161–164), KwaZulu-Natal Ndumo – Shokwe, 30.III.2017, 26.874930°S 32.210920°E, leg. P. Just, F. Šťáhlavský, V. Opatová, C. Haddad, R. Booysen, A. Gomez, J. Ruch & J. Schneider, JA1418 (CUPC).

Pseudolychas transvaalicus Lawrence, 1961
1juv. (Figs. 629–634, 639–640), Mpumalanga, God's Window, 24.874719°S 30.890959°E, 6.IV.2017, leg. F. Šťáhlavský (CUPC).

Appendix 3. Anatomical atlas of representative '*Grosphus*' group scorpions.

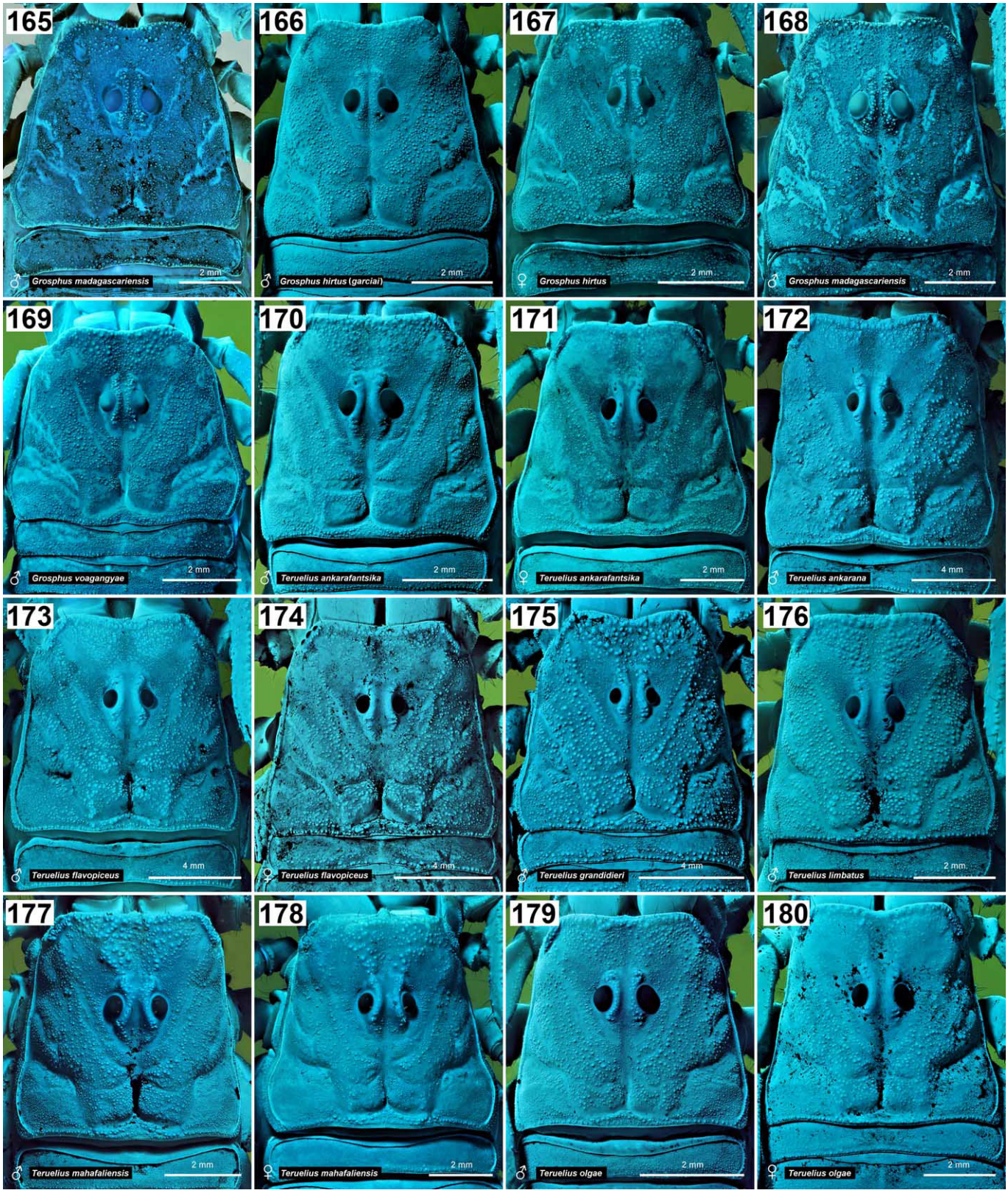

Figures 165–180. Carapace of representative *Grosphus* and *Teruelius* **gen**. **n**. *G. madagascariensis* (165, 168), *G. hirtus* (166–167), *G. voahangyae* (169), *T. ankarafantsika* (170–171), *T. ankarana* (172), *T. flavopiceus* (173–174), *T. grandidieri* (175), *T. limbatus* (176), *T. mahafaliensis* (177–178) and *T. olgae* (179–180). UV fluorescence, ♂ male, ♀ female. Scale bars: 2 mm (165–171, 176–180), 4 mm (172–175).

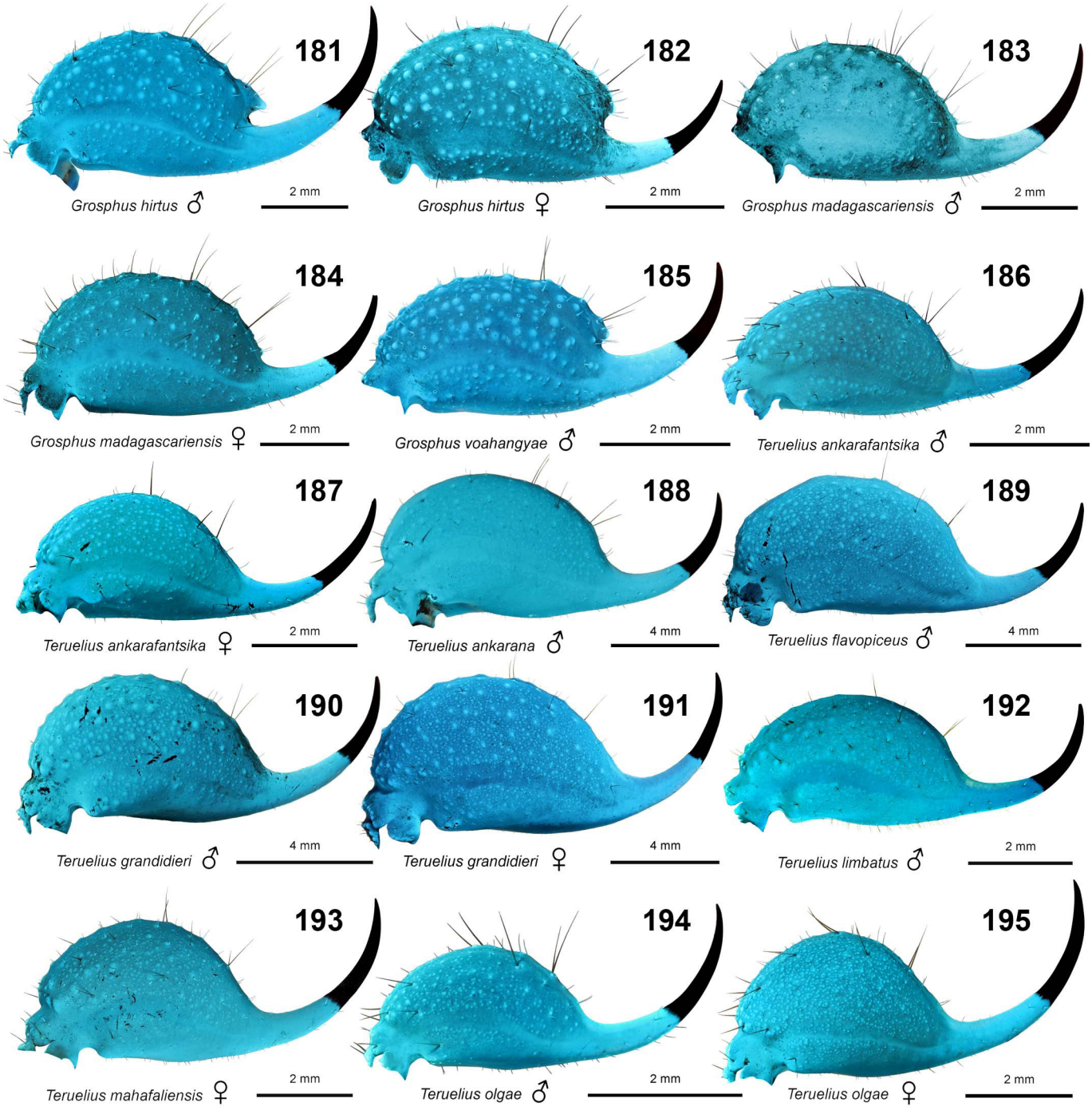

Figures 181–195. Telson of representative *Grosphus* and *Teruelius* **gen. n**. *G. hirtus* (181–182), *G. madagascariensis* (183–184), *G. voahangyae* (185), *T. ankarafantsika* (186–187), *T. ankarana* (188), *T. flavopiceus* (189), *T. grandidieri* (190–191), *T. limbatus* (192), *T. mahafaliensis* (193) and *T. olgae* (194–195). UV fluorescence, ♂ male, ♀ female. Scale bars: 2 mm (181–187, 192–195), 4 mm (188–191).

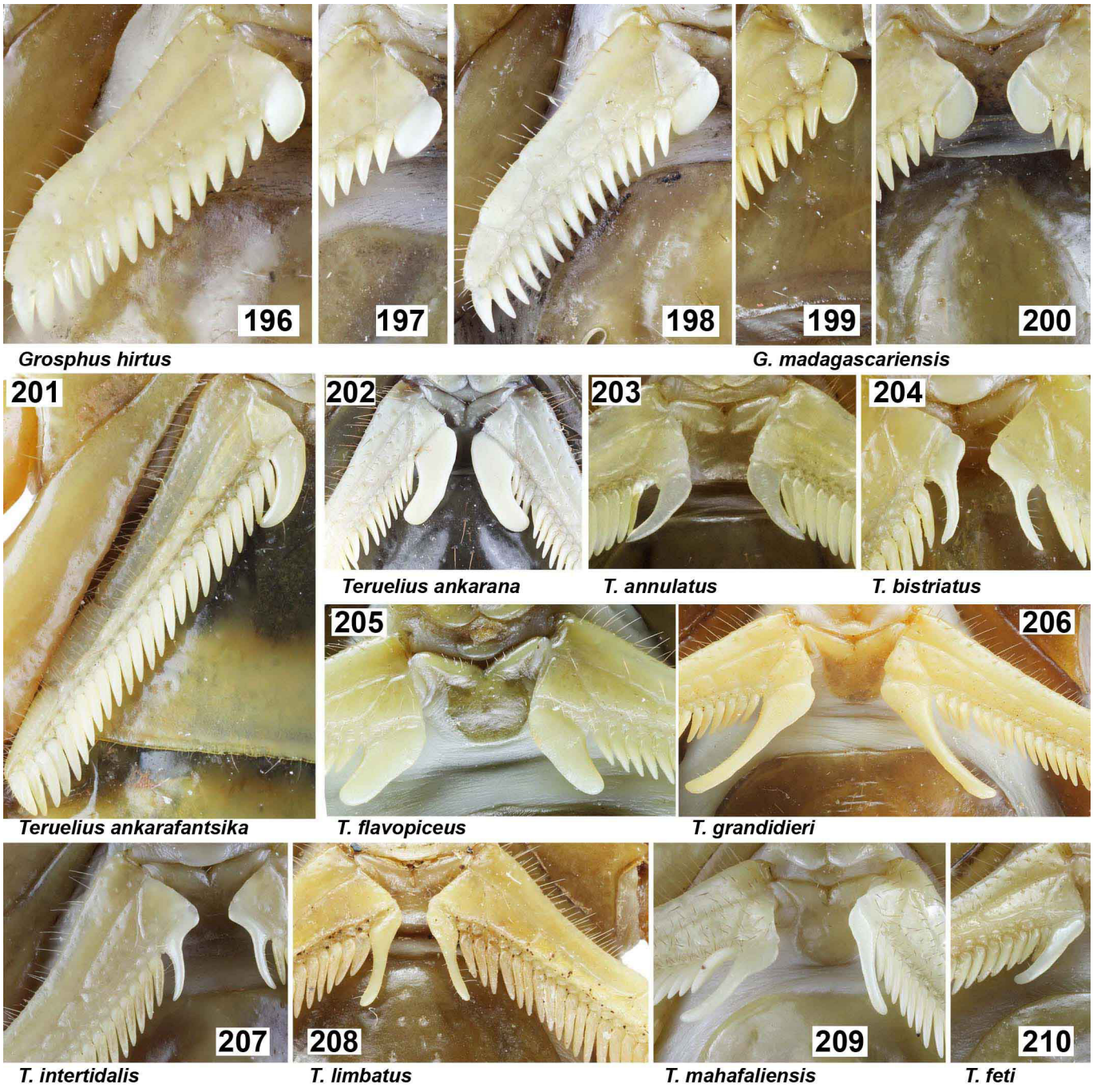

Figures 196–210. Female basal pectinal teeth of representative *Grosphus* and *Teruelius* **gen**. **n**. *G. hirtus* (196–198), *G. madagascariensis* (199), *G. madagascariensis*, paratype of *G. mandena* (200), *T. ankarafantsika* (201), *T. ankarana* (202), *T. annulatus* (203), *T. bistriatus* (204), *T. flavopiceus* (205), *T. grandidieri* (206), *T. intertidalis* (207), *T. limbatus* (208), *T. mahafaliensis* (209), *T. feti* (210).

Figures 211–226. Ventral tarsal setation of legs III or IV in *Grosphus* and *Teruelius* **gen. n**. *G. goudoti* (211), *G. hirtus* (212), *G. hirtus* (G. *garciai*) (213), *G. madagascariensis* (214), *G. madagascariensis* (*G. mandena*) (215), *Teruelius ankarana* (216), *T. flavopiceus* (217), *T. annulatus* (218), *T. ankarafantsika* (219–220), *T. bistriatus* (221), *T. intertidalis* (222), *T. grandidieri* (223), *T. mahafaliensis* (224), *T. limbatus* (225), *T. feti* (226).

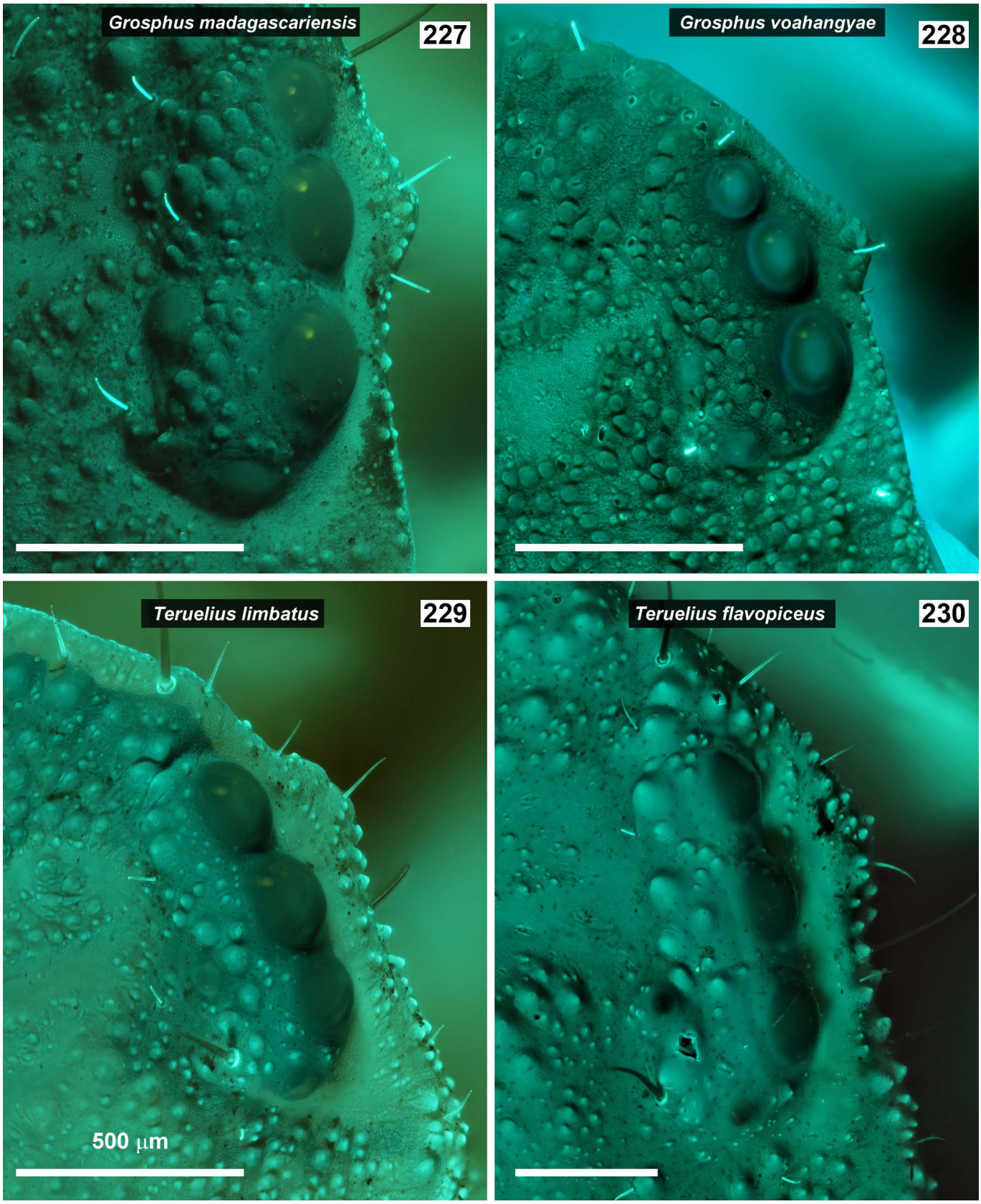

Figures 227–230. Right lateral eyes of *Grosphus* and *Teruelius* **gen**. **n**. *G. madagascariensis* (227), *G. voahangyae* (228), *T. limbatus* (229) and *T. flavopiceus* (230). All species comply with the 5-eye buthid pattern with series of 3 larger ocelli in lower position, and two smaller ocelli in posterior and upper positions. UV fluorescence, males. Scale bars: 500 μm.

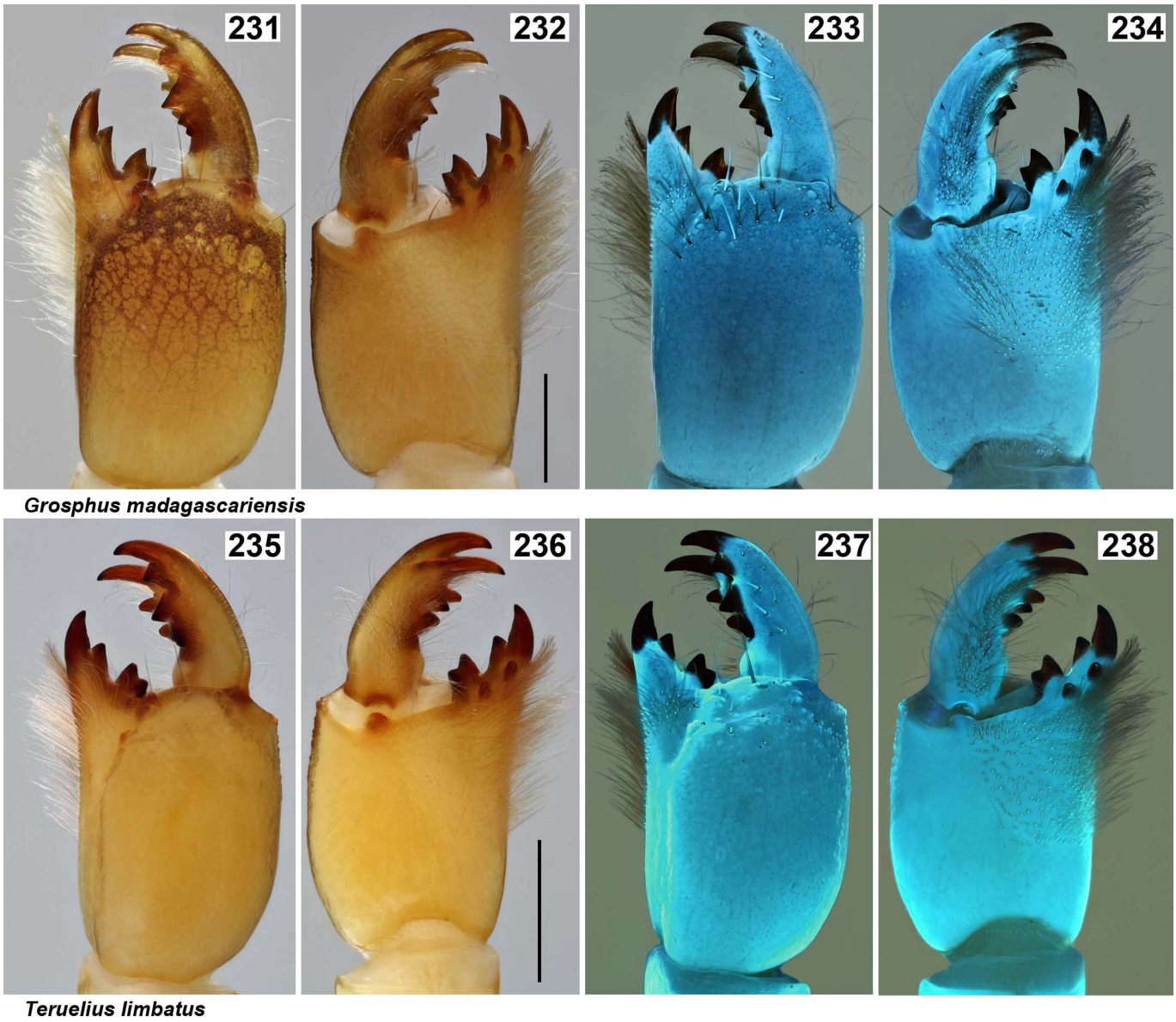

Figures 231–**238**. Males. Right chelicera. **Figures 231**–**234**. *Grosphus madagascariensis*, dorsal (231, 233) and ventral (232, 234) views, under white light (231–232) and UV fluorescence (233–234). **Figures 235**–**238**. *Teruelius limbatus*, dorsal (235, 237) and ventral (236, 238) views, under white light (235–236) and UV fluorescence (237–238). Scale bars: 1 mm.

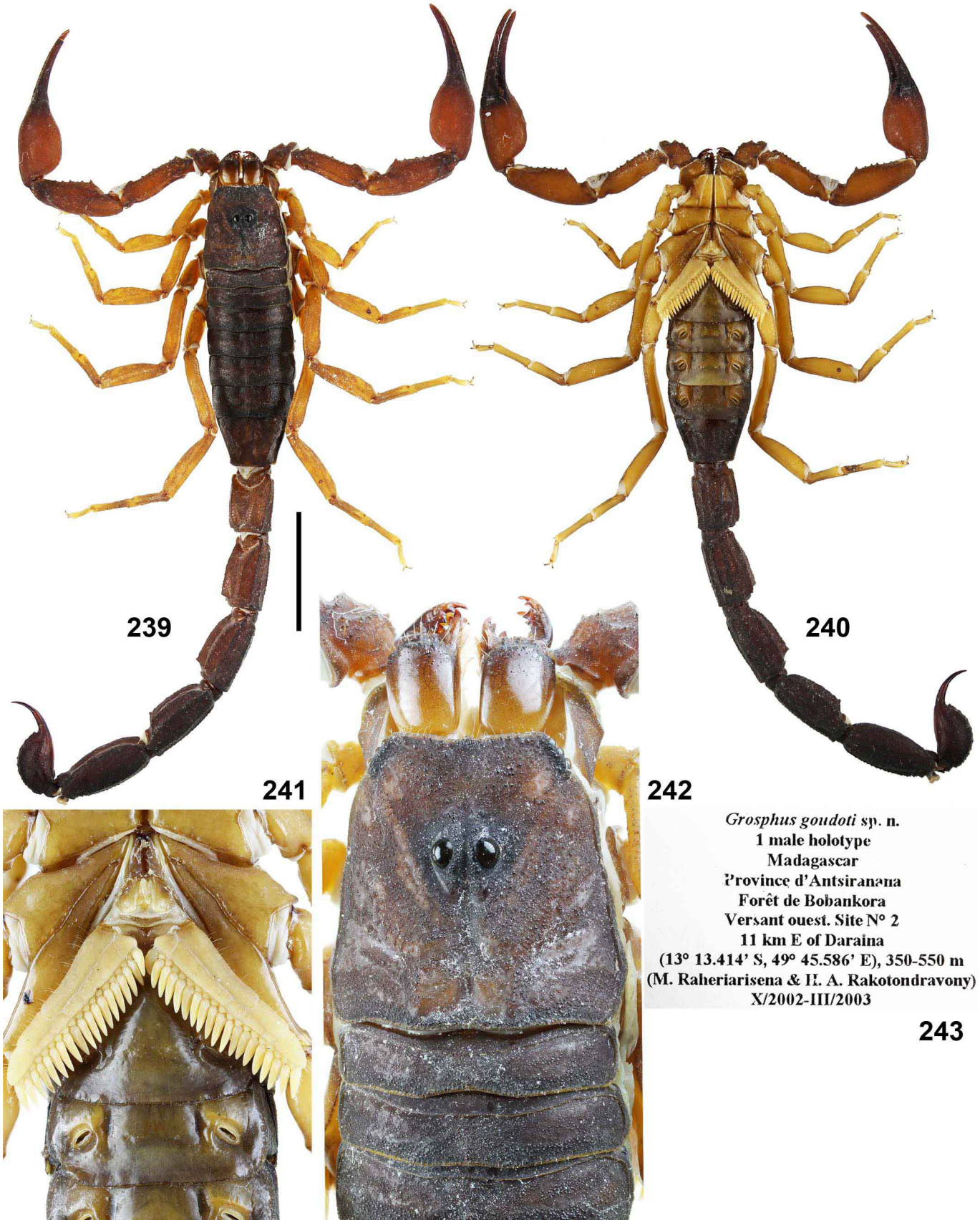

Figures 239–243. *Grosphus goudoti*, male holotype, dorsal (239) and ventral (240) views, sternopectinal region and sternites III–IV (241), carapace and tergites I–III (242), and original label (243). Scale bar: 10 mm (239–240).

Figures 244–**258**. *Grosphus goudoti*, male holotype, pedipalp chela, dorsal (244), external (245), and ventrointernal (246) views; pedipalp patella, dorsal (247), external (248), and ventral (249) views; pedipalp femur and trochanter, internodorsal (250) and dorsal (251) views; pedipalp chela, movable finger dentate margin (252); right chelicera, dorsal (253) and ventral (254) views; telson lateral view (255); metasoma and telson, lateral (256), dorsal (257) and ventral (258) views.

Figures 259–262. *Grosphus goudoti*, male holotype, distal segments of right legs I–IV, retrolateral views.

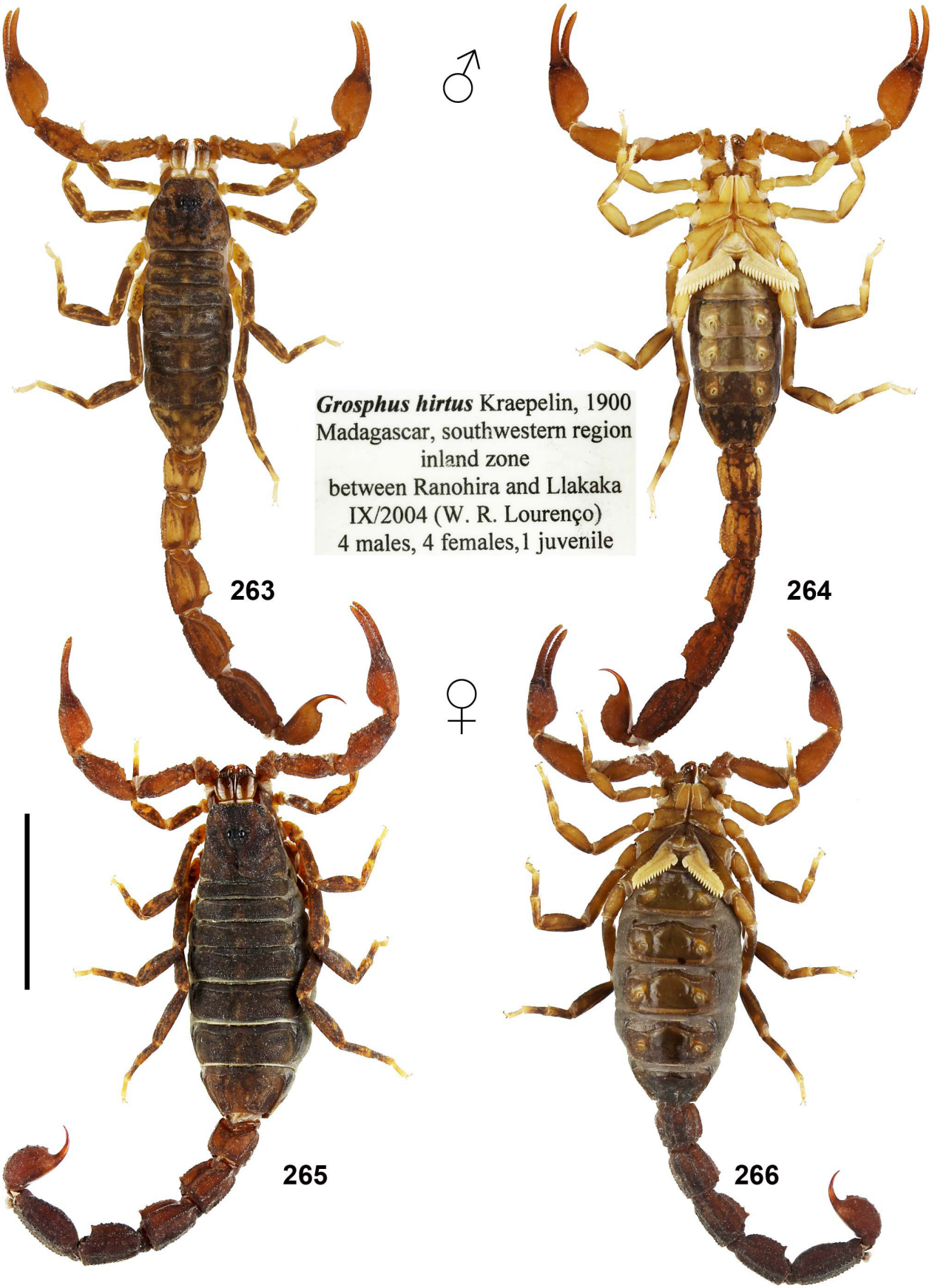

Figures 263–266. *Grosphus hirtus*, habitus. Male (263–264) and female (265–266), in dorsal (263, 265) and ventral (264, 2662) views. Scale bar: 10 mm.

Figures 267–274. *Grosphus hirtus*, telson lateral view in male (267) and female (268); metasoma and telson in male and female, lateral (269, 272), ventral (270, 273) and dorsal (271, 274) views. Scale bar: 10 mm (269–274).

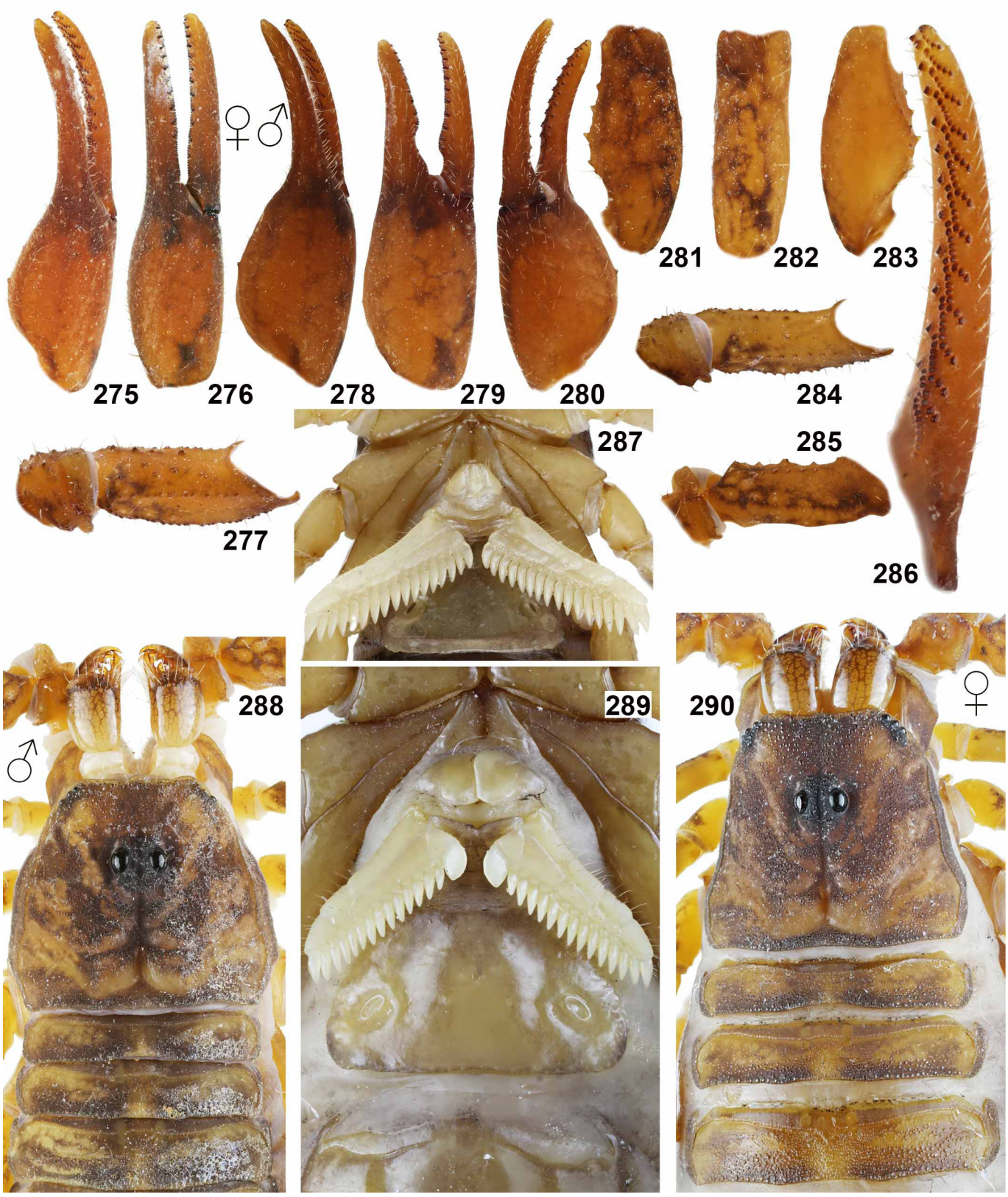

Figures 275–290. *Grosphus hirtus*. **Figures 275–277**, **289–290**. Female, pedipalp chela, dorsal (275) and external (276) views, pedipalp femur and trochanter, internodorsal (277) view; sternopectinal region and sternite III (289) and carapace and tergites I–III (290). **Figures 278–288**. Male, pedipalp chela, dorsal (278), external (279) and ventrointernal (280) views; pedipalp patella, dorsal (281), external (282) and ventral (283) views; pedipalp femur and trochanter, internodorsal (284) and dorsoexternal (285) views; pedipalp chela, movable finger dentate margin (286); sternopectinal region and sternite III (287) and carapace and tergites I–III (288).

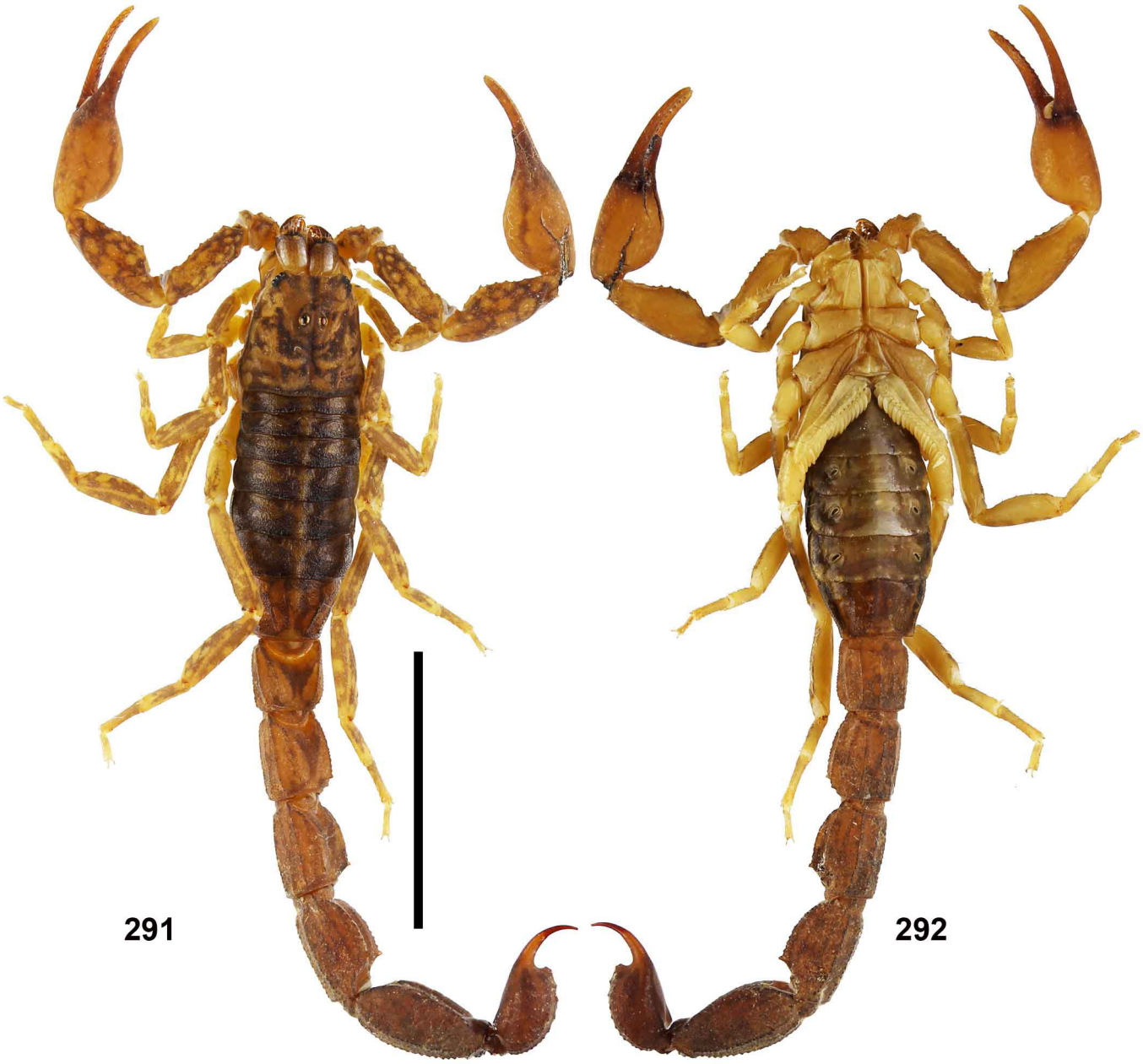

Figures 291–292. *Grosphus hirtus*, male holotype of *G. garciai*, dorsal (291) and ventral (292) views. Scale bar: 10 mm.

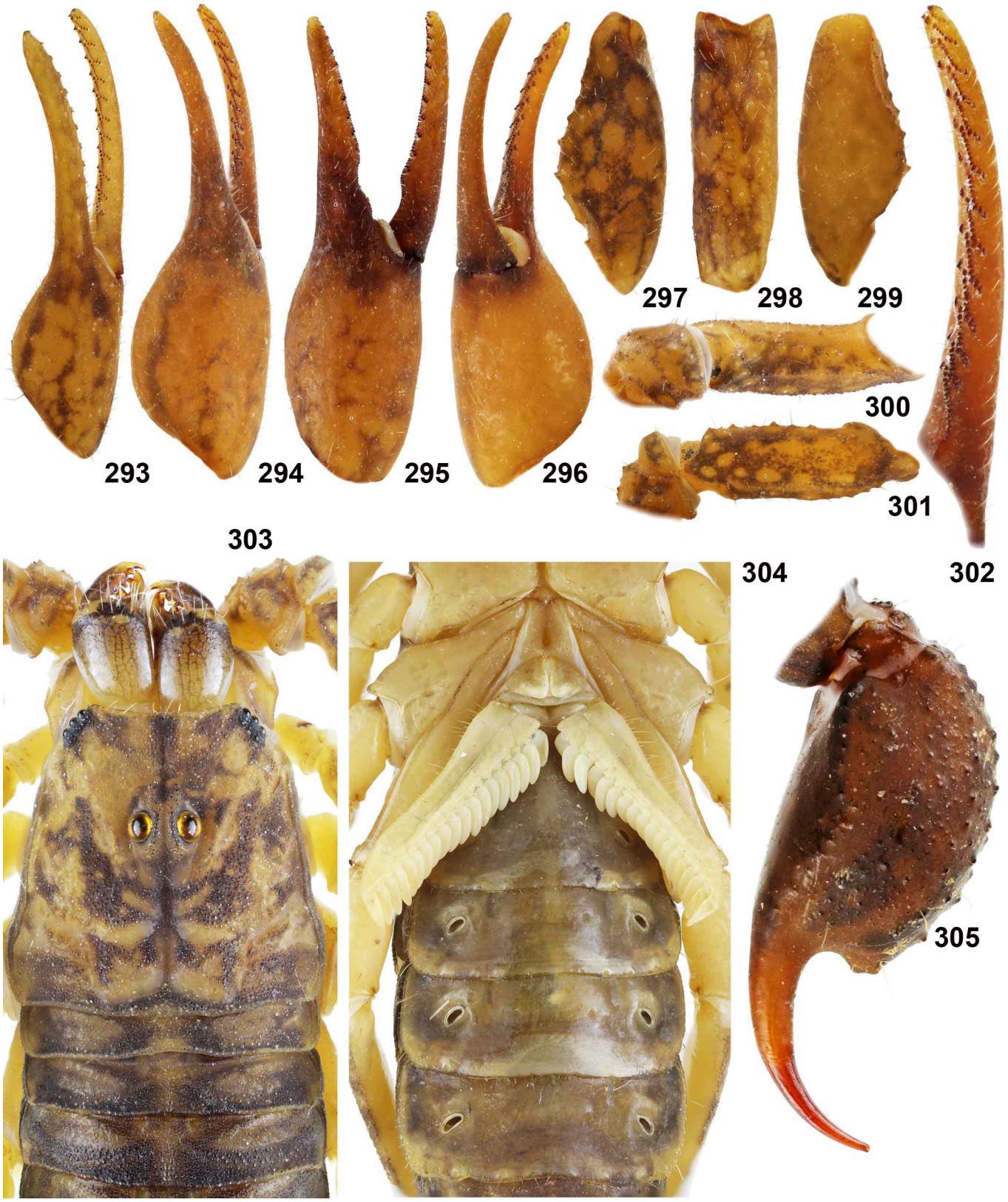

Figures 293–305. *Grosphus hirtus*. **Figure 293**. Juvenile paratype of *G. garciai*, pedipalp chela dorsal. **Figures 294–305**. *Grosphus hirtus*, male holotype of *G. garciai*. **Figures 294–302**. Left pedipalp (mirrored), pedipalp chela, dorsal (294), external (295) and ventrointernal (296) views; pedipalp patella, dorsal (297), external (298) and ventral (299) views; pedipalp femur and trochanter, internodorsal (300) and dorsal (301) views; pedipalp chela, movable finger dentate margin (302). **Figures 303–305**. Carapace and tergites I–III (303), sternopectinal region and sternites III–VI (304) and telson lateral view (305).

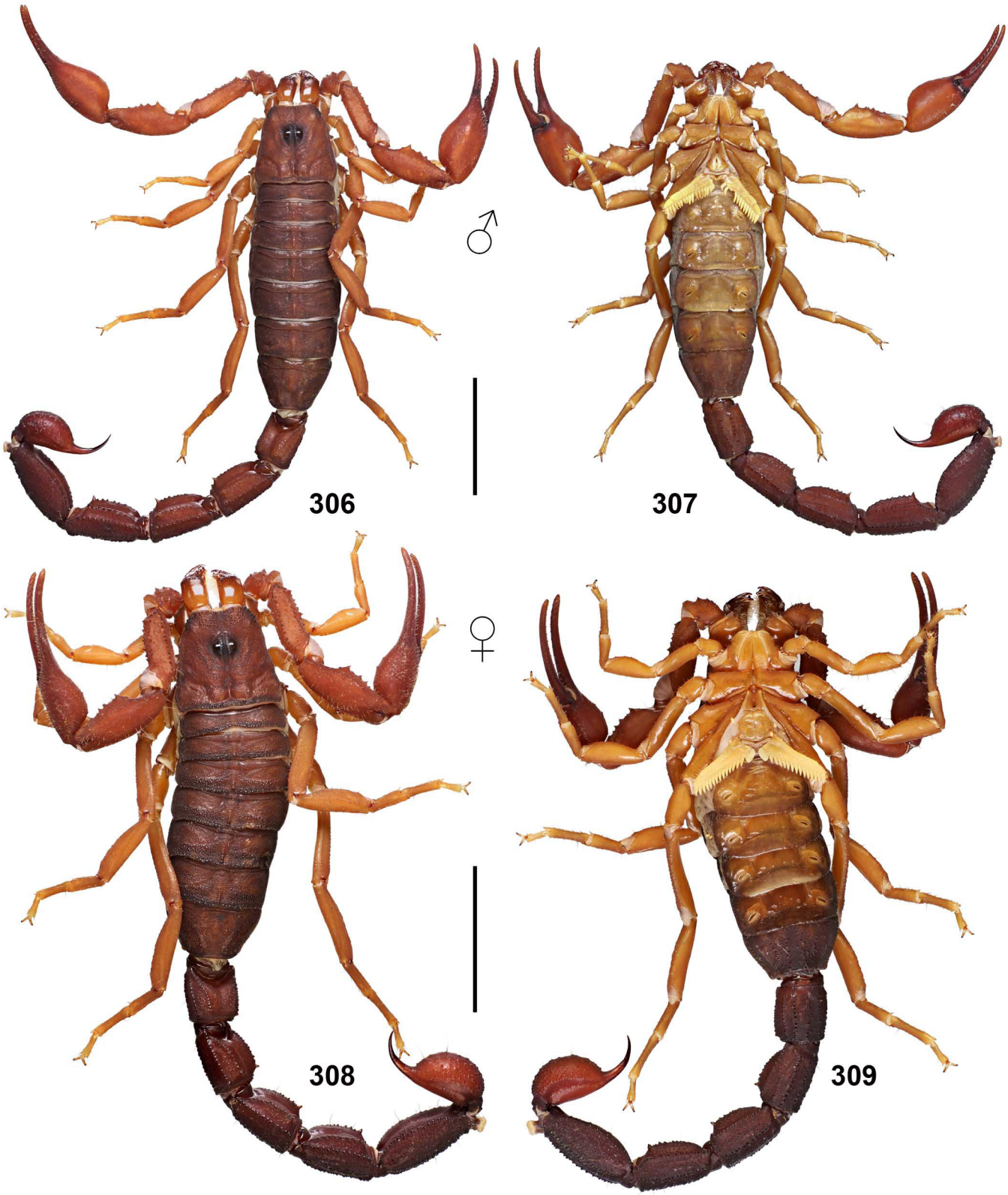

Figures 306–309. *Grosphus madagascariensis*. Habitus. Male (306–307) and female (308–309), dorsal (306, 308) and ventral (307, 309) views. Scale bars: 10 mm..

Figures 310–315. *Grosphus madagascariensis*. Metasoma and telson. Male (310–312) and female (313–315), dorsal (310, 313), lateral (311, 314) and ventral (312, 315) views. Scale bars: 4 mm.

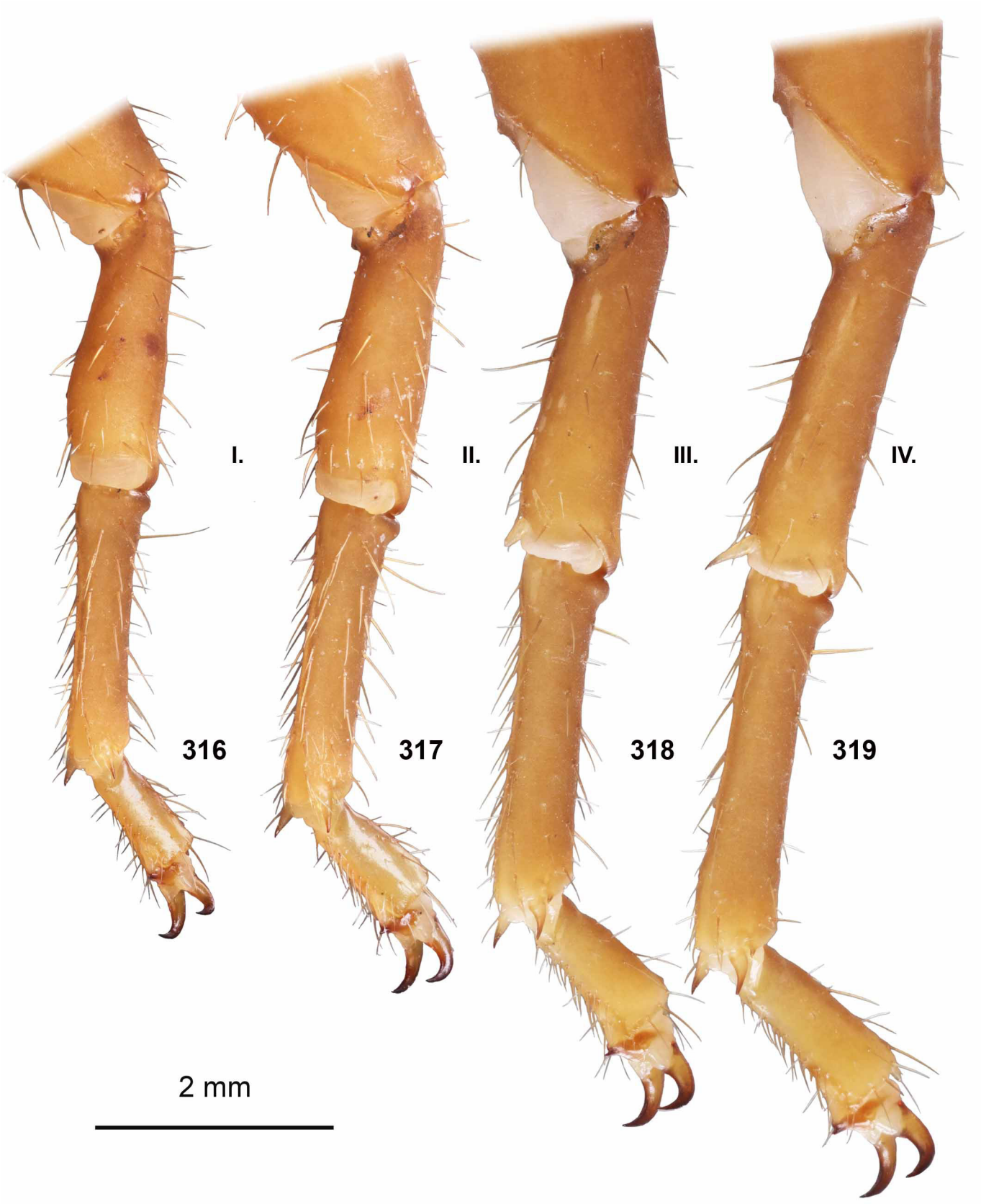

Figures 316–319. *Grosphus madagascariensis*, male, right legs I–IV tibia, basitarsus and telotarsus, retrolateral views. Scale bar: 2 mm.

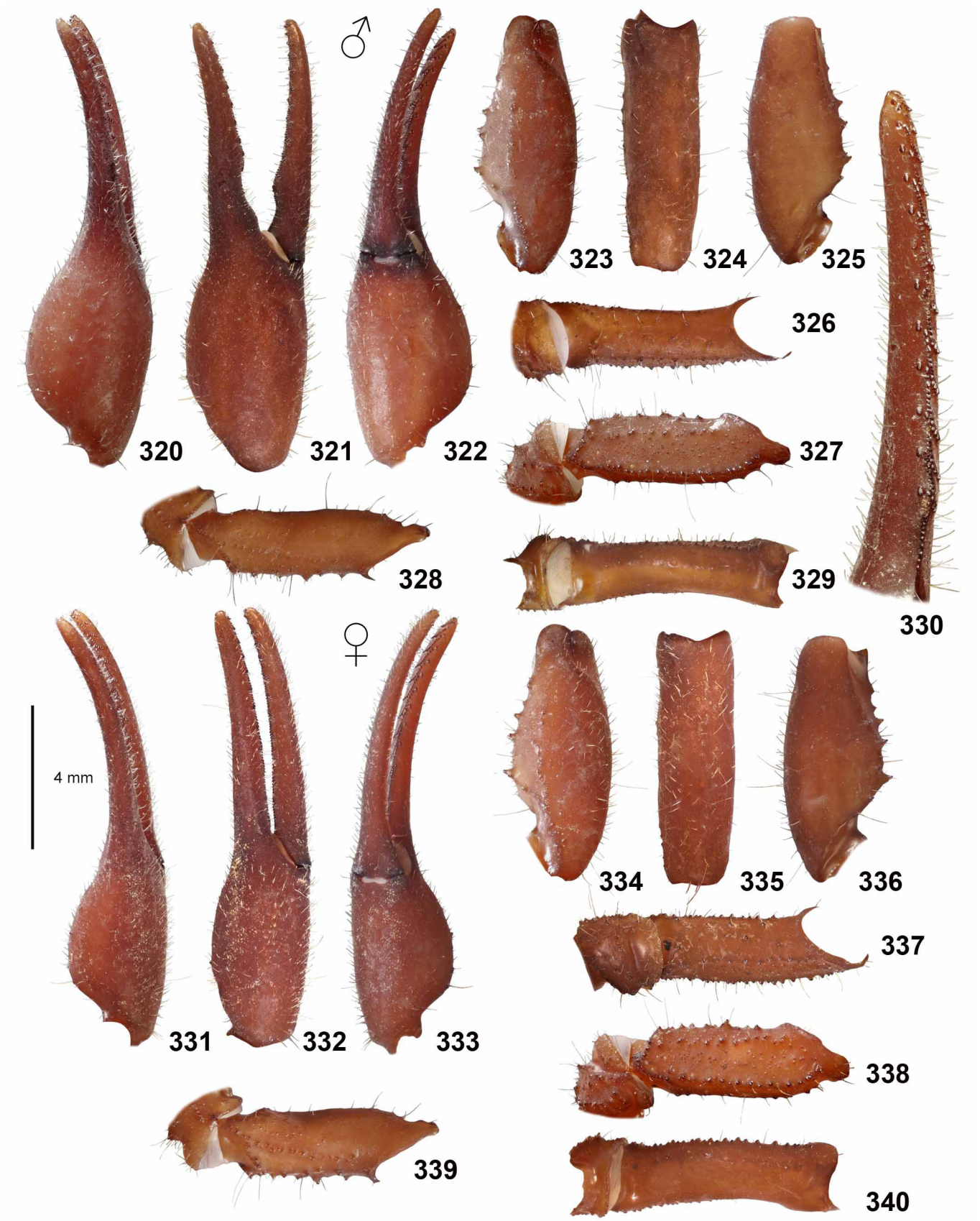

Figures 320–340. *Grosphus madagascariensis*. Pedipalp. Male (320–330) and female (331–340). Chela in dorsal (320, 331), external (321, 332) and ventrointernal (322, 333) views. Patella in dorsal (323, 334), external (324, 335) and ventral (325, 336) views. Femur and trochanter in internal (326, 337), dorsal (327, 338), ventral (329, 339) and external (329, 340) views. Pedipalp chela, movable finger dentate margin (330). Scale bar: 4 mm.

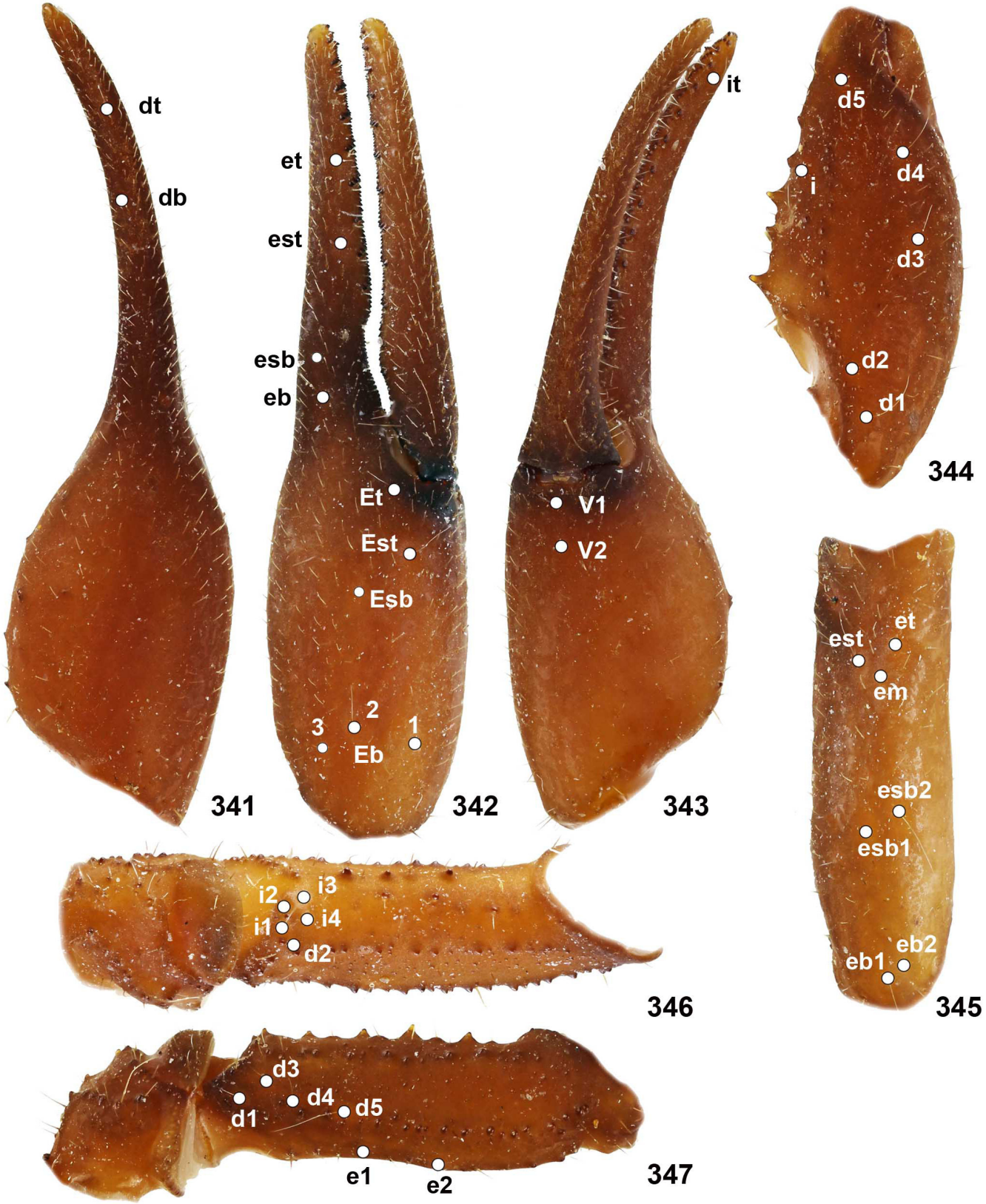

Figures 341–347. *Grosphus madagascariensis*. Pedipalp. Male. Chela in dorsal (341), external (342) and ventrointernal (343) views. Patella in dorsal (344) and external (345) views. Femur and trochanter in internal (346) and dorsoexternal (347) views. The trichobothrial pattern is indicated by white circles.

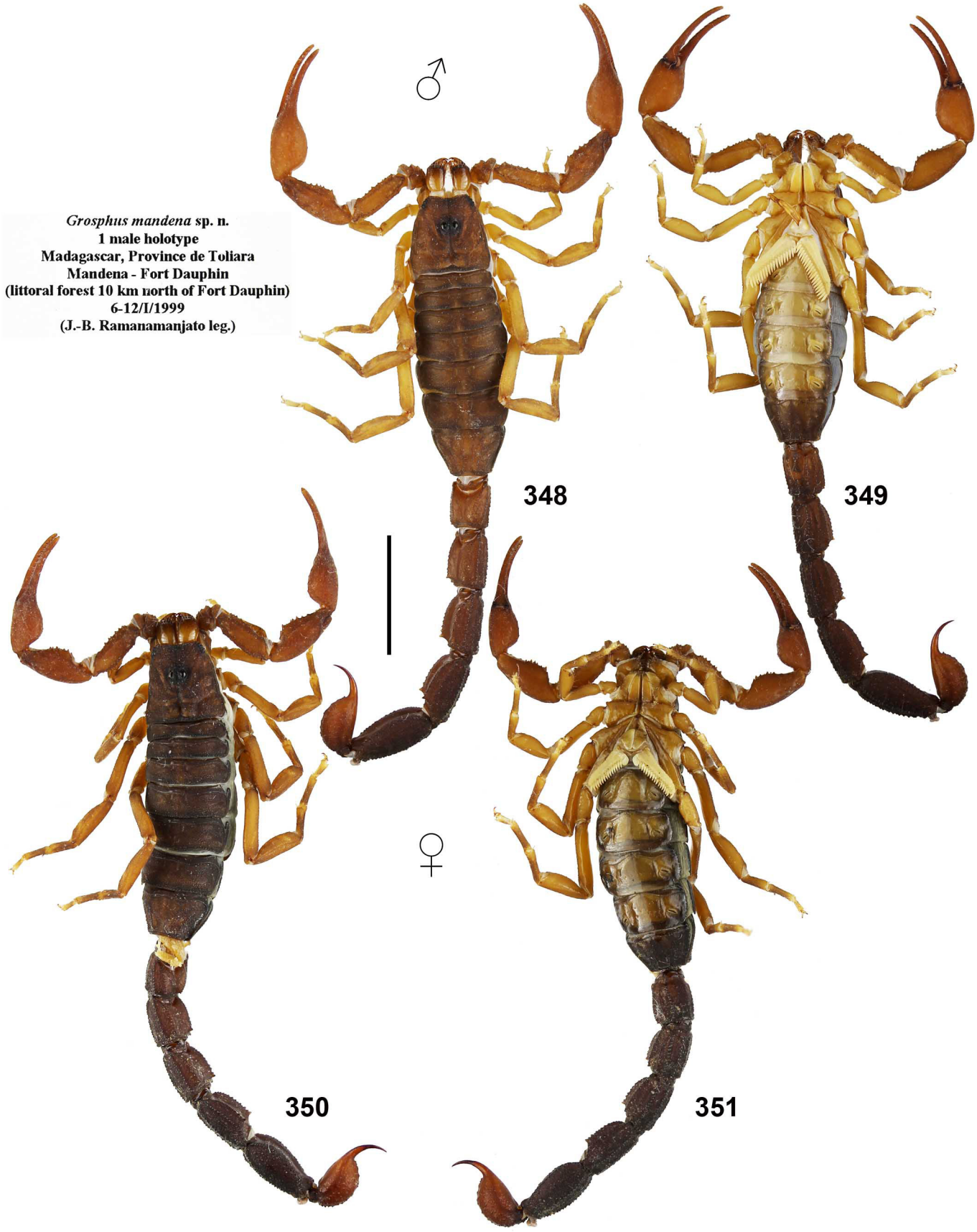

Figures 348–351. *Grosphus madagascariensis*. Habitus. Male holotype (348–349) and female paratype (350–351) of *Grosphus mandena* in dorsal (348, 350) and ventral (349, 351) views. Scale bar: 10 mm.

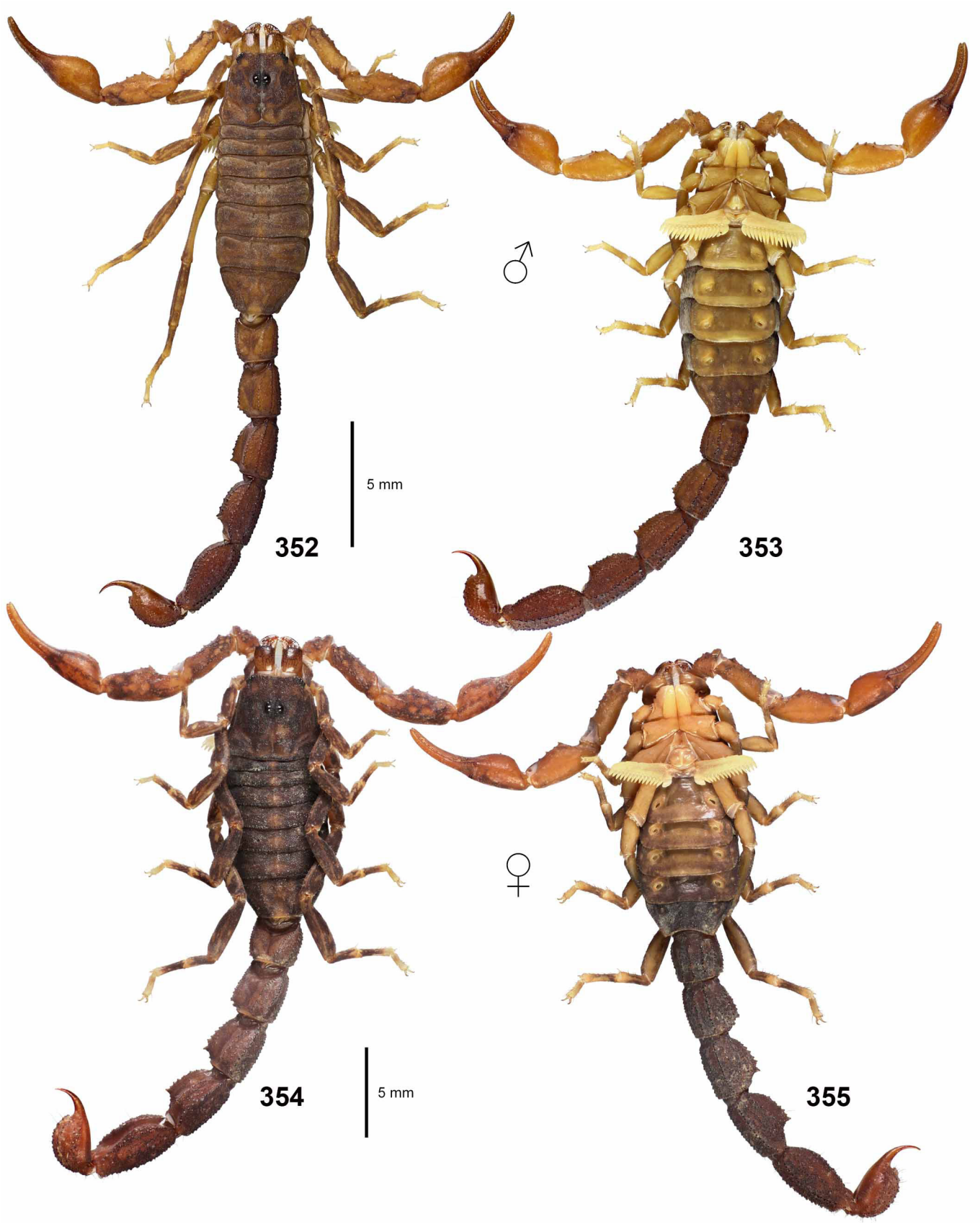

Figures 352–355. *Grosphus voahangyae*. Habitus. Male (352–353) and female (354–355), dorsal (352, 354) and ventral (353, 355) views. Scale bars: 5 mm.

Figures 356–361. *Grosphus voahangyae*. Metasoma. Male (356–358) and female (359–361), dorsal (356, 359), lateral (357, 360) and ventral (358, 361) views. Scale bars: 2 mm.

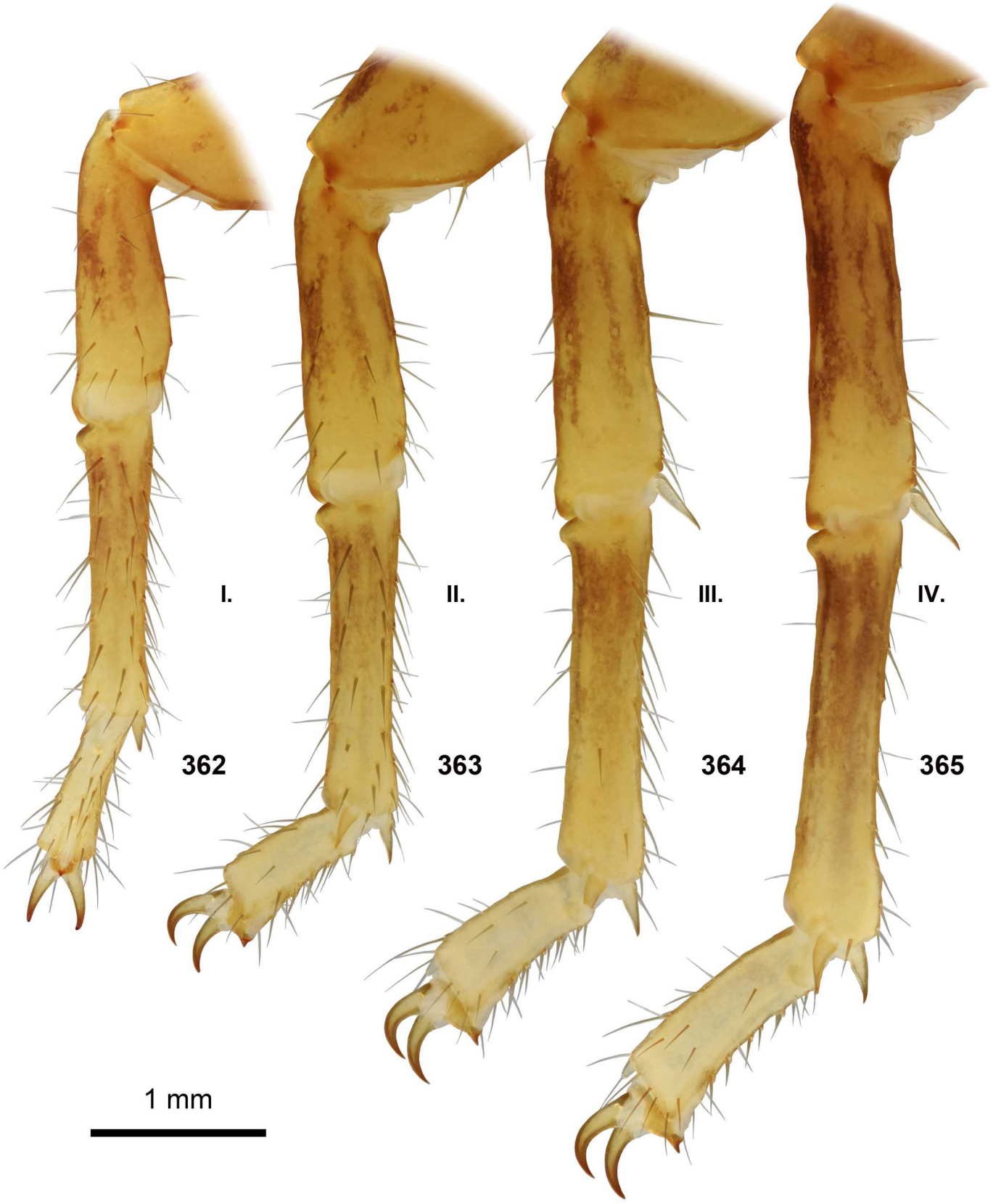

Figures 362–365. *Grosphus voahangyae*, male, left legs I–IV tibia, basitarsus and telotarsus, retrolateral views. Leg I (362), leg II (363), leg III (364), leg IV (365). Scale bar: 1 mm.

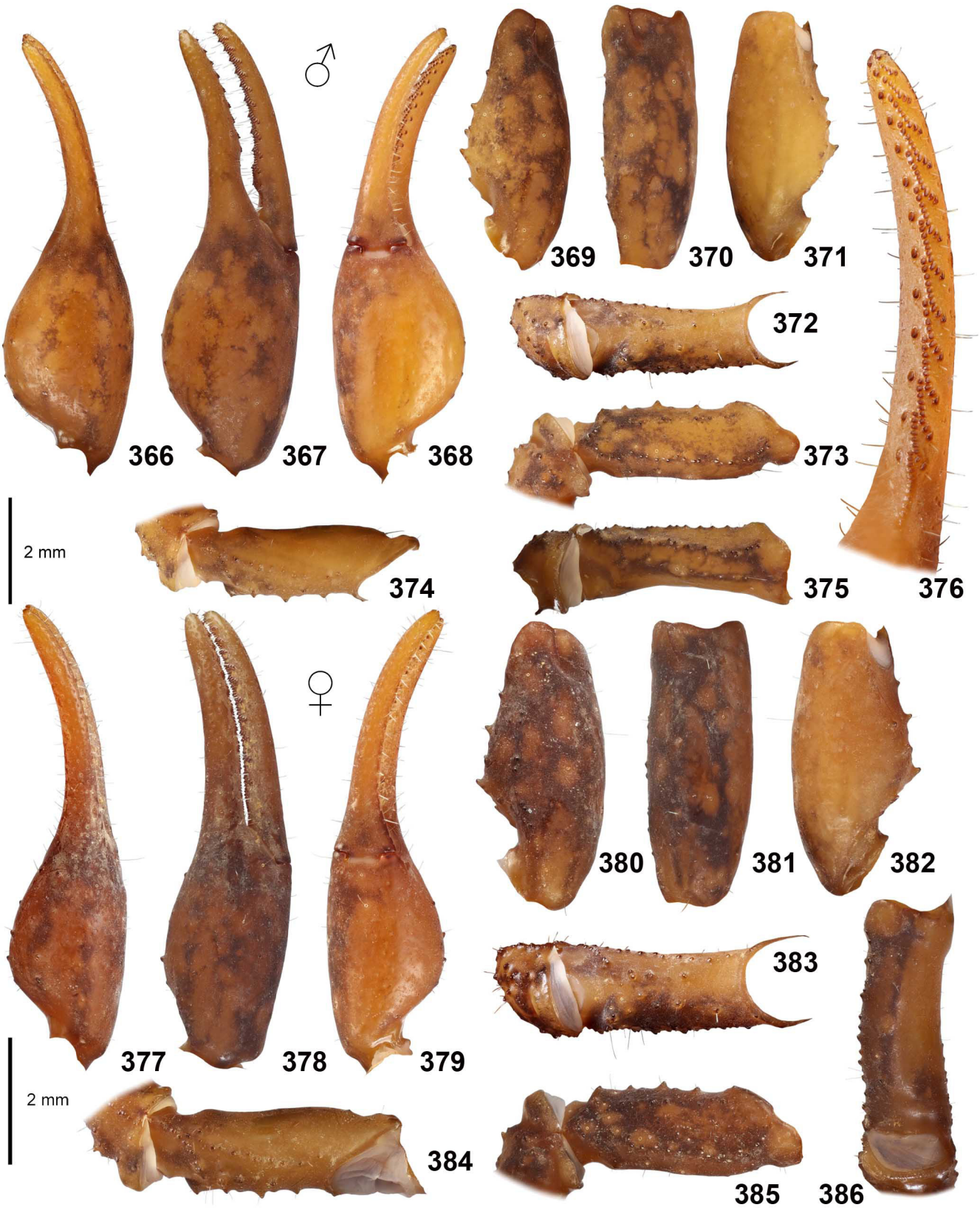

Figures 366–386. *Grosphus voahangyae*. Pedipalp. Male (366–376) and female (377–386). Chela in dorsal (366, 377), external (367, 378) and ventral (368, 379) views. Patella in dorsal (369, 380), external (370, 381) and ventral (371, 382) views. Femur and trochanter in internal (372, 383), dorsal (373, 385), external (375, 386) and ventral (374, 384) views. Pedipalp chela, movable finger dentate margin (376). Scale bars: 2 mm (366–375, 377–386).

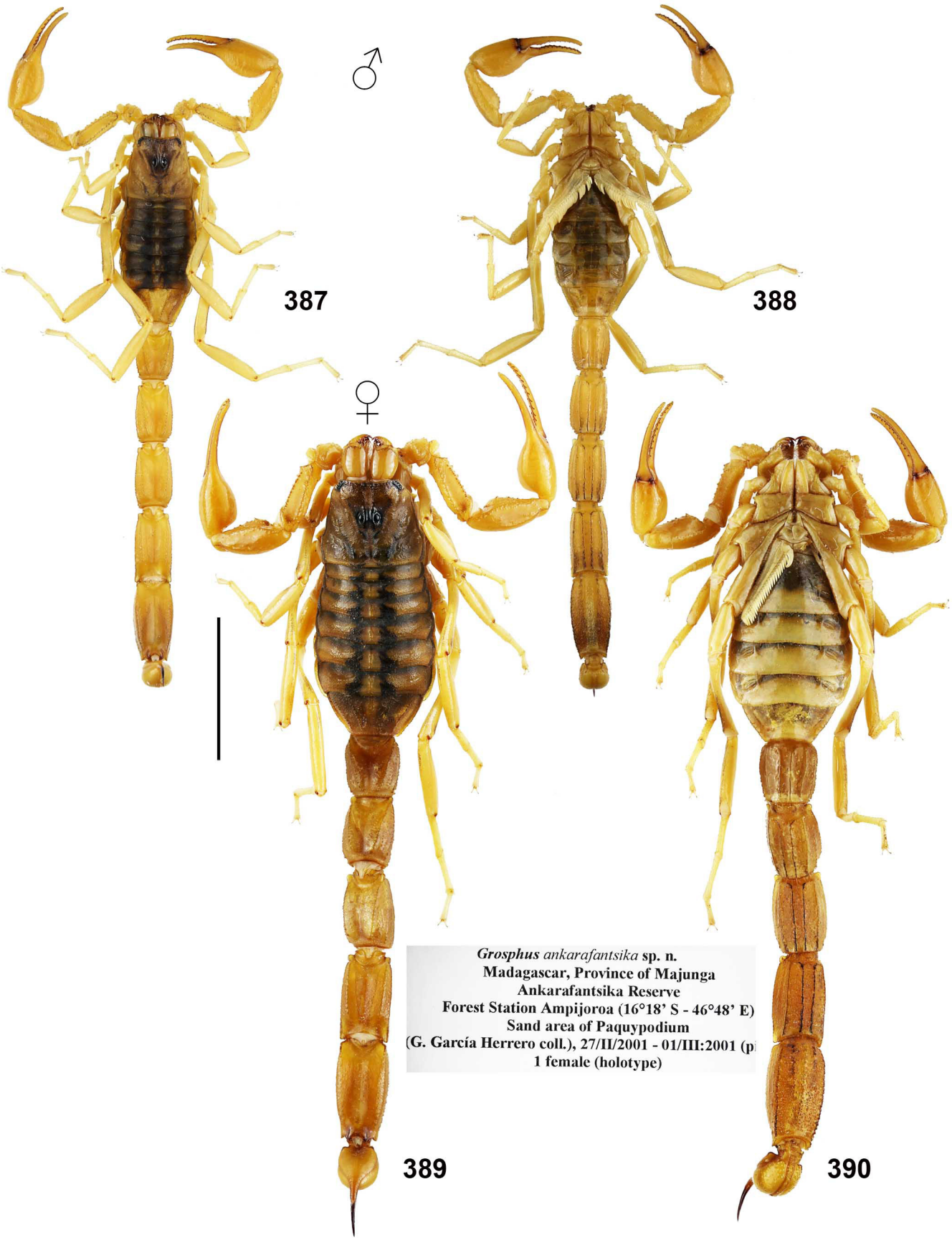

Figures 387–390. *Teruelius ankarafantsika*. Habitus. Male paratype (387–388) and female holotype (389–390), dorsal (387, 389) and ventral (388, 390) views. Scale bar: 10 mm.

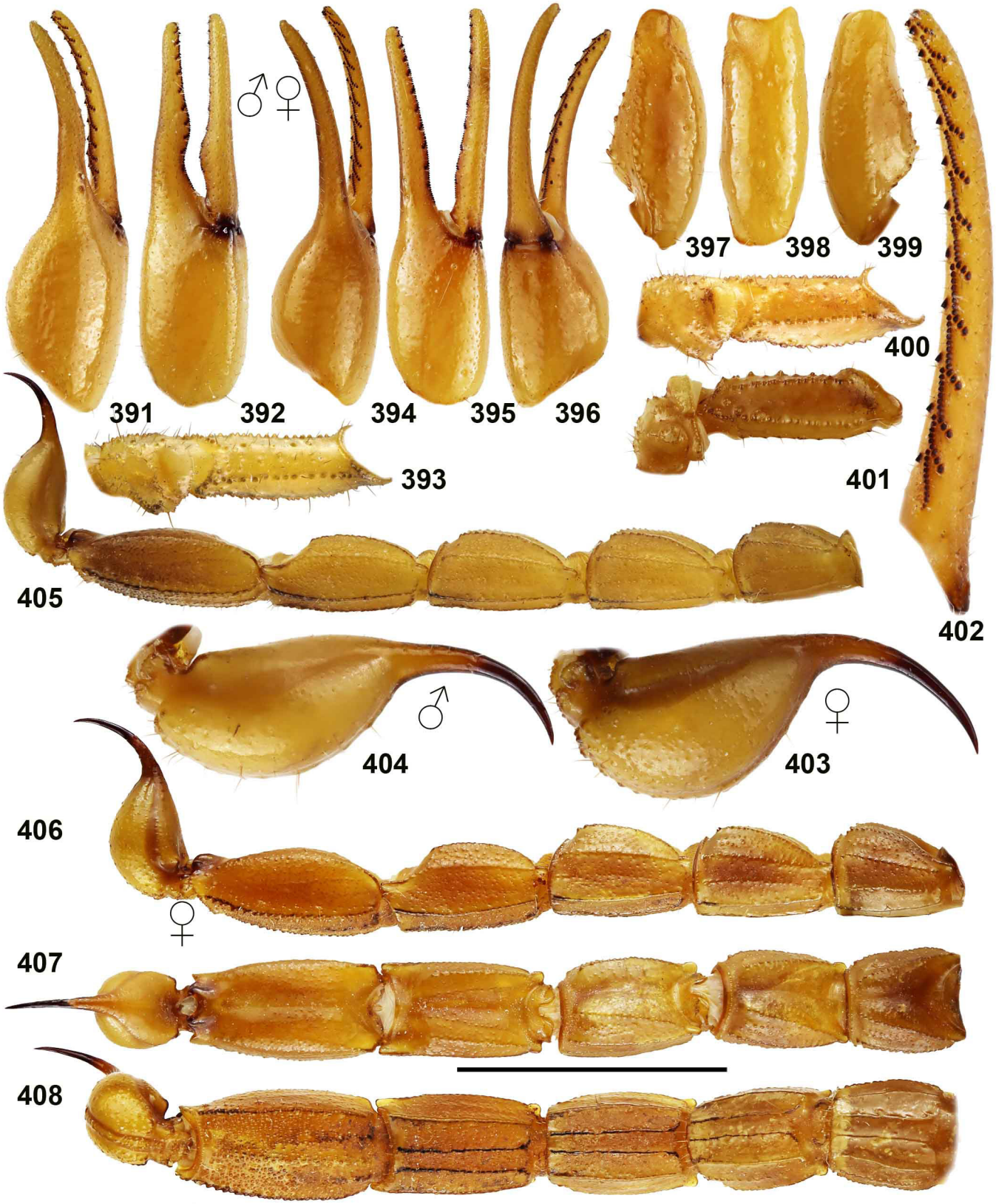

Figures 391–**408**. *Teruelius ankarafantsika*. Male paratype (391–393, 404–405) and female holotype (394–403, 406–408). **Figures 391**–**402**. Pedipalp. Chela in dorsal (391, 394), external (392, 395) and ventral (396) views. Patella in dorsal (397), external (398) and ventral (399) views. Femur and trochanter in internal (393, 400) and dorsal (401) views. Pedipalp chela, movable finger dentate margin (402). **Figures 403**–**408**. Telson in lateral (403, 404) views. Metasoma and telson in lateral (405, 406), dorsal (407) and ventral (408) views. Scale bar: 10 mm (406–408).

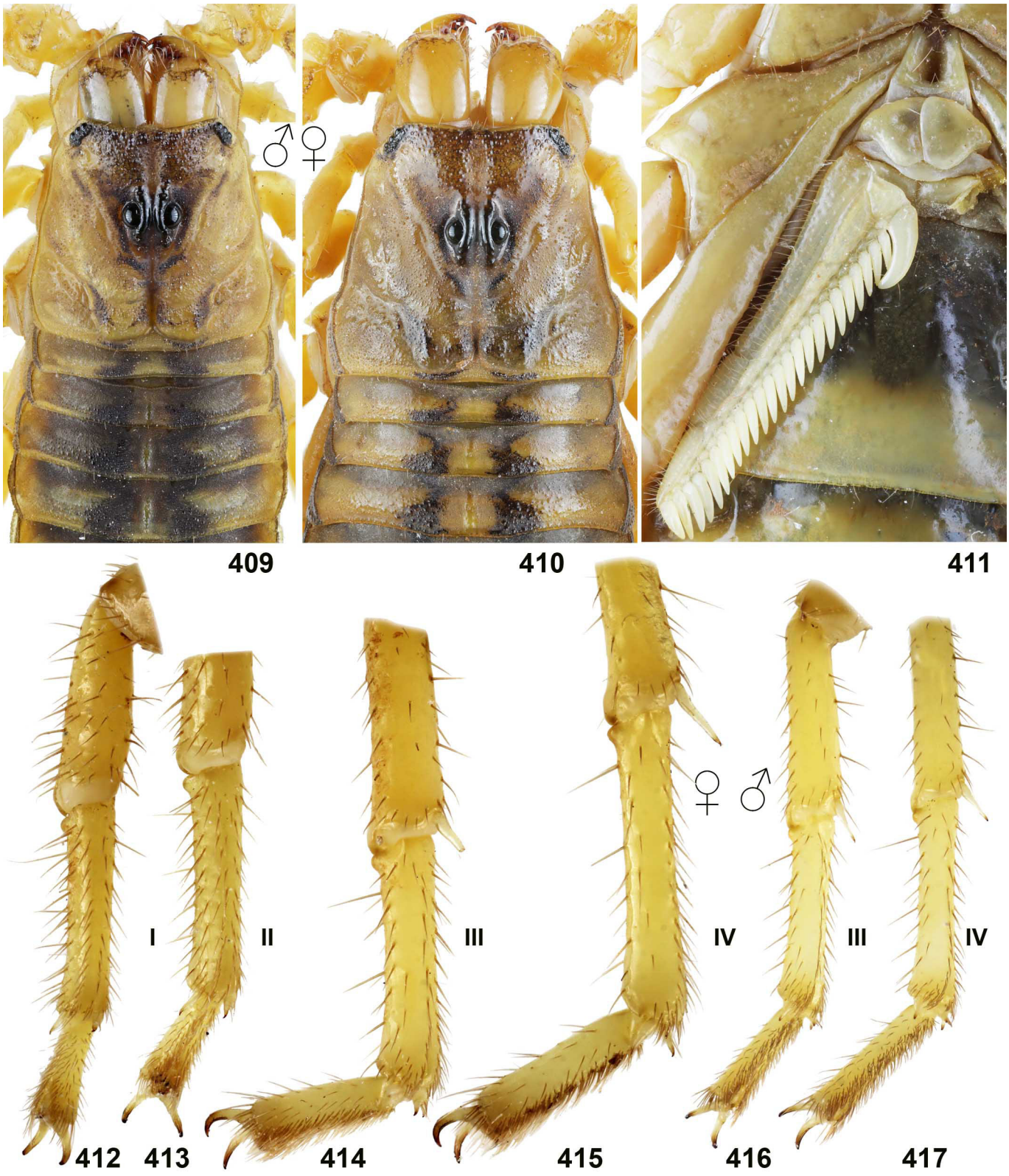

Figures 409–417. *Teruelius ankarafantsika*. Male paratype (409, 416–417) and female holotype (410–415). **Figures 409–411**. Carapace and tergites I–III (409–410) and sternopectinal region (411). **Figures 412–417**. Left legs tibia, basitarsus and telotarsus, retrolateral views. Leg I (412), leg II (413), leg III (414, 416), leg IV (415, 417).

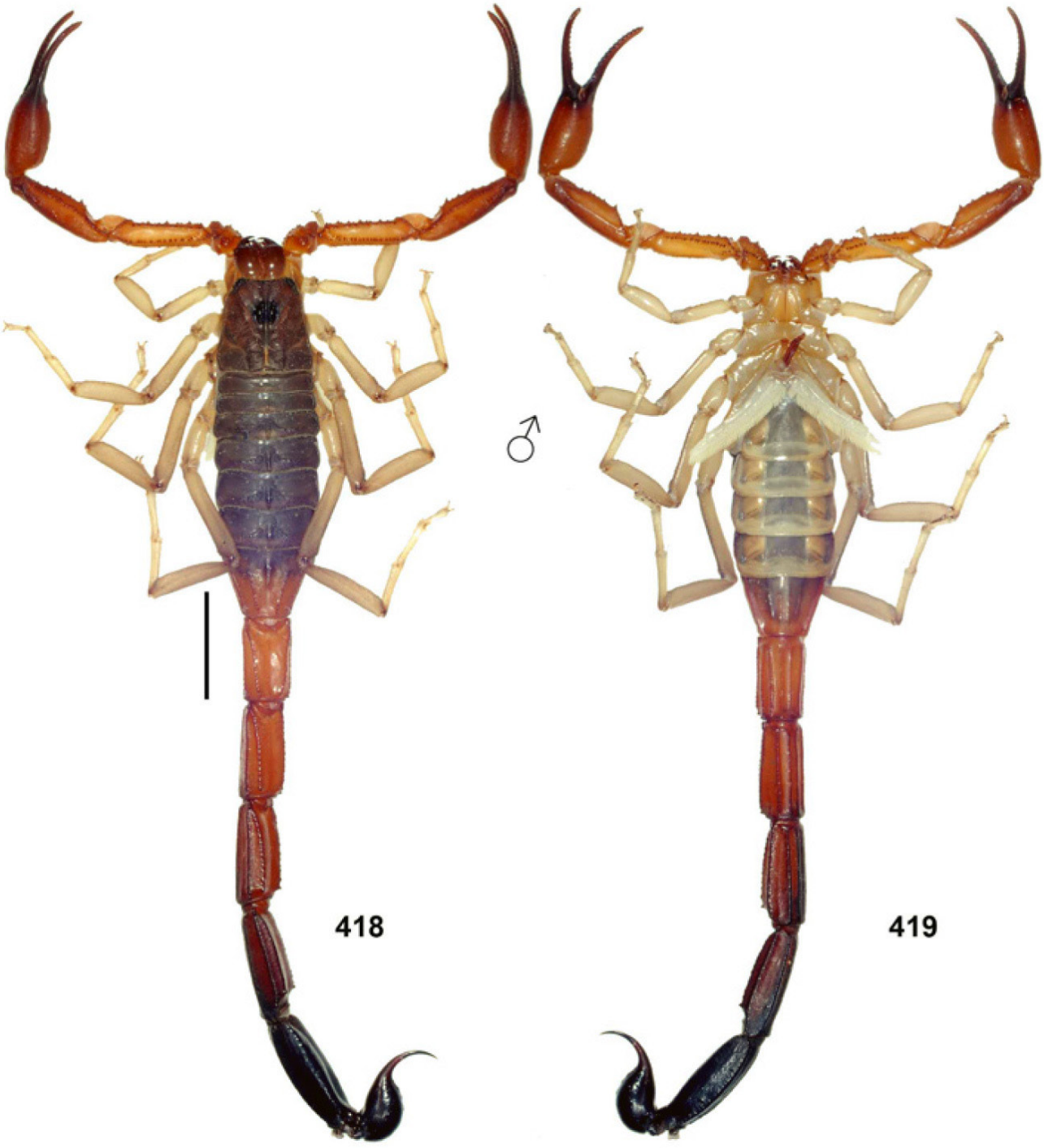

Figures 418–419. *Teruelius ankarana*. Habitus. Male in dorsal (418) and ventral (419) views. Scale bar: 10 mm.

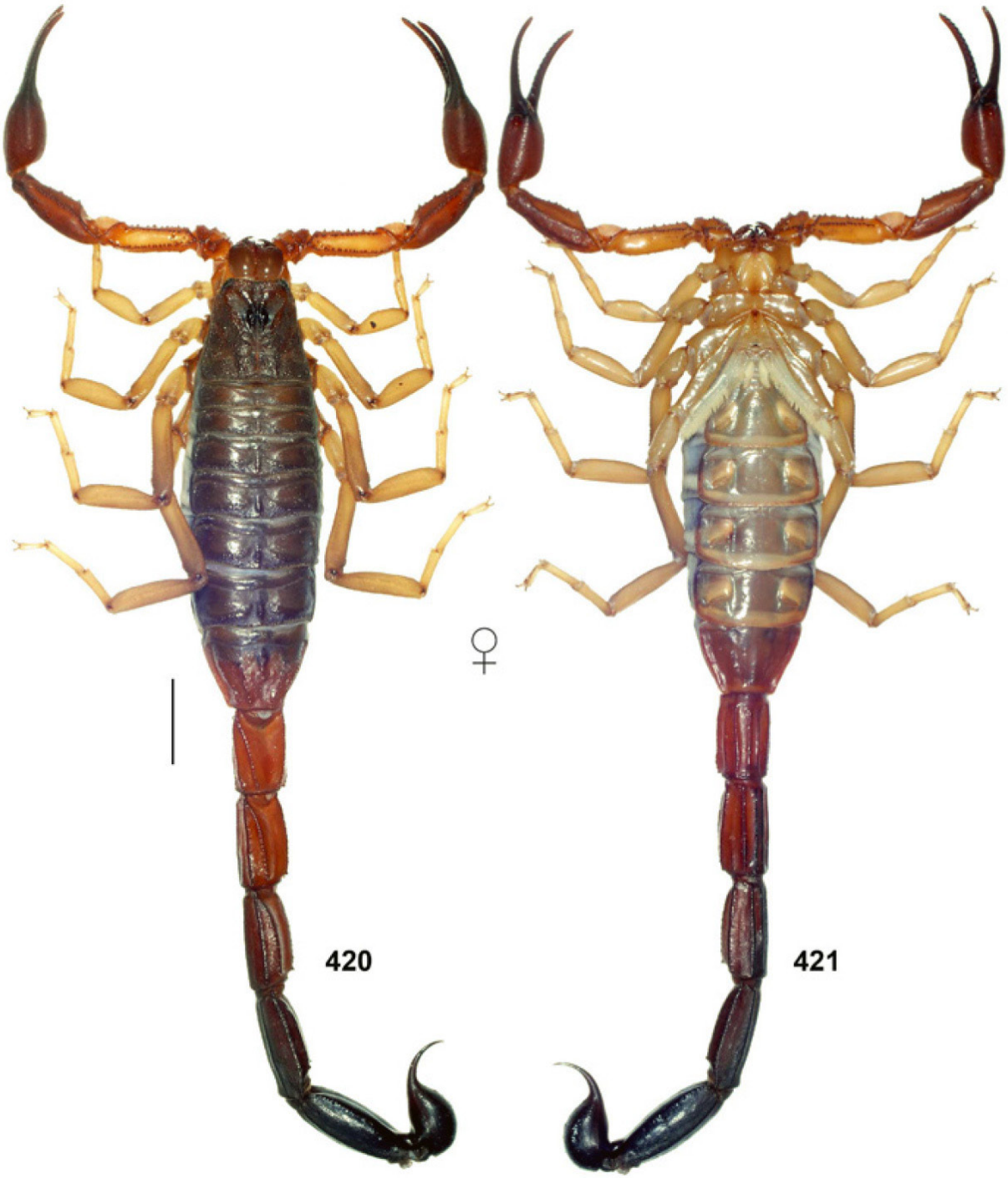

Figures 420–421. *Teruelius ankarana*. Habitus. Female in dorsal (420) and ventral (421) views. Scale bar: 10 mm.

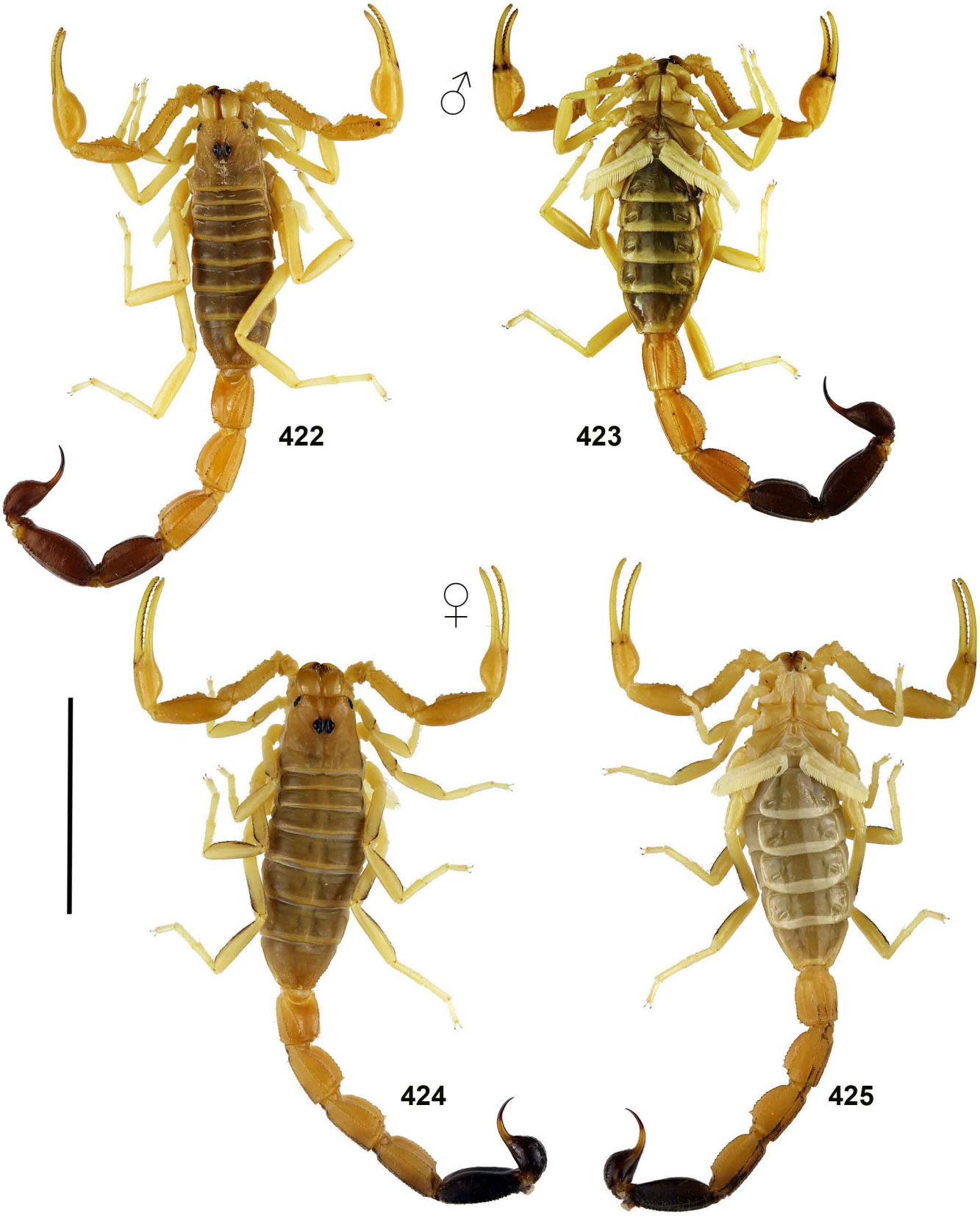

Figures 422–425. *Teruelius annulatus*. Habitus. Male (422–423) and female (424–425), dorsal (422, 424) and ventral (423, 425) views. Scale bar: 10 mm.

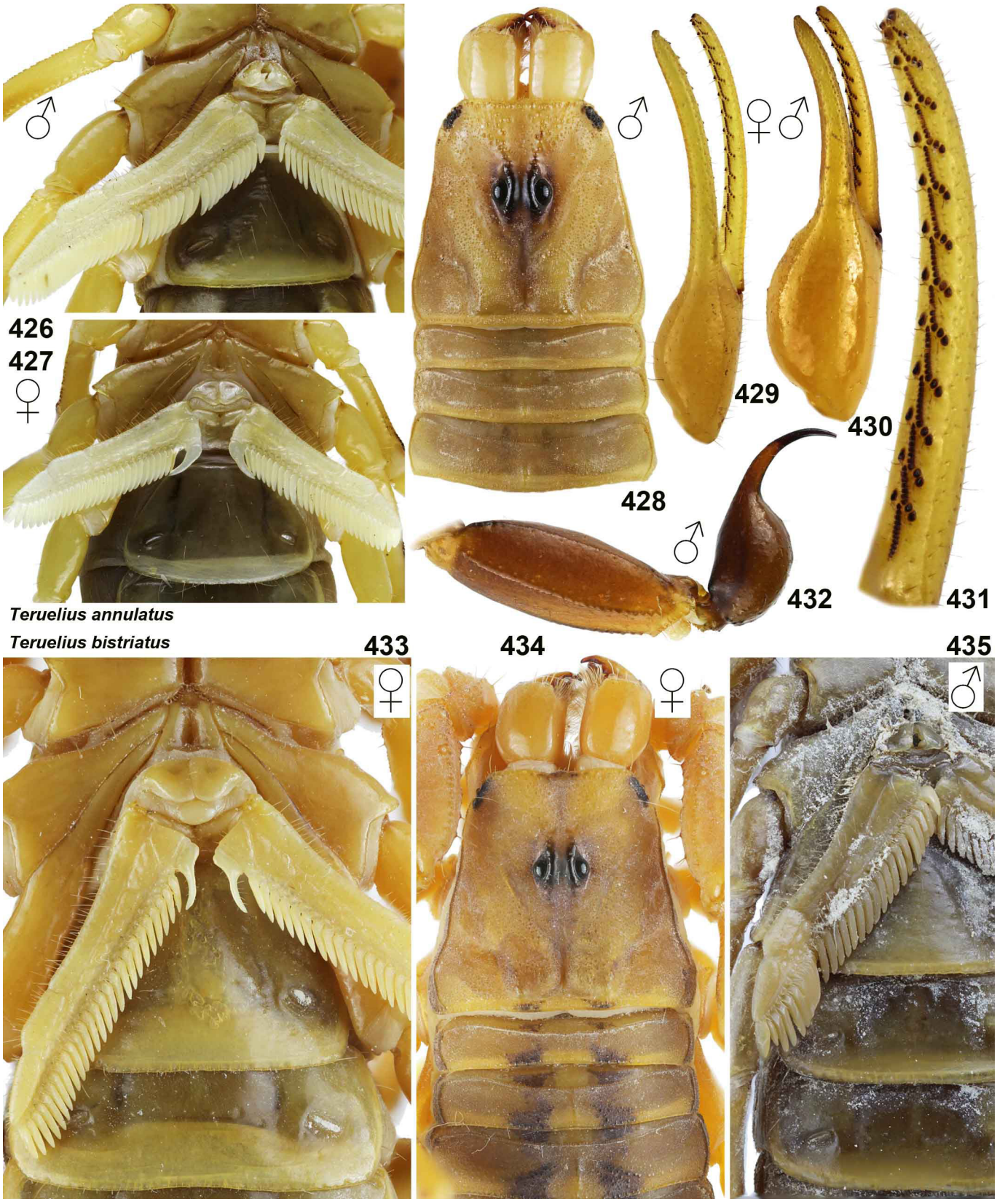

Figures 426–435. **Figures 426–432**. *Teruelius annulatus*. Male (426, 428, 430–431) and female (427, 429). Sternopectinal region (426–427). Carapace and tergites I–III (428). Pedipalp chela dorsal (429–430). Pedipalp chela, movable finger dentate margin (431). Metasoma V and telson lateroventral view (432). **Figures 433–435**. *Teruelius bistriatus*. Female (433–434) and male (435) syntypes. Sternopectinal region (433, 435). Carapace and tergites I–III (434).

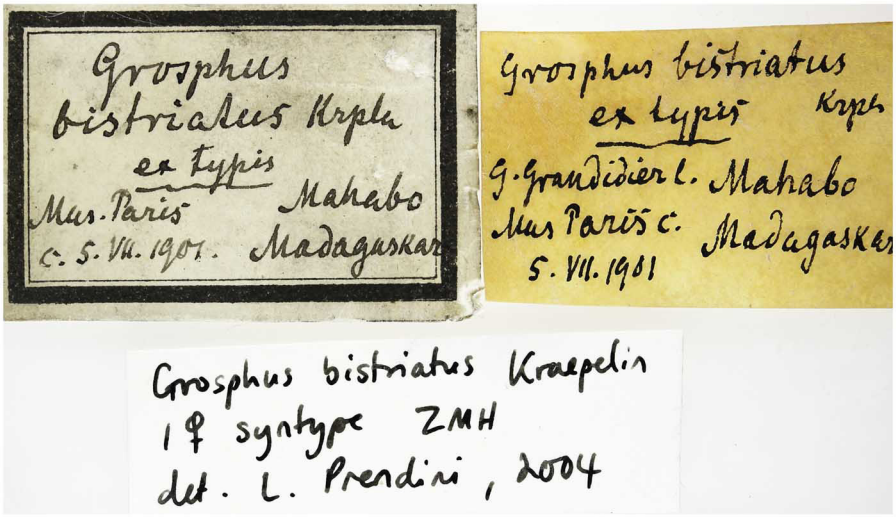

Figures 436–438. *Teruelius bistriatus*. Habitus. Female syntype in dorsal (436) and ventral (437) views, and original labels (438). Scale bar: 10 mm.

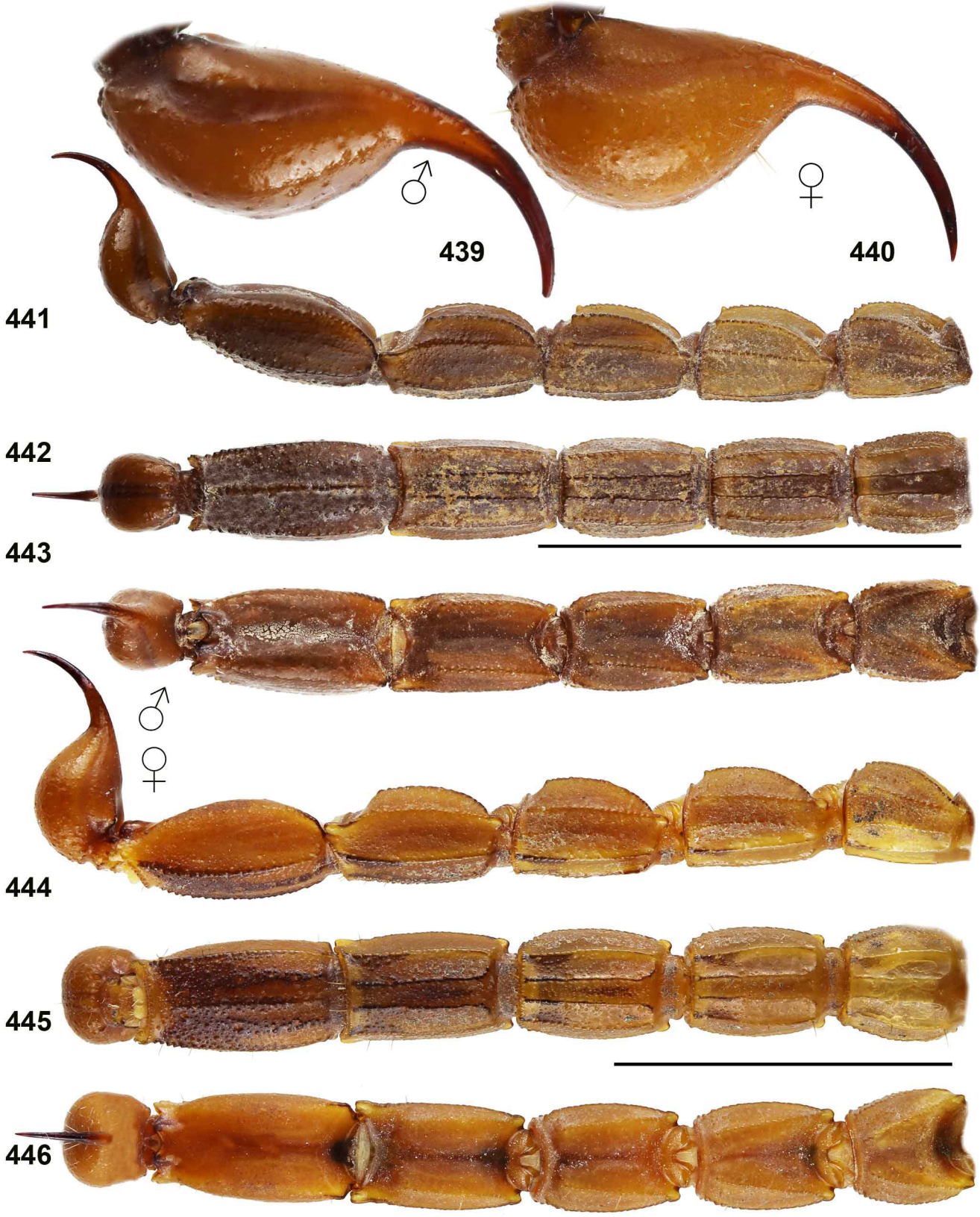

Figures 439–446. *Teruelius bistriatus*. Metasoma and telson. Male (439, 441–443) and female syntypes (440, 444–446), lateral (439–441, 444), ventral (442, 445) and dorsal (443, 446) views. Scale bars: 10 mm (441–443, 444–446).

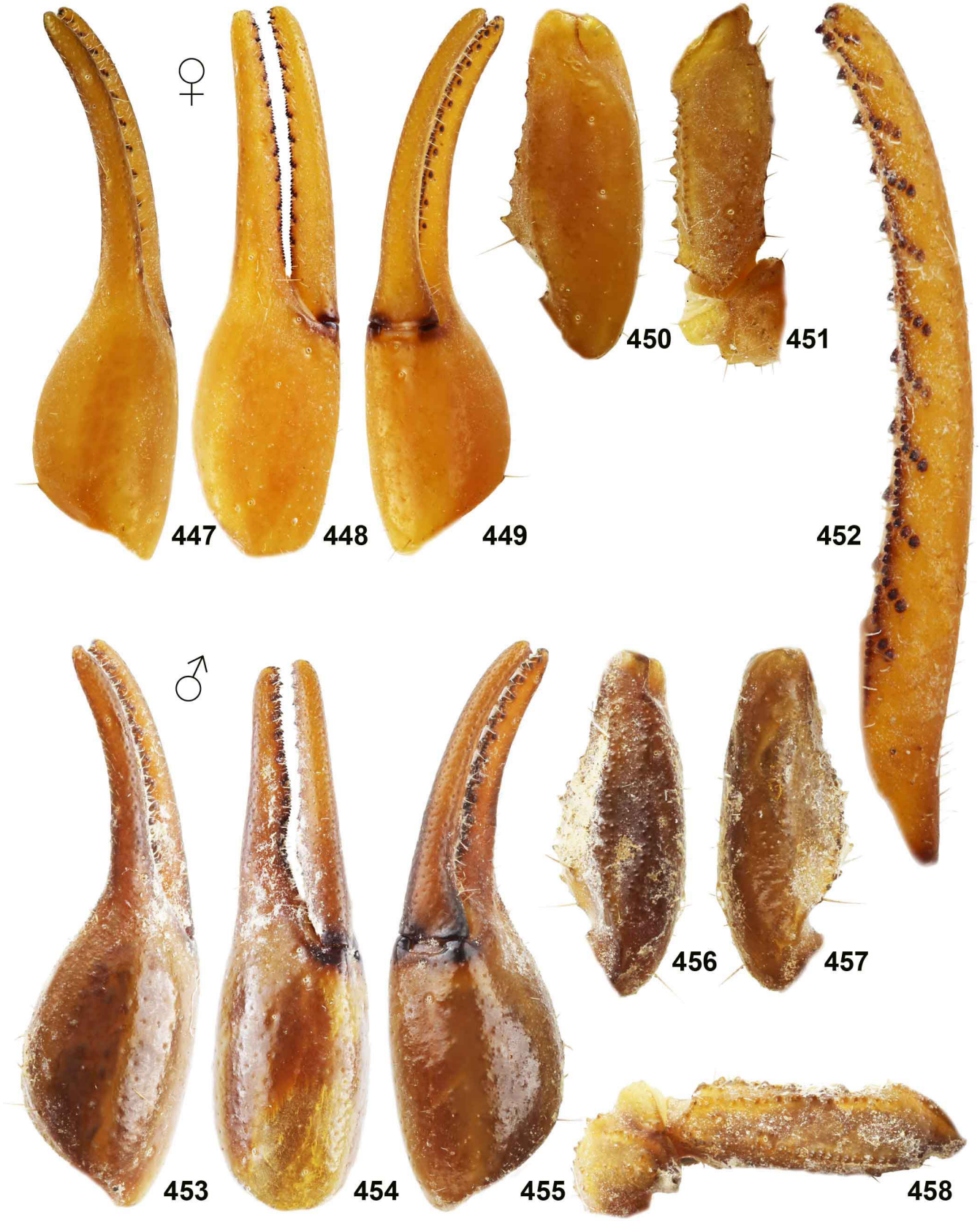

Figures 447–458. *Teruelius bistriatus*. Pedipalp. Female (447–452) and male (453–458) syntypes. Pedipalp chela, dorsal (447, 453), external (448, 454) and ventrointernal (449, 455) views; pedipalp patella, dorsal (450, 456) and ventral (457) views; pedipalp femur and trochanter in dorsal (451, 458) views; pedipalp chela, movable finger dentate margin (452). Pedipalp of male is mirrored.

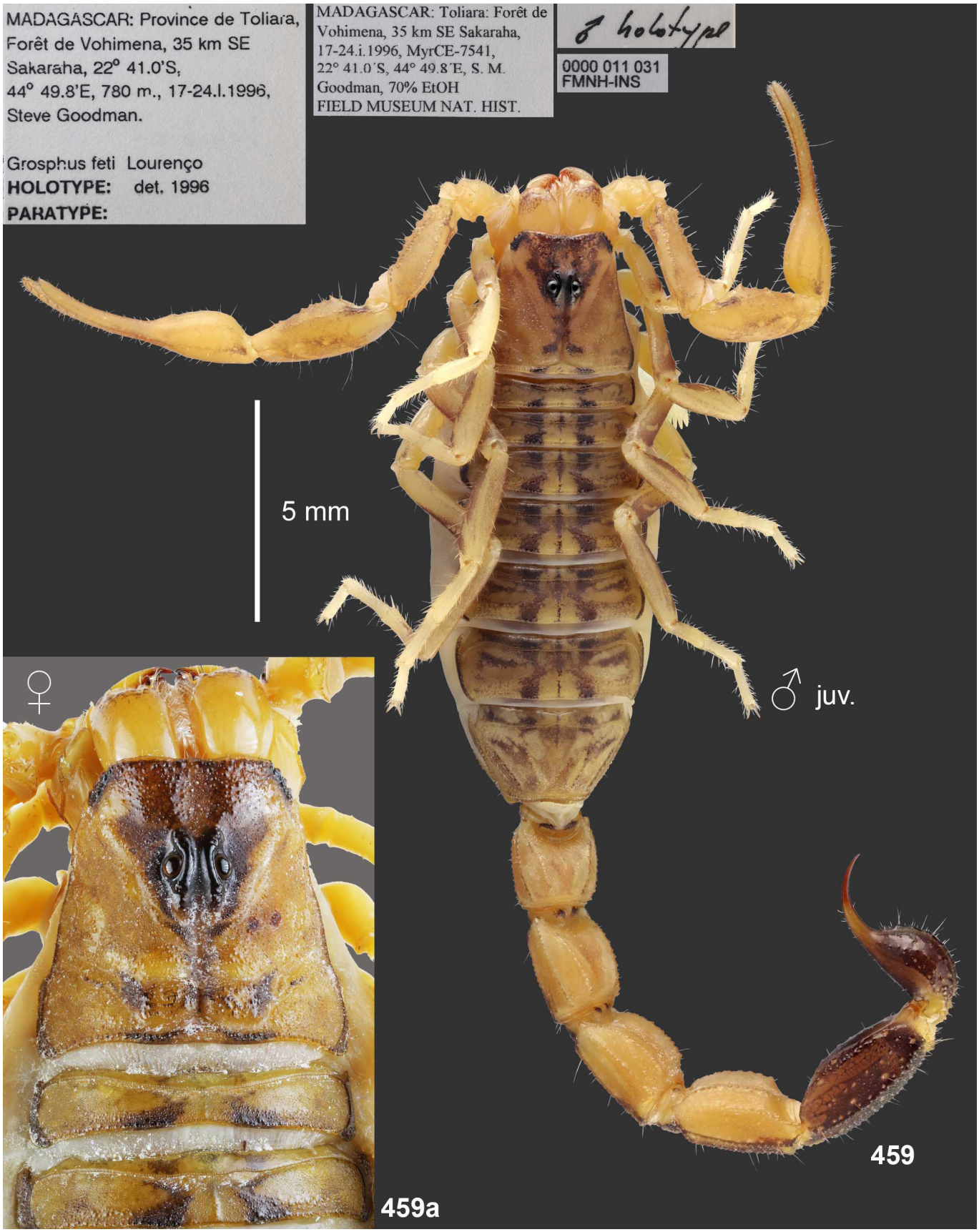

Figure 459. *Teruelius feti*. Holotype juvenile male. Habitus, dorsal view, with specimen labels (FMNH). Scale bar: 5 mm (holotype).
Figure 459a. Adult female from Makay Mts., carapace and tergites I–II.

Figures 460–472. *Teruelius feti*. Holotype male. Metasoma and pedipalp. **Figures 460–462**. Metasoma in dorsal (460), lateral (461) and ventral (462) views. **Figures 463–472**. Pedipalp. Chela in dorsal (463), external (464) and ventral (465) views. Patella in dorsal (466), external (467) and ventral (468) views. Femur and trochanter in internal (469), dorsal (470), ventral (471) and external (472) views. Right femur shows developmental anomaly (Figs. 469, 472). Scale bars: 2 mm (460–462, 463–472).

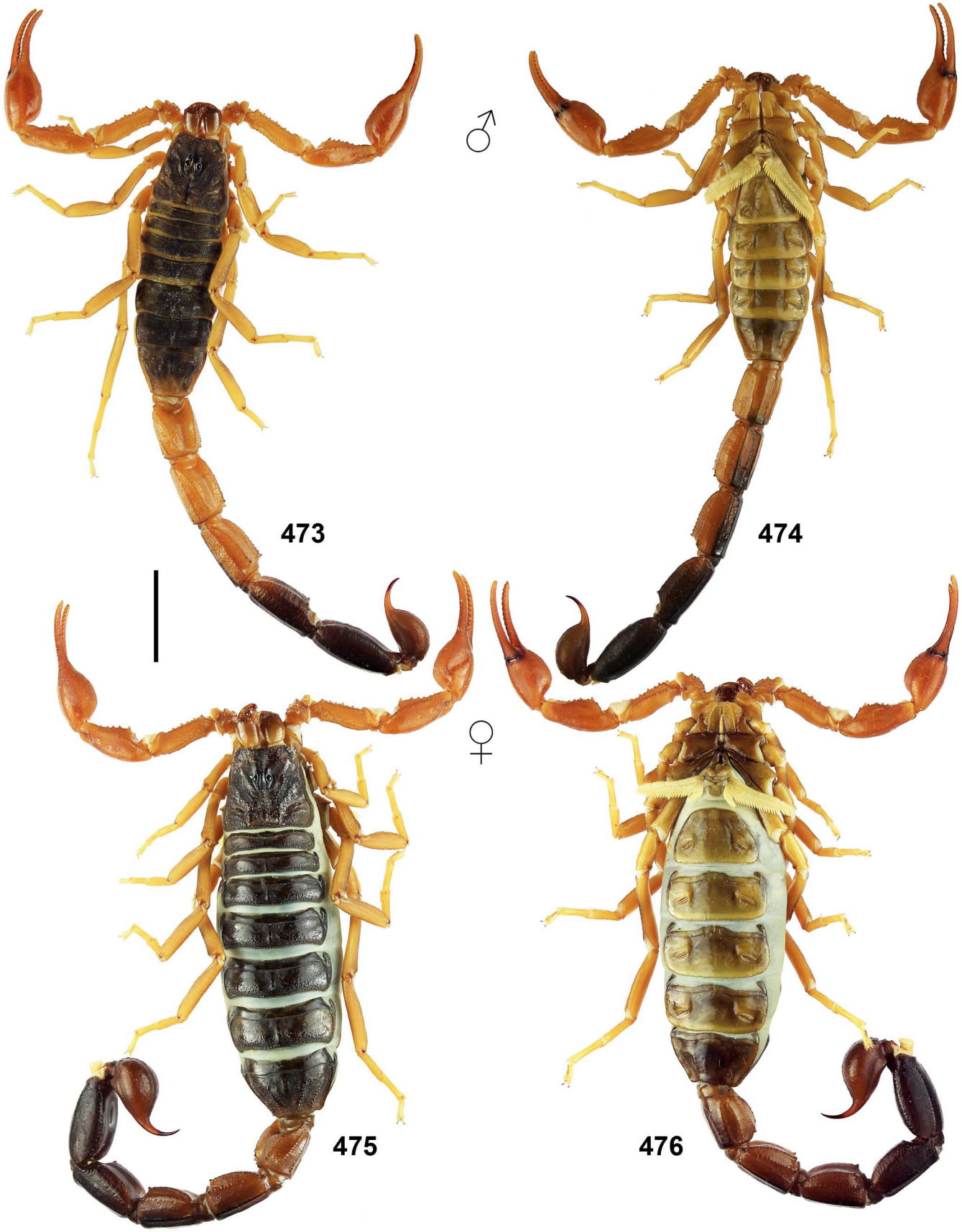

Figures 473–476. *Teruelius flavopiceus*. Habitus. Male (473–474) and female (475–476), dorsal (473, 475) and ventral (474, 476) views. Scale bar: 10 mm.

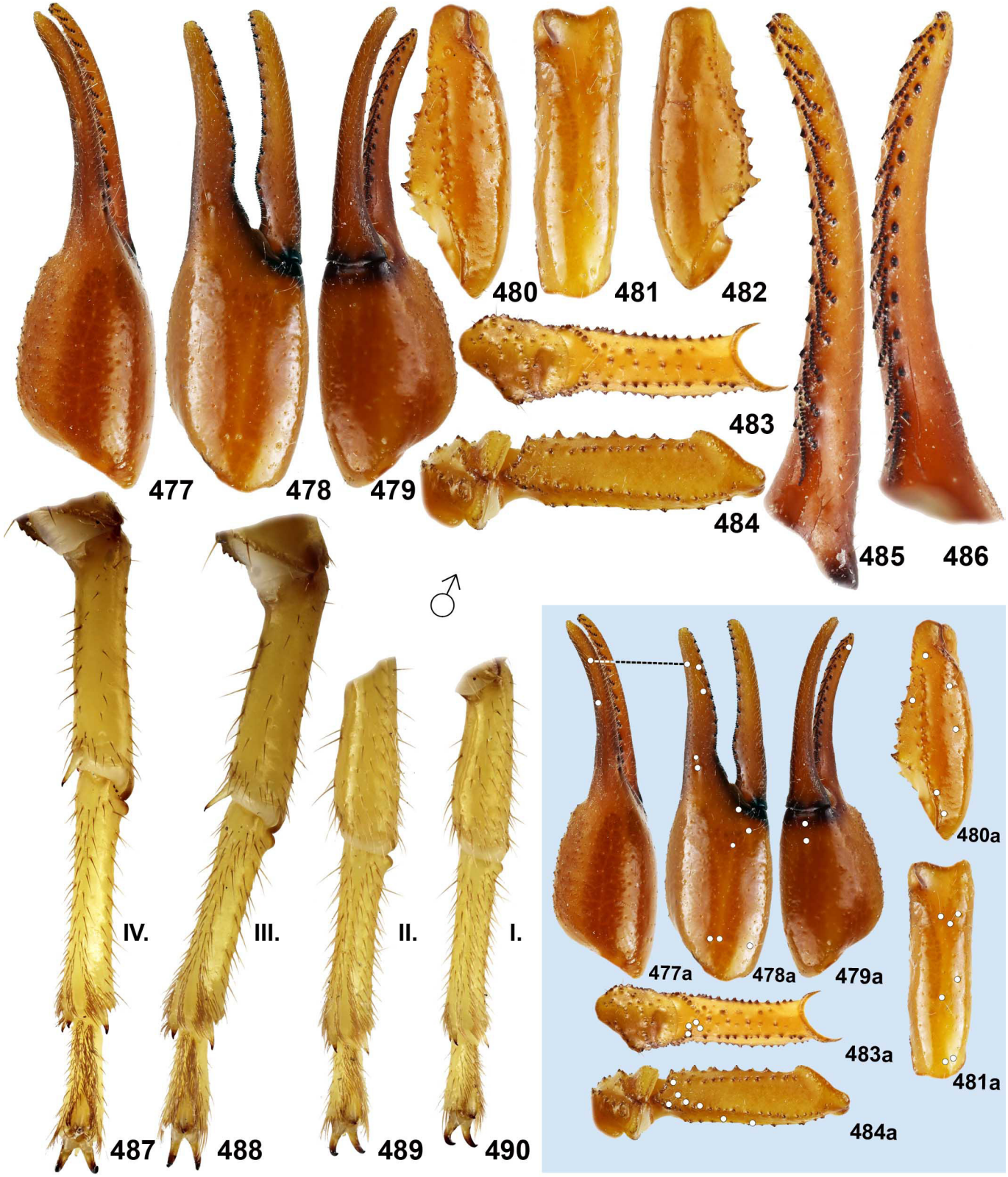

Figures 477–490. *Teruelius flavopiceus*, male. **Figures 477–486**. Pedipalp chela, dorsal (477), external (478) and ventrointernal (479) views; pedipalp patella, dorsal (480), external (481) and ventral (482) views; pedipalp femur and trochanter, internal (483) and dorsal (484) views; pedipalp chela, movable (485) and fixed (486) finger dentate margin. The trichobothrial pattern is indicated by white circles in Figures 477a–484a. **Figures 487–490**. Right legs tibia, basitarsus and telotarsus, retrolateral views. Leg IV (487), leg III (488), leg. II (489), leg I (490).

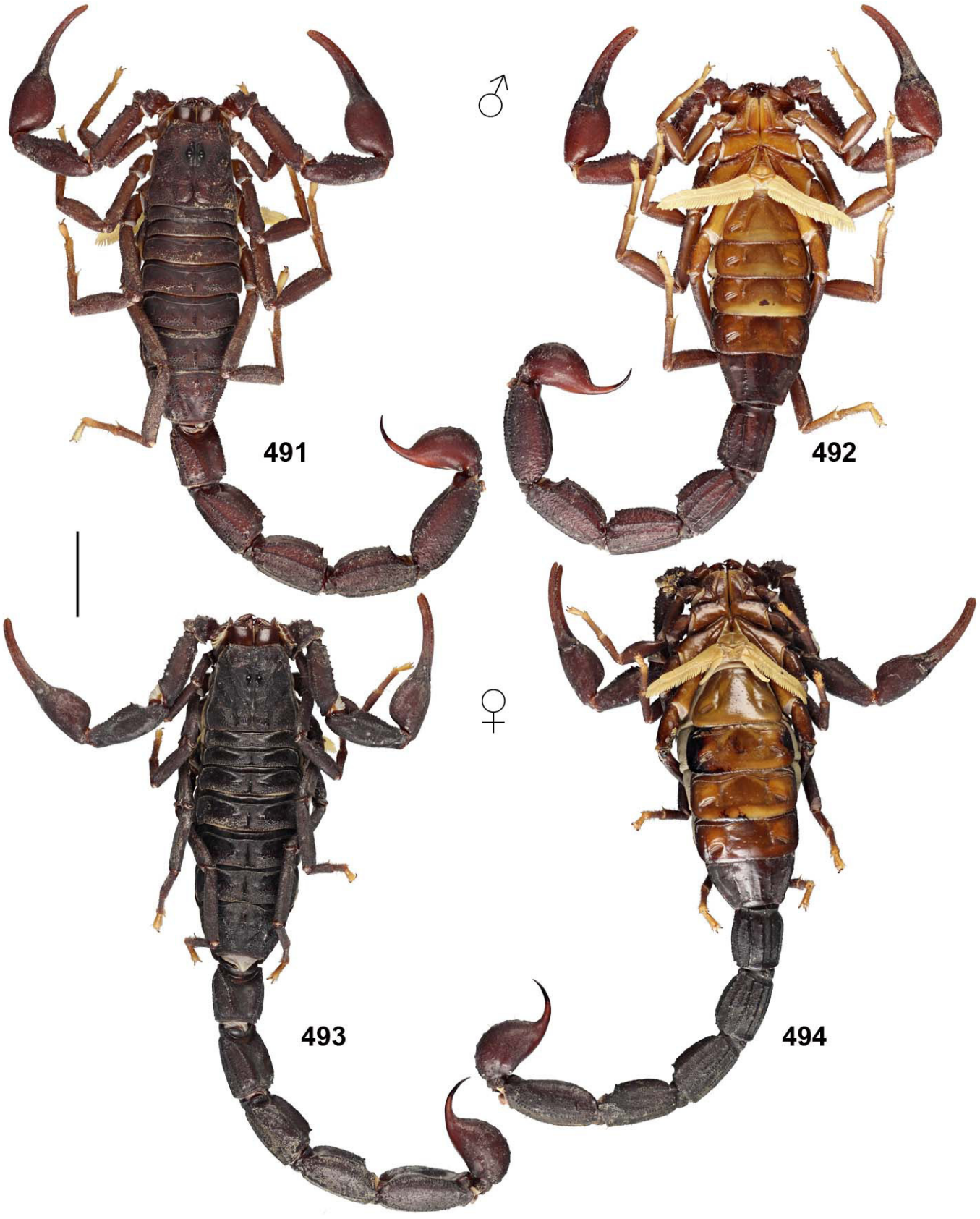

Figures 491–494. *Teruelius grandidieri*. Habitus. Male (491–492) and female (493–494), dorsal (491, 493) and ventral (492, 494) views. Scale bar: 10 mm.

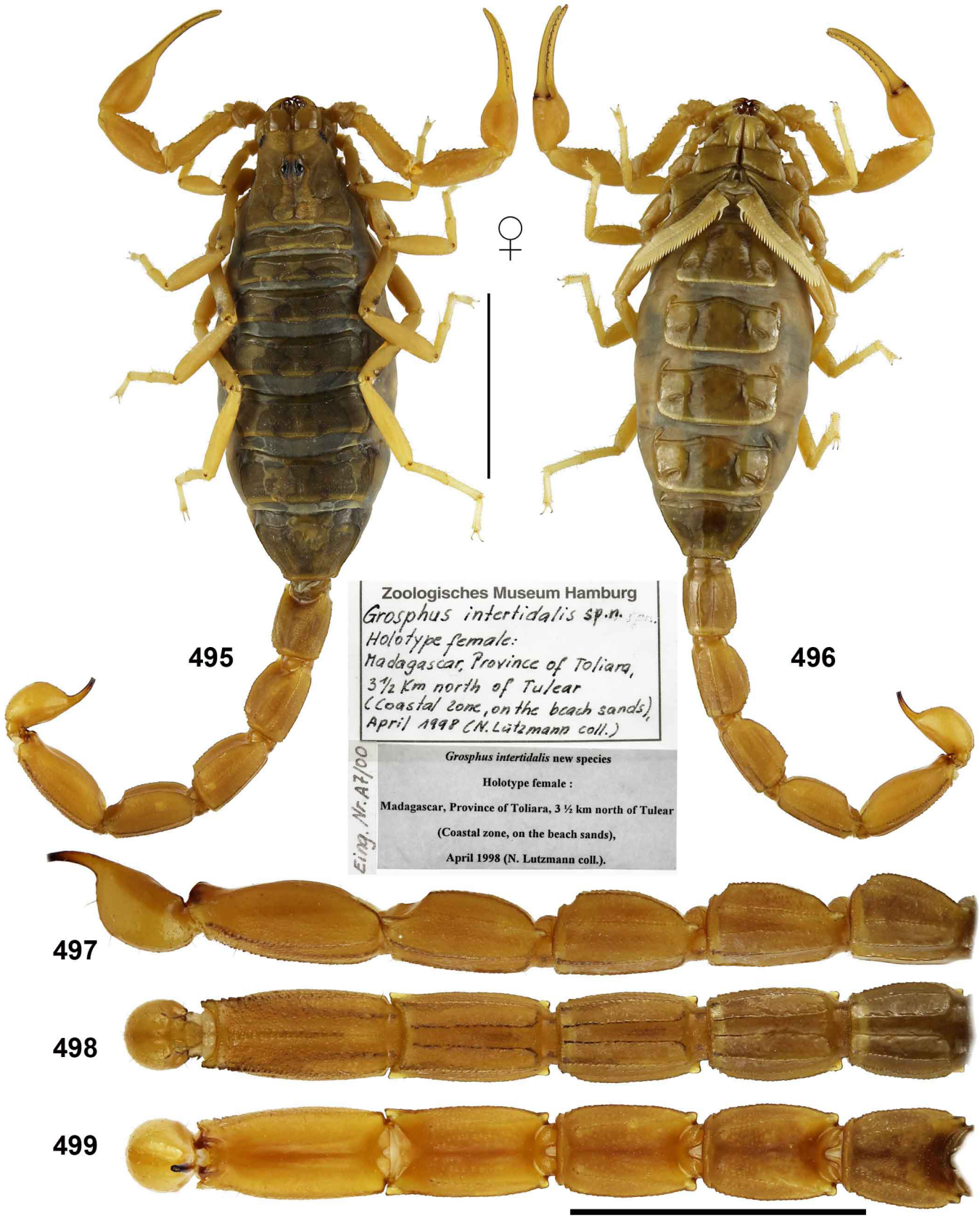

Figures 495–499. *Teruelius intertidalis*, female holotype. **Figures 495–496**. Habitus in dorsal (495) and ventral (496) views, and original labels. **Figures 497–499**. Metasoma in lateral (497), ventral (498) and dorsal (499) views. Scale bars: 10 mm.

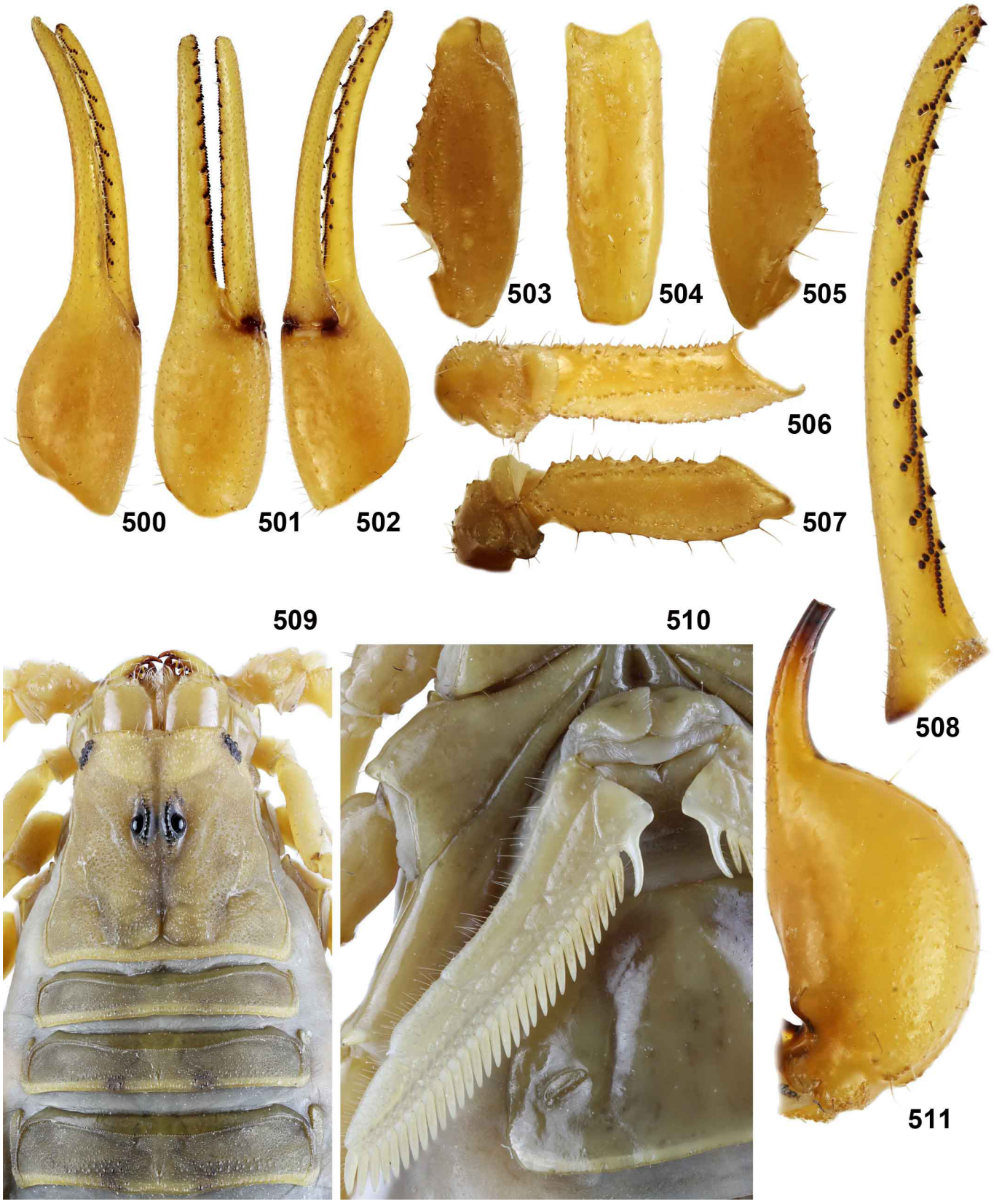

Figures 500–511. *Teruelius intertidalis*, female holotype. **Figures 500–508**. Pedipalp chela, dorsal (500), external (501) and ventrointernal (502) views; pedipalp patella, dorsal (503), external (504) and ventral (505) views; pedipalp femur and trochanter, internal (506) and dorsal (507) views; pedipalp chela, movable finger dentate margin (508). **Figure 509**. Carapace and tergites I–III. **Figure 510**. Sternopectinal region. **Figure 511**. Telson lateral view.

Figures 512–515. *Teruelius intertidalis*, female holotype. Left legs tibia, basitarsus and telotarsus, retrolateral views. Leg I (512), leg II (513), leg III (514), leg IV (515).

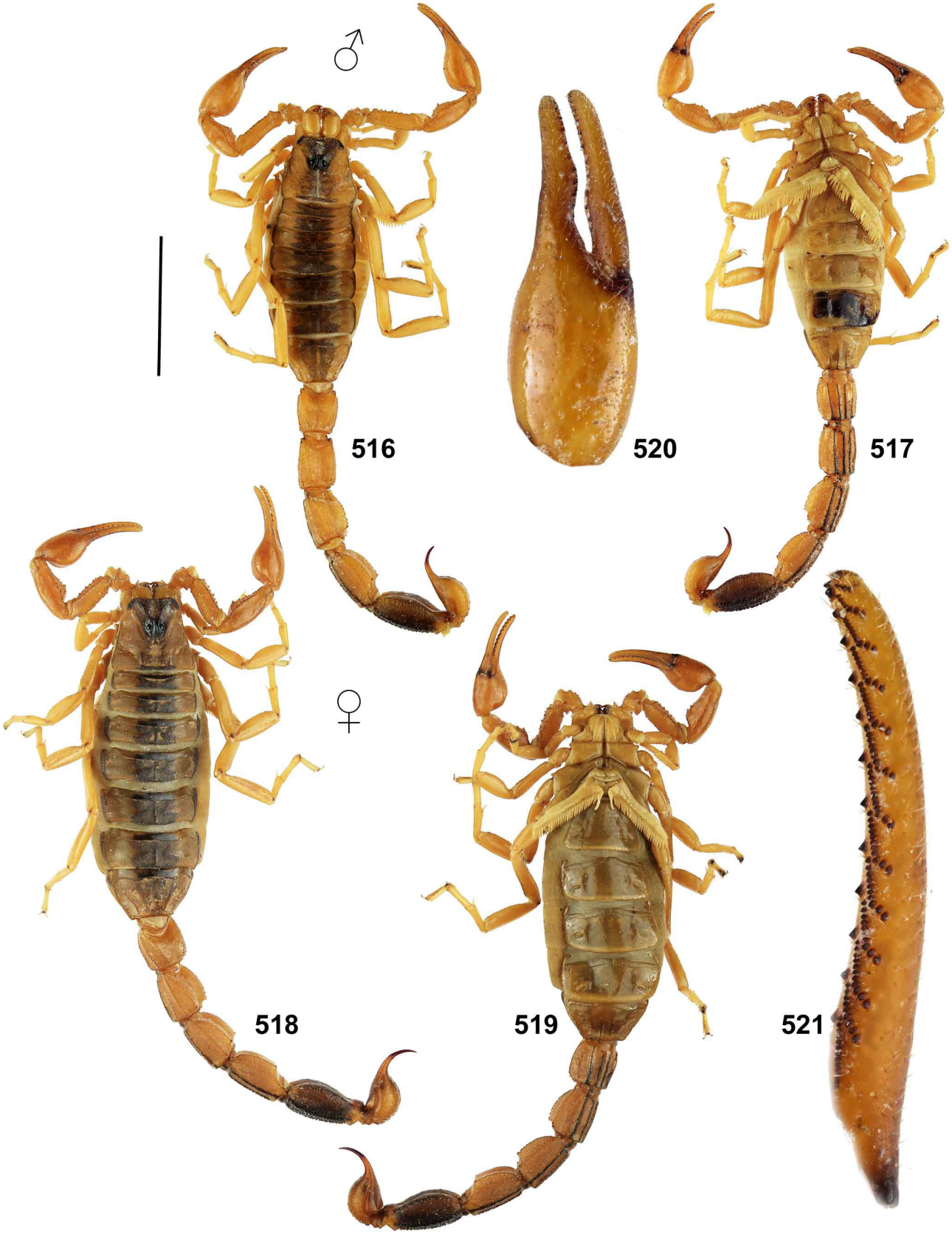

Figures 516–521. *Teruelius limbatus*. **Figures 516–519**. Habitus. Male (516–517) and female (518–519), dorsal (516, 518) and ventral (517, 519) views. **Figure 520**. Pedipalp chela external, male. **Figure 521**. Pedipalp chela, movable finger dentate margin, female. Scale bar: 10 mm (516–519).

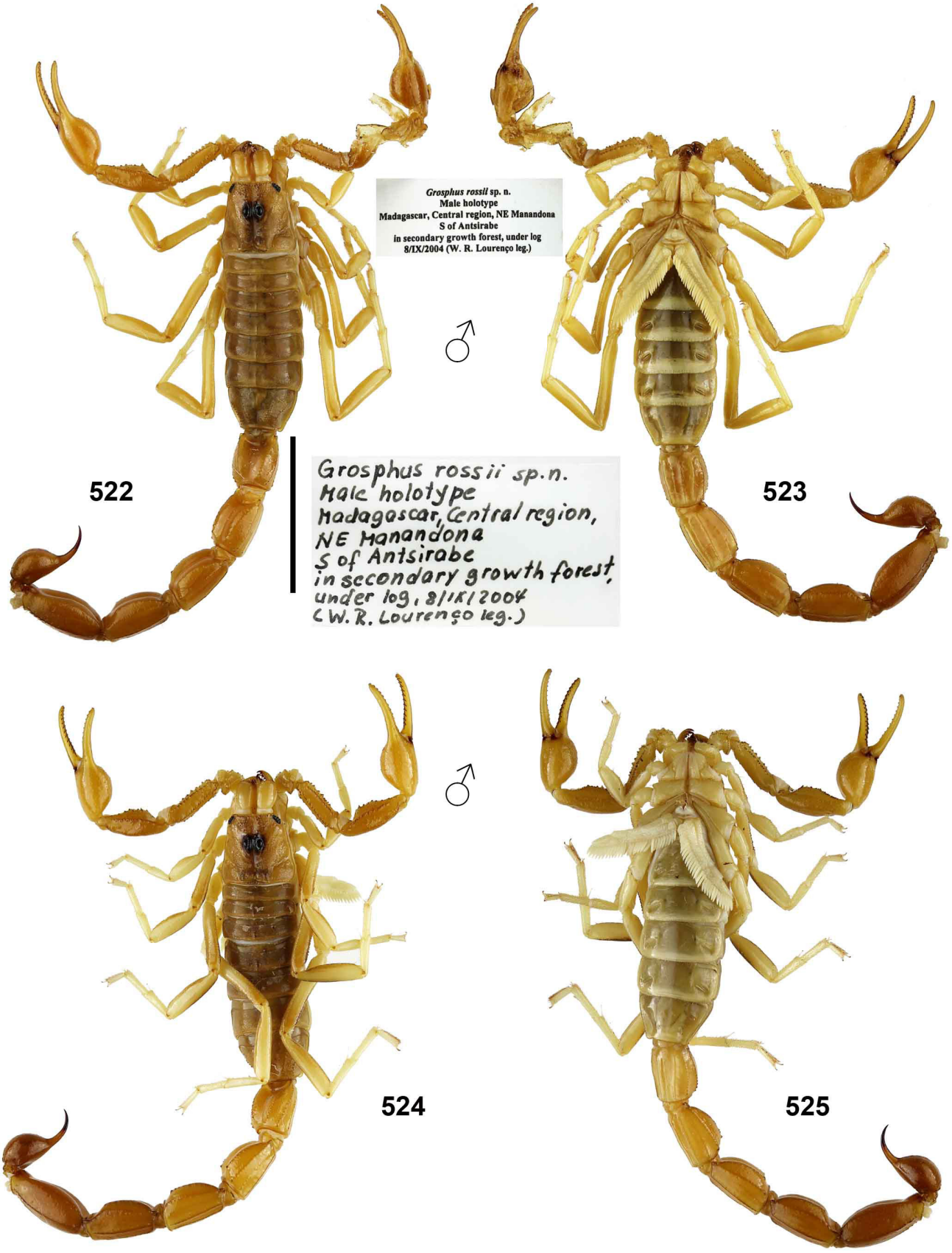

Figures 522–525. *Teruelius mahafaliensis*. Habitus. Male holotype of *G. rossii* (522–523) and male from near the type locality of *T. mahafaliensis* (524–525), dorsal (522, 524) and ventral (523, 525) views. Scale bar: 10 mm.

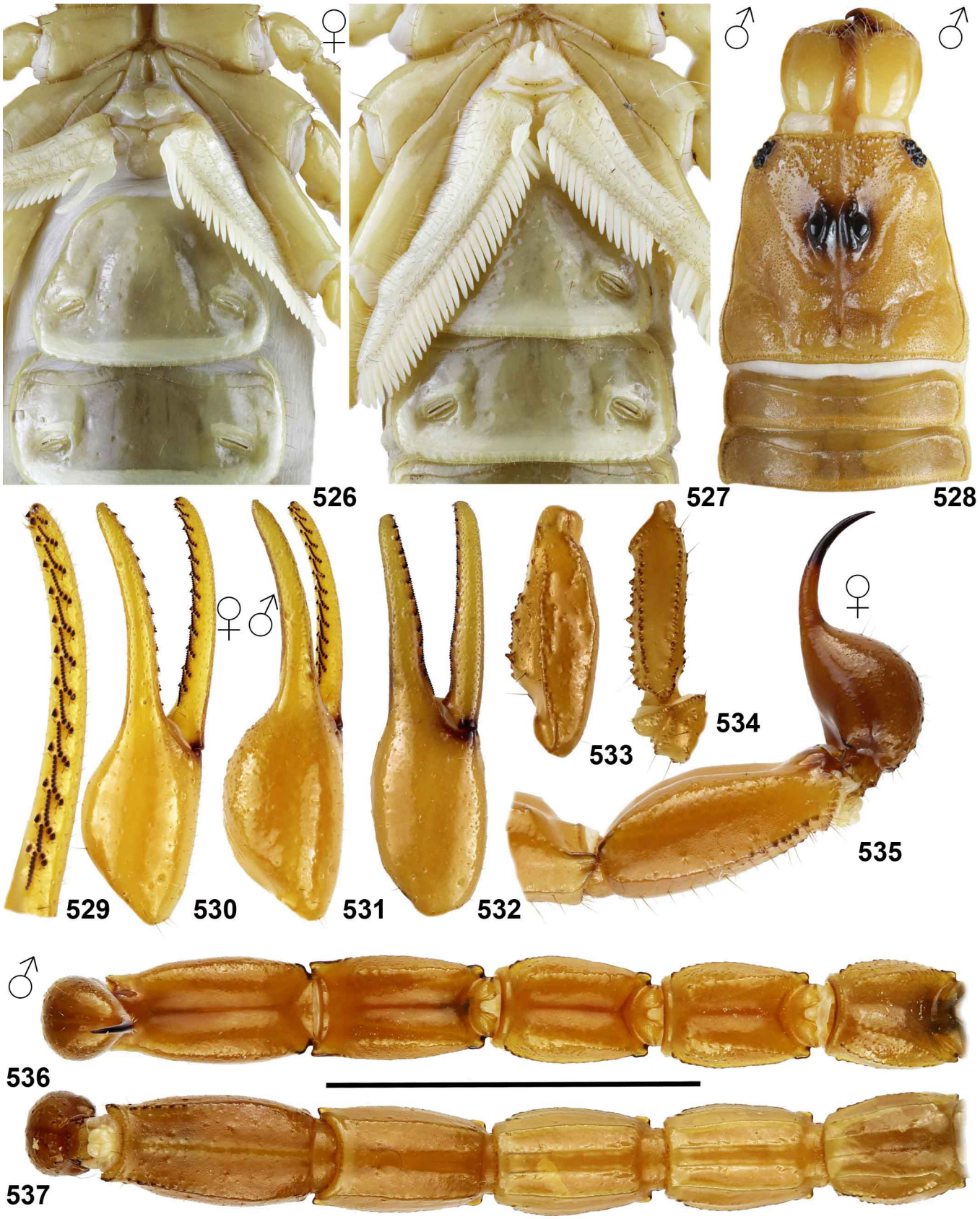

Figures 526–537. *Teruelius mahafaliensis*, female (526, 529–530, 535), male (527–528, 531–534) and male holotype of *G. rossii* (536–537). Sternopectinal region (526–527). Carapace and tergites I–II (528). Pedipalp chela, movable finger dentate margin (529). Pedipalp chela dorsal (530–531) and external (532) views. Pedipalp patella dorsal (533) view. Pedipalp femur and trochanter dorsal (534) view. Metasoma V and telson lateral (535) view. Metasoma and telson dorsal (536) and ventral (537) views. Scale bar: 10 mm (536–537).

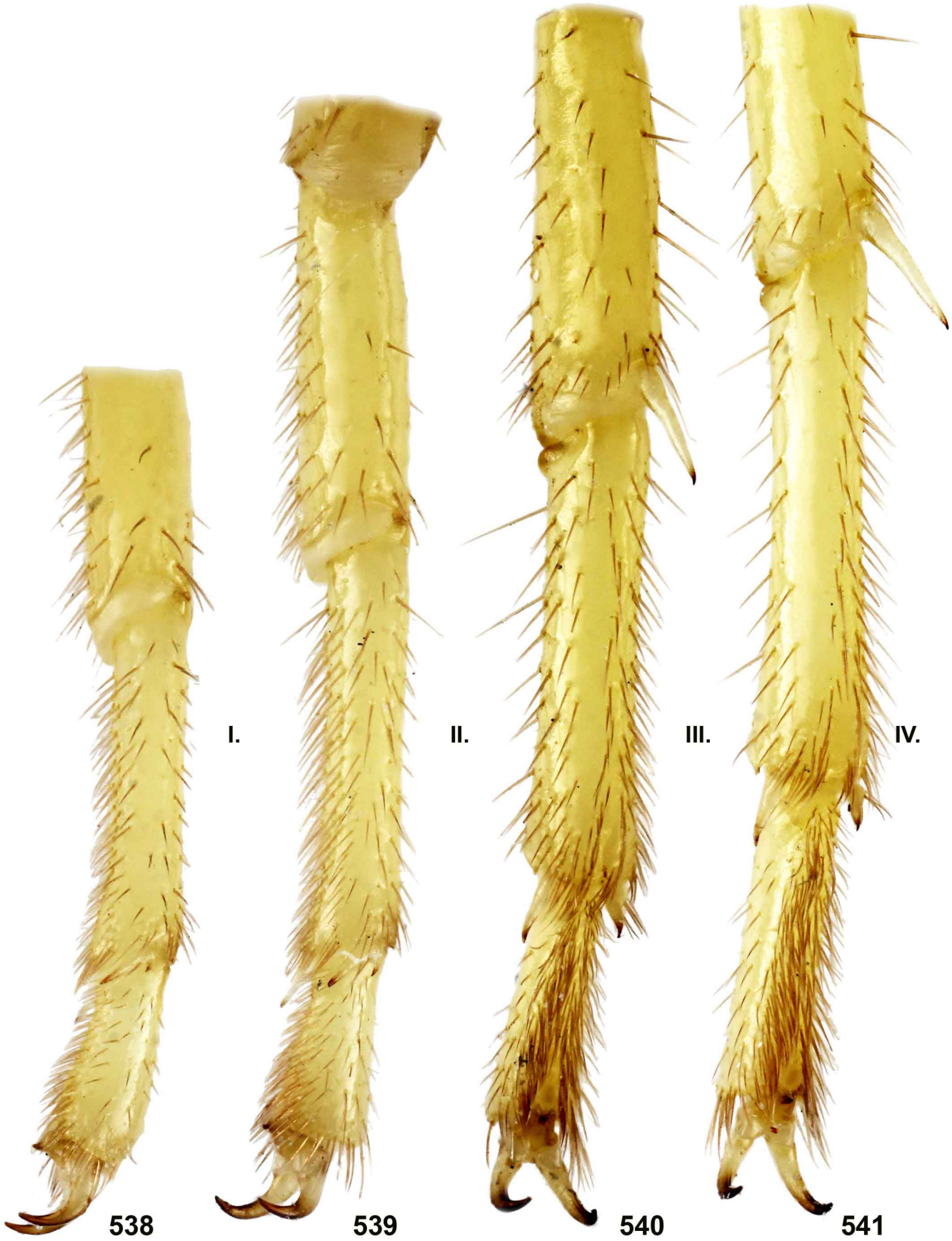

Figures 538–541. *Teruelius mahafaliensis*, male holotype of *G. rossii*. Left legs tibia, basitarsus and telotarsus, retrolateral views. Leg I (538), leg II (539), leg. III (540), leg IV (541).

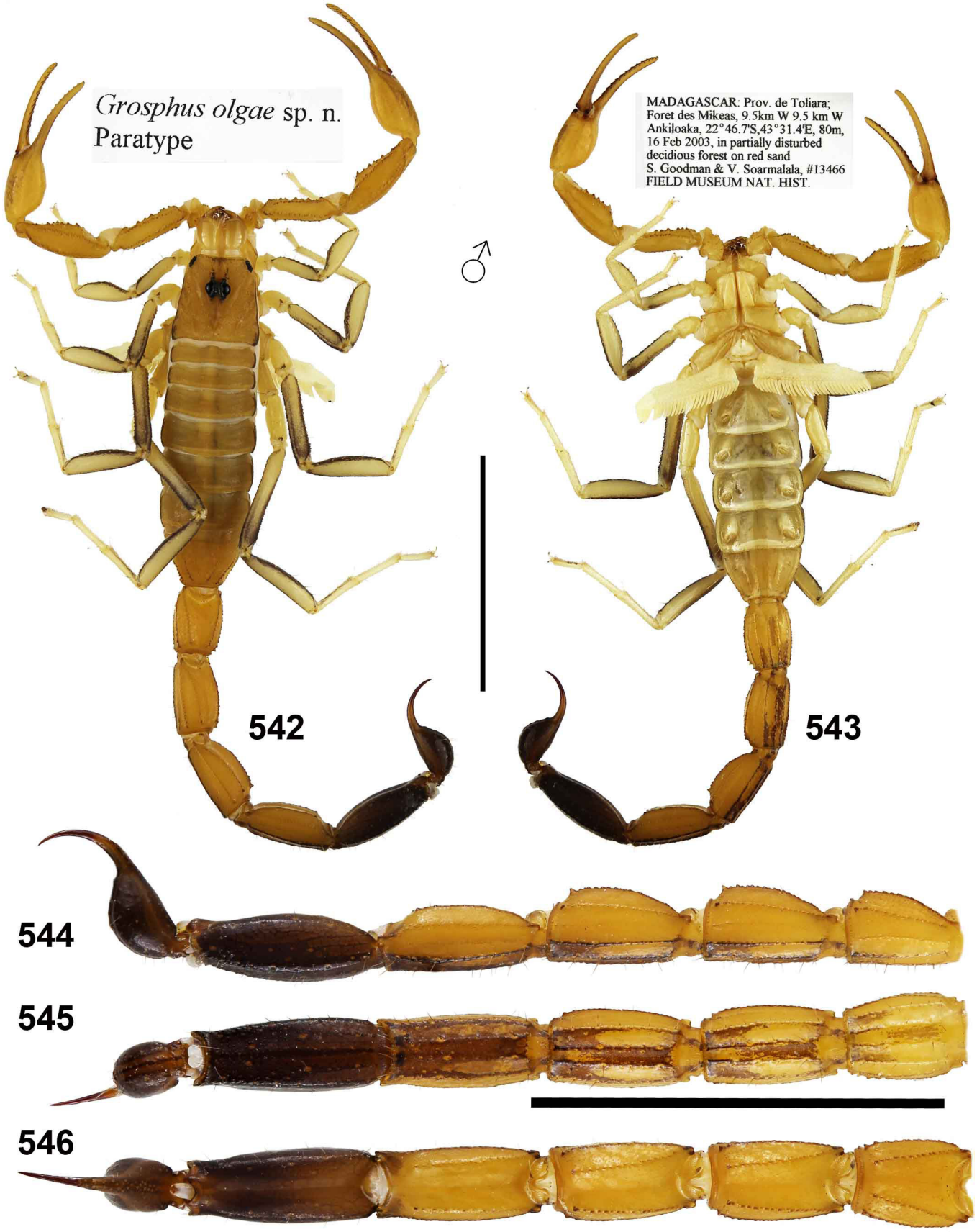

Figures 542–546. *Teruelius olgae*, male paratype. **Figures 542–543**. Habitus, dorsal (542) and ventral (543) views, and original labels. **Figures 544–546**. Metasoma and telson in lateral (544), ventral (545) and dorsal (546) views. Scale bars: 10 mm (542–543, 544–546).

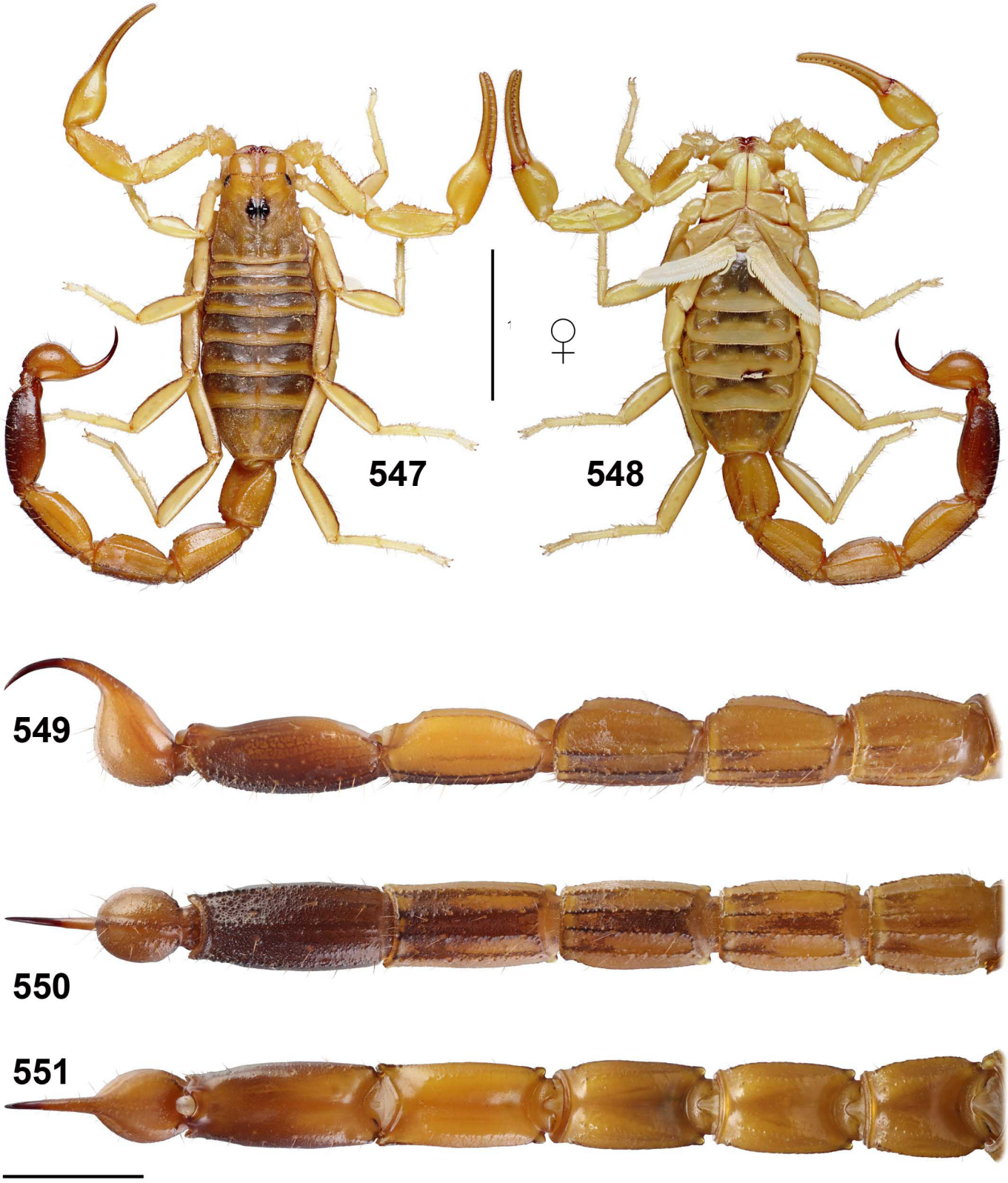

Figures 547–551. *Teruelius olgae*, female. **Figures 547–548**. Habitus, dorsal (547) and ventral (548) views. Scale bar: 10 mm. **Figures 549–551**. Metasoma and telson. lateral (549), ventral (550) and dorsal (551) views. Scale bar: 5 mm.

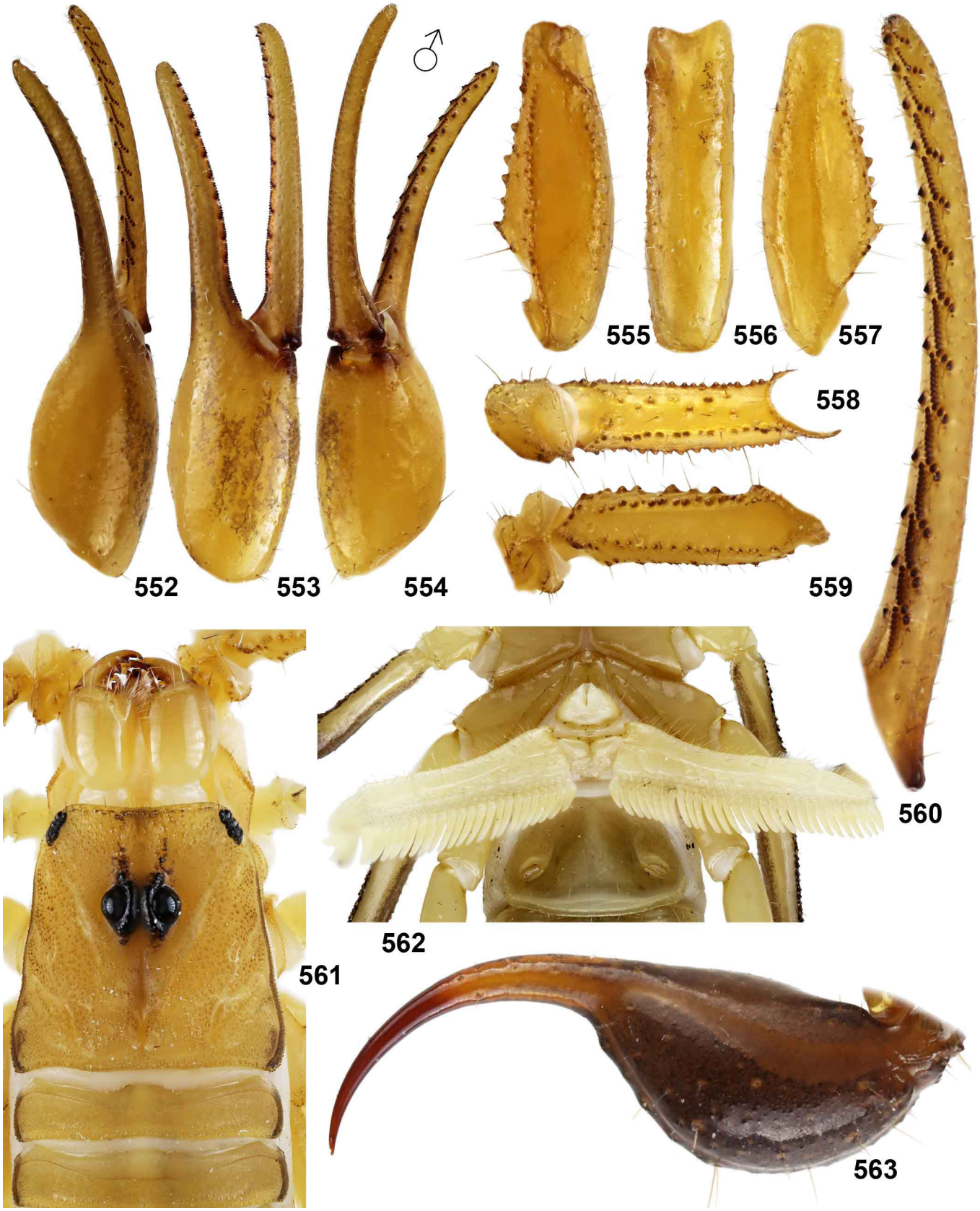

Figures 552–**563**. *Teruelius olgae*, male paratype. **Figures 552**–**560**. Pedipalp chela, dorsal (552), external (553) and ventrointernal (554) views; pedipalp patella, dorsal (555), external (556) and ventral (557) views; pedipalp femur and trochanter, internal (558) and dorsal (559) views; pedipalp chela, movable finger dentate margin (560). **Figure 561**. Carapace and tergites I–II. **Figure 562**. Sternopectinal region. **Figure 563**. Telson lateral view.

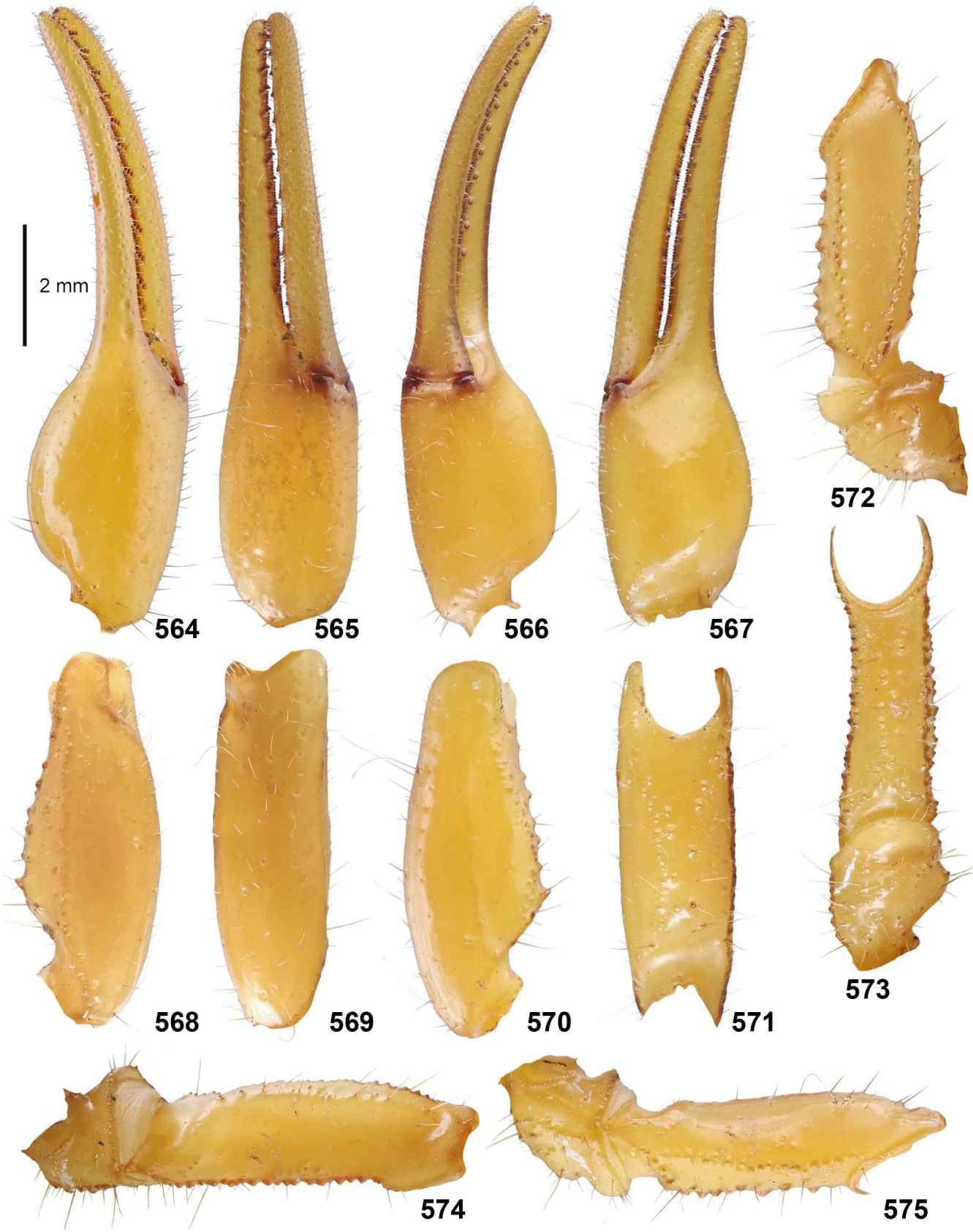

Figures 564–575. *Teruelius olgae*. Female pedipalp. Chela in dorsal (564), external (565), ventral (566) and internal (567) views. Patella in dorsal (568), external (569), ventral (570) and internal (571) views. Femur and trochanter in dorsal (572), internal (573), external (574) and ventral (575) views. Scale bar: 2 mm.

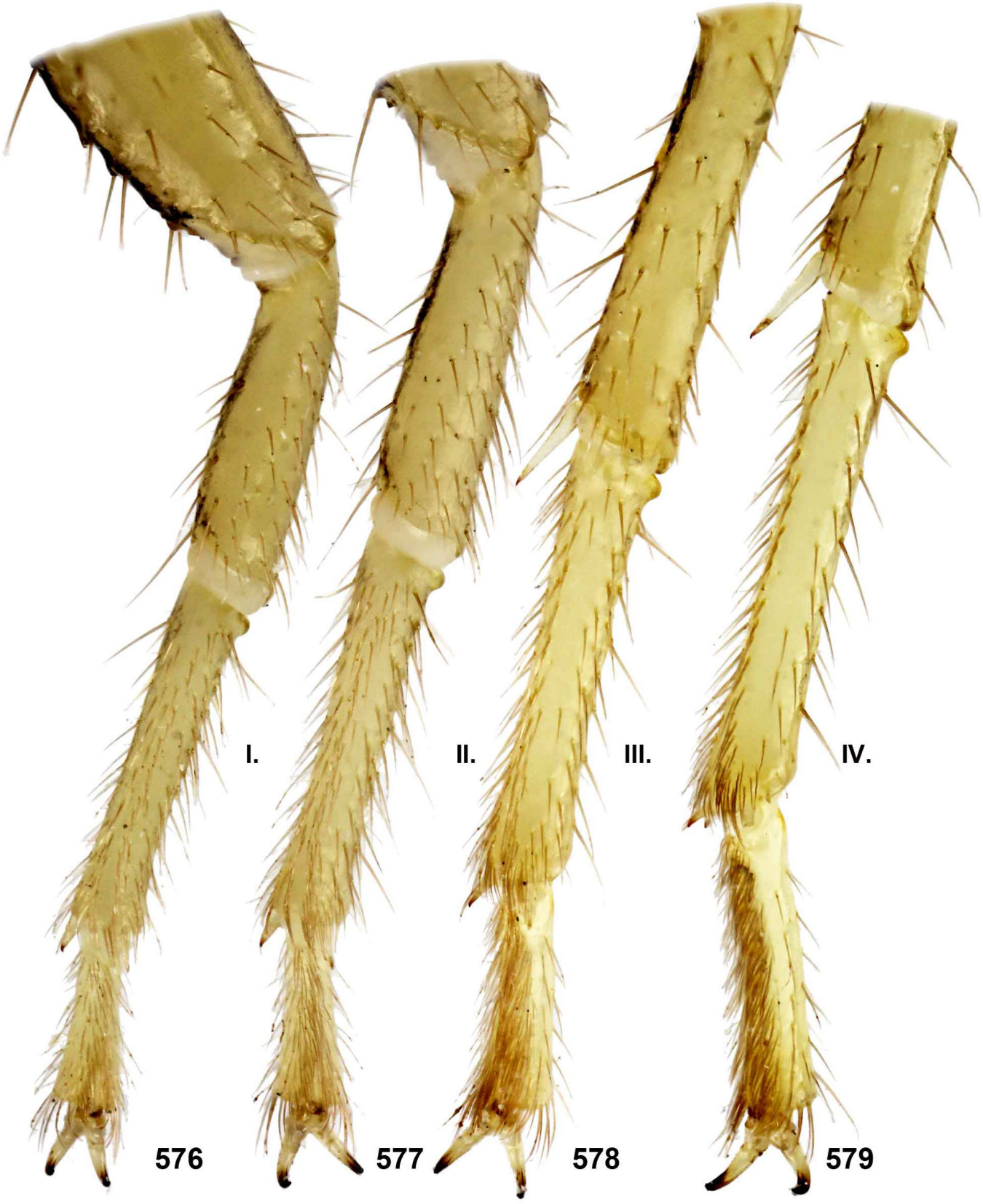

Figures 576–579. *Teruelius olgae*, male paratype. Right legs tibia, basitarsus and telotarsus, retrolateral and ventral views. Leg I (576), leg II (577), leg III (578), leg IV (579).

Figures 580–581. *Grosphus madagascariensis*. Male and female, in vivo habitus (580) and female with newborns (581).

Figures 582–583. *Grosphus madagascariensis*. Female with newborns (582) and with juveniles after first ecdysis (583).

Figures 584–**587**. *Teruelius ankarana*. Juveniles before second (584 top), after second (584 below and 585), third (586) and fourth (587) ecdysis.

Figures 588–589. *Teruelius ankarana*. Male (588) and female (589), in vivo habitus.

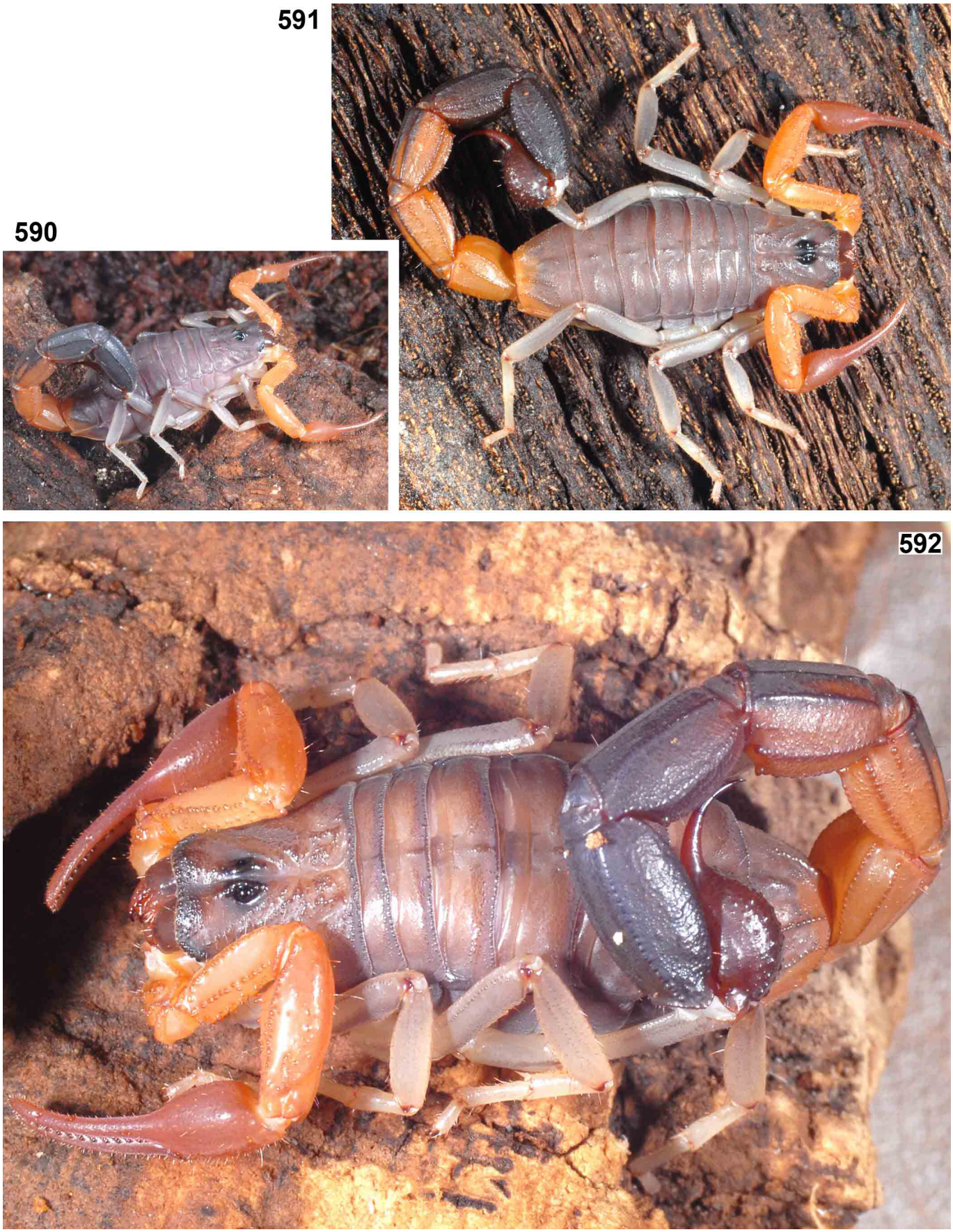

Figures 590–592. *Teruelius flavopiceus*. Juveniles after second (590), third (591) and fourth (592) ecdysis.

Figures 593–594. *Teruelius flavopiceus*. Male (593) and female (594), in vivo habitus.

Figures 595–596. *Teruelius flavopiceus*. Female with newborns (595) and with juveniles after first ecdysis (596).

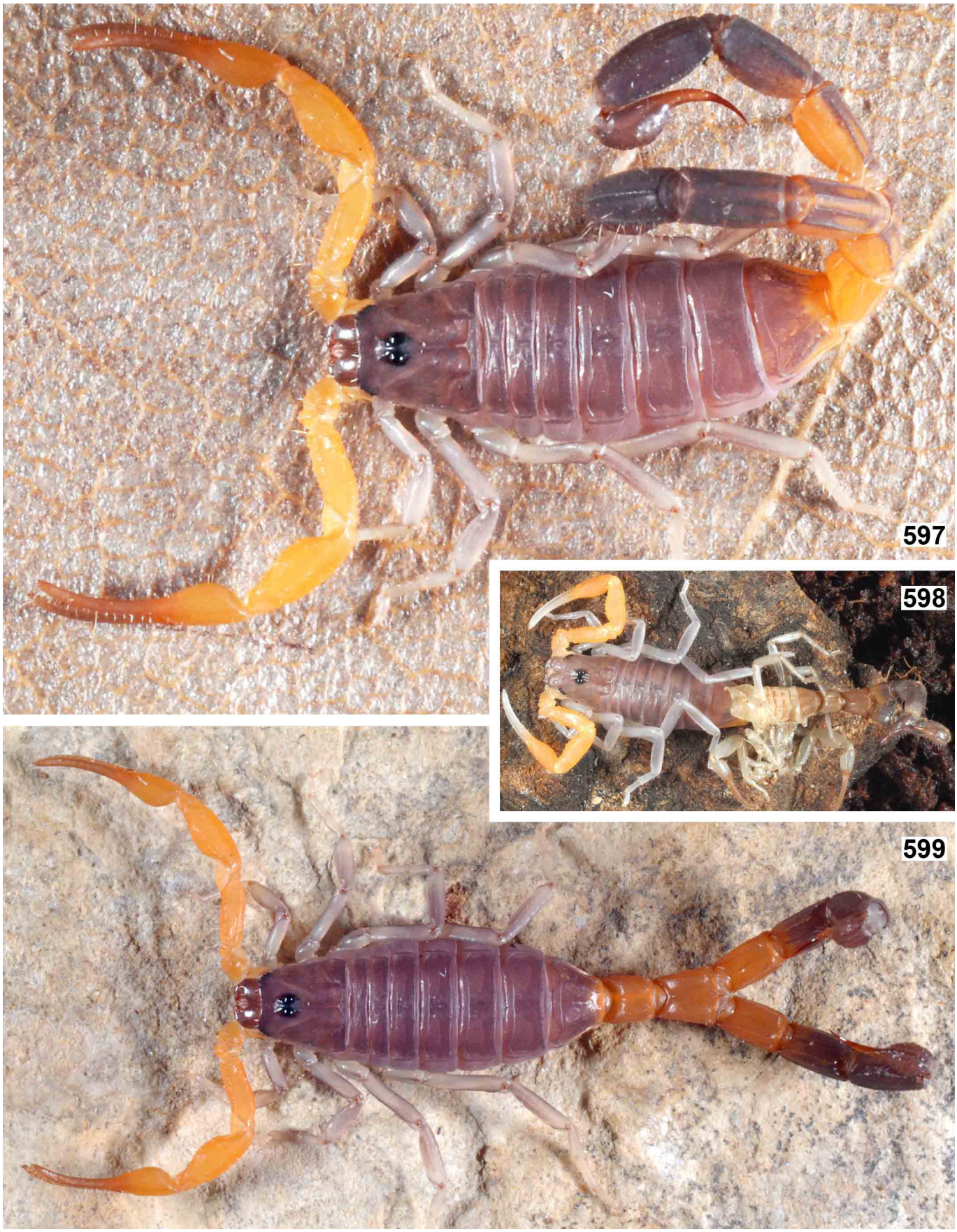

Figures 597–599. *Teruelius flavopiceus*. Juvenile with duplicated metasoma (597, 599) and its unsuccesful second ecdysis (598).

Figures 600–601. *Teruelius grandidieri*. Male (600) and female (601) in vivo habitus.

Figures 602–603. *Teruelius grandidieri*. Female with newborns (602) and with juveniles after first ecdysis (603).

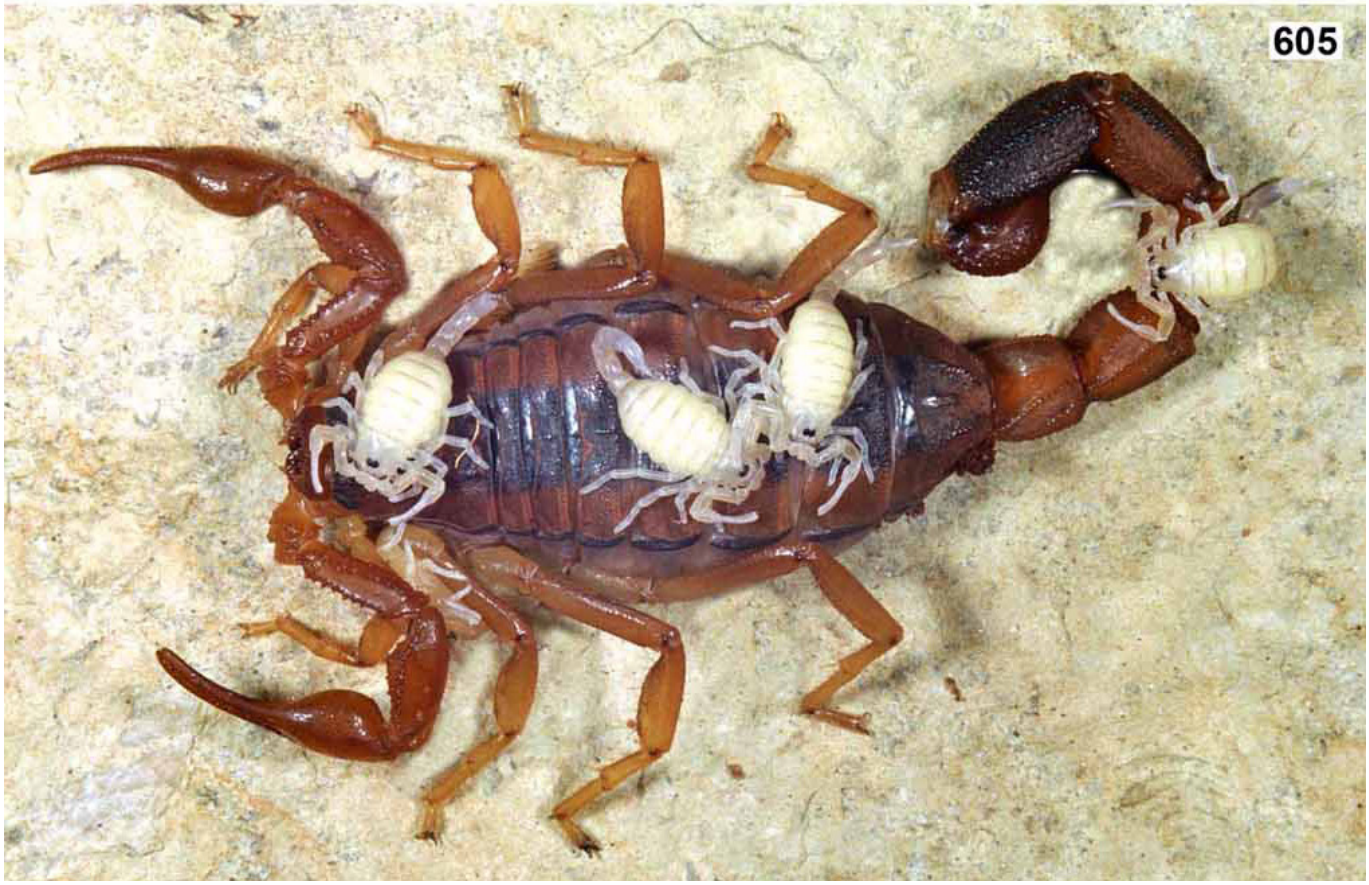

Figures 604–605. *Teruelius limbatus*. Male (in the middle) and females (604) and female with newborns (605).

Figures 606–609. *Neogrosphus griveaudi*. Habitus. Male (606–607) and female (608–609), dorsal (606, 608) and ventral (607, 609) views. Scale bar: 10 mm.

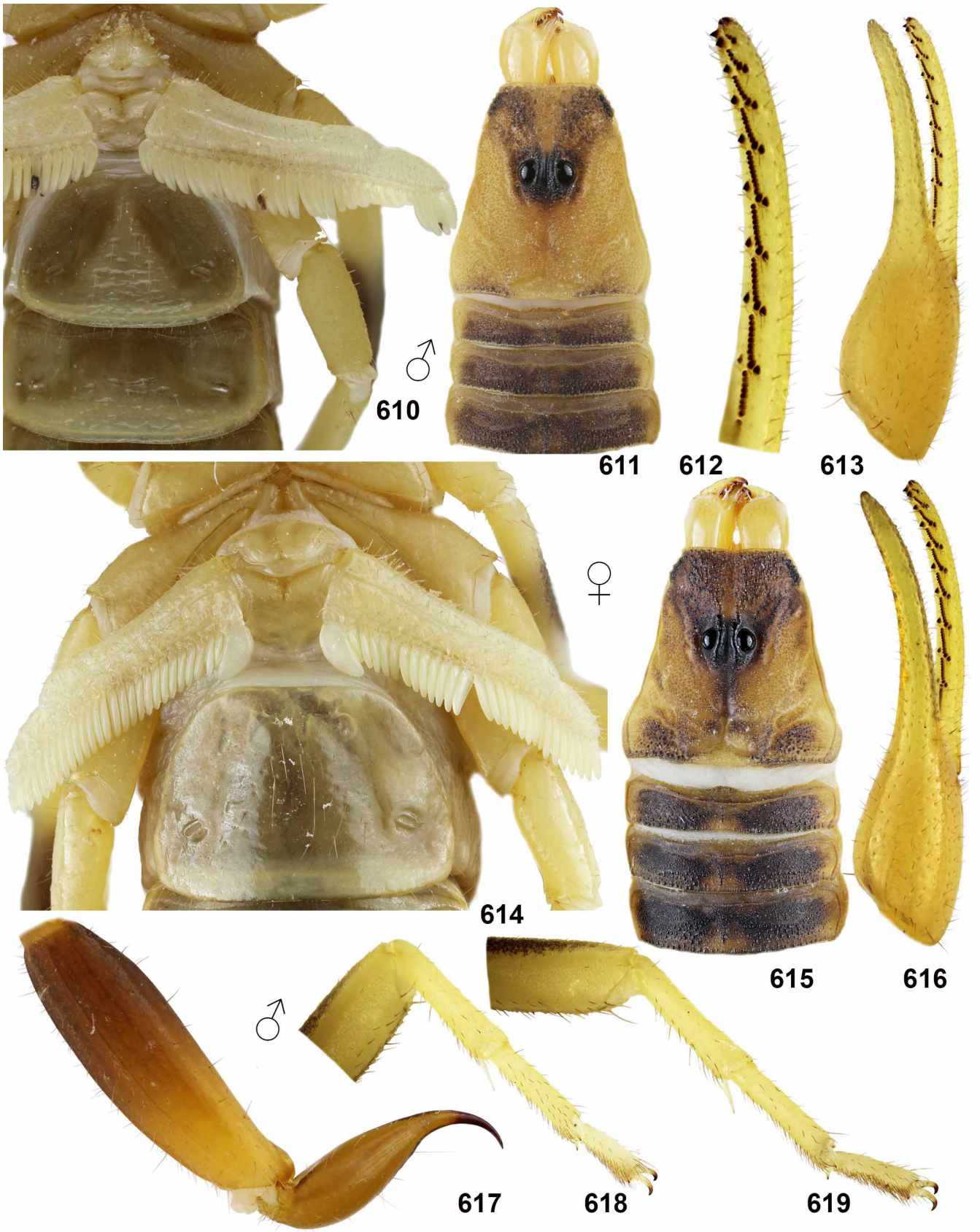

Figures 610–619. *Neogrosphus griveaudi*, male (610–613, 617–619) and female (614–616). **Figures 610**, **614**. Sternopectinal region. **Figures 611**, **615**. Carapace and tergites I–III. **Figure 612**. Pedipalp chela, movable finger dentate margin. **Figures 613**, **616**. Pedipalp chela in dorsal views. **Figure 617**. Metasoma V and telson lateral view. **Figures 618–619**. Right leg III (618) and leg IV (619), tibia, basitarsus and telotarsus, retrolateral views.

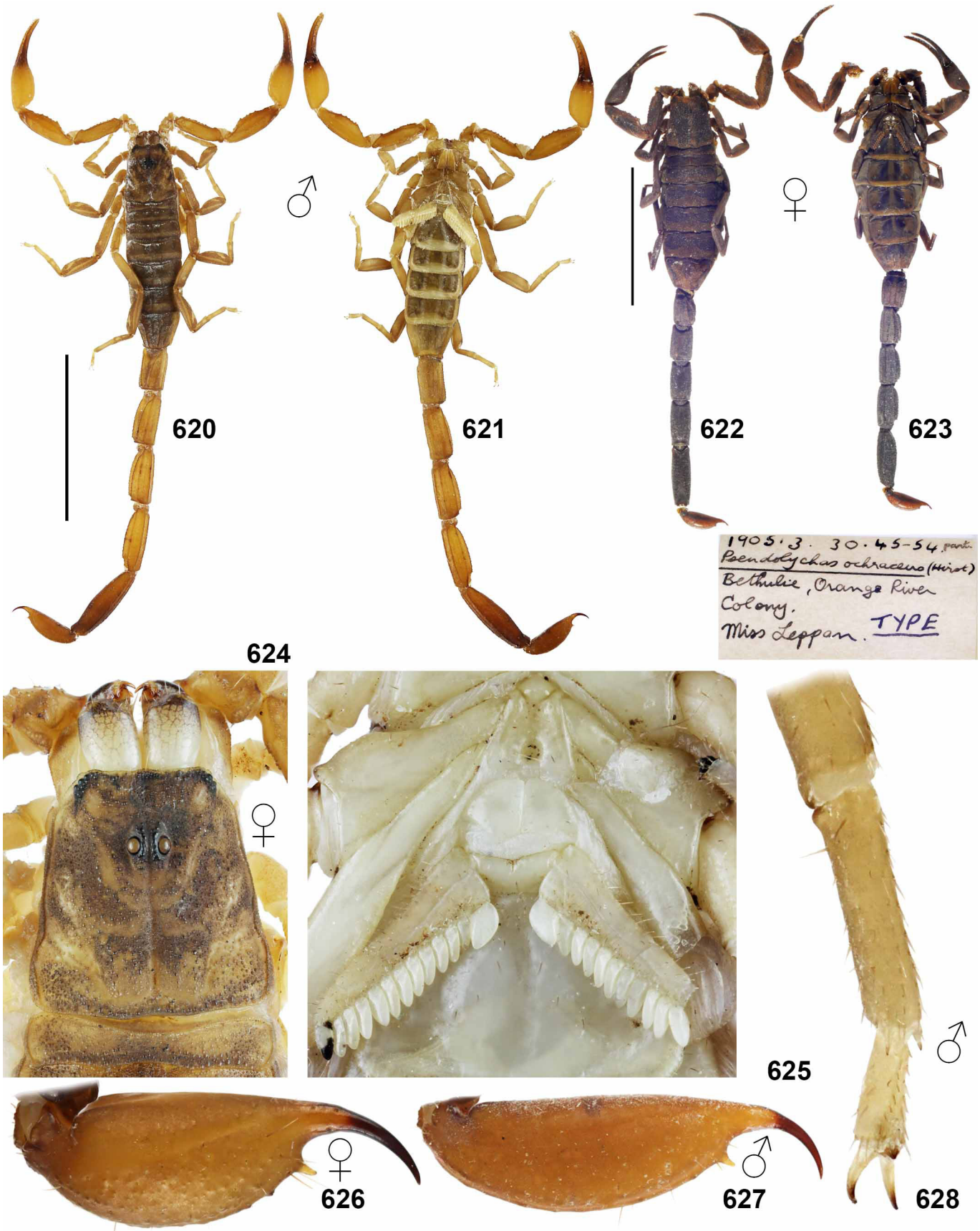

Figures 620–**628**. *Pseudolychas ochraceus*. **Figures 620**–**623**. Habitus. Male (620–621) and female holotype (622–623), dorsal (620, 622) and ventral (621, 623) views. Scale bars: 10 mm. **Figures 624**–**625**. Female, carapace and tergite I (624) and sternopectinal region (625). **Figures 626**–**627**. Telson lateral in female (626) and male (627). **Figure 628**. Male, leg III basitarsus and telotarsus, retrolateral views.

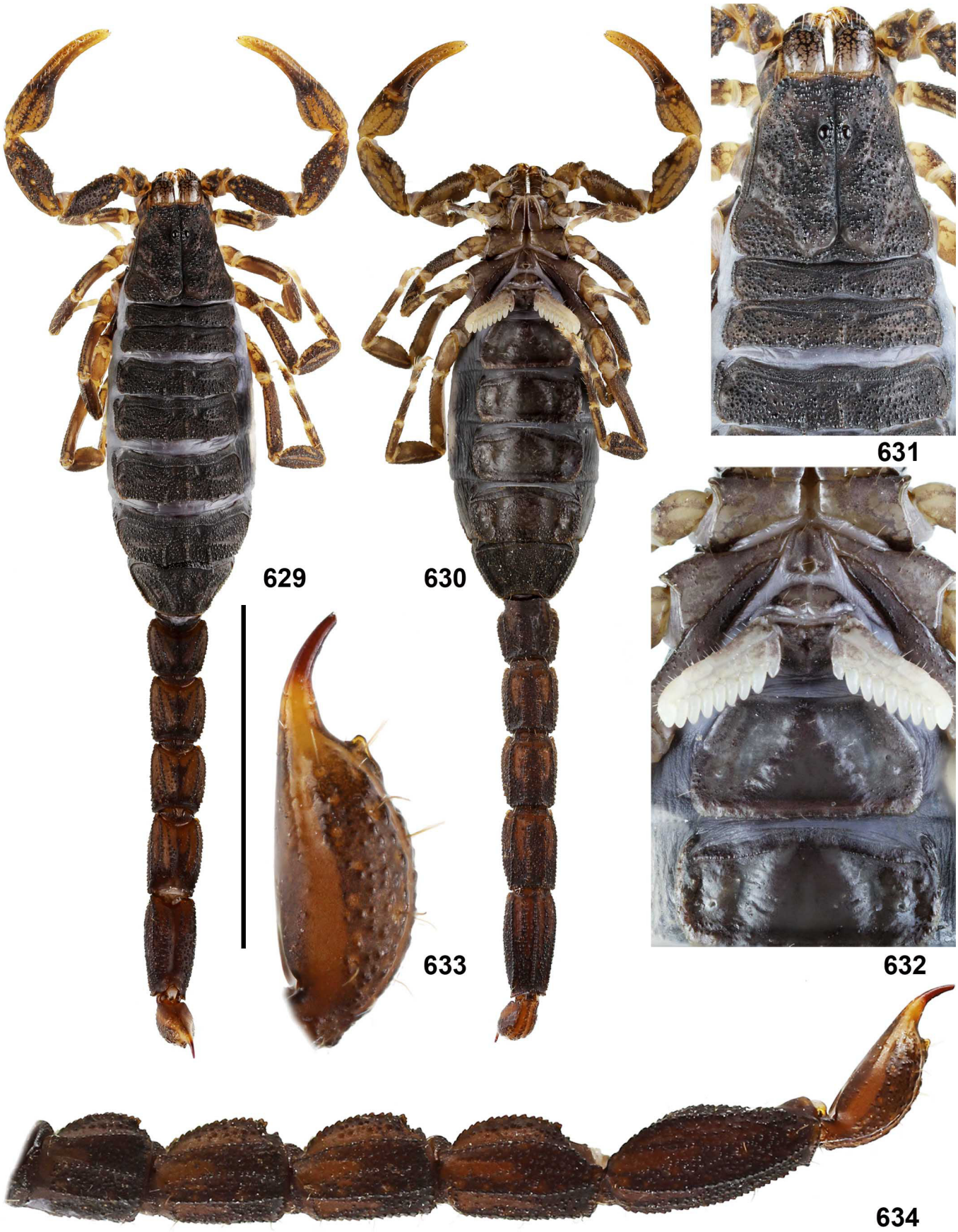

Figures 629–634. *Pseudolychas transvaalicus*, juvenile female, habitus in dorsal (629) and ventral (630) views, carapace and tergites I–III (631), sternopectinal region and sternites III–IV (632), telson lateral (633) and telson and metasoma in dorsal view (634). Scale bar: 10 mm (629–630).

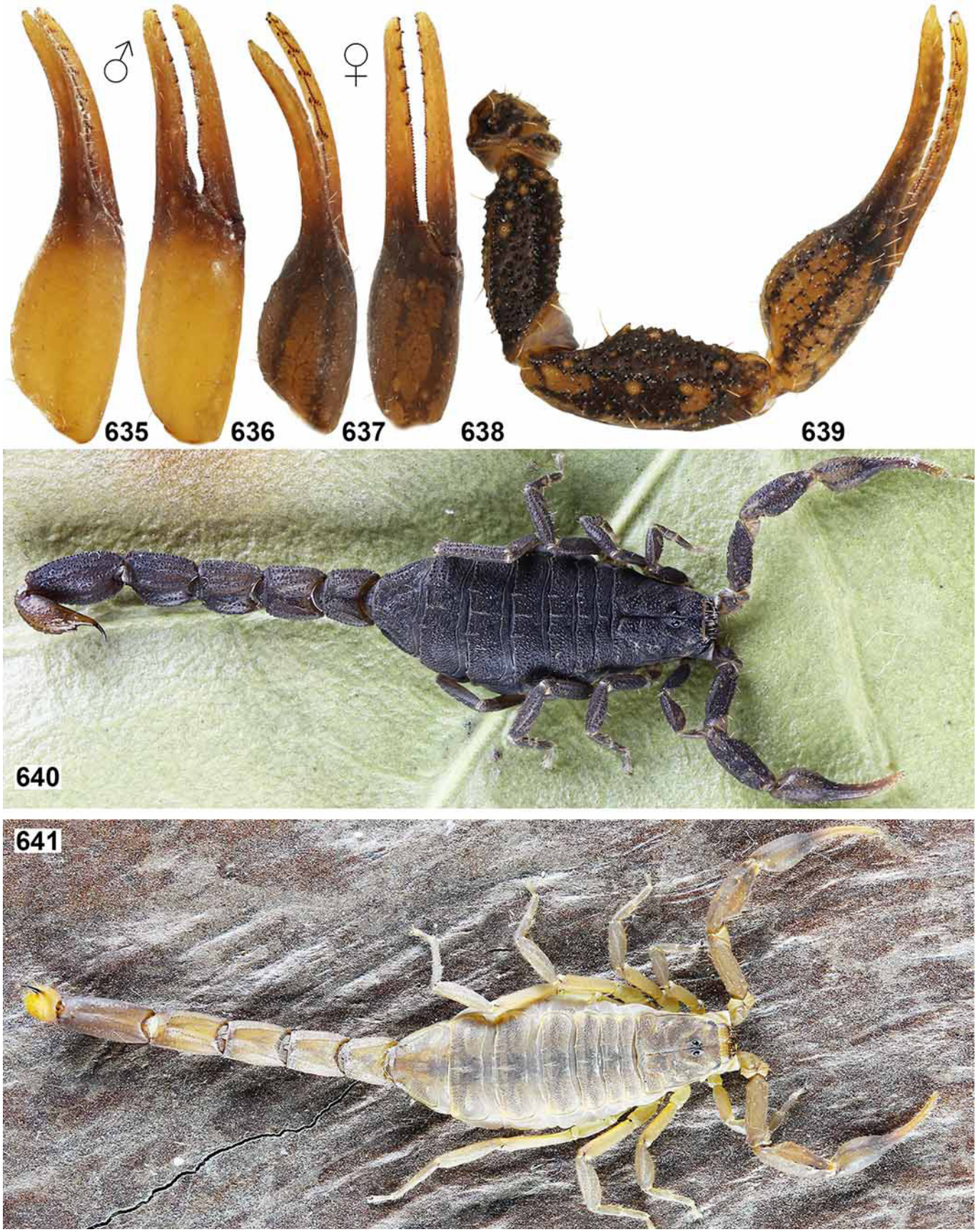

Figures 635–641. *Pseudolychas*. **Figures 635–638**. *P. ochraceus*, pedipalp chela dorsal (635, 637) and external (636, 638) in male (635–636) and female (637–638). **Figures 639–640**. *P. transvaalicus*, juvenile female, right pedipalp (639) and in vivo habitus 640. **Figure 641**. *P. ochraceus*, female in vivo habitus.